



THE HONG KONG
POLYTECHNIC UNIVERSITY

香港理工大學

Pao Yue-kong Library

包玉剛圖書館

Copyright Undertaking

This thesis is protected by copyright, with all rights reserved.

By reading and using the thesis, the reader understands and agrees to the following terms:

1. The reader will abide by the rules and legal ordinances governing copyright regarding the use of the thesis.
2. The reader will use the thesis for the purpose of research or private study only and not for distribution or further reproduction or any other purpose.
3. The reader agrees to indemnify and hold the University harmless from and against any loss, damage, cost, liability or expenses arising from copyright infringement or unauthorized usage.

IMPORTANT

If you have reasons to believe that any materials in this thesis are deemed not suitable to be distributed in this form, or a copyright owner having difficulty with the material being included in our database, please contact lbsys@polyu.edu.hk providing details. The Library will look into your claim and consider taking remedial action upon receipt of the written requests.

Pao Yue-kong Library, The Hong Kong Polytechnic University, Hung Hom, Kowloon, Hong Kong

<http://www.lib.polyu.edu.hk>

**DESIGN AND SYNTHESIS OF AMIDE-BASED
HYDROGEN BOND DONOR-ACCEPTOR-DONOR
ORGANOCATALYSTS FOR CONJUGATE
ADDITION**

LEUNG KING CHI

M.Phil

The Hong Kong Polytechnic University

2014

The Hong Kong Polytechnic University

Department of Applied Biology and Chemical Technology

**Design and Synthesis of Amide-Based Hydrogen Bond
Donor-Acceptor-Donor Organocatalysts for Conjugate
Addition**

LEUNG KING CHI

A Thesis Submitted in Partial Fulfillment of the Requirements
for the Degree of Master of Philosophy

June, 2013

Certificate of Originality

I hereby declare that this thesis entitled “DESIGN AND SYNTHESIS OF AMIDE-BASED HYDROGEN BOND DONOR-ACCEPTOR-DONOR ORGANOCATALYSTS FOR CONJUGATE ADDITION” is my own work within the period of July, 2011 to June, 2013 and that, to the best of my knowledge and belief, it reproduces no material previously published or written, nor material that have been accepted for award of any other degree or diploma, except where due acknowledgement has been made in text.

Franco King-Chi LEUNG

Abstract

Organocatalysis has emerged as an appealing strategy for addressing important synthetic challenges in chemistry. In this thesis, a new class of amide-based hydrogen bond donor-acceptor-donor (HB-DAD) organocatalysts has been developed as efficient organocatalysts for conjugate addition of benzylidene barbiturates. Through mechanistic studies, a good correlation between binding constants of hydrogen bonding and reaction rates has been found to support the substrate activation mode.

A modular approach to identify essential moieties in the organocatalysts for substrate activation has been employed. A series of amide-based HB-DAD organocatalysts **1a-1c**, **2a-2c**, **3a-3b** and **4a** with tunable functionalities including [1] nitrogen-heterocyclic ring as hydrogen bond acceptor (HBA), [2] nitrogen-hydrogen bond (N-H bond) as hydrogen bond donor (HBD), and [3] electron-withdrawing activator (A) to increase the acidity of the N-H bond have been constructed. Systematic screening of organocatalysts **1a-1c**, **2a-2c**, **3a-3b** and **4a** in catalyzing conjugate addition of benzylidene barbiturates has been performed. We have found that organocatalyst **1a** (featuring *para*-chloro-pyrimidine as the HBA, N-H as the HBD and trifluoroacetyl group as the activator) is able to activate the substrates through complementary DAD-ADA hydrogen bonding resulting in reaction rate

enhancement.

Organocatalyst **1a** together with other newly developed HB-DAD organocatalysts **1c**, **2a** and **2c** were found to be efficient in catalyzing conjugate addition of 2-methylfuran to benzylidene barbiturates in dichloromethane at room temperature. Using 20 mol% of organocatalysts, a two-fold reaction rate enhancement in conjugate addition of furans to barbiturates was obtained with good isolated yield (up to 70 %). In particular, benzylidene barbiturates bearing aliphatic ether and thioether substituents were most significantly activated by the organocatalysts.

Mechanistic studies of the amide-based HB-DAD catalyzed conjugate addition have been conducted. Using ^1H NMR spectroscopy, pseudo first-order kinetic studies were conducted. The rate constant ($k = 1.48 \times 10^{-3} \text{ s}^{-1}$, $R^2 = 0.95$, $k_{\text{rel}} = 2.22$) of **1a** in catalyzing conjugate addition of benzylidene barbiturates was obtained. Hence, the role of the trifluoroacetamide as HBD and activator in **1a** has been supported by reaction rate enhancement in the conjugate addition of benzylidene barbiturates. By UV/vis titration experiments, high binding constants (up to $K = 8936 \text{ M}^{-1}$, $R^2 = 0.95$, $\Delta G = -22.5 \text{ kJ/mol}$) of the amide-based HB-DAD organocatalysts with benzylidene barbiturate chromophores in dichloromethane were obtained. The excellent

correlation ($R^2 = 0.92$) between the binding constants and reaction rate constants of amide-based HB-DAD organocatalysts provides support for HB-DAD as the activation moiety in organocatalysis. In addition, adjustable electrophilic substrate control in the conjugate addition of benzylidene barbiturates has been realized.

On the basis of the above findings, rational design and synthesis of C_2 -symmetric chiral amide-based HB-DAD organocatalysts, **10a-10f**, have been achieved. Using chiral organocatalysts **10a-10f**, asymmetric conjugate addition of dibenzoylmethane to maleimide in dichloromethane at room temperature has been performed. Adducts were obtained in excellent isolated yield (up to 90 %) with enantioselectivities of 8-15 %ee indicating the feasibility of catalyst-to-product chirality transfer.

Acknowledgement

I appreciate to my supervisor, Dr. Man-Kin Wong for offering me a chance to study on hydrogen bond donor-acceptor-donor organocatalysis. I would like to express my deepest gratitude to his invaluable advice, supervision and guidance throughout my study, in both experimental work and writing up of this thesis.

I am grateful to my group members, Dr. Ka-Yan Karen Kung, Ms. Gai-Li Li, Mr. Yat-Sing Fung, Mr. Hok-Ming Ko, Mr. Kong-Fan Wong and Dr. Jian-Fang Cui for sharing of their research experience and technical skills with me and giving me an unforgettable memory.

I would like to thank all academic and technical staffs of the Department of Applied Biology and Chemical Technology for their technical support, especially thank Prof. Zhong-Yuan Zhou for X-ray crystallographic study, Dr. Siu-Cheong Yan for his guidance in NMR analysis, and Dr. Pui-Kin So for recording MS spectra.

I am very grateful to work with members of Dr. Wong's group. It is my pleasure to work with you all, for this enjoyable experimental research experience.

Table of Content

Certificate of Originality	i
Abstract	ii
Acknowledgement.....	v
List of Figures	x
List of Tables.....	xii
List of Schemes	xiii
Chapter 1 Introduction	1
1.1 Introduction to Organocatalysis	1
1.2 Organocatalysis	2
1.2.1 Amine-Catalysts: Iminium Ion, Enamine, Dienamine, Guanidine, and SOMO Organocatalysis	3
1.2.1.1 Iminium Ion Organocatalysis	3
1.2.1.2 Enamine Organocatalysis	4
1.2.1.3 Guanidine Organocatalysis.....	7
1.2.1.4 SOMO Organocatalysis.....	8
1.2.2 Non-Amine Lewis Base Catalysts: Phosphine and NHC Organocatalysis	9
1.2.2.1 Phosphine Organocatalysis.....	9
1.2.2.2 NHC Organocatalysis	10
1.2.3 Ion-Pairing Catalysis	11
1.2.3.1 Cation-Binding Catalysts: Phase-Transfer Catalysis.....	11
1.2.3.2 Brønsted Acid Catalysis	13
1.2.4 Hydrogen-Bonding Catalysis	14
1.2.4.1 Hydrogen-Bonding Donor-Donor (DD) Catalysis - Thiourea.....	15
1.2.4.2 Hydrogen-Bonding Donor-Donor (DD) Catalysis - Guanidinium	16
1.2.4.3 Hydrogen-Bonding Donor-Donor (DD) Catalysis - Squaramide	17
1.3 Hydrogen-Bonding Donor-Acceptor-Donor (HB-DAD) Catalysis.....	19

1.4 The Objectives and Achievement of the Thesis	20
1.5 References	21
Chapter 2	
Design and Synthesis of Hydrogen Bond Donor-Acceptor-Donor Organocatalysts	26
2.1 Introduction	26
2.1.1 Design of HB-DAD Organocatalysts	26
2.1.2 The Objectives of This Chapter	28
2.2 Results and Discussion	29
2.2.1 Synthesis of HB-DAD Organocatalysts	29
2.2.2 Studies on Catalytic Conjugate Addition of Benzylidene Barbiturates	33
2.2.3 Binding Mode Study.....	39
2.2.3.1 Binding Mode Study - HB-DAD Organocatalysts Modifications	39
2.3 Conclusion.....	42
2.4 Experimental Section.....	43
2.4.1 Experimental Procedure	43
2.4.2 Literature Reference of 2a-e , 4a-4c , 5a-5c and Thiourea B.....	44
2.4.3 Characterization.....	46
2.5 Reference.....	50
Chapter 3	
Hydrogen Bond Donor-Acceptor-Donor Organocatalysts for Conjugate Addition of Benzylidene Barbiturates.....	53
3.1 Introduction	53
3.1.1 History of Barbiturates	54
3.1.2 Applications of Benzylidene Barbiturates	55
3.1.3 Reactions of Benzylidene Barbiturates.....	57
3.1.4 The Objectives of This Chapter.....	59
3.2 Results and Discussion.....	60
3.2.1 Design and Synthesis of HB-ADA Based Benzylidene Barbiturates.....	60

3.2.2 Optimization of Reaction Conditions of Conjugate Additions of Benzylidene Barbiturates	64
3.2.3 Substrate Scopes.....	68
3.2.3.1 Substrate Scopes - Conjugate Additions of N-n-Butyl Substituted Benzylidene Barbiturates	68
3.2.3.2 Substrate Scopes - Conjugate Additions of N-Methyl and N-m-toluene Substituted Benzylidene Barbiturates.....	72
3.2.3.3 Substrate Scope - Conjugate Additions of Benzylidene Barbiturate with other Nucleophiles.....	74
3.3 Conclusion.....	76
3.4 Experimental Section.....	77
3.4.1 Experimental Procedures.....	77
3.4.2 Characterizations	78
3.5 Reference.....	91
Chapter 4	
Kinetic and Binding Studies of Amide-Based HB-DAD Organocatalysis.....	94
4.1 Introduction	94
4.1.1 Kinetics Studies of Hydrogen Bonding Organocatalysts	94
4.1.2 UV. / Vis. Titration Binding Constant Study	95
4.2 Results and Discussion.....	97
4.2.1 Kinetics Study of Amide-Based HB-DAD Organocatalysts	97
4.2.2 Binding Study of Amide-Based HB-DAD Organocatalysts	103
4.2.3 Correlation of Rate Constants and Binding Constants of Amide-Based HB-DAD Organocatalysts	107
4.3 Conclusion.....	110
4.4 Experimental Section.....	111
4.4.1 ¹ H NMR Kinetics Study of Conjugate Addition of Benzylidene Barbiturate	111

4.4.2 Results in ¹ H NMR Kinetic Study of Conjugate Addition of Benzylidene Barbiturates	112
4.4.3 UV / Vis. Titration Binding Study of Benzylidene Barbiturate Chromophore with Amide-Based HB-DAD Organocatalysts	113
4.5 References	115
Chapter 5	
Studies on Asymmetric Conjugate Addition by C₂ Symmetric Chiral Hydrogen Bond Donor-Acceptor-Donor Organocatalysts	
5.1 Introduction	119
5.1.1 Design of C ₂ Symmetric Chiral HB-DAD Organocatalysts	120
5.1.2 The Objective of This Chapter	121
5.2 Results and Discussion	122
5.2.1 Synthesis of C ₂ Symmetric Chiral HB-DAD Organocatalysts	122
5.2.2 Catalytic Activity Studies - C ₂ Symmetric Chiral HB-DAD Organocatalysts in Conjugate Additions of Maleimide with Dibenzoylmethane	125
5.3 Conclusion	128
5.4 Experimental Section	129
5.4.1 Experimental Procedures	129
5.4.2 Characterizations	134
5.4.3 HPLC Spectra of 11	139
5.5 References	144
Appendices	

List of Figures

Figure 1.1	Structure of HB-DAD catalysts and HB-ADA electrophiles	19
Figure 2.1	Design of HB-DAD organocatalysts containing (1) HBA, (2) HBD, and (3) Activator	26
Figure 2.2	X-ray crystallographic structure of 1a	30
Figure 3.1	Diethyl barbiturate (Veronal)	54
Figure 3.2	Chemical structure of Phenobarbital	54
Figure 3.3	Modification of the C-5 position of barbituric acid	55
Figure 3.4	Chemical structures of benzylidene barbiturates	55
Figure 3.5	Conjugate additions, cycloadditions and reductions of benzylidene barbiturates	58
Figure 3.6	Constituents of benzylidene barbiturates (1) HB-ADA motif, (2) N-substituted group and (3) aryl group	60
Figure 3.7	Synthesis of benzylidene barbiturates (1) Electron donating aryl substituents	62
Figure 3.8	Synthesis of benzylidene barbiturates (2) Electron neutral aryl substituents	62
Figure 3.9	Synthesis of benzylidene barbiturates (3) Electron withdrawing aryl substituents	63
Figure 3.10	Synthesis of N-methyl and N- <i>m</i> -tolyl substituted benzylidene barbiturates	63
Figure 4.1	Kinetics data of conjugate addition of 6a and 2-methylfuran catalyzed by HB-DAD organocatalysts	97
Figure 4.2	Correlation of natural logarithm relative rate and binding	107

constant of HB-DAD organocatalysts

Figure 5.1 X-ray crystallography structure of **10a**

121

List of Tables

Table 3.1	Solvent screening study of the organocatalytic conjugate addition	65
Table 3.2	Study of 1a loading in organocatalytic conjugate addition	66
Table 3.3	Reaction temperature optimization in organocatalytic conjugate addition	67
Table 3.4	Substrate scope of organocatalytic conjugate addition of electron rich benzylidene barbiturates	69
Table 3.5	Substrate scope of organocatalytic conjugate addition of electron neutral benzylidene barbiturates	71
Table 3.6	Substrate scope of organocatalytic conjugate addition of electron deficient benzylidene barbiturates	72
Table 3.7	Substrate scope of organocatalytic conjugate addition of N-methyl and N-m-toluene substituted benzylidene barbiturates	73
Table 3.8	Substrate scope of organocatalytic conjugate addition of 6a with other nucleophiles	75
Table 4.1	Rate constant determinations by ¹ H NMR studies	99
Table 4.2	Binding constants of HB-DAD organocatalysts	104
Table 4.3	Treatment of relative rate and binding constant of HB-DAD organocatalysts	106
Table 4.4	Rate constants determinations with ¹ H NMR studies	110
Table 4.5	Binding constant determinations with UV / Vis. titration method	112
Table 5.1	10a and 10b in catalyzing conjugate addition of maleimide	124
Table 5.2	10c , 10d , 10e and 10f in catalyzing conjugate addition of	125

List of Schemes

Scheme 1.1	General Classification of Organocatalysis	2
Scheme 1.2	Iminium organocatalysis with chiral imidazolinones	3
Scheme 1.3	Iminium organocatalysis with cinchona-derived primary amines	4
Scheme 1.4	Enamine organocatalysis with cinchona-derived primary amines	5
Scheme 1.5	Enamine organocatalysis with chiral amino diol catalysts	5
Scheme 1.6	Dienamine organocatalysis with bifunctional squaramide-based aminocatalyst	6
Scheme 1.7	Dienamine organocatalysis with diphenylprolinol silyl ether catalyst	7
Scheme 1.8	Guanidine organocatalysis with chiral guanidine derived catalyst	7
Scheme 1.9	Organocatalytic protonation with chiral guanidine derived catalyst	8
Scheme 1.10	SOMO organocatalysis with chiral benzyl-substituted imidazolidinone	8
Scheme 1.11	Phosphine-catalyzed addition with chiral phosphine	9
Scheme 1.12	NHC-catalyzed Michael / Stetter reaction	10
Scheme 1.13	NHC-catalyzed annulation	11
Scheme 1.14	Chiral ammonium bromide phase-transfer catalyst in	12

	catalyzing alkylation of modified 2-arylcyclohexanones	
Scheme 1.15	Chiral pentanidium based phase-transfer catalyst in catalyzing the Michael addition	12
Scheme 1.16	Chiral confined chiral Brønsted acid in catalyzing the oxidations	13
Scheme 1.17	Chiral phosphoric acid in catalyzing the asymmetric bromination	14
Scheme 1.18	Schiff-base hydrogen-bonding catalyst in catalyzing the Strecker reaction	15
Scheme 1.19	Amino acid-derived bifunctional thiourea in catalyzing the Michael addition	16
Scheme 1.20	Saccharide-derived organocatalyst in catalyzing the Mannich addition	16
Scheme 1.21	Gunidinium BArF catalyst in catalyzing the Claisen rearrangement	17
Scheme 1.22	Squaramide derived hydrogen bonding catalysts in catalyzing the α -amination	18
Scheme 1.23	Squaramide-tertiary amine catalyst in catalyzing the sulfa-Michael/ Michael addition	18
Scheme 2.1	Synthesis of amide-based HB-DAD organocatalysts	29
Scheme 2.2	Synthesis of amine-based HB-DAD organocatalysts	31
Scheme 2.3	Synthesis of amide-based hydrogen bonding organocatalysts	32
Scheme 2.4	Hydrogen bonding organocatalysts reactivity studies in conjugate addition of 6a	33
Scheme 2.5	HB-DAD organocatalysts reactivity studies in conjugate	36

	addition of 6a	
Scheme 2.6	HB-DAD organocatalysts reactivity studies in conjugate addition of 6a	37
	addition of 6a	
Scheme 2.7	HB-DAD organocatalysts reactivity studies in conjugate addition of 6a	38
	addition of 6a	
Scheme 2.8	2a and 5a in catalyzing conjugate addition of 6a	39
Scheme 2.9	2a and 5b in catalyzing conjugate addition of 6a	40
Scheme 2.10	5b and 5c in catalyzing conjugate addition of 6a	40
Scheme 3.1	Synthesis of benzylidene barbiturates 6 and 8	61
Scheme 4.1	The calculation of the relative rate constant of HB-DAD organocatalyst 1a	100
Scheme 4.2	The relative rate constants scale of HB-DAD organocatalysts in catalyzing conjugate addition of benzylidene barbiturate 6a	101
Scheme 4.3	The scale of yield of 7a of HB-DAD organocatalysts in catalyzing conjugate addition of benzylidene barbiturate 6a	102
Scheme 4.4	The polarization of [1a-6a]	105
Scheme 5.1	Design of C_2 symmetric chiral HB-DAD organocatalysts	118
Scheme 5.2	Synthetic route of 10a and 10b	120
Scheme 5.3	Synthetic route of C_2 symmetric chiral HB-DAD organocatalysts 10c , 10d , 10e and 10f	122

Abbreviation

δ	Chemical shift (NMR)
s	Singlet
d	Doublet
t	Triplet
q	Quartet
m	Multiplet
MS	Mass spectrometry
NMR	Nuclear magnetic resonance spectroscopy
equi.	Equivalent
h	Hour
rt	Room temperature
ee	Enantiomeric excess
THF	Tetrahydrofuran
MeOH	Methanol
EtOH	Ethanol
Et ₂ O	Diethyl ether
EA	Ethyl acetate
R	Generalized alkyl group
Me	Methyl
Et	Ethyl
<i>n</i> -Bu	<i>n</i> -butyl
<i>i</i> -Pr	isopropyl
<i>t</i> -Bu	<i>t</i> -butyl
Ar	Aryl

Ph	Phenyl
Bn	Benzyl
Cy	Cyclohex

Chapter 1

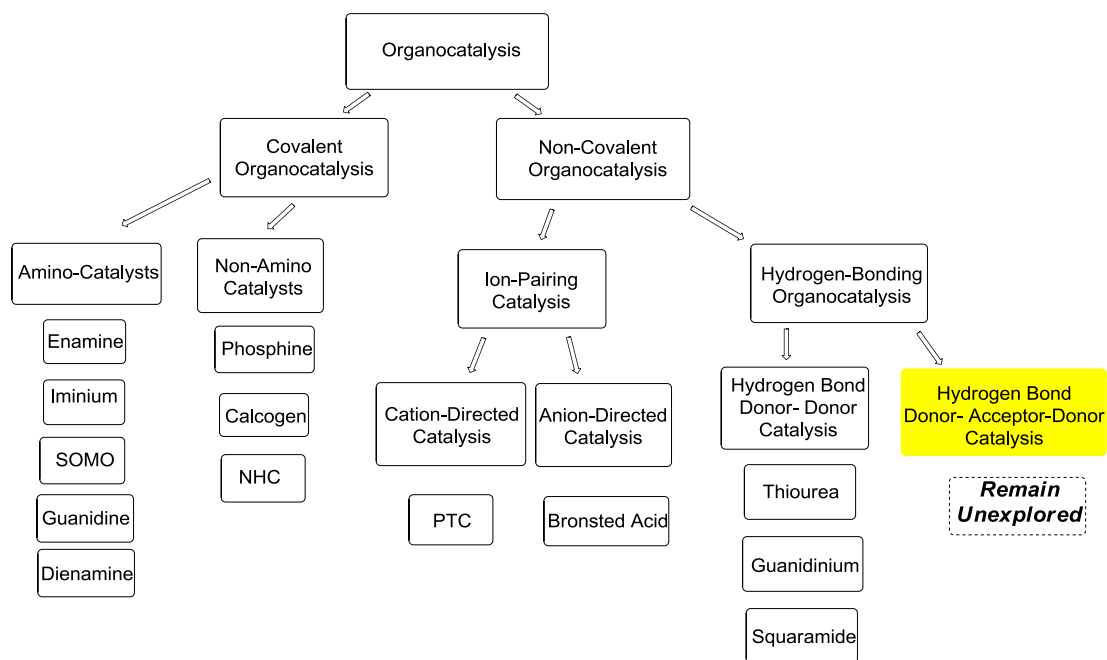
Introduction

1.1 Introduction to Organocatalysis

Organocatalysis has emerged as an important research area in Organic Chemistry.^[1-5] The features of organocatalysis including excellent selectivity, tunable reactivity and exceptional insensitivity to air/moisture reaction conditions offer remarkable advantages in catalyzing a wide variety of organic reactions that may not be achieved by using transition metal catalysis. Therefore, the search for new organocatalysts, new organocatalytic activation modes and synthetic applications has attracted considerable attention.

As no transition metals are involved, organocatalysis may provide compelling synthetic routes for the preparation of pharmaceutical products that tolerate no metal contamination. The significant development in organocatalysis research in recent years has been reflected by the mounting amount of publications in top scientific journals including *Science*, *Nature*, *J. Am. Chem. Soc.*, and *Angew. Chem Int. Ed.*

1.2 Organocatalysis



Scheme 1.1 General Classification of Organocatalysis^[3]

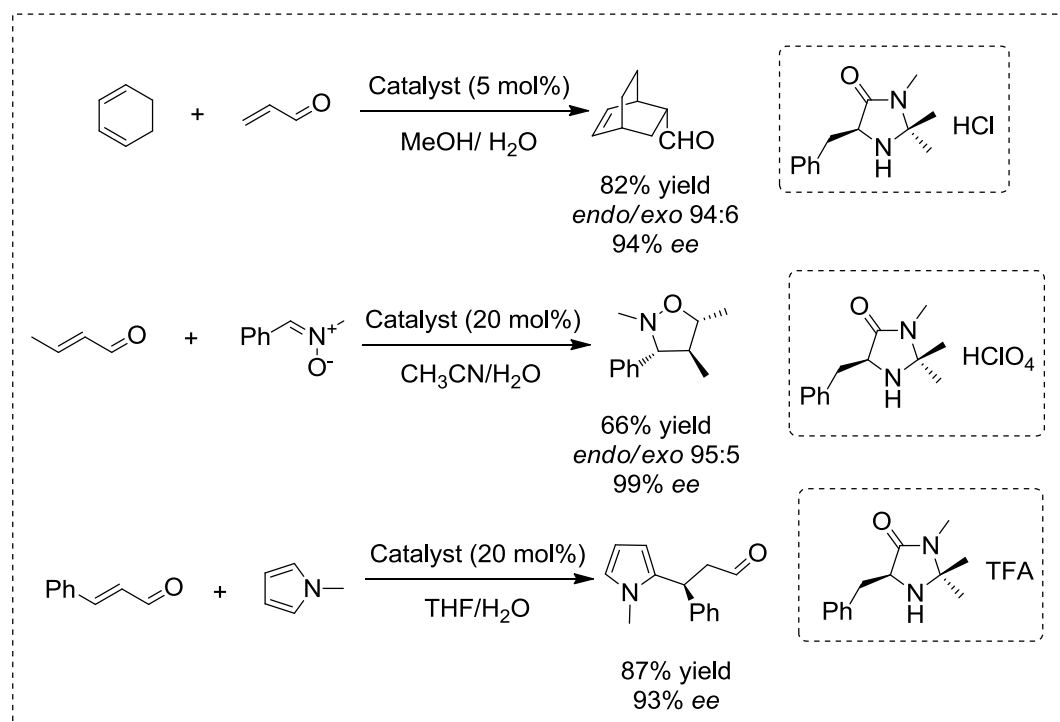
In 2010, Jacobsen and MacMillan reviewed that the generic modes of reactivity in organocatalysis were executed by various types of catalyst scaffolds.^[6] The amino-catalysts, non-amino catalysts and catalysis through non-covalent interaction were highlighted as the generic modes of reactivity. In addition, Jacobsen and co-workers discussed the concept of anion-directed catalysis proceeds via cationic intermediates through ion-pairing with anionic catalysts.^[7] List and coworkers highlighted counter anion-directed catalysis that shared similar idea in anion-directed catalysis.^[8] According to their views, the ion-pairing catalysis was classified as one of the non-covalent catalysis.

1.2.1 Amine-Catalysts: Iminium Ion, Enamine, Dienamine, Guanidine, and SOMO

Organocatalysis

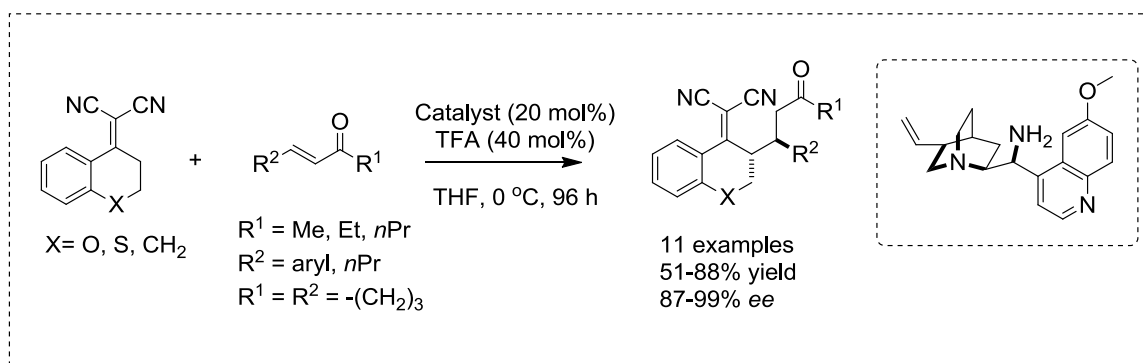
1.2.1.1 Iminium Ion Organocatalysis

Iminium organocatalysis activation mode features the reversible condensation of chiral amines with an unsaturated aldehyde to form iminium ion intermediates. The LUMO energy of the π system was effectively lowered. In addition, the susceptibility of iminium ions toward nucleophilic attack was enhanced.^[9]



Scheme 1.2 Iminium organocatalysis with chiral imidazolinones

Particularly, MacMillan and co-workers established effective chiral imidazolinones to promote transformations of α,β -unsaturated aldehydes in a highly enantioselective fashion (Scheme 1.2).^[10]

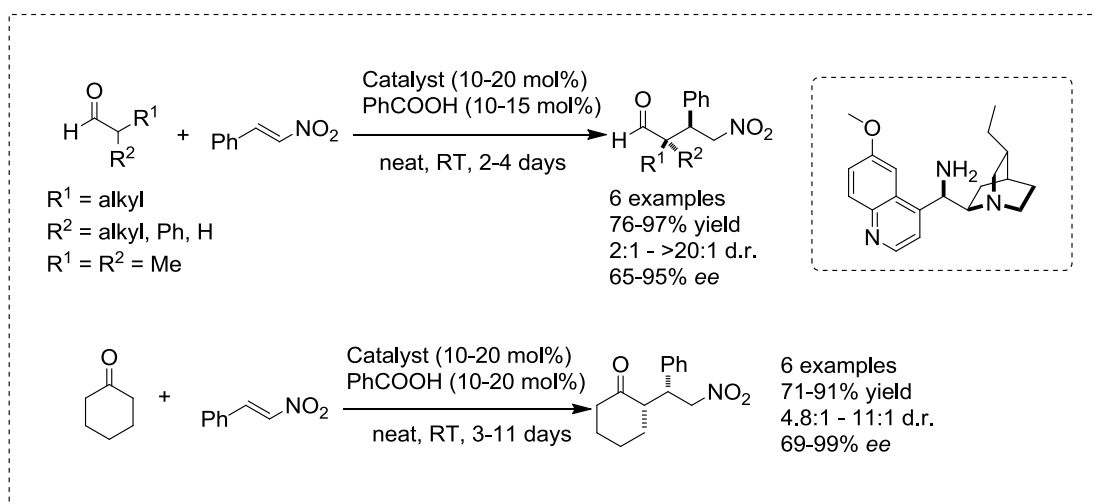


Scheme 1.3 Iminium organocatalysis with cinchona-derived primary amines

In 2007, Chen and co-workers developed cinchona-derived primary amines as iminium ion-based catalysts in catalyzing asymmetric Michael addition of α,α -dicyanoalkenes to afford enones (Scheme 1.3).^[11]

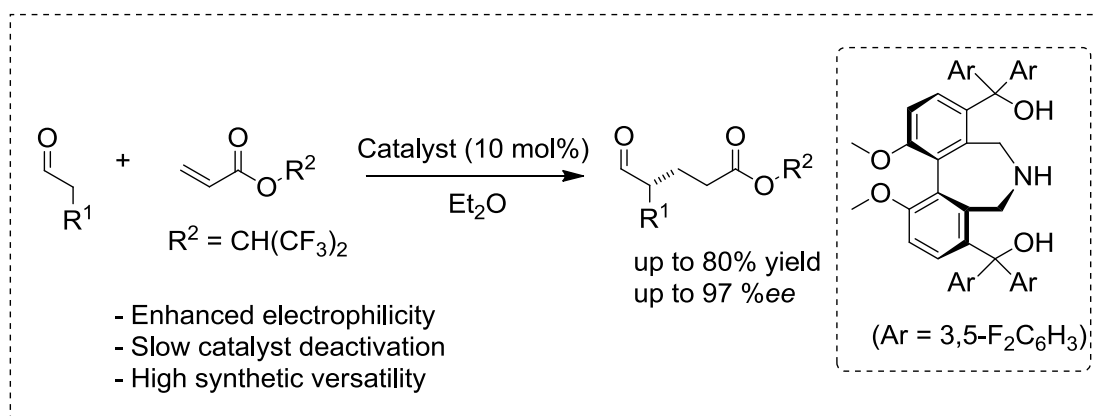
1.2.1.2 Enamine Organocatalysis

In addition to iminium ion activation of enones, cinchona-based primary amines have potential in the α -functionalization of enolizable carbonyl compounds. Specifically, 9-*epi* hydroquinidine derived catalyst was efficient in catalyzing Michael addition of nitroalkanes by enamine activation of linear and cyclic ketones as well as linear and α -branched aldehydes (Scheme 1.4).^[12]



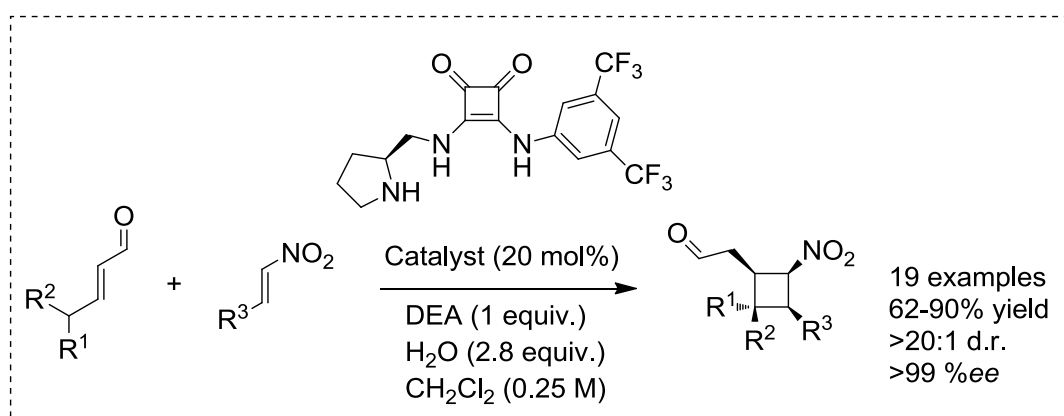
Scheme 1.4 Enamine organocatalysis with cinchona-derived primary amines

In 2012, Maruoka and co-workers reported axially chiral amino diol-catalysts in catalyzing Michael addition of di-*tert*-butyl methylmalonate with acrylates to give excellent yield (up to 80%) and enantioselective products (up to 97 %*ee*; Scheme 1.5).^[13]



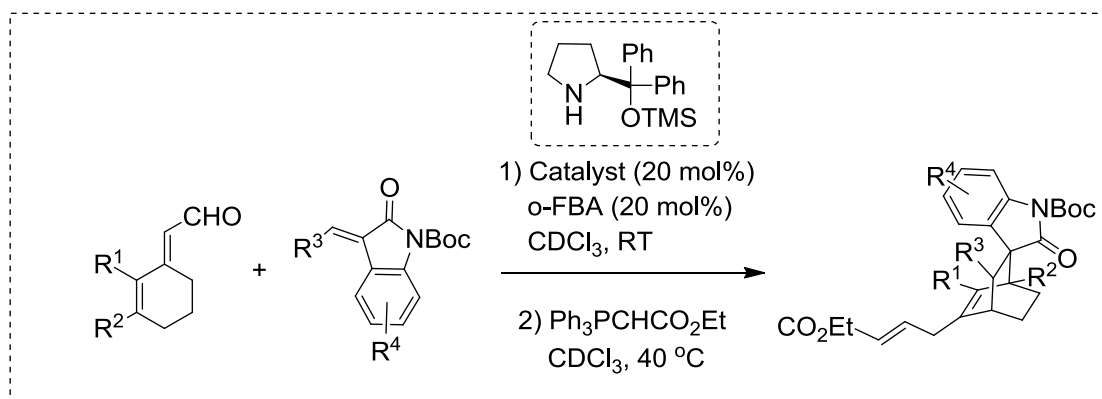
Scheme 1.5 Enamine organocatalysis with chiral amino diol-catalysts

In 2012, Jørgensen and co-workers reported an asymmetric organocatalytic formal [2+2]-cycloaddition through H-bond directing dienamine catalysis (Scheme 1.6).^[14] The bifunctional squaramide-based aminocatalysts catalyzed the cycloaddition of α,β -unsaturated aldehydes with nitroolefins to give good to excellent yield (62-90%) and excellent enantioselectivity (up to >99 %*ee*).



Scheme 1.6 Dienamine organocatalysis with bifunctional squaramide-based aminocatalyst

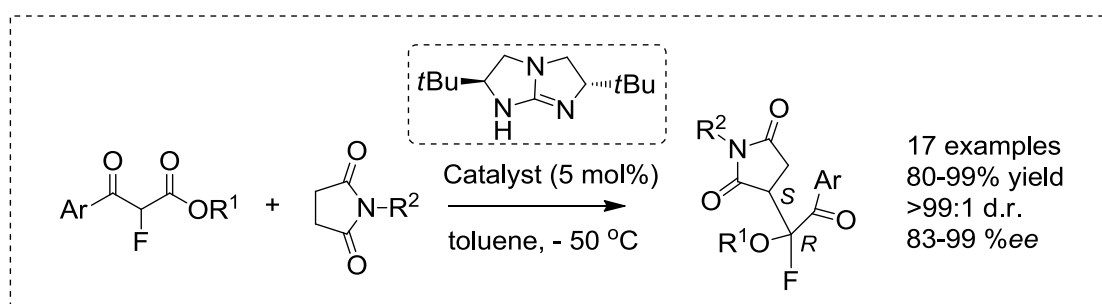
For trienamine of organocatalysis, Jørgensen and co-workers developed asymmetric organocatalyzed Diels-Alder reactions via cross-trienamine intermediates to provide enantioselective functionalization at the γ,δ -carbon centers of cyclic dienals (Scheme 1.7).^[15]



Scheme 1.7 Dienamine organocatalysis with diphenylprolinol silyl ether catalyst

1.2.1.3 Guanidine Organocatalysis

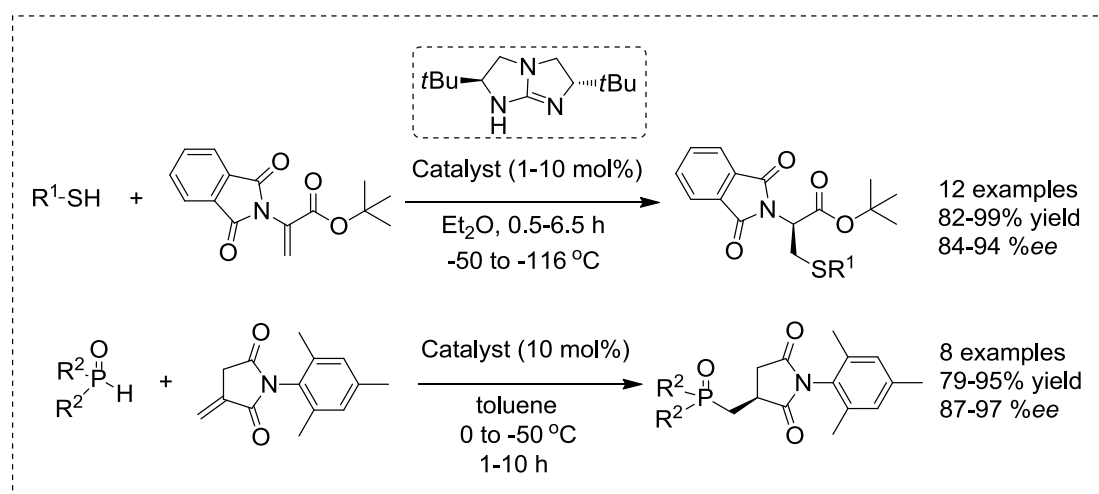
In addition to enamine and iminium ion catalysis, guanidine catalysis is one of the organocatalysis of amino-catalysts. Tan and co-workers recognized the potential catalytic function of guanidinium, to take part in dual hydrogen bonding.^[16]



Scheme 1.8 Guanidine organocatalysis with chiral guanidine derived catalyst

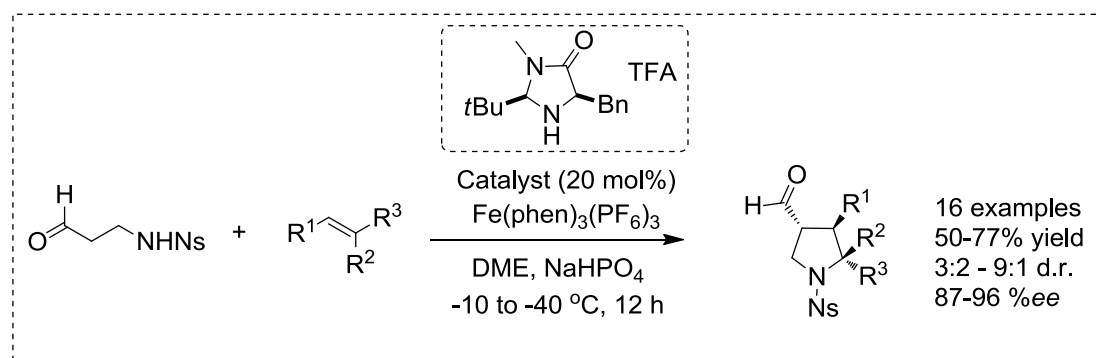
In 2009, Tan and co-workers reported the guanidine-catalyzed highly enantioselective and diastereoselective reactions between α -fluoro- β -ketoesters and

N-alkyl maleimides to give excellent yield (80-99%) and enantioselectivity (83-99 %*ee*; Scheme 1.8).^[17] Furthermore, Tan and co-workers reported asymmetric protonation of *tert*-butyl 2-phthalimidoacrylate with thiols and N-(2,4,6-trimethylphenyl)itaconimide with secondary phosphine oxides (Scheme 1.9).^[18]



Scheme 1.9 Organocatalytic protonation with chiral guanidine derived catalyst

1.2.1.4 SOMO Organocatalysis



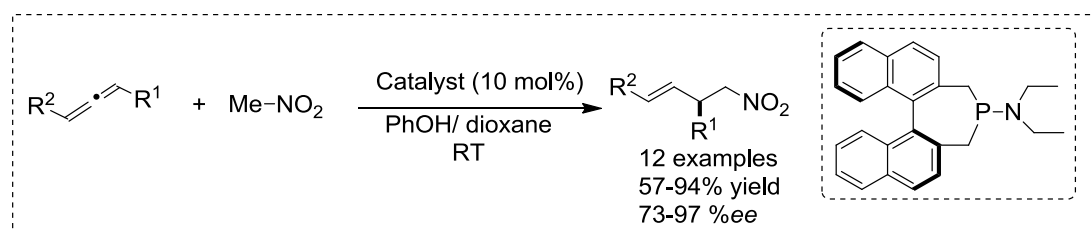
Scheme 1.10 SOMO organocatalysis with chiral benzyl-substituted imidazolidinone

In 2012, MacMillan and co-workers reported a rapid generation of pyrrolidines through SOMO-activated enantioselective [3+2] coupling of aldehydes and conjugated olefins in the presence of benzyl-substituted imidazolidinones (Scheme 1.10).^[19]

1.2.2 Non-Amine Lewis Base Catalysts: Phosphine and NHC Organocatalysis

1.2.2.1 Phosphine Organocatalysis

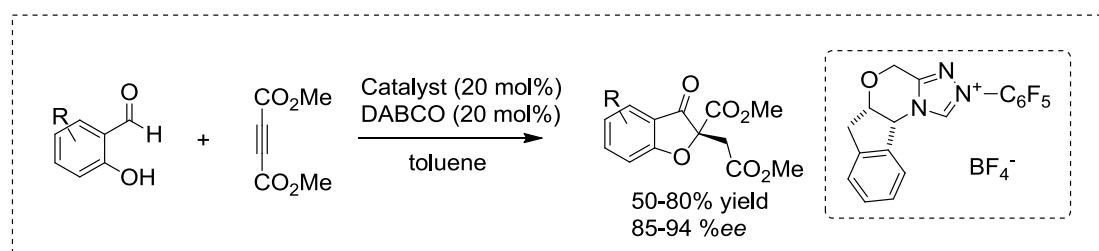
A class of phosphine-catalyzed asymmetric carbon-carbon bond formations at the γ -position of carbonyl compounds has been developed.^[20a] Particularly, in 2009, Fu and co-workers reported the phosphine-catalyzed additions of nitromethane to allenes with good to excellent yield (57-94%) and highly enantioselective products (73-97 %*ee*; Scheme 1.11).^[20b]



Scheme 1.11 Phosphine-catalyzed addition with chiral phosphine

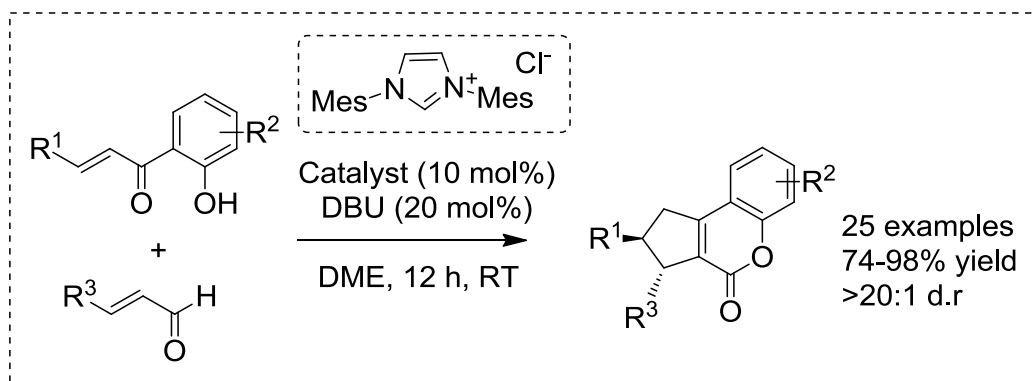
1.2.2.2 NHC Organocatalysis

N-Heterocyclic carbene (NHC) organocatalysis offers unique transformations in an umpolung way.^[21] Particularly, Rovis and co-workers reported the development of a multi-catalysis, one-pot, asymmetric Michael / Stetter reaction with salicylaldehydes and electron-deficient alkynes to give good yield (50-80%) and good to excellent enantioselectivity in products (85-94 %*ee*; Scheme 1.12).^[22]



Scheme 1.12 NHC-catalyzed Michael / Stetter reaction

Furthermore, Biju and co-workers reported a NHC-catalyzed annulation of enal with 2'-hydroxychalcones to afford cyclopentane-fused coumarin compounds in good to excellent yield (74-98%) and excellent level of diastereocontrol (d.r. >20:1; Scheme 1.13).^[23]

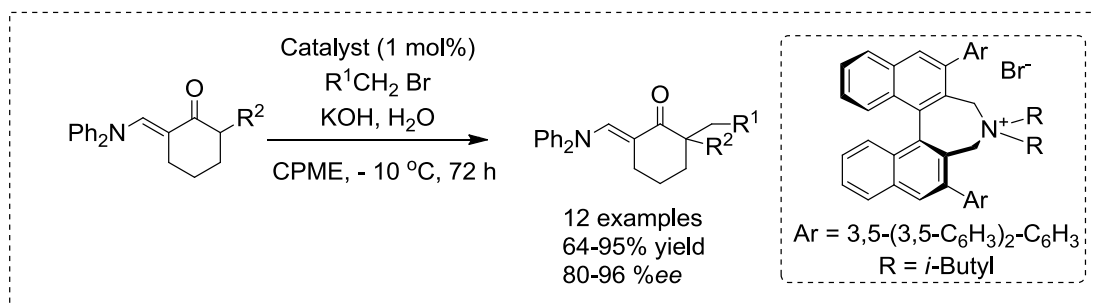


Scheme 1.13 NHC-catalyzed annulation

1.2.3 Ion-Pairing Catalysis

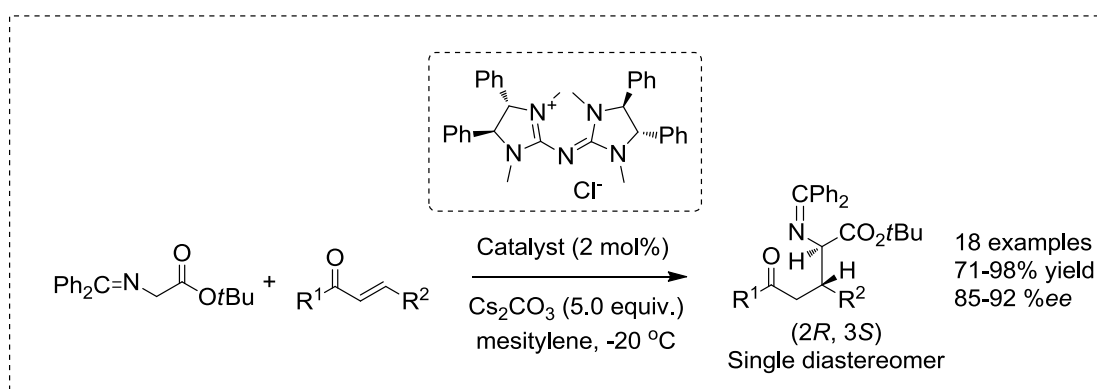
1.2.3.1 Cation-Binding Catalysts: Phase-Transfer Catalysis^[7,8]

Phase-transfer catalysis has been recognized as a versatile methodology for organic transformations in both industrial and academic areas.^[24] In 2013, Maruoka and co-workers reported an asymmetric alkylation of modified 2-arylcyhexanones catalyzed by a novel ammonium bromide as phase-transfer catalyst to give good to excellent yield (64-95%) and highly enantioselective products (80-96 %*ee*; Scheme 1.14).^[25]

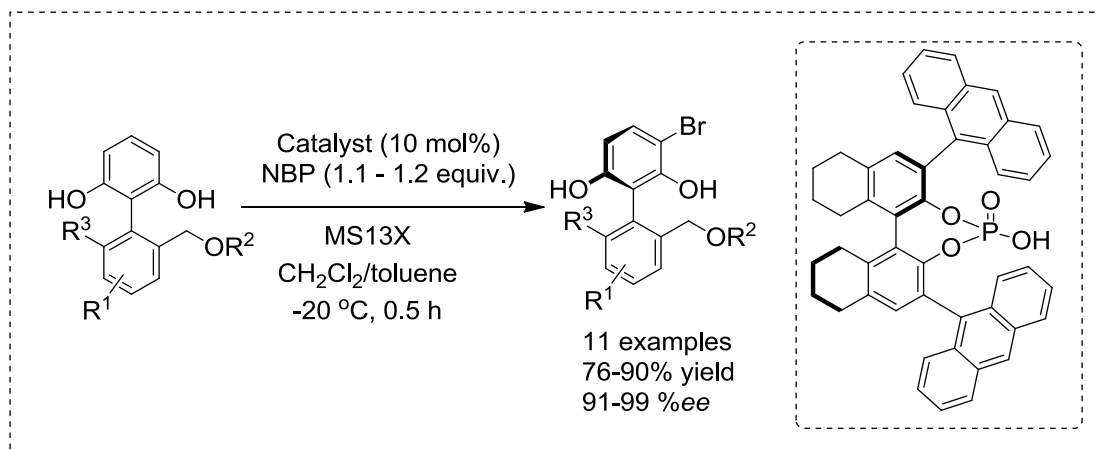


Scheme 1.14 Chiral ammonium bromide phase-transfer catalyst in catalyzing alkylation of modified 2-arylcyclohexanones

Furthermore, a novel pentanidium-based phase-transfer catalyst was developed by Tan's group. The Michael additions of *tert*-butyl glycinate-benzophenone Schiff base with various α,β -unsaturated compounds were catalyzed by pentanidium-based phase-transfer catalyst to provide adducts with high enantioselectivities (82-92 %ee; Scheme 1.15).^[26]



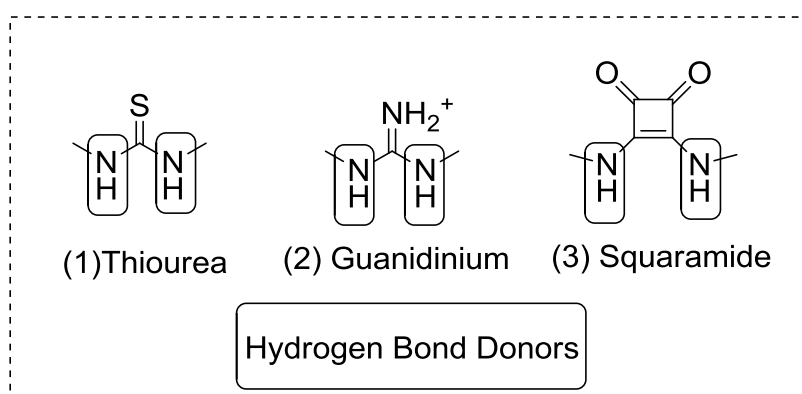
Scheme 1.15 Chiral pentanidium based phase-transfer catalyst in catalyzing the Michael addition



Scheme 1.17 Chiral phosphoric acid in catalyzing the asymmetric bromination

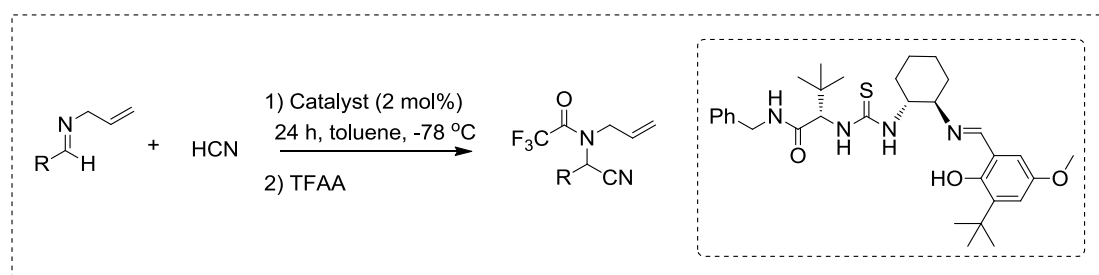
1.2.4 Hydrogen-Bonding Catalysis

Hydrogen bonding organocatalysis is one of the activation modes in which substrate binding and activation are solely achieved through multiple and concerted non-covalent interactions.^[29] In brief, dual-hydrogen bond donor or hydrogen bond donor-donor (DD) has been reported in three major catalyst types: (1) thiourea, (2) guanidinium, and (3) squaramide.



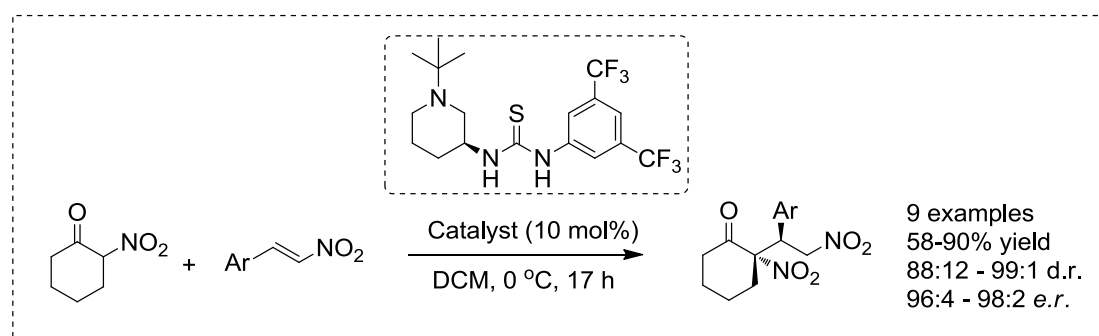
1.2.4.1 Hydrogen-Bonding Donor-Donor (DD) Catalysis - Thiourea

In 1998, Jacobsen and co-workers developed Schiff base-hydrogen bonding catalyst to enhance the rate of asymmetric Strecker reactions and to give high yield (65-92%) and good enantioselective products (up to 91% *ee*; Scheme 1.18).^[30]

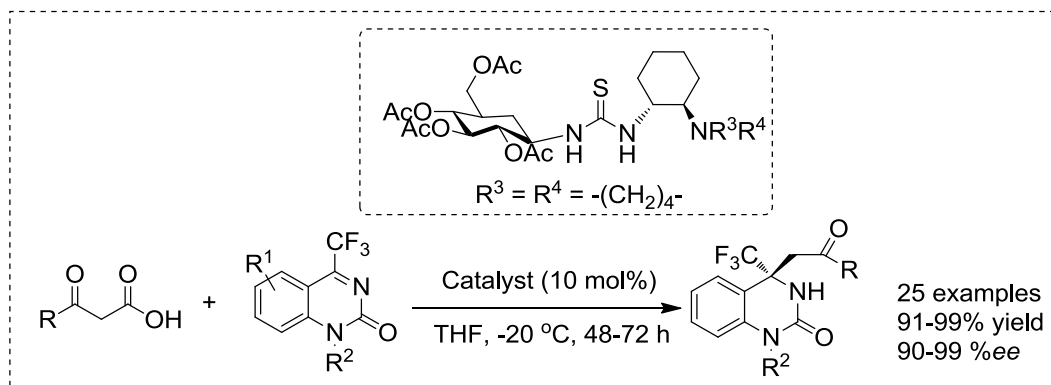


Scheme 1.18 Schiff-base hydrogen-bonding catalyst in catalyzing the Strecker reaction

Furthermore, Bolm and co-workers reported asymmetric Michael additions of α -nitrocyclohexanone to aryl nitroalkenes catalyzed by natural amino acid-derived bifunctional thiourea (Scheme 1.19).^[31]



Scheme 1.19 Amino acid-derived bifunctional thiourea in catalyzing the Michael addition

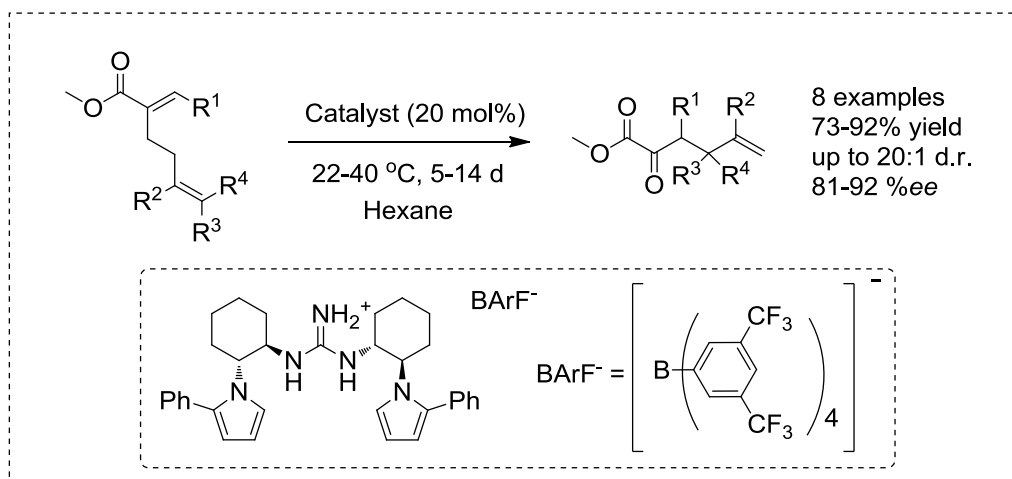


Scheme 1.20 Saccharide-derived organocatalyst in catalyzing the Mannich addition

In 2013, Ma and co-workers developed a hydrogen-bond directed enantioselective decarboxylative Mannich reaction of β -ketoacids with ketamines in order to synthesize anti-HIV drug DPC 083 (Scheme 1.20).^[32]

1.2.4.2 Hydrogen-Bonding Donor-Donor (DD) Catalysis - Guanidinium

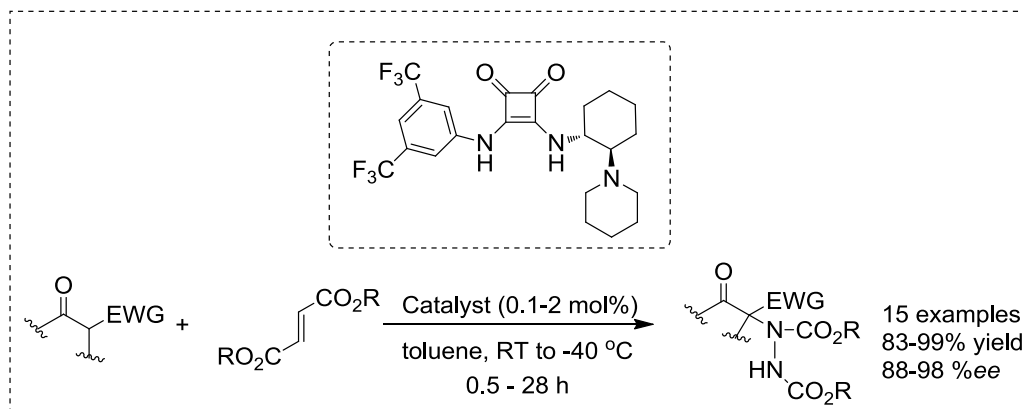
Guanidinium is the conjugated acid of guanidine.^[16, 33] In 2008, Jacobsen and co-workers reported enantioselective Claisen rearrangements with hydrogen bond donor catalysts to give good to excellent yield (73-92%) and enantioselective products (up to 92 %*ee*; Scheme 1.21).^[34]



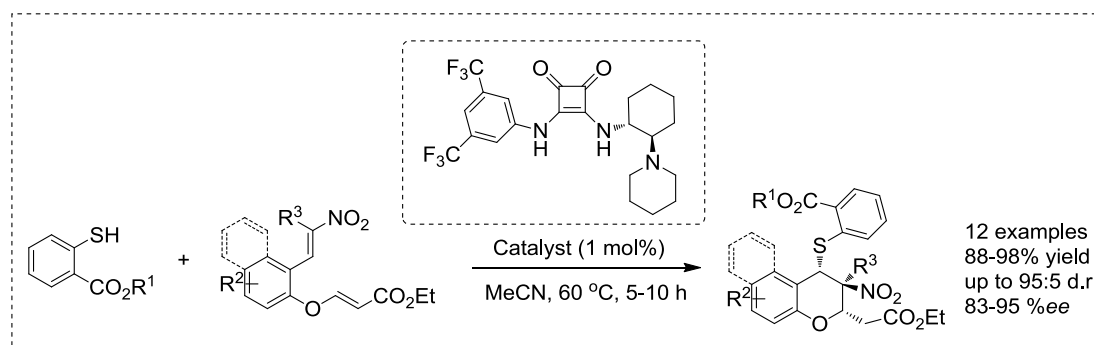
Scheme 1.21 Guanidinium BArF⁻ catalyst in catalyzing the Claisen rearrangement

1.2.4.3 Hydrogen-Bonding Donor-Donor (DD) Catalysis - Squaramide^[35]

In 2010, Rawal and co-workers developed the enantioselective α -amination of 1,3-dicarbonyl compounds using squaramide-derived hydrogen bonding catalysts to give good to excellent yield (83-99%) and to afford excellent enantioselective products (88-98 %ee; Scheme 1.22).^[36] In 2013, Du and co-workers reported asymmetric cascade sulfa-Michael / Michael addition through dynamic kinetic resolution catalyzed by squaramide-tertiary amine (Scheme 1.23).^[37]



Scheme 1.22 Squaramide derived hydrogen bonding catalysts in catalyzing the α -amination



Scheme 1.23 Squaramide-tertiary amine catalyst in catalyzing the sulfa-Michael/
Michael addition

1.3 Hydrogen-Bonding Donor-Acceptor-Donor (HB-DAD) Catalysis

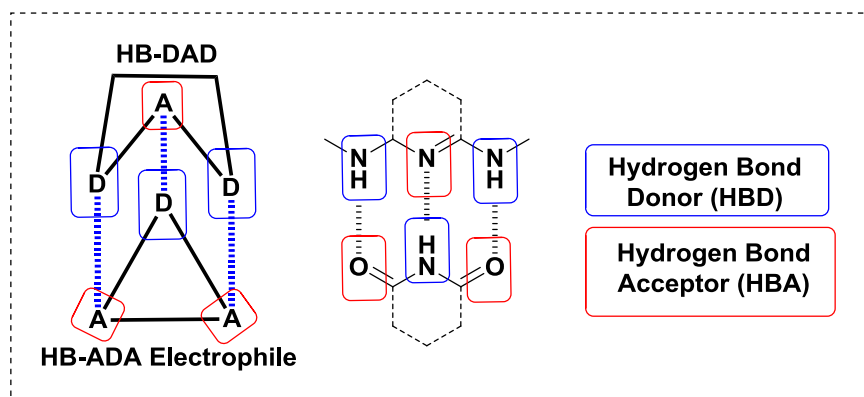


Figure 1.1 Structure of HB-DAD catalysts and HB-ADA electrophiles

Hydrogen bonding donor-donor organocatalysis has largely been developed as efficient catalysts to achieve synthetic transformations. However, other modes of hydrogen bonding catalysis remain largely unexplored.

HB-DAD and HB-ADA systems are common in supramolecular chemistry, mainly acting as supramolecular linking units in non-covalent polymer assembly.^[38] This class of hydrogen bonding system is of high utility in various applications in materials science because it is highly directional. In addition, the three complementary hydrogen bondings are strong binding array.^[39]

We envision that this highly directional and strong complementary HB-DAD and HB-ADA systems could be developed as a new and efficient activation mode of hydrogen bonding organocatalysis.

1.4 The Objectives and Achievement of the Thesis

The objective of this project is to develop efficient methods for catalytic conjugate addition by HB-DAD organocatalysts. Amide-based HB-DAD organocatalysts were chosen as the catalyst, and HB-ADA benzylidene barbiturates were used as the electrophile. The catalytic conjugate addition of HB-ADA benzylidene barbiturates was achieved by complementary binding mode of DAD-ADA. As a result, the HB-ADA benzylidene barbiturates would give desired products with enhanced reaction rate.

This work focuses on (1) the design and synthesis of efficient HB-DAD organocatalysts for conjugate addition of various HB-ADA benzylidene barbiturates, (2) the investigations of kinetics and binding of the amide-based HB-DAD organocatalysts, and (3) the investigation of C_2 symmetric chiral HB-DAD organocatalysts on asymmetric conjugate addition.

1.5 References

- (1) Berkessel, A.; Groeger, H. *Asymmetric Organocatalysis: from Biomimetic Concepts to Applications in Asymmetric Synthesis*; University Science Books: Mill Valley, CA, 2005.
- (2) Hegedus, L.S. *J. Am. Chem. Soc.* **2009**, *131*, 177995-17997.
- (3) MacMillan, D. W. C. *Nature* **2008**, *455*, 304-308.
- (4) List, B. *Chem. Rev.* **2007**, *107*, 5413-5415.
- (5) List B.; Yang, J. W. *Science* **2006**, *313*, 1584-1586.
- (6) Jacobsen, E. N.; MacMillan, D. W. C. *Proc. Natl. Acad. Sci. USA* **2010**, *107*, 20618-20619.
- (7) Brak, K.; Jacobsen, E. N. *Angew. Chem. Int. Ed.* **2013**, *52*, 534-561.
- (8) Mahlau, M.; List, B. *Angew. Chem. Int. Ed.* **2013**, *52*, 518-533.
- (9) Melchiorre, P.*; Marigo, M.*; Carlone, A.; Bartoli, G. *Angew. Chem. Int. Ed.* **2008**, *47*, 6138-6171.
- (10) a) Ahrendt, K. A.; Borths, C. J.; MacMillan, D. W. C. *J. Am. Chem. Soc.* **2000**, *122*, 4243-4244. b) Jen, W. S.; Wiener, J. J. M.; MacMillan, D. W. C. *J. Am. Chem. Soc.* **2000**, *122*, 9874-9875. c) Paras, N. A.; MacMillan, D. W. C. *J. Am. Chem. Soc.* **2001**, *123*, 4370-4371.

- (11) Xie, J.W.; Chem, W.; Li, R.; Zeng, M.; Du, W.; Yue, L.; Chen, Y. C.; Wu, Y.; Zhu, J.; Deng, J. G. *Angew. Chem. Int. Ed.* **2007**, *46*, 389-392.
- (12) a) Melchiorre, P. *Angew. Chem. Int. Ed.* **2012**, *51*, 9748-9770. b) MacCooney, S. H.; Connon, S. J. *Org. Lett.* **2007**, *9*, 599-602.
- (13) Kano, T.; Shirozu, F.; Akakura, M.; Maruoka, K. *J. Am. Chem. Soc.* **2012**, *134*, 16068-16073.
- (14) Albrecht, Ł.; Dickmeiss, G.; Acosta, F. C.; Rodríguez-Escrih, C.; Davis, R. L.; Jørgensen K. A. *J. Am. Chem. Soc.* **2012**, *134*, 2543-2546.
- (15) Halskov, K. S.; Johansen, T. K.; Davis, R. L.; Steurer, M.; Jensen, F.; Jørgensen K. A. *J. Am. Chem. Soc.* **2012**, *134*, 12943-12946.
- (16) For recent reviews of Guanidines and Guanidinium organocatalysis: (a) Fu, X.; Tan, C. H. *Chem. Commun.* **2011**, *47*, 8210-8222. b) Leow, D.; Tan, C. H. *Synlett* **2010**, *11*, 1589-1605. c) Leow, D.; Tan, C. H. *Chem. Asian. J.* **2009**, *4*, 488-507. d) Shen, J.; Tan, C. H. *Org. Biomol. Chem.* **2007**, *6*, 3229-3236.
- (17) Jiang, Z.; Pan, Y.; Zhao, Y.; Lee, T. M. R.; Yang, Y.; Huanh, K. W.; Wong, M. W.; Tan, C. H. *Angew. Chem. Int. Ed.* **2009**, *48*, 3627-3631.
- (18) Leow, D.; Lin, S.; Chittmalla, S. K.; Fu, X.; Tan, C. H. *Angew. Chem. Int. Ed.* **2008**, *47*, 5641-5645.
- (19) Jui, N. T.; Garber, J. A. O.; Finelli, F. G.; MacMillan, D. W. C. *J. Am. Chem. Soc.*

2012, *134*, 11400-11403.

- (20) a) Sinisi, R.; Sun, J.; Fu, G. C. *Proc. Natl. Acad. Sci. USA* **2010**, *107*, 20652-20654. b) Smith, S. W.; Fu, G. C. *J. Am. Chem. Soc.* **2009**, *135*, 14231-14233.
- (21) For reviews of NHC: a) Ender, D.; Niemeier, O.; Henseler, A. *Chem. Rev.* **2007**, *107*, 5606-5655. b) Grossmann, A.; Ender, D. *Angew. Chem. Int. Ed.* **2012**, *51*, 314-325. c) Biju, A. T.; Kuhl, N.; Glorius, F. *Acc. Chem. Res.* **2011**, *44*, 1182-1195.
- (22) Filloux, C. M.; Lathrop, S. P.; Rovis, T. *Proc. Natl. Acad. Sci. USA* **2010**, *107*, 20666-20671.
- (23) Bhunia, A.; Patra, A.; Puranik, V. G.; Biju, A. T. *Org. Lett.* **2013**, *15*, 1756-1759.
- (24) For recent reviews of PTC: a) Shirakawa, S.; Maruoka, K. *Angew. Chem. Int. Ed.* **2013**, *52*, 4312-4348. b) Maruoka, K. *Chem. Rec.* **2010**, *10*, 254-257.
- (25) Kano, T.; Hayashi, Y.; Maruoka, K. *J. Am. Chem. Soc.* **2013**, *135*, 7134-7137.
- (26) Ma, T.; Fu, X.; Kee, C. W.; Zong, L.; Pan, Y.; Huang, K. W.; Tan, C. H. *J. Am. Chem. Soc.* **2011**, *133*, 2828-2831.
- (27) Liao, S.; Čorić, I.; Wang, Q.; List, B. *J. Am. Chem. Soc.* **2012**, *134*, 10765-10768.
- (28) Mori, K.; Ichikawa, Y.; Kobayashi, M.; Shibata, Y.; Yamanaka, M.; Akiyama, T. *J. Am. Chem. Soc.* **2013**, *135*, 3964-3970.

- (29) For reviews of hydrogen bonding catalysis: a) Zhang, Z.; Schreiner, P. R. *Chem. Soc. Rev.* **2009**, *38*, 1187-1198. b) Yu, X.; Wang, W. *Chem.-Asian J.* **2008**, *3*, 516-532. c) Doyle, A. G.; Jacobsen, E. N. *Chem. Rev.* **2007**, *107*, 5713-5743. d) Connon, S. J. *Chem.-Eur. J.* **2006**, *12*, 5418-5427. e) Taylor, M. S.; Jacobsen, E. N. *Angew. Chem. Int. Ed.* **2006**, *45*, 1520-1543. f) Takemoto, Y. *Org. Biomol. Chem.* **2005**, *3*, 4299-4306. g) Schreiner, P. R. *Chem. Soc. Rev.* **2003**, *32*, 289-296.
- (30) Sigman, M. S.; Jacobsen, E. N. *J. Am. Chem. Soc.* **1998**, *120*, 4901-4902.
- (31) Jörres, M.; Schiffers, I.; Atodiresei, I.; Bolm, C. *Org. Lett.* **2012**, *14*, 4518-4521.
- (32) Yuan, H. N.; Wang, S.; Nie, J.; Meng, W.; Yao, Q.; Ma, J. A. *Angew. Chem. Int. Ed.* **2013**, *52*, 3869-3873.
- (33) Coles, M. P. *Chem. Commun.* **2009**, *45*, 3659-3676.
- (34) Uyeda, C.; Jacobsen, E. N. *J. Am. Chem. Soc.* **2008**, *130*, 9228-9229.
- (35) For reviews of Squaramides: a) Storer, R. I.; Aciro, C.; Jones, L. H. *Chem. Soc. Rev.* **2011**, *40*, 2330-2346. b) Alemán, J.; Parra, A.; Jiang, H.; Jørgensen, K. A. *Chem.-Eur. J.* **2011**, *17*, 6890-6899.
- (36) Konishi, H.; Lam, T. Y.; Malerich, J. P.; Rawal, V. H. *Org. Lett.* **2010**, *12*, 2028-2031.
- (37) Yang, W.; Yang, Y.; Du, D. M. *Org. Lett.* **2013**, *15*, 1190-1193.

- (38) a) Seiffert, S.; Sprakel, J. *Chem. Soc. Rev.* **2012**, *41*, 909-930. b) Nair, K. P.; Breedveld, V.; Weck, M. *Macromoleculae* **2008**, *41*, 3429-3438. c) Nair, K. P.; Breedveld, V.; Weck, M. *Soft Matter* **2011**, *7*, 533-559. d) Herbst, F.; Schroeter, K.; Gunkel, I.; Groeger, S.; Thurn-Albrecht, T.; Balbach, J.; Binder, W. H. *Macromoleculae* **2010**, *43*, 10006-10016.
- (39) a) Beijer, F. H.; Kooijman, H.; Spek, A. L.; Sijbesma, R. P.; Meijer, E. W. *Angew. Chem. Int. Ed.* **1998**, *37*, 75-78. b) Jorgensen, W. L.; Pranata, J. *J. Am. Chem. Soc.* **1990**, *112*, 2008-2010. c) Pranta, J.; Wierschke, S. G.; Jorgensen, W. L. *J. Am. Chem. Soc.* **1991**, *113*, 2810-2819. d) Sartorius, J.; Schneider, H. J. *Chem. Eur. J.* **1996**, *2*, 1446-1452. e) Ducharme, Y.; Wuest, J. D. *J. Org. Chem.* **1988**, *53*, 5787-5789.

Chapter 2

Design and Synthesis of Hydrogen Bond

Donor-Acceptor-Donor Organocatalysts

2.1 Introduction

2.1.1 Design of HB-DAD Organocatalysts

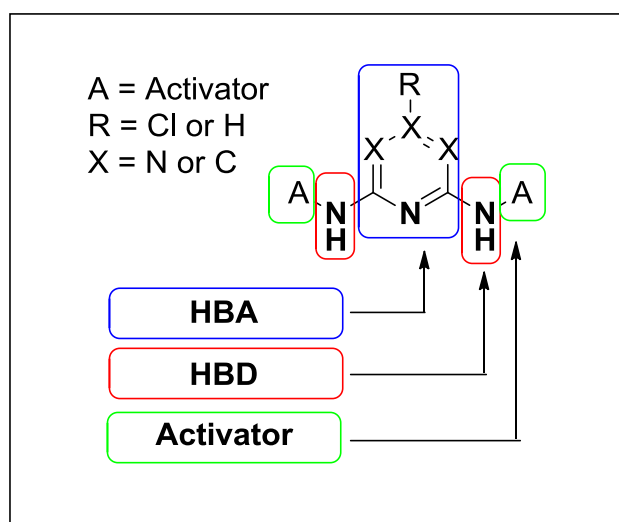


Figure 2.1 Design of HB-DAD organocatalysts containing (1) HBA, (2) HBD, and (3) Activator

HB-DAD organocatalysts consisting of three components (1) Hydrogen bond acceptor (HBA), (2) Hydrogen bond donor (HBD), and (3) Activator (A) were designed (Figure 2.1).

HBA is an N-heterocyclic aromatic ring. A variety of N-heterocyclic aromatic

rings were selected, e.g. pyridine, pyrazine, chloro-pyrimidine and chloro-triazine.

The nitrogen lone-pair of HBA could contribute to the tunable electrophilicity of HB-DAD organocatalysts and function as an acceptor in hydrogen bonding with the substrates.^[1]

Nitrogen-hydrogen (N-H bond), one of the most electronegative hydrogen bonds, was chosen as HBD in our design.^[2] In addition, the amine group acted as a linker to connect the HBA and the activator.

Activator is an electron withdrawing group to adjust the electrophilicity of the N-H bond. For example, the acyl group of amide could increase the acidity of the N-H bond.

2.1.2 The Objectives of This Chapter

We set out to design and synthesize a series of HB-DAD organocatalysts with different combinations of HBA, HBD, and activators. We also plan to identify key structural elements that facilitate the catalytic conjugate addition.

Amide-based HB-DAD organocatalysts **2a**,^[3] **2b**,^[4] **2c**,^[5] **2d**^[6] and **2e**^[7] were synthesized and characterized according to literature reports (Scheme 2.1). New HB-DAD organocatalysts **1a** was prepared with 58% isolated yield by amide coupling of 2,6-diamino-4-chloropyrimidine (1 mmol) and trifluoroacetic anhydride (3 mmol). In addition, the molecular structure of **1a** was revealed by X-ray crystallography (Figure 2.2). HB-DAD organocatalyst **3a** was prepared in 68% isolated yield by reaction of 2,6-diaminopyrazine (1 mmol) and trifluoroacetic anhydride (3 mmol).

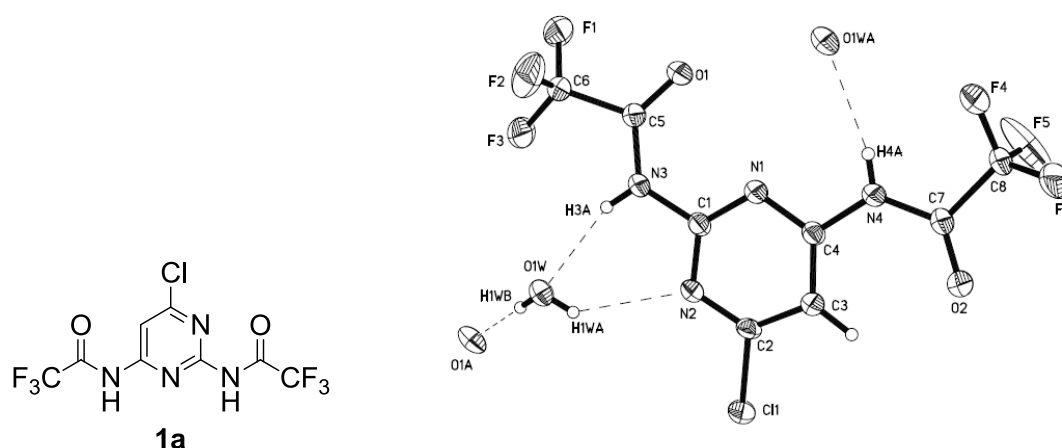
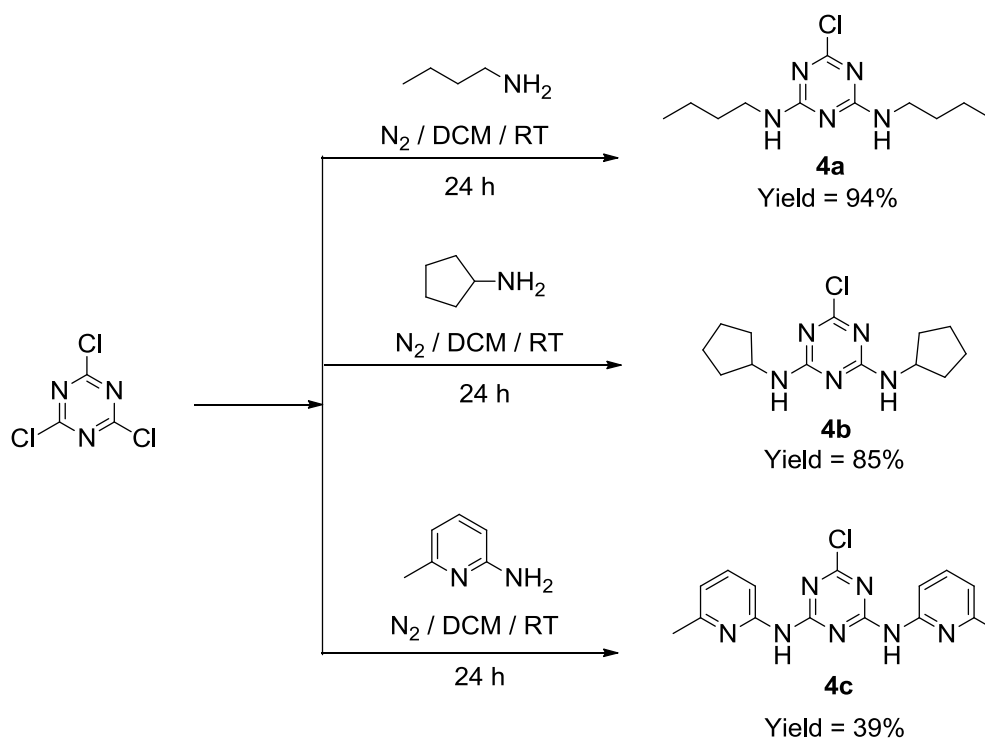


Figure 2.2 X-ray crystallographic structure of **1a**

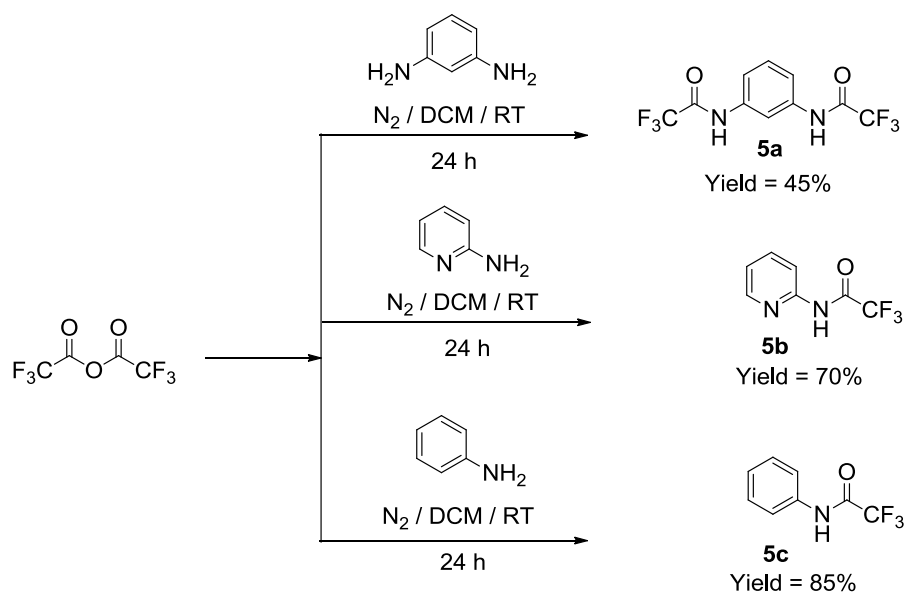
HB-DAD organocatalysts **1b** bearing hexanoyl-group as well as **1c** and **3c** bearing pivaloyl-group were prepared by treatment of acid chloride (2.5 mmol) with 2,6-diamino-4-chloropyrimidine (1 mmol) and 2,6-diamino-pyrazine (1 mmol) respectively. As a result, **1c** and **2c** were obtained in 62% isolated yield.

Amine-based HB-DAD organocatalysts **4a**,^[8] **4b**^[9] and **4c**^[8] were synthesized and characterized according to literature reports (Scheme 2.2).



Scheme 2.2 Synthesis of amine-based HB-DAD organocatalysts

Amide-based hydrogen bonding organocatalysts **5a**, **5b** and **5c** were prepared by condensation of aryl-amines (1 mmol) and trifluoroacetic anhydride (3 mmol). Then, **5a-5c** were obtained in 45-85% isolated yield (Scheme 2.3).^[10, 11]

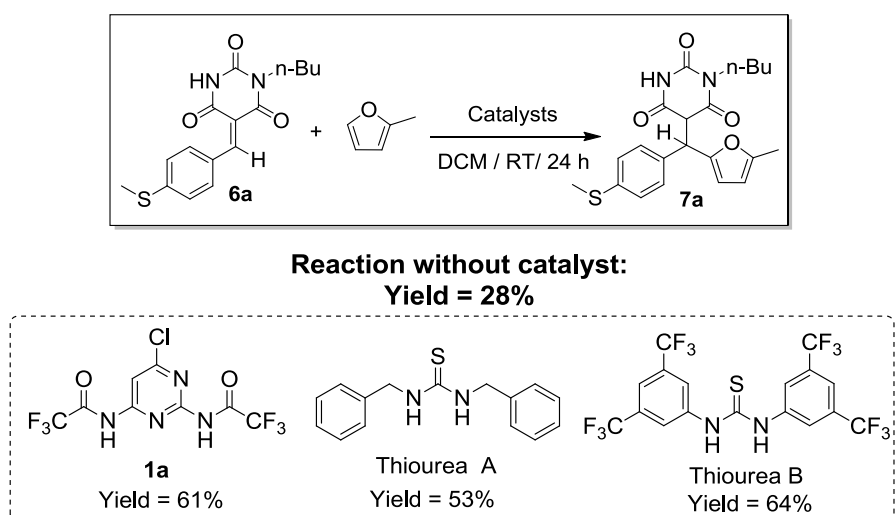


Scheme 2.3 Synthesis of amide-based hydrogen bonding organocatalysts

2.2.2 Studies on Catalytic Conjugate Addition of Benzylidene Barbiturates

A mixture of benzylidene barbiturate **6a** (0.05 mmol), 2-methylfuran (0.05 mmol) and HB-DAD organocatalyst **1a** (0.01 mmol) in dichloromethane was stirred at room temperature for 24 h. The yield of reaction adduct **7a** was monitored by ^1H NMR with toluene as internal standard (Scheme 2.4). Adduct **7a** was obtained with 61% yield. Yet, **7a** was obtained in 28% yield in the absence of HB-DAD organocatalyst **1a** (background reaction).

Thioureas are efficient hydrogen bond donor organocatalysts.^[12,13] As a control, Thiourea A and Thiourea B were found to give adduct **7a** in 53% and 64% yield, respectively (Scheme 2.4) that were comparable to that using **1a**. In this connection, we are pleased to find that *the newly developed HB-DAD organocatalyst 1a exhibited comparable catalytic activity to the commonly used Thiourea A and Thiourea B.*



Scheme 2.4 Hydrogen bonding organocatalysts reactivity studies in conjugate addition of **6a**

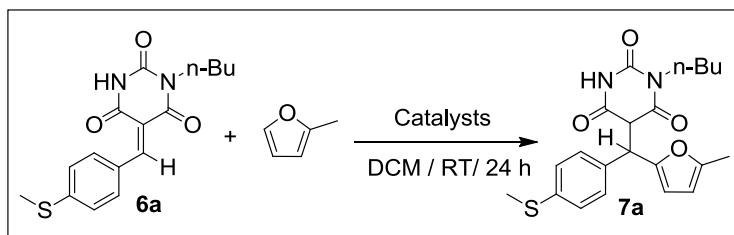
Studies on the catalytic activities of 20 mol% of **1a**, **1b** and **1c** with chloro-pyrimidine as the HBA in the conjugate addition of benzylidene barbiturate **6a** (0.05 mmol) and 2-methylfuran (0.05 mmol) for adduct **7a** synthesis are depicted in Scheme 2.5.

Using HB-DAD organocatalyst **1a** with trifluoroacetyl-group as the activator, adduct **7a** was obtained in 61% yield at 20 °C in 24 h. Yet, 40% yield of **7a** was obtained with **1b** (bearing hexanoyl-group as the activator). These results indicate that the electron withdrawing trifluoroacetyl-group is important to achieve high catalytic activity.^[14]

HB-DAD organocatalyst **1c** with pivaloyl-group as the activator exhibited poor catalytic activity. Using **1c**, only gave 28% yield of **7a** that is comparable to yield of **7a** in the absence of catalyst. These findings indicate that the steric effect of pivaloyl-group led to poor catalytic activity in the reaction.

The catalytic activities of **2a**, **2b** and **2c** with pyridine as the HBA in the conjugate addition of **6a** and 2-methylfuran were also studied. Using **2a**, adduct **7a** was obtained in 49% yield. The reaction using **2b** gave 44% yield while using **2c** could give 28% yield of **7a**. These results indicate that using chloro-pyrimidine as the HBA afforded higher catalytic activity than that of using pyridine as the HBA.

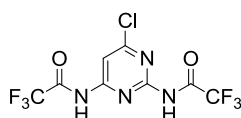
Sulfonamides and phosphoramides are effective hydrogen bond donor organocatalysts.^[15] The catalytic activities of **2d** and **2e** in the conjugate addition of **6a** and 2-methylfuran were studied. Using **2d** bearing sulfonyl group as the activator gave 63% yield while using **2e** bearing phosphinic group as the activator led to 28% yield of **7a**. Our results revealed that the HB-DAD organocatalyst **1a** afforded comparable catalytic activity to the effective sulfonamide-based hydrogen bond donor organocatalyst **2d**.



Reaction without catalyst:
Yield = 28%

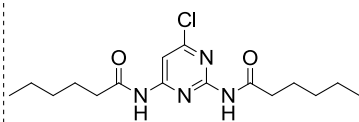
Organocatalysts

Chloro-Pyrimidine HBA



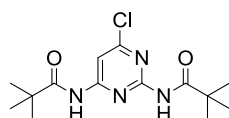
1a

Yield = 61%



1b

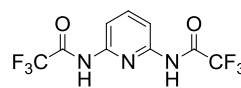
Yield = 40%



1c

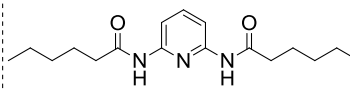
Yield = 28%

Pyridine HBA



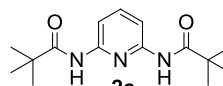
2a

Yield = 49%



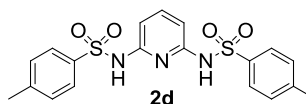
2b

Yield = 44%



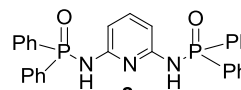
2c

Yield = 28%



2d

Yield = 63%



2e

Yield = 28%

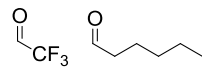
HBA:



HBD:



Activator:



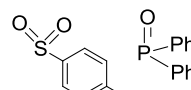
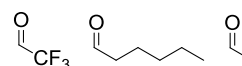
HBA:



HBD:

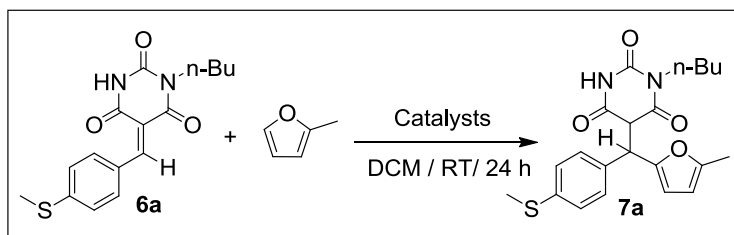


Activator:

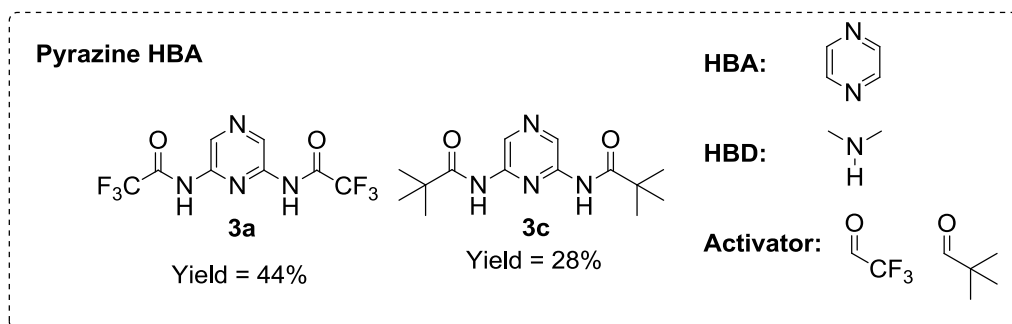


Scheme 2.5 HB-DAD organocatalysts reactivity studies in conjugate addition of **6a**

Studies on the catalytic activities of **3a** and **3c** with pyrazine as the HBA in the conjugate addition of benzylidene barbiturate **6a** (0.05 mmol) and 2-methylfuran (0.05 mmol) for adduct **7a** synthesis are depicted in Scheme 2.6. Using 20 mol% of HB-DAD organocatalyst **3a** with trifluoroacetyl group as the activator, adduct **7a** was obtained in 44% yield at 20 °C in 24 h. For the reaction using 20 mol% of **3c**, adduct **7a** was obtained only in 28% yield. In this regard, the chloro-pyrimidine is a better HBA than pyrazine.

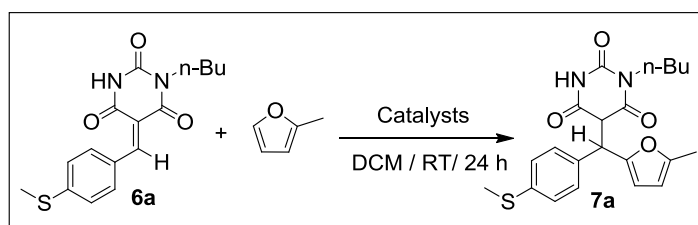


**Reaction without catalyst:
Yield = 28%**

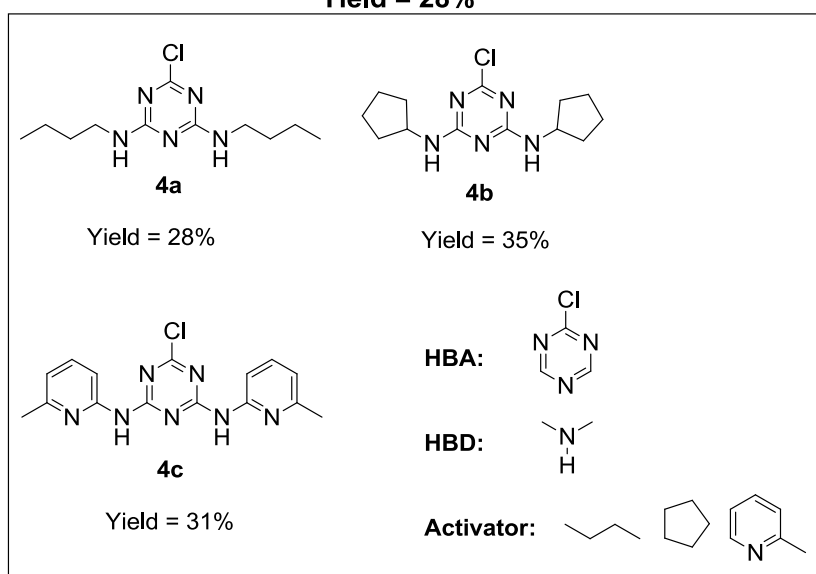


Scheme 2.6 HB-DAD organocatalysts reactivity studies in conjugate addition of **6a**

To investigate the catalytic activities of **4a**, **4b** and **4c** in the conjugate addition of **6a** and 2-methylfuran for adduct **7a** synthesis is depicted in Scheme 2.7. The reaction using **4a** and **4b** bearing alkyl-groups as the activator, adduct **7a** were obtained in 28% and 35% yield, respectively (Scheme 2.7). Using **4c** bearing aryl-group as activator, 31% yield of adduct **7a** was obtained. These results indicate that electron withdrawing acyl groups are better activators than amine groups.



Reaction without catalyst:
Yield = 28%



Scheme 2.7 HB-DAD organocatalysts reactivity studies in conjugate addition of **6a**

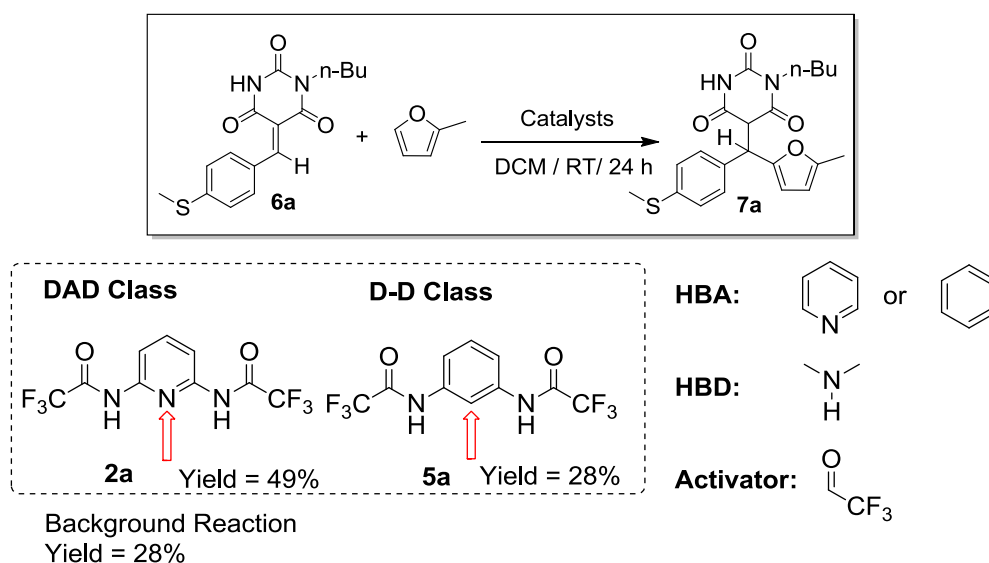
Our results revealed that HB-DAD organocatalysts **1a**, **1b**, **2a**, **2c**, **2d** and **3a** could catalyze the conjugate addition of **6a** with 2-methylfuran. Note that, **1a** was chosen for further studies in the substrate scope of the conjugate addition in chapter 3.

2.2.3 Binding Mode Study

2.2.3.1 Binding Mode Study - HB-DAD Organocatalysts Modifications

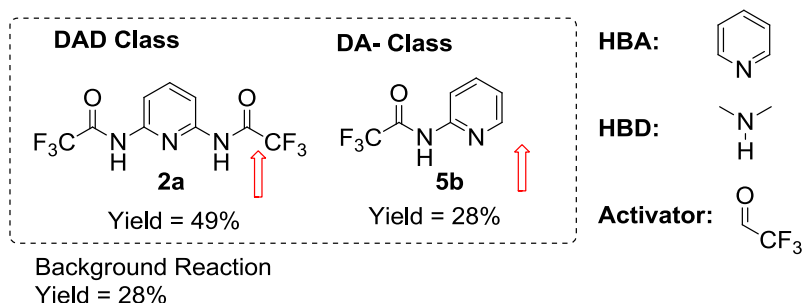
With reference to the catalytic effect of **2a**, the binding mode studies on the catalytic activity of hydrogen bonding organocatalysts D-D class **5a**, DA- class **5b** and D-- class **5c** in the conjugate addition of benzylidene barbiturate **6a** (0.05 mmol) and 2-methylfuran (0.05mmol) are depicted in Scheme 2.8. Using 20 mol% of **5a**, adduct **7a** was obtained in 28% yield that is comparable to the yield obtained in the absence of catalyst. Notably, the reaction using **2a** gave adduct **7a** in 49% yield.

The significantly higher catalytic activity of DAD class **2a** than D-D class **5a** could be attributed to their structural difference in HBA motifs. **2a** has a nitrogen lone-pair, yet **5a** bears a C-H bond. The nitrogen lone-pair of **2a** could form hydrogen bond to HBD (N-H) in **6a**, but the C-H bond of **5a** could not form.



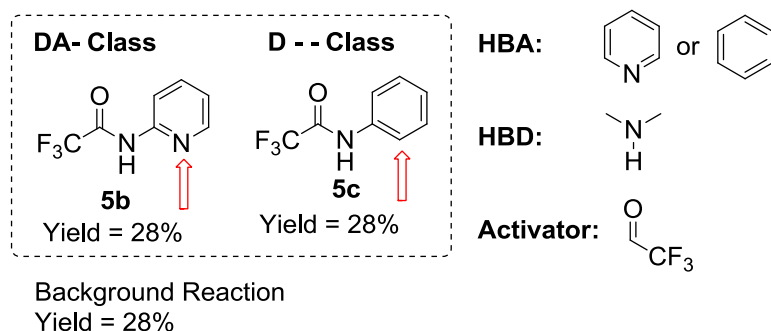
Scheme 2.8 **2a** and **5a** in catalyzing conjugate addition of **6a**

For the reaction using DA- class **5b**, adduct **7a** was obtained in 28% yield (Scheme 2.9) while using DAD class **2a** gave 49% yield. The higher catalytic activity of **2a** than **5b** was observed probably due to their structural difference on HBD and activator motifs. **2a** bears two trifluoroacetamide groups, yet **5a** only has one trifluoroacetamide group. Thus, the two HBDs in the DAD class catalysts are essential to give catalytic effect in the reaction of **6a**.



Scheme 2.9 **2a** and **5b** in catalyzing conjugate addition of **6a**

For the reaction using D-- class **5c**, adduct **7a** was obtained in 28% yield (Scheme 2.10) while using DA- class **5b** gave 28% yield. These results indicate that both HBD and HBA in the DAD class are also important to afford catalytic activity in the reaction.



Scheme 2.10 **5b** and **5c** in catalyzing conjugate addition of **6a**

Our results revealed that the HBA, HBD and activator in the structure of **2a** has significant effect on conjugate addition of HB-ADA benzylidene barbiturate **6a**.

2.3 Conclusion

We have identified that HB-DAD organocatalyst **1a** featuring (1) chloro-pyrimidine as HBA, (2) N-H as HBD, and (3) trifluoroacetyl group as activator is the most effective catalyst in catalyzing conjugate addition of benzylidene barbiturates. The DAD-ADA binding mode was found to be a crucial factor in catalyzing the conjugate addition.

2.4 Experimental Section

2.4.1 Experimental Procedure

Procedure for Catalytic Conjugate Additions of Benzylidene Barbiturates

A mixture of benzylidene barbiturates (0.05 mmol), 2-methylfuran (0.05 mmol) and amide-based HB-DAD organocatalyst (0.01 mmol), in DCM (1 mL) was stirred at RT (25 °C) for 24 h. The reaction mixture was concentrated. The product yield was determined by ¹H NMR with toluene (0.02 mmol) as internal standard.

*General Procedure for Synthesis of Amide-Based HB-DAD Organocatalysts **1a** and*

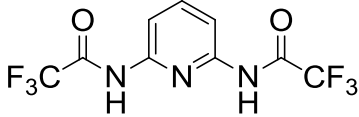
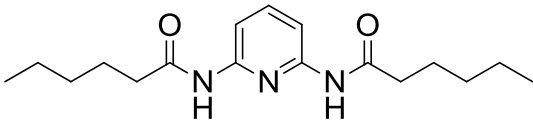
3a

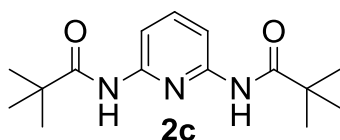
A mixture of 2,6-diamino-N-heterocyclic compounds (1 mmol) and trifluoroacetic anhydride (3 mmol) in DCM (10 mL) was stirred under nitrogen atmosphere at room temperature for 24 h. The reaction mixture was treated with water (5 mL), and extracted with ethyl acetate (3 × 10 mL). The combined organic layers were dried over anhydrous Na₂SO₄, filtered, and concentrated. The residue was purified by flash column chromatography on silica gel using ethyl acetate-hexane as eluent.

General Procedure for Synthesis of Amide-Based HB-DAD Organocatalysts 1b, 1c and 3c

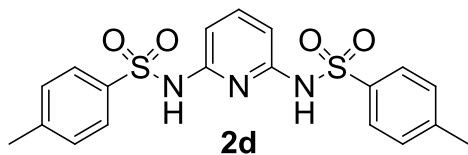
A mixture of 2,6-diamino-N-heterocyclic compounds (1 mmol), acid chloride (2.5 mmol), 4-dimethylaminopyridine (0.2 mmol) and triethylamine (2.5 mmol) in DCM (10 mL) was stirred under nitrogen atmosphere at room temperature for 24 h. The reaction mixture was treated with water (5 mL), and extracted with ethyl acetate (3 × 10 mL). The combined organic layers were dried over anhydrous Na₂SO₄, filtered, and concentrated. The residue was purified by flash column chromatography on silica gel using ethyl acetate-hexane as eluent.

2.4.2 Literature Reference of 2a-e, 4a-4c, 5a-5c and Thiourea B

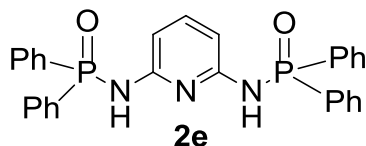
Compounds	Reference
 2a	<i>Angew. Chem. Int. Ed.</i> , 2009 , 48, 7440.
 2b	<i>Organometallics</i> , 2006 , 25, 1900.



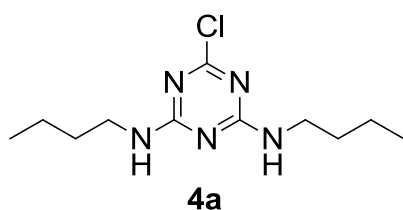
Eur. J. Org. Chem., **2009**, 4581.



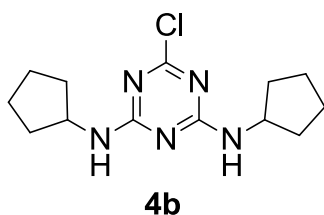
Chem. Commun., **1991**, 514.



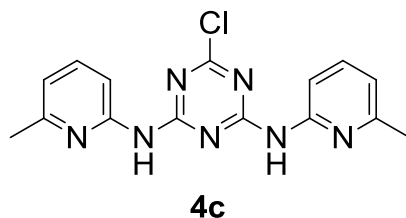
Mendeleev Communications, **2010**, 223.



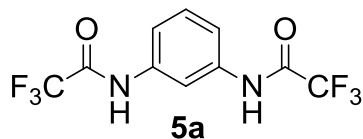
J. Am. Chem. Soc., **2001**, 123, 8914.



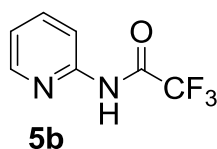
Journal of the Institution of Chemists (India), **1981**, 53, 141.



J. Am. Chem. Soc., **2001**, 123, 8914.



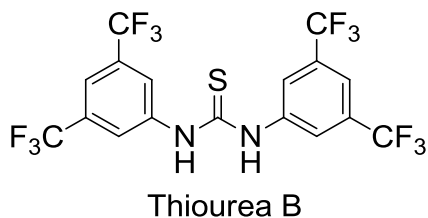
Eur. J. Org. Chem., **1998**, 1471.



Journal of Chemical and Engineering Data, **1981**, 234.

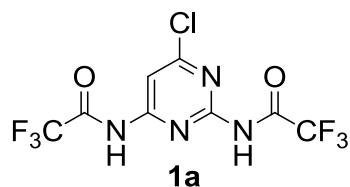


Angew. Chem. Int. Ed., **2007**, *46*, 1281.

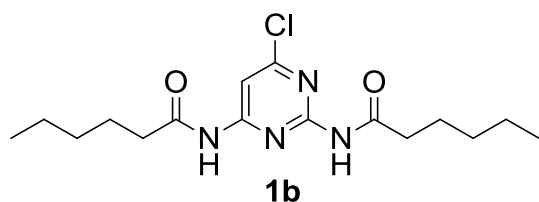


Chem. Eur. J., **2003**, *9*, 409.

2.4.3 Characterization

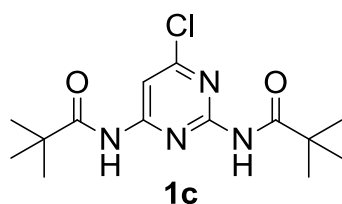


Transparent crystal, analytical TLC (silica gel 60) (25% ethyl acetate in n-hexane) R_f = 0.6; 58% isolated yield; ^1H NMR (400 MHz, CDCl_3) δ 11.84 (br s, 1H), 10.94 (br s, 1H), 7.95 (s, 1H); ^{13}C NMR (100 MHz, D-Acetone) δ 162.63, 158.80, 156.46 (q, $^2J_{\text{CF}}$ = 157.6), 155.76, 154.14 (q, $^2J_{\text{CF}}$ = 154.4), 115.39 (q, $^1J_{\text{CF}}$ = 1146.8), 115.31 (q, $^1J_{\text{CF}}$ = 1143.2), 107.06 ; ESIMS m/z 337 $[\text{M}+\text{H}^+]$; X-ray crystallography obtained.

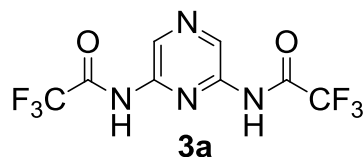


Transparent crystal, analytical TLC (silica gel 60) (25% ethyl acetate in n-hexane) R_f

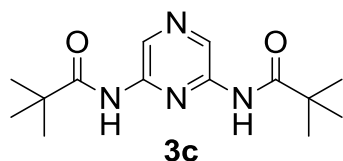
= 0.6; 15% isolated yield; ^1H NMR (400 MHz, CDCl_3) δ 10.89 (br s, 1H), 9.66 (br s, 1H), 8.08 (s, 1H), 2.98 (m, 2H), 2.51-5.54 (m, 2H), 1.70-1.74 (m, 4H), 1.36-1.39 (m, 8H), 0.91-0.94 (m, 6H); ^{13}C NMR (100 MHz, CDCl_3) δ 174.42, 162.61, 160.48, 156.41, 105.08, 37.50, 31.62, 31.55, 25.05, 24.68, 22.67, 22.56, 14.13, 14.10; ESIMS m/z 341 $[\text{M}+\text{H}^+]$.



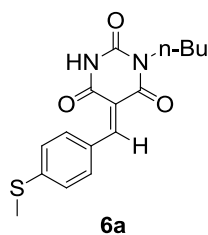
White solid, analytical TLC (silica gel 60) (25% ethyl acetate in n-hexane) $R_f = 0.6$; 62% isolated yield; ^1H NMR (400 MHz, D-Acetone) δ 10.11 (br s, 1H), 9.01 (br s, 1H), 7.92 (s, 1H), 1.34 (s, 9H), 1.32 (s, 9H); ^{13}C NMR (100 MHz, D-Acetone) δ 178.61, 176.01, 161.58, 160.71, 157.26, 103.96, 40.29, 40.21, 26.59, 26.44; ESIMS m/z 313 $[\text{M}+\text{H}^+]$.



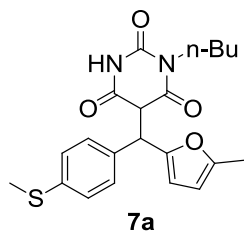
White solid, analytical TLC (silica gel 60) (25% ethyl acetate in n-hexane) $R_f = 0.4$; 68% isolated yield; ^1H NMR (400 MHz, D-Acetone) δ 11.00-11.02 (br s, 1H), 9.19 (s, 1H); ^{13}C NMR (100 MHz, D-Acetone) δ 155.62 (q, $^2J_{\text{CF}} = 123.2$), 145.13, 134.03, 115.89 (q, $^1J_{\text{CF}} = 915.2$); ESIMS m/z 303 $[\text{M}+\text{H}^+]$.



Yellow solid, analytical TLC (silica gel 60) (50% ethyl acetate in n-hexane) $R_f = 0.5$;
 62% isolated yield; ^1H NMR (400 MHz, CDCl_3) δ 9.28 (s, 1H), 1.34 (s, 18H); ^{13}C
 NMR (100 MHz, CDCl_3) δ 176.92, 145.81, 131.62, 39.97, 27.62, 0.196; ESIMS m/z
 279 $[\text{M}+\text{H}^+]$.



Yellow Crystal, analytical TLC (silica gel 60) (25% ethyl acetate in n-hexane) $R_f =$
 0.5; 73% isolated yield; ^1H NMR (400 MHz, CDCl_3) δ 8.51 (br s, 2H), 8.22 (d, $J =$
 8.0 Hz, 2H), 7.28 (d, $J = 8.0$ Hz, 2H), 3.94-3.98 (m, 2H), 2.55 (s, 3H), 1.65-1.68 (m,
 2H), 1.38-1.40 (m, 2H), 0.97 (t, $J = 7.2$ Hz, 3H); ^{13}C NMR (100 MHz, CDCl_3) δ
 163.48, 160.41, 159.50, 148.45, 135.50, 128.66, 124.66, 115.37, 41.83, 30.17, 20.18,
 14.63, 13.82; ESIMS m/z 319 $[\text{M}+\text{H}^+]$.



Yellow oil, analytical TLC (silica gel 60) (30% ethyl acetate in n-hexane) $R_f = 0.6$;
 55% isolated yield; ^1H NMR (400 MHz, CDCl_3) δ 8.39 (br s, 1H), 7.18-7.28 (m, 4H),
 5.96-5.99 (m, 1H), 5.91-5.92 (m, 1H), 5.00 (d, $J = 3.9$ Hz, 1H), 4.15-4.18 (m, 1H),
 3.68-3.80 (m, 2H), 2.48 (s, 3H), 2.28 (s, 3H), 1.42-1.46 (m, 2H), 1.25-1.30 (m, 2H),
 0.89-0.949 (m, 3H); ^{13}C NMR (100 MHz, CDCl_3) δ 167.69, 167.57, 167.13, 166.92,
 152.05, 152.02, 150.42, 150.37, 150.10, 138.87, 133.56, 133.53, 129.57, 126.64,
 126.61, 109.88, 109.80, 106.72, 53.47, 53.44, 47.76, 41.50, 41.47, 30.01, 29.97, 20.17,
 20.13, 15.75, 13.88, 13.76, 13.71; ESIMS m/z 401 $[\text{M}+\text{H}^+]$.

2.5 Reference

- (1) a) Nigst, T. A.; Ammer, J.; Mayr, H. *J. Phys. Chem. A* **2012**, *116*, 8494-8499. b) Rycke, N. D.; Berionni, G.; Couty, F.; Mayr, H.; Goumont, R.; David, O. R. P. *Org. Lett.* **2011**, *13*, 530-533. c) Campodonico, P. R.; Aizman, A.; Contreras, R. *Chemical Physics Letters* **2006**, *422*, 204-209. d) Streidl, N.; Denegri, B.; Kronja, O.; Mayr, H. *Acc. Chem. Res.* **2010**, *43*, 1537-1549. e) Baidya, M.; Horn, M.; Zipse, H.; Mayr, H. *J. Org. Chem.* **2009**, *74*, 7157-7164. f) Brotzel, F.; Chu, Y. C.; Mayr, H. *J. Org. Chem.* **2007**, *72*, 3679-3688.
- (2) a) Huheey, J. E. *J. Org. Chem.* **1971**, *36*, 204-205. b) Reed, J. L. *J. Phys. Chem.* **1994**, *98*, 10477-10483. c) Chattaraj, P. K.; Sarkar, U.; Roy, D. R. *Chem.Rev.* **2006**, *106*, 2065-2091. d) Chattaraj, P. K.; Giri, S.; Duley, S. *Chem.Rev.* **2011**, *111*, 43-75.
- (3) Bolz, I.; Schaarschmidt, D.; Ruffer, T.; Lang, H.; Spange, S. *Angew. Chem. Int. Ed.*, **2009**, *48*, 7440-7443.
- (4) Benito-Garagorri, D.; Becker, E.; Wiedermann, J.; Lackner, W.; Pollak, M.; Mereiter, K.; Kisala, J.; Kirchner, K. *Organometallics*, **2006**, *25*, 1900-1903.
- (5) Xu, Z.; Daka, P.; Budik, I.; Wang, H.; Bai, F. Q.; Zhang, H. X. *Eur. J. Org. Chem.*, **2009**, 4581-4585.
- (6) Tsai, M. S; Peng, S. M. *Chem. Commun.*, **1991**, 514-515.

- (7) Lempert, P. S.; Ostapchuk, P. N.; Bobrikova, A. A.; Petrovskii, P. V.; Kagramanov, N. D.; Bodrin, G. V.; Nifant'ev, E. E. *Mendeleev Communications*, **2010**, 223-225.
- (8) Zhang, W.; Nowlan, D. T.; Thomson, L. M.; Lackowski, W. M.; Simanek, E. E. *J. Am. Chem. Soc.*, **2001**, 8914-8922.
- (9) Cowper, A. J. *Journal of the Institution of Chemists (India)*, **1981**, 53, 141-144.
- (10) Habel, M.; Niederal, C.; Grimme, S.; Nieger, M.; Vogtle, F. *Eur. J. Org. Chem.*, **1998**, 1471-1477.
- (11) Barluenga, J.; Álvarez-Gutiérrez, J. M.; Ballesteros, A.; González, J. M. *Angew. Chem. Int. Ed.*, **2007**, 46, 1281-1283.
- (12) a) Zhang, Z.; Schreiner, P. R. *Chem. Soc. Rev.* **2009**, 38, 1187-1198. b) Yu, X.; Wang, W. *Chem.-Asian J.* **2008**, 3, 516-532. c) Doyle, A. G.; Jacobsen, E. N. *Chem. Rev.* **2007**, 107, 5713-5743. d) Connon, S. J. *Chem.-Eur. J.* **2006**, 12, 5418-5427. e) Taylor, M. S.; Jacobsen, E. N. *Angew. Chem. Int. Ed.* **2006**, 45, 1520-1543. f) Takemoto, Y. *Org. Biomol. Chem.* **2005**, 3, 4299-4306. g) Schreiner, P. R. *Chem. Soc. Rev.* **2003**, 32, 289-296.
- (13) a) Jakab, G.; Tancon, C.; Zhang, Z.; Lippert, K. M.; Schreiner, P. R. *Org. Lett.* **2012**, 14, 1724-1727. b) Wang, J.; Li, H.; Yu, X.; Zu, L.; Wang, W. *Org. Lett.* **2005**, 7, 4293-4296. c) Sohtome, Y.; Tanatani, A.; Hashimoto, Y.; Nagasawa, K.

Tetrahedron Lett. **2004**, *45*, 5589–5592. d) Vakulya, B.; Varga, S.; Csampai, A.; Soos, T. *Org. Lett.* **2005**, *7*, 1967–1969. e) Zhang, Z.; Lippert, K. M.; Hausmann, H.; Kotke, M.; Schreiner, P. R. *J. Org. Chem.* **2011**, *76*, 9764–9776. f) Klausen, R. S.; Jacobsen, E. N. *Org. Lett.* **2009**, *11*, 887–890. g) Herrera, R. P.; Sgarzani, V.; Bernardi, L.; Ricci, A. *Angew. Chem., Int. Ed.* **2005**, *44*, 6576–6579. h) Cao, C.-L.; Ye, M.-C.; Sun, X.-L.; Tang, Y. *Org. Lett.* **2006**, *8*, 2901–2904. i) Okino, T.; Hoashi, Y.; Takemoto, Y. *J. Am. Chem. Soc.* **2003**, *125*, 12672–12673. j) Wittkopp, A.; Schreiner, P. R. *Chem.-Eur. J.* **2003**, *9*, 407–414.

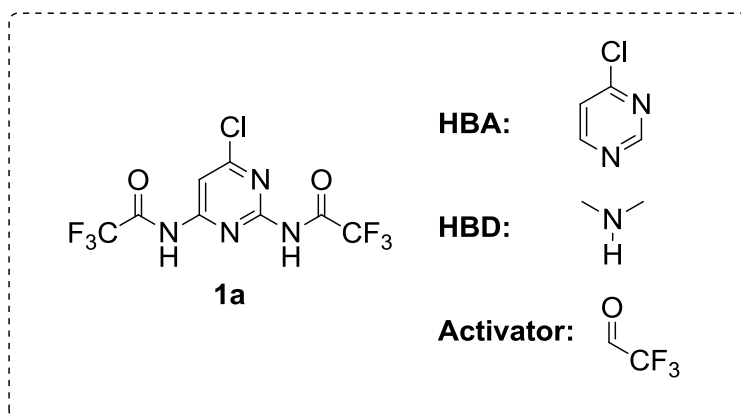
(14) a) Tian, Z.; Fattahi, A.; Lis, L.; Kass, S. R. *J. Am. Chem. Soc.*, **2009**, *131*, 16984-16988. b) Shokri, A.; Wang, X. B.; Kass, S. R. *J. Am. Chem. Soc.*, **2013**, DOI: 10.1021/ja4036384.

(15) a) Zu, L.; Wang, J.; Li, H.; Wang, W. *Org. Lett.* **2006**, *8*, 3077-3079. b) Zu, L.; Xie, H.; Li, H.; Wang, J.; Wang, W. *Org. Lett.* **2008**, *10*, 1211-1214. c) Yang, H.; Carter, R. G. *J. Org. Chem.* **2009**, *74*, 5151-5156. d) Chen, L. Y.; He, H.; Chan, W. H.; Lee, A. W. M. *J. Org. Chem.* **2001**, *76*, 7141-7147.

Chapter 3

Hydrogen Bond Donor-Acceptor-Donor Organocatalysts for Conjugate Addition of Benzylidene Barbiturates

3.1 Introduction



In chapters 1 and 2, the design and synthesis of HB-DAD organocatalysts were described. Through systematic studies, the DAD-ADA binding mode was examined. The binding mode was found to be a crucial factor in catalyzing conjugate addition of HB-ADA benzylidene barbiturates with 2-methylfuran. Notably, **1a** was the most efficient catalyst in this conjugate addition. In this chapter, we focus on the use of HB-DAD organocatalyst **1a** in conjugate addition of structurally diverse benzylidene barbiturates with 2-methylfuran.

3.1.1 History of Barbiturates

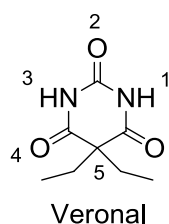


Figure 3.1 Diethyl barbiturate (Veronal)

In 1903, Fischer and von Mering synthesized the first therapeutically active barbiturate derivative. The C-5 hydrogen of barbiturate acid ring was replaced with ethyl group.^[1a] This new diethyl barbiturate, commonly called Veronal (Figure 3.1), is the first known hypnotics active derivative synthesized from barbiturate acid.^[1a,b]

In the early 20th Century, chemists realized the problem with metabolic degradation of Veronal. Human subjects administered with Veronal would sleep for several days with regard to the early scientific amount.^[1]

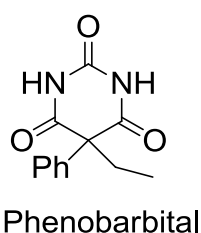


Figure 3.2 Chemical structure of Phenobarbital

In 1912, the active drug Phenobarbital was produced from early advances in the understanding of the SAR of barbiturates.^[1] Phenobarbital was classified as medicinal

compound possessing hypnotic and anticonvulsant activity to keep epileptic seizures under control (Figure 3.2).

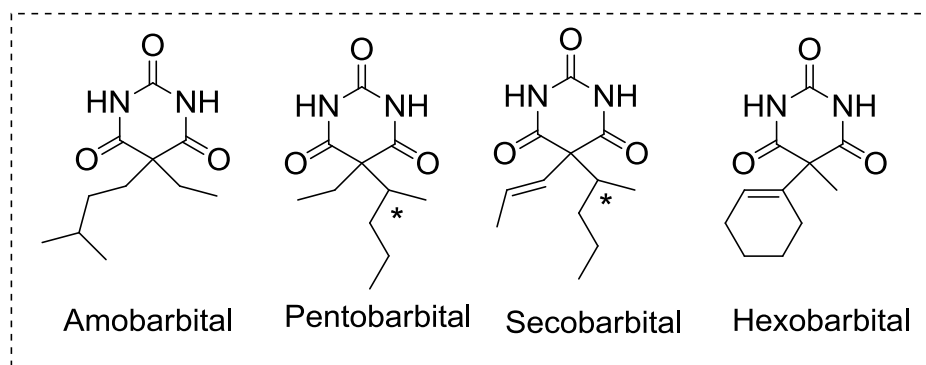


Figure 3.3 Modification of the C-5 position of barbituric acids

The modifications of barbiturates by functional substitutions of barbituric acid stem from either C-5 substitutions or C-2 substitutions to produce compounds with various medical activities.^[1] For instance, modifications of C-5 position has led to the synthesis of amobarbital, pentobarbital, secobarbital and hexobarbital (Figure 3.3).

3.1.2 Applications of Benzylidene Barbiturates

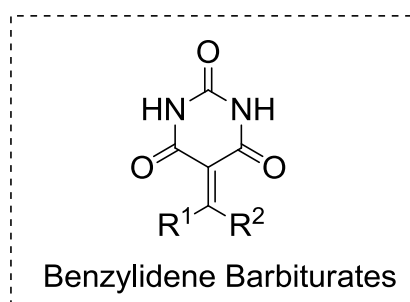


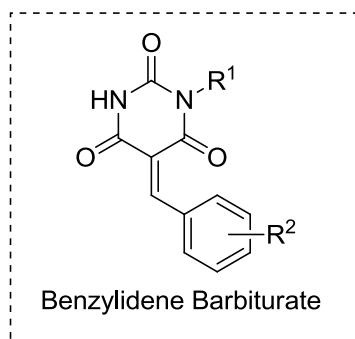
Figure 3.4 Chemical structures of benzylidene barbiturates

Benzylidene barbiturates are considered as significant biologically active

compounds (Figure 3.4). Benzylidene barbiturates are synthetic building blocks in the preparation of oxadeazaflavines,^[2] for asymmetric synthesis of disulfides,^[3] and being potential organic oxidizers.^[4] In addition, benzylidene barbiturates could be used as nonlinear optical materials.^[5]

We envision that benzylidene barbiturates are excellent HB-ADA electrophiles because of the (1) imide functionality acting as HB-ADA sequence to bind with HB-DAD organocatalysts and (2) carbon-carbon double bond acting as electrophilic center for nucleophilic attack. Thus, benzylidene barbiturates are chosen as HB-ADA electrophiles in following studies.

3.1.3 Reactions of Benzylidene Barbiturates



Benzylidene barbiturates were easily prepared using a modular approach,^[6] and used as important building blocks for the synthesis of versatile heterocyclic compounds.^[7] The electron deficient C=C bond of benzylidene barbiturates was highly reactive towards conjugate addition of furans, cycloaddition of amines and reduction (Figure 3.5).^[8]

However, these reactions were very slow. For examples, the conjugate addition of benzylidene barbiturate with 2-methylfuran needs 4 days to complete.^[8c] In this regard, we set out to employ HB-DAD organocatalyst **1a** for catalytic conjugate addition of benzylidene barbiturates with 2-methylfuran. In addition, other nucleophilic aromatic heterocyclic compounds e.g. indole, thiophene were studied.

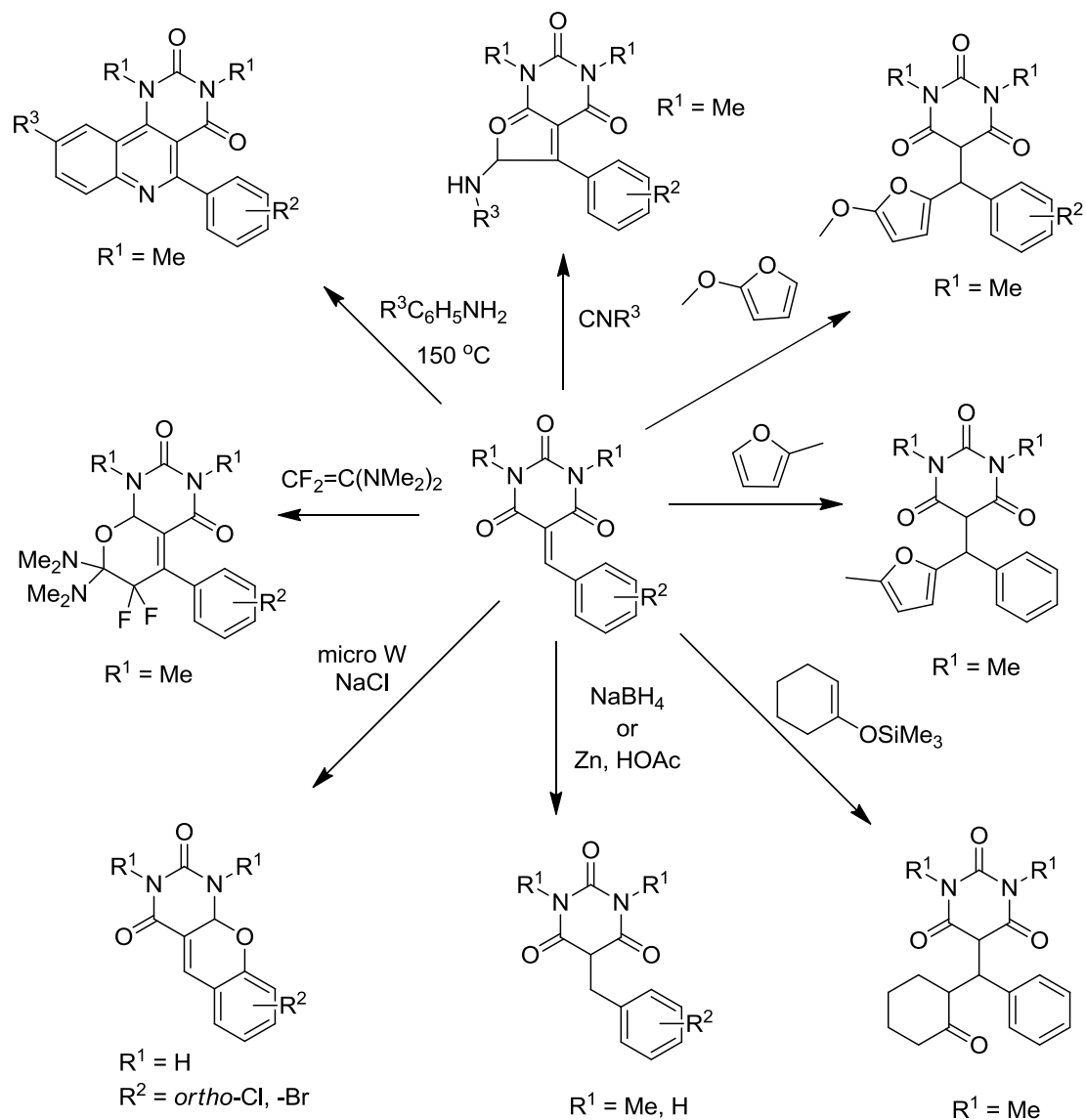


Figure 3.5 Conjugate additions, cycloadditions and reductions of benzylidene barbiturates

3.1.4 The Objectives of This Chapter

HB-DAD organocatalyst **1a** is chosen for studies on the conjugate addition of benzylidene barbiturates with 2-methylfuran. We set out to: (1) design and synthesize HB-ADA based benzylidene barbiturates, (2) optimize conjugate additions of benzylidene barbiturates with 2-methylfuran, and (3) study the substrate scope of benzylidene barbiturates.

3.2 Results and Discussion

3.2.1 Design and Synthesis of HB-ADA Based Benzylidene Barbiturates

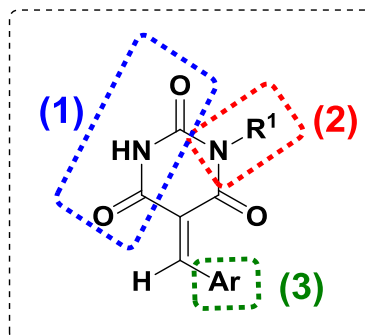
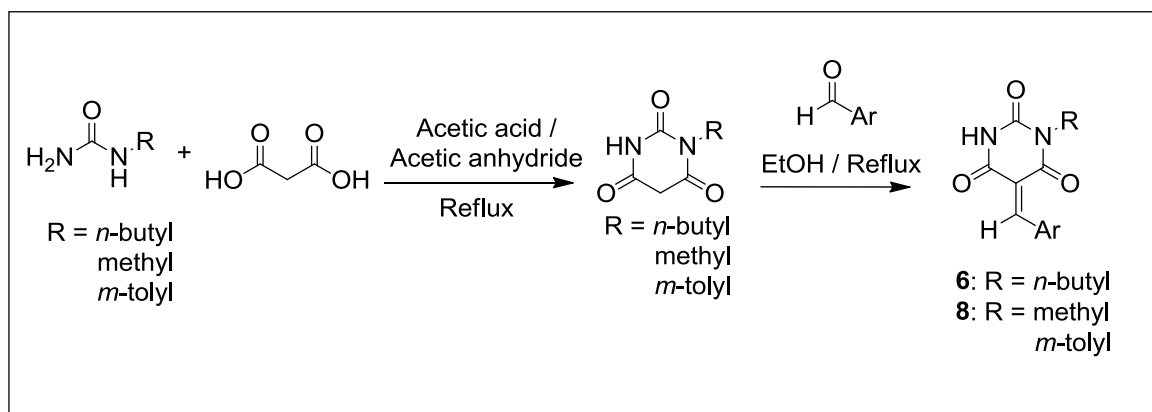


Figure 3.6 Constituents of benzylidene barbiturates (1) HB-ADA motif, (2) N-substituted group and (3) aryl group

Generally, benzylidene barbiturates could be prepared by reaction of substituted barbituric acids and aryl aldehydes in ethanol under refluxing conditions with good to excellent yield. Three motifs were generated (1) HB-ADA motif for binding to HB-DAD organocatalysts, (2) substituent on barbiturate acid, and (3) aromatic substituent originated from benzaldehyde (Figure 3.6). Note that, the N-substituted and aryl groups of benzylidene barbiturates could be easily introduced through the incorporation of functionalized ureas and aromatic aldehydes.



Scheme 3.1 Synthesis of benzylidene barbiturates **6** and **8**

Particularly, benzylidene barbiturates used in this study were prepared from the two-step synthesis (Scheme 3.1). The first step was synthesis of barbituric acids from ureas and malonic acid. In this step, N-substituted ureas (R = *n*-butyl, methyl, and *m*-tolyl groups) were chosen based on known literature procedures,^[2] which could lead to three major types of barbituric acids. The second step, reaction of barbituric acids and aldehydes was involved that could introduce various aryl substitutes to benzylidene barbiturates.

The first class of benzylidene barbiturates with N-substituted *n*-butyl group was obtained as new compounds (24-86% yield; *E* : *Z* = 1:1). In addition, this class of benzylidene barbiturates gave better solubility in polar aprotic organic solvents for reactivity screening.

Three sub-categories of benzylidene barbiturates bearing (1) Electron donating aryl substituents, (2) Electron neutral aryl substituents, and 3) Electron withdrawing aryl substituents were synthesized.

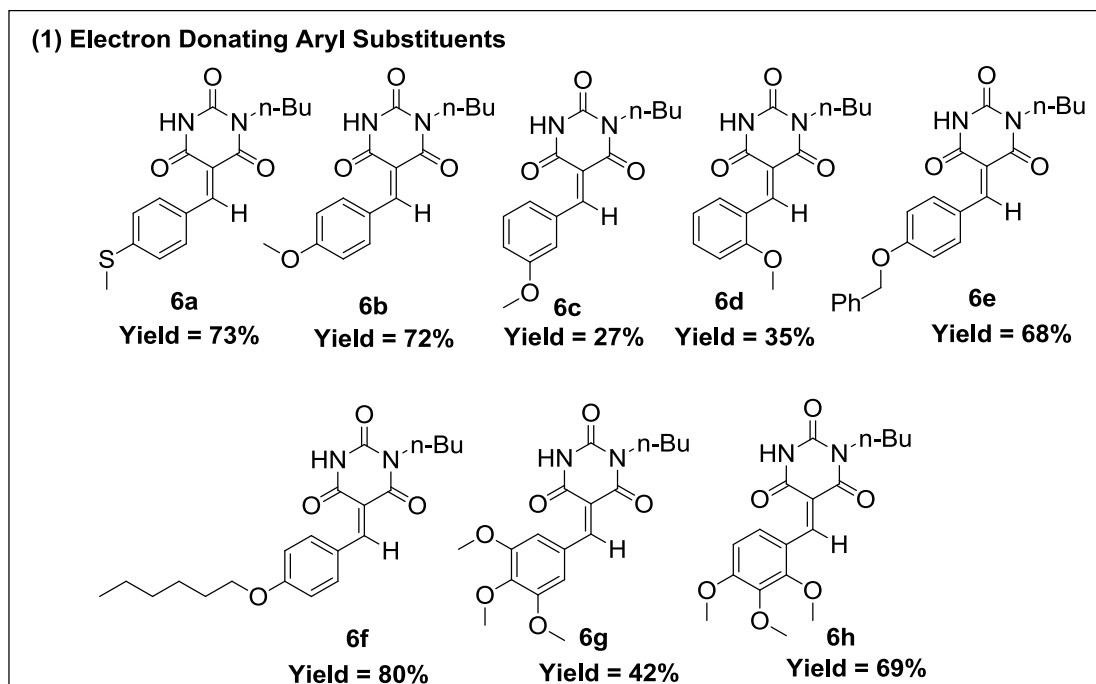


Figure 3.7 Synthesis of benzylidene barbiturates (1) Electron donating aryl substituents

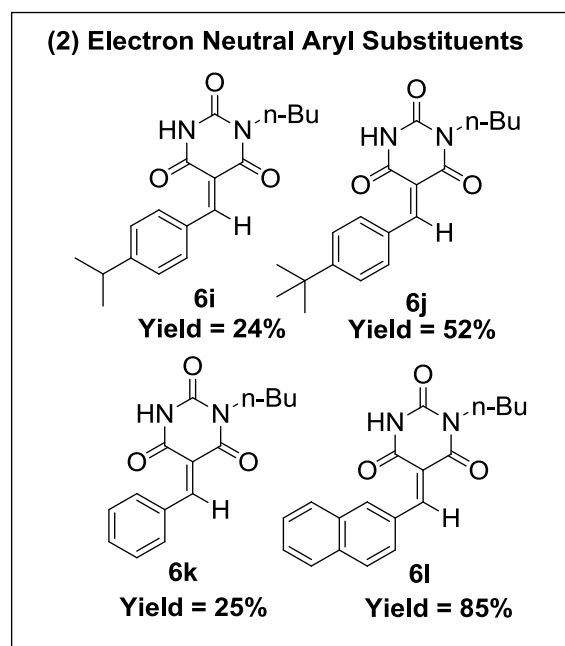


Figure 3.8 Synthesis of benzylidene barbiturates (2) Electron neutral aryl substituents

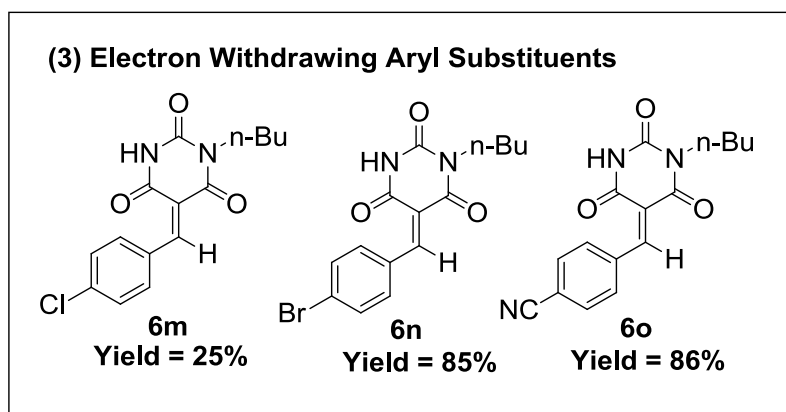


Figure 3.9 Synthesis of benzylidene barbiturates (3) Electron withdrawing aryl substituents

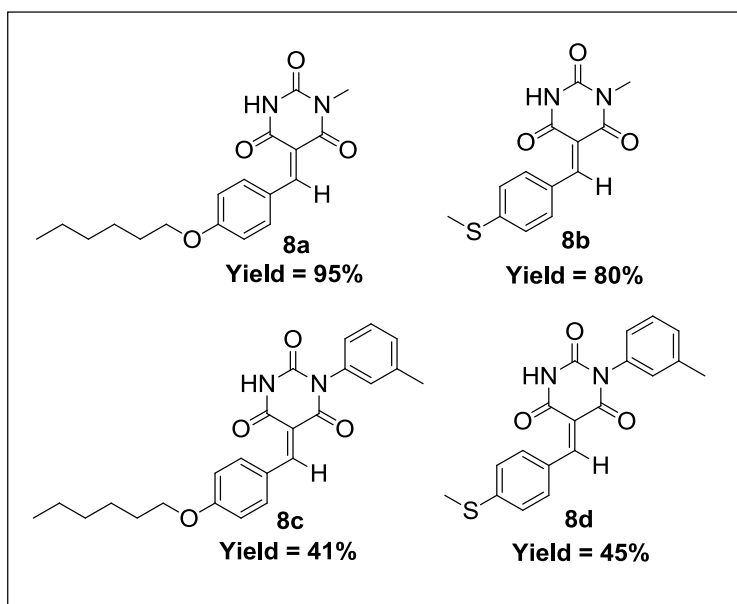


Figure 3.10 Synthesis of N-methyl and N-*m*-tolyl substituted benzylidene barbiturates

The N-methyl substituted and N-*m*-tolyl substituted benzylidene barbiturates were synthesized from the two step synthesis.^[2] **8a**, **8b**, **8c** and **8d** were prepared in good to excellent yield (41-95%; Figure 3.10) in order to further extend the substrate scope of this organocatalytic conjugate addition.

3.2.2 Optimization of Reaction Conditions of Conjugate Additions of Benzylidene Barbiturates

A preliminary study of the conjugate addition of benzylidene barbiturate **6a** with 2-methylfuran was carried out by stirring **6a** (0.05 mmol), 2-methylfuran (0.05 mmol) and HB-DAD organocatalyst (0.01 mmol) in dichloromethane at room temperature for 24 h. ¹H NMR yield was determined with toluene as an internal standard. The effect of solvent systems, reaction temperature and catalyst loading of **1a** were also screened in this optimization study.

Yield enhancement (product yield with catalyst / product yield without catalyst) of the conjugate addition was calculated according to equation 1. It was used in the optimization and substrate scope studies for comparison.

$$\text{Yield Enhancement} = \frac{\text{product yield with catalyst}}{\text{product yield without catalyst}} \quad (\text{Equation 1})$$

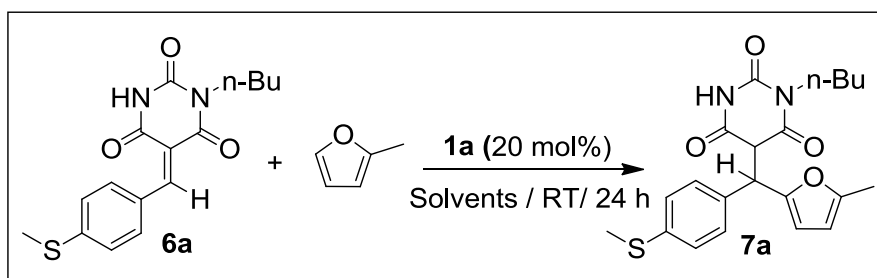
For instance, **Table 3.1**, entry 1 stated

$$\begin{aligned} \text{Yield Enhancement} &= 61\% / 28\% \\ &= 2.2 \end{aligned}$$

In the solvent screening, dichloromethane and chloroform were found to be good solvents with better yield (up to 61%) and yield enhancement (up to 2.2; entries 1-2, Table 3.1). Poor yield enhancement was observed in acetonitrile (1.3; entry 3). No yield enhancement was observed with acetone (1.0; entry 4). The benzylidene barbiturates were found to be insoluble in non-polar solvent (entry 5). Thus, dichloromethane was chosen for subsequent studies.

No increase in conversion was observed when the reaction was prolonged to 48 h in dichloromethane (62% yield; entry 6). Notably, the reaction conducted in dried dichloromethane could give better yield enhancement (3.0; entry 7).

Table 3.1 Solvent screening study of the organocatalytic conjugate addition^[a]



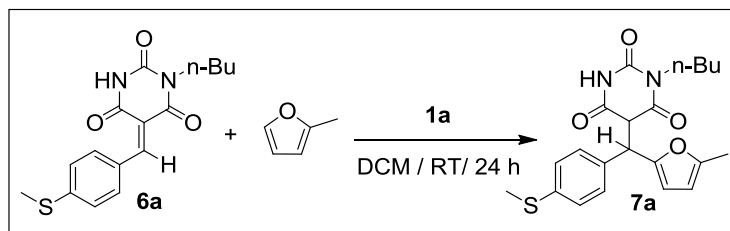
Entry ^[a]	Solvent	Yield (%) ^[b]	Background Yield (%) ^[c]	Yield Enhancement
1	CH ₂ Cl ₂	61	28	2.2
2	CHCl ₃	51	24	2.1
3	CH ₃ CN	21	16	1.3
4	Acetone	14	14	1
5 ^[f]	Toluene	2	0	-----
6 ^[d]	CH ₂ Cl ₂	60	30	2.0
7 ^[e]	CH ₂ Cl ₂	69	23	3.0

^[a] Unless noted otherwise, reaction were performed with **6a** (0.05 mmol), 2-methylfuran (0.05 mmol),

1a (0.01 mmol), solvents (1 mL), 25 °C, 24 h. ^[b] Yield determined by ¹H NMR of the crude product using toluene as the internal standard. ^[c] Without addition of **1a**. ^[d] For 48 h. ^[e] Dried CH₂Cl₂ ^[f] Ethyl acetate as the internal standard.

Studies on the loading of HB-DAD organocatalyst **1a** (0.05-0.5 equiv.) in conjugate addition of **6a** (0.05 mmol) with 2-methylfuran (0.05 mmol) to give adduct **7a** is depicted in Table 3.2. Using 0.05 equiv. of **1a**, adduct **7a** was obtained in 28% yield (entry 1) while the reaction without addition of **1a** gave 28% yield of **7a** (entry 5). Using of **1a** (0.1 equiv.), adduct **7a** was obtained in 49% yield (entry 2) while the reaction using of 0.2 equiv. and 0.5 equiv. of **1a** could give 61% and 62% yield of **7a** respectively (entries 3 and 4). Thus, 0.2 equiv. of **1a** was used for latter studies.

Table 3.2 Study of **1a** loading in organocatalytic conjugate addition of **6a**^[a]

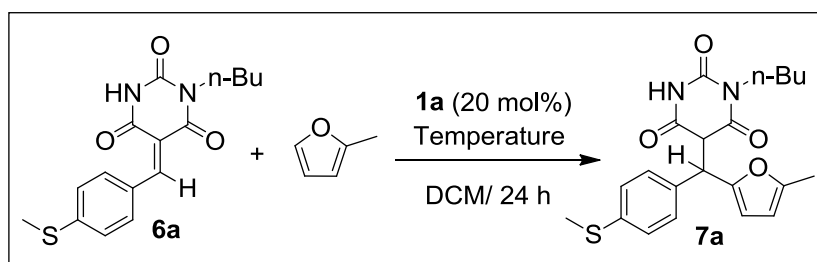


Entry ^[a]	Loading of 1a	Yield (%) ^[b]
1	0.05	28
2	0.1	49
3	0.2	61
4	0.5	62
5	-----	28

^[a] Conditions: **6a** (0.05 mmol), 2-methylfuran (0.05 mmol), **1a** (0.05-0.5 equiv.), CH₂Cl₂ (1 mL), 25 °C, 24 h. ^[b] Yield determined by ¹H NMR of the crude product using toluene as the internal standard.

As depicted in Table 3.3, screening experiments of reaction temperature (-20 °C to 40 °C) using **1a** (0.01 mmol) in catalyzing conjugate addition of **6a** (0.05 mmol) with 2-methylfuran (0.05 mol) for 24 h were performed to give adduct **7a** with 1.3-3.0 yield enhancement (entries 1-4). For **1a** catalyzing conjugate addition carried out at 0 °C and -20 °C, adduct **7a** were obtained in 3% and 25% yields with yield enhancements of 3.0 and 2.5, respectively (entries 1-2). The reaction conducted in 20 °C gave adduct **7a** in good yield (61%; entry 3) with good yield enhancement (2.1). A lower yield enhancement of the reaction was observed in 40 °C (1.3; entry 4). Considering the product yield and yield enhancement, the reaction carried out in 25 °C was chosen for further studies on substrate scope.

Table 3.3 Reaction temperature optimization in organocatalytic conjugate addition^[a]



Entry ^[a]	Temperature (°C)	Yield (%) ^[b]	Background Yield (%) ^[c]	Yield Enhancement
1	-20	3	1	3.0
2	0	25	10	2.5
3	20	61	28	2.1
4	40	62	49	1.3

^[a] Conditions: **6a** (0.05 mmol), 2-methylfuran (0.05 mmol), **1a** (0.01 mmol), CH₂Cl₂ (1 mL), 24 h. ^[b] Yield determined by ¹H NMR of the crude product using toluene as the internal standard. ^[c] Without addition of **1a**.

3.2.3 Substrate Scopes

3.2.3.1 Substrate Scopes - Conjugate Additions of *N*-*n*-Butyl Substituted Benzylidene

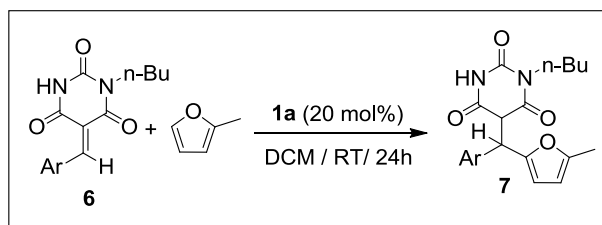
Barbiturates

Substrate scope of conjugate addition using **1a** (0.01 mmol) with different combinations of benzylidene barbiturates (0.05 mmol) (R = *n*-butyl; Ar = aryl) and 2-methylfuran (0.05 mmol) was examined (Tables 3.4-3.6).

The **1a**-catalyzed conjugate addition worked well for electron rich benzylidene barbiturates **6a-6h** (Table 3.4), with good yield enhancements (1.8-3.1; entries 1-8) except **6c** (1.2; entry 3). Particularly, **1a**-catalyzed conjugate addition of **6b** and **6e-6h** bearing *para*-alkoxy phenyl group afforded good yield enhancements (1.8-2.9; entry 2, and 5-8) while the conjugate addition of **6d** bearing *ortho*-methoxy phenyl group could give even higher yield enhancement (3.1; entry 4). The results indicated that benzylidene barbiturates bearing *para*- and *ortho*-alkoxy phenyl groups led to better yield enhancement as the electrophilicities of benzylidene barbiturates were lowered.

Table 3.4 Substrate scope of organocatalytic conjugate addition of electron rich

benzylidene barbiturates



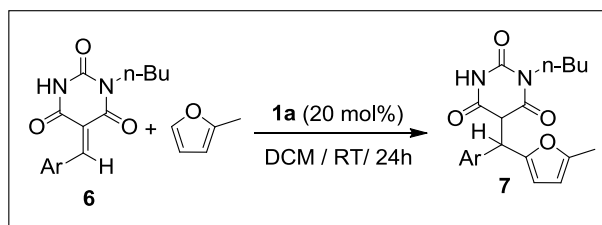
Entry ^[a]	Substrate	Ar	Product	Isolated	NMR	Background	Yield
				Yield (%)	Yield (%) ^[b]	Yield (%) ^[c]	Enhancement
1	6a		7a	55	61	28	2.2
2	6b		7b	52	57	25	2.3
3	6c		7c	78	80	65	1.2
4	6d		7d	25	22	7	3.1
5	6e		7e	30	30	17	1.8
6	6f		7f	16	20	7	2.9
7	6g		7g	65	70	31	2.3
8	6h		7h	47	50	21	2.4

^[a] Condition: **6** (0.05 mmol), 2-methylfuran (0.05 mmol), **1a** (0.01 mmol), DCM (1 mL), 25 °C, 24 h. ^[b]

Yield determined by ¹H NMR of the crude product using toluene as the internal standard. ^[c] Without addition of **1a**.

Varying the substitutions on benzylidene barbiturates afforded adducts **7i-7l** in good yield enhancements (2.0-2.4; Table 3.5; entries 1-2, 4) except **7k** (1.4; entry 3). Notably, the **1a**-catalyzed conjugate addition of **6j** led to adduct **7j** in 73% isolated yield with 2.0 yield enhancement (entry 2). In addition, the **1a**-catalyzed reaction of **6l** gave adduct **7l** in 35% isolated yield with good yield enhancement (2.4; entry 4). These findings indicate that benzylidene barbiturates bearing electron neutral substituents could lead to good yield enhancement as compared with the electron rich benzylidene barbiturates

Table 3.5 Substrate scope of organocatalytic conjugate addition of electron neutral benzylidene barbiturates



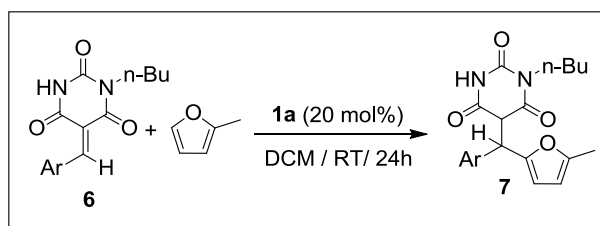
Entry ^[a]	Substrate	Ar	Product	Isolated Yield (%)	NMR Yield (%) ^[b]	Background NMR Yield (%) ^[c]	Yield Enhancement
1	6i		7i	66	69	30	2.3
2	6j		7j	73	71	36	2.0
3	6k		7k	79	84	60	1.4
4	6l		7l	35	38	16	2.4

^[a] Condition: **6** (0.05 mmol), 2-methylfuran (0.05 mmol), **1a** (0.01 mmol), DCM (1 mL), 25 °C, 24 h. ^[b] Yield determined by ¹H NMR of the crude product using toluene as the internal standard. ^[c] Without addition of **1a**.

As depicted in Table 3.6, conjugate additions of **6m-6o** to give corresponding adducts **7m-7o** in excellent yield (up to 99%) yet with poor yield enhancements (1.0-1.3). The conjugate additions of **6m** and **6n** led to adducts **7m** and **7n** with 1.1 and 1.3 yield enhancements, respectively (entries 1 and 2). In particular, the reaction of **6o** gave adduct **7o** in 99 % yields without yield enhancement (1.0; entry 3). These

findings indicated that benzylidene barbiturates bearing electron deficient substituents e.g. -Cl, -Br, -CN led to poor enhancements as the electrophilicity of benzylidene barbiturates increased.

Table 3.6 Substrate scope of organocatalytic conjugate addition of electron deficient benzylidene barbiturates



Entry ^[a]	Substrate	Ar	Product	NMR Yield (%) ^[b]	Background NMR Yield (%) ^[c]	Yield Enhancement
1	6m		7m	96	87	1.1
2	6n		7n	97	76	1.3
3	6o		7o	99	99	1.0

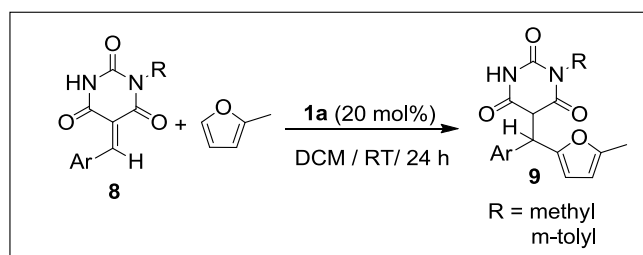
^[a] Condition: **6** (0.05 mmol), 2-methylfuran (0.05 mmol), **1a** (0.01 mmol), DCM (1 mL), 25 °C, 24 h. ^[b] Yield determined by ¹H NMR of the crude product using toluene as the internal standard. ^[c] Without addition of **1a**.

3.2.3.2 Substrate Scopes - Conjugate Additions of *N*-Methyl and *N*-*m*-toluene Substituted Benzylidene Barbiturates

Varying the substitutions on benzylidene barbiturates **8a-8d** afforded adducts **9a-9d** in good yield enhancements, respectively (1.8-5.0; Table 3.7, entries 1-3)

except **9d** (1.2; entry 4). In particular, conjugate additions of **8a** and **8b** (R = methyl) gave adducts **9a** and **9b** in 5.0 and 3.0 yield enhancements, respectively (entries 1-2). In addition, the reactions of **8c** and **8d** (R = *m*-tolyl) led to **9c** and **9d** in 1.8 and 1.2 yield enhancements, respectively (entries 3-4). The results indicated that N-methyl benzylidene barbiturates gave better yield enhancement than N-*m*-tolyl benzylidene barbiturates.

Table 3.7 Substrate scope of organocatalytic conjugate addition of N-methyl and N-*m*-toluene substituted benzylidene barbiturates



Entry ^[a]	Substrate	R	Ar	Product	Isolated	NMR	Background	Yield Enhancement
					Yield (%)	Yield (%) ^[b]	NMR Yield (%) ^[c]	
1	8a	methyl		9a	20	25	5	5.0
2	8b	methyl		9b	20	18	6	3.0
3	8c	<i>m</i> -tolyl		9c	46	48	27	1.8
4	8d	<i>m</i> -tolyl		9d	75	73	61	1.2

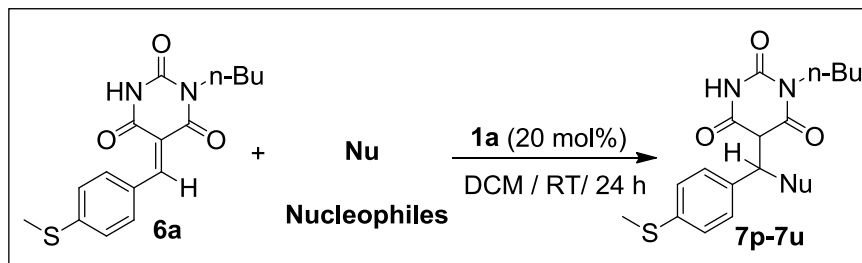
^[a] Condition: **8** (0.05 mmol), 2-methylfuran (0.05 mmol), **1a** (0.01 mmol), DCM (1 mL), 25 °C, 24 h. ^[b]

Yield determined by ¹H NMR of the crude product using toluene or ethyl acetate as the internal standard. ^[c] Without addition of **1a**.

3.2.3.3 Substrate Scope - Conjugate Additions of Benzylidene Barbiturate with other Nucleophiles

We attempted to extend the substrate scope of **1a**-catalyzed conjugate addition of benzylidene barbiturates by coupling the benzylidene barbiturate **6a** (0.05 mmol) with different nucleophiles (Table 3.8). Using **6a** and nucleophiles including 1-methylindole, indole and 5-methylindole, the corresponding adducts (**7p-7r**) were obtained with no yield enhancements (0.8-0.9; entries 1-3). However, the conjugate additions of **6a** with thiophene, dibenzoylmethane and ethylbenzylacetate gave no conversion of starting materials (entries 4-6).

Table 3.8 Substrate scope of organocatalytic conjugate addition of **6a** with other nucleophiles



Entry ^[a]	Nucleophiles	Product	NMR Yield (%)	Background NMR Yield (%) ^[c]	Yield Enhancement
1		7p	62	72	0.9
2		7q	63	76	0.8
3		7r	39	45	0.9
4		7s	0	0	-----
5		7t	0	0	-----
6		7u	0	0	-----

^[a] Condition: **6a** (0.05 mmol), Nucleophile (0.05 mmol), **1a** (0.01 mmol), DCM (1 mL), 25 °C, 24 h. ^[b] Yield determined by ¹H NMR of the crude product using toluene as the internal standard. ^[c] Without addition of **1a**.

3.3 Conclusion

A new class of barbiturates **7a-7b**, **7f-7h**, **8a** and **8c** have been synthesized and well characterized. The **1a**-catalyzed conjugate addition of *N-n*-butyl, *N*-methyl and *N-m*-tolyl substituted benzylidene barbiturates with 2-methylfuran have been conducted. Significant yield enhancements were observed (up to 5.0).

3.4 Experimental Section

3.4.1 Experimental Procedures

General Preparation Procedure for Benzylidene Barbiturates

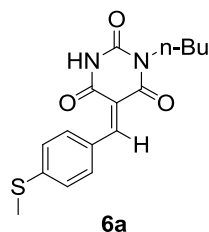
A mixture of ureas (2 mmol) and aryl aldehyde (2 mmol) in EtOH (10 mL) was refluxed for 2-12 h. The reaction mixture was allowed to cool to room temperature and filtered to obtain solid/crystalline crude products. The residue was purified by flash column chromatography on silica gel using ethyl acetate-hexane as eluent.

Procedure for Catalytic Conjugate Additions of Benzylidene Barbiturates

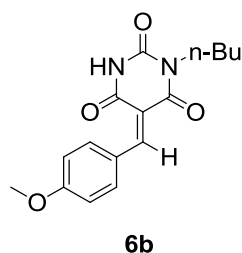
A mixture of benzylidene barbiturates (0.05 mmol), 2-methylfuran (0.05 mmol) and HB-DAD organocatalyst **1a** (0.01 mmol), in DCM (1 mL) was stirred at RT (25 °C) for 24 h. The product yield was determined by crude ¹H NMR with toluene (0.02 mmol) as internal standard. The reaction mixture was concentrated. The residue was purified by flash column chromatography on silica gel using ethyl acetate-hexane as eluent.

3.4.2 Characterizations

Characterization of **6a**, **6b**, **6f-6j**, **6l**, **8a** and **8c**

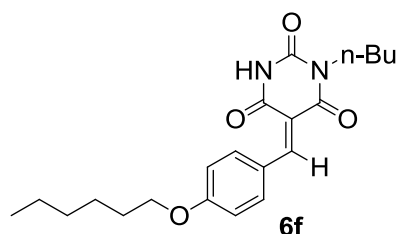


Yellow crystal, analytical TLC (silica gel 60) (25% ethyl acetate in n-hexane) $R_f = 0.5$;
73% isolated yield; $^1\text{H NMR}$ (400 MHz, CDCl_3) δ 8.51 (br s, 2H), 8.22 (d, $J = 8.0$ Hz, 2H), 7.28 (d, $J = 8.0$ Hz, 2H), 3.94-3.98 (m, 2H), 2.55 (s, 3H), 1.65-1.68 (m, 2H), 1.38-1.40 (m, 2H), 0.97 (t, $J = 7.2$ Hz, 3H); $^{13}\text{C NMR}$ (100 MHz, CDCl_3) δ 163.48, 160.41, 159.50, 148.45, 135.50, 128.66, 124.66, 115.37, 41.83, 30.17, 20.18, 14.63, 13.82; ESIMS m/z 319 $[\text{M}+\text{H}^+]$.

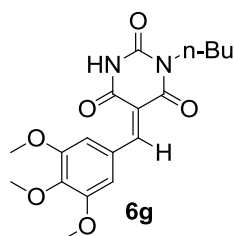


Yellow crystal, analytical TLC (silica gel 60) (25% ethyl acetate in n-hexane) $R_f = 0.4$;
72% isolated yield; $^1\text{H NMR}$ (400 MHz, CDCl_3) δ 8.53 (br s, 1H), 8.38 (d, $J = 8.8$ Hz, 2H), 8.33 (br s, 1H), 6.99 (d, $J = 9.2$ Hz, 2H), 3.96 (t, $J = 7.6$ Hz, 2H), 3.92 (s, 3H), 1.63-1.66 (m, 2H), 1.37-1.42 (m, 2H), 0.96 (t, $J = 7.6$ Hz, 3H); $^{13}\text{C NMR}$ (100 MHz, CDCl_3) δ 164.86, 164.80, 163.91, 161.55, 160.86, 160.82, 159.95, 159.13, 150.37,

150.33, 138.66, 138.54, 125.72, 125.57, 114.34, 114.30, 114.14, 114.07, 55.86, 41.90, 41.33, 30.31, 20.36, 20.31, 13.97, 13.95; ESIMS m/z 303 $[M+H^+]$.

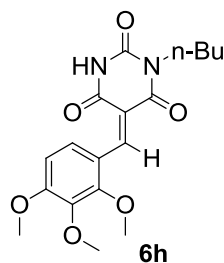


Yellow crystal, analytical TLC (silica gel 60) (25% ethyl acetate in n-hexane) R_f = 0.6; 80% isolated yield; ^1H NMR (500 MHz, CDCl_3) δ 8.52 (s, 1H), 8.38 (d, J = 8.0 Hz, 2H), 6.97 (d, J = 8.5 Hz, 2H), 4.07 (t, J = 6.0 Hz, 2H), 3.96 (t, J = 7.5 Hz, 2H), 1.79-1.84 (m, 2H), 1.61-1.67 (m, 2H), 1.46-1.48 (m, 2H), 1.34-1.41 (m, 6H), 0.97 (t, J = 7.5 Hz, 3H), 0.90-0.93 (m, 3H); ^{13}C NMR (100 MHz, CDCl_3) δ 164.60, 164.03, 159.96, 138.88, 125.52, 114.78, 113.82, 68.74, 41.87, 41.86, 41.85, 31.73, 30.33, 29.20, 25.84, 22.79, 14.24, 13.99; ESIMS m/z 373 $[M+H^+]$.

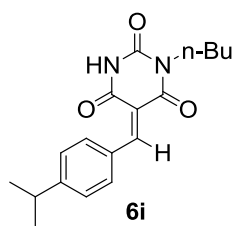


Yellow solid, analytical TLC (silica gel 60) (25% ethyl acetate in n-hexane) R_f = 0.6; 42% isolated yield; ^1H NMR (400 MHz, CDCl_3) δ 9.46-9.60 (br s, 1H), 8.49 (d, J =

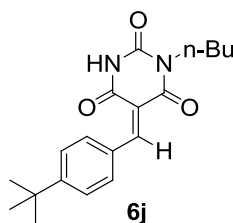
8.8 Hz, 1H), 7.82 (s, 1H), 7.74 (s, 1H), 3.94-4.01 (m, 11H), 1.62-1.67 (m, 2H), 1.37-1.42 (m, 2H), 0.94-0.99 (m, 3H); ^{13}C NMR (100 MHz, CDCl_3) δ 163.75, 163.25, 161.30, 161.29, 160.33, 159.26, 152.59, 152.55, 150.31, 144.14, 143.98, 127.52, 127.40, 115.54, 115.35, 113.73, 113.50, 61.32, 56.55, 56.52, 41.97, 41.24, 30.30, 30.26, 20.28, 13.93; ESIMS m/z 363 $[\text{M}+\text{H}^+]$.



Yellow Crystal, analytical TLC (silica gel 60) (25% ethyl acetate in n-hexane) $R_f = 0.4$; 69% isolated yield; ^1H NMR (400 MHz, CDCl_3) δ 8.87 (br s, 1H), 8.32-8.35 (br s, 2H), 6.76 (d, $J = 9.2$ Hz, 1H), 4.02 (s, 3H), 3.96 (s, 3H), 3.89-3.93 (m, 2H), 3.86 (s, 3H), 1.58-1.66 (m, 2H), 1.33-1.42 (m, 2H), 0.95 (t, $J = 7.2$ Hz, 3H); ^{13}C NMR (100 MHz, CDCl_3) δ 162.85, 161.26, 159.19, 156.31, 154.15, 150.43, 141.15, 129.98, 119.55, 115.03, 106.41, 62.15, 60.92, 56.24, 41.09, 30.11, 20.16, 13.78; ESIMS m/z 363 $[\text{M}+\text{H}^+]$.

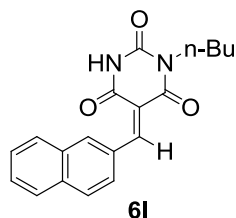


Pale yellow crystal, analytical TLC (silica gel 60) (25% ethyl acetate in n-hexane) R_f = 0.7; 24% isolated yield; ^1H NMR (400 MHz, CDCl_3) δ 8.79 (br s, 1H), 8.60 (s, 1H), 8.20 (d, J = 8.4 Hz, 2H), 7.36 (d, J = 8.0 Hz, 2H), 3.98 (t, J = 7.6 Hz, 2H), 2.97-3.04 (m, 1H), 1.63-1.71 (m, 2H), 1.41-1.46 (m, 1H), 1.30 (d, J = 7.2, Hz, 3H), 0.99 (t, J = 7.6 Hz, 3H); ^{13}C NMR (100 MHz, CDCl_3) δ 163.37, 160.38, 160.24, 155.95, 150.13, 135.15, 130.18, 126.71, 115.97, 41.79, 34.52, 30.11, 23.53, 20.14, 13.77; ESIMS m/z 315 $[\text{M}+\text{H}^+]$.



Pale yellow crystal, analytical TLC (silica gel 60) (25% ethyl acetate in n-hexane) R_f = 0.7; 52% isolated yield; ^1H NMR (400 MHz, CDCl_3) δ 9.49 (br s, 1H), 8.58 (s, 1H), 8.13-8.22 (m, 2H), 7.48-7.51 (m, 2H), 3.92-3.98 (m, 2H), 1.62-1.67 (m, 2H), 1.30-1.42 (m, 11H), 0.94-0.98 (m, 3H); ^{13}C NMR (100 MHz, CDCl_3) δ 163.61, 163.18, 161.17, 160.77, 160.28, 159.60, 158.25, 150.67, 150.53, 135.14, 134.85, 130.02, 129.93, 125.72, 125.66, 116.34, 41.93, 35.57, 31.16, 30.29, 20.34, 20.31,

13.97, 13.96; ESIMS m/z 329 $[M+H]^+$.



Yellow crystal, analytical TLC (silica gel 60) (25% ethyl acetate in n-hexane) $R_f = 0.6$;

85% isolated yield; 1H NMR (400 MHz, $CDCl_3$) δ 9.25 (s, 1H), 8.25 (br s, 1H), 8.01

(d, $J = 8.4$ Hz, 2H), 7.88-7.93 (m, 2H), 7.54-7.58 (m, 3H), 3.84-3.88 (m, 2H),

1.54-1.62 (m, 2H), 1.30-1.36 (m, 2H), 0.89-0.93 (t, $J = 7.2$ Hz, 3H); ^{13}C NMR (100

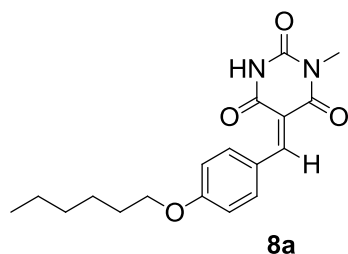
MHz, $CDCl_3$) δ 162.79, 161.48, 161.45, 161.44, 160.36, 159.29, 158.39, 157.82,

149.92, 149.89, 149.86, 149.84, 133.41, 133.08, 132.85, 132.00, 131.83, 130.35,

130.13, 129.97, 129.87, 127.73, 127.69, 126.69, 124.95, 124.91, 124.23, 124.16,

119.43, 119.30, 45.01, 42.03, 41.46, 30.33, 30.22, 20.35, 20.29, 13.94, 13.89; ESIMS

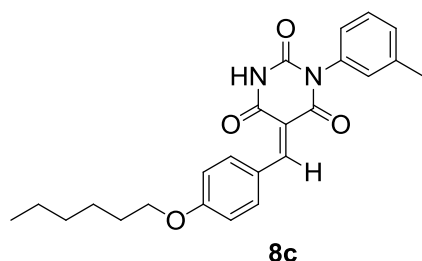
m/z 323 $[M+H]^+$.



Yellow crystal, analytical TLC (silica gel 60) (25% ethyl acetate in n-hexane) $R_f = 0.5$;

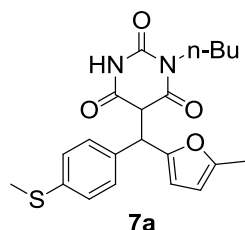
95% isolated yield; 1H NMR (500 MHz, $CDCl_3$) δ 8.61-8.64 (br s, 1H), 8.53 (s, 1H),

8.39 (d, $J = 8.5$ Hz, 2H), 6.97 (d, $J = 8.5$ Hz, 2H), 4.07 (t, $J = 6.5$ Hz, 2H), 3.39 (s, 3H), 1.79-1.84 (m, 2H), 1.46-1.48 (m, 2H), 1.35-1.36 (m, 4H), 0.90-0.93 (m, 3H); ^{13}C NMR (100 MHz, CDCl_3) δ 164.74, 164.31, 160.16, 150.63, 138.93, 125.44, 114.83, 113.54, 68.79, 45.00, 31.72, 29.19, 28.55, 25.83, 22.79, 14.24; ESIMS m/z 331 $[\text{M}+\text{H}^+]$.

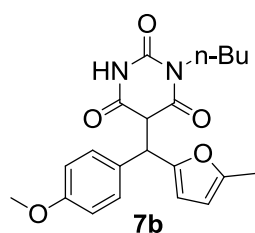


Yellow crystal, analytical TLC (silica gel 60) (25% ethyl acetate in n-hexane) $R_f = 0.5$; 41% isolated yield; ^1H NMR (500 MHz, CDCl_3) δ 8.60 (s, 1H), 8.39 (d, $J = 7.2$ Hz 2H), 8.67 (br s, 1H), 7.41 (t, $J = 6.0$ Hz, 1H), 7.27-2.29 (m, 2H), 7.07-7.09 (m, 2H), 6.91 (d, $J = 6.8$ Hz, 2H), 4.04 (t, $J = 5.2$ Hz, 2H), 2.49 (s, 3H), 1.77-1.82 (m, 2H), 1.58 (br s, 2H), 1.43-1.46 (m, 2H), 1.33-1.34 (m, 4H), 0.88-0.92 (3H); ^{13}C NMR (100 MHz, CDCl_3) δ 164.98, 164.93, 164.24, 162.96, 161.92, 160.78, 160.72, 160.16, 149.97, 139.71, 139.63, 139.37, 139.04, 134.56, 134.31, 130.22, 130.12, 129.46, 129.41, 129.38, 129.24, 125.81, 125.65, 125.44, 125.28, 114.89, 114.84, 113.54, 113.36, 68.83, 68.80, 31.70, 31.68, 29.18, 29.14, 25.81, 25.78, 22.76, 22.74, 21.54, 21.52, 14.19; ESIMS m/z 407 $[\text{M}+\text{H}^+]$.

Characterization of **7a**, **7b**, **7f-7j**, **7l**, **9a** and **9c**

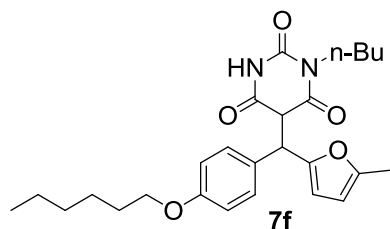


Yellow oil, analytical TLC (silica gel 60) (30% ethyl acetate in n-hexane) $R_f = 0.6$;
55% isolated yield; $^1\text{H NMR}$ (400 MHz, CDCl_3) δ 8.39 (br s, 1H), 7.18-7.28 (m, 4H),
5.96-5.99 (m, 1H), 5.91-5.92 (m, 1H), 5.00 (d, $J = 3.9$ Hz, 1H), 4.15-4.18 (m, 1H),
3.68-3.80 (m, 2H), 2.48 (s, 3H), 2.28 (s, 3H), 1.42-1.46 (m, 2H), 1.25-1.30 (m, 2H),
0.89-0.949 (m, 3H); $^{13}\text{C NMR}$ (100 MHz, CDCl_3) δ 167.69, 167.57, 167.13, 166.92,
152.05, 152.02, 150.42, 150.37, 150.10, 138.87, 133.56, 133.53, 129.57, 126.64,
126.61, 109.88, 109.80, 106.72, 53.47, 53.44, 47.76, 41.50, 41.47, 30.01, 29.97, 20.17,
20.13, 15.75, 13.88, 13.76, 13.71; ESIMS m/z 401 $[\text{M}+\text{H}^+]$.

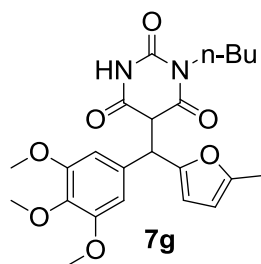


Yellow oil, analytical TLC (silica gel 60) (30% ethyl acetate in n-hexane) $R_f = 0.6$;
52% isolated yield; $^1\text{H NMR}$ (400 MHz, CDCl_3) δ 8.35 (br s, 1H), 7.23-7.26 (m, 2H),
6.82-6.85 (m, 2H), 5.95 (d, $J = 9.2$ Hz, 1H), 5.89-5.90 (m, 1H), 4.97 (d, $J = 3.6$ Hz,

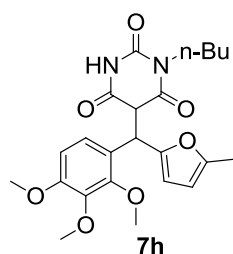
1H), 4.16 (dd, $J = 3.6, 6.8$ Hz, 1H), 3.79 (s, 3H), 3.64-3.75 (m, 2H), 2.27 (s, 3H), 1.35-1.48 (m, 2H), 1.17-1.29 (m, 2H), 0.86-0.92 (m, 3H); ^{13}C NMR (100 MHz, CDCl_3) δ 167.91, 167.58, 167.32, 166.90, 159.59, 151.93, 151.91, 150.86, 150.84, 150.09, 130.25, 128.54, 114.21, 114.17, 109.75, 109.68, 106.67, 106.65, 55.41, 53.71, 53.69, 47.91, 47.83, 41.47, 41.43, 30.01, 29.96, 20.19, 20.13, 13.87, 13.77, 13.73; ESIMS m/z 359 $[\text{M}+\text{H}^+]$.



Yellow oil, analytical TLC (silica gel 60) (10% ethyl acetate in n-hexane) $R_f = 0.6$; 16% isolated yield; ^1H NMR (400 MHz, CDCl_3) δ 8.21 (br s, 1H), 7.23 (t, $J = 8.4$ Hz, 2H), 6.82-6.86 (m, 2H), 5.90-5.99 (m, 2H), 4.97 (d, $J = 3.6$ Hz, 1H), 4.18 (dd, $J = 3.6, 7.2$ Hz, 1H), 3.94 (t, $J = 6.4$ Hz, 2H), 3.65-3.79 (m, 2H), 2.29 (s, 3H), 1.75-1.82 (m, 2H), 1.19-1.49 (m, 10H), 0.89-0.94 (m, 6H); ^{13}C NMR (100 MHz, CDCl_3) δ 167.94, 167.58, 167.25, 166.79, 159.22, 151.89, 151.86, 151.82, 150.94, 150.88, 150.00, 149.96, 149.92, 130.19, 130.05, 129.99, 129.97, 128.21, 114.75, 114.72, 114.59, 109.72, 109.66, 109.57, 106.63, 68.19, 53.74, 53.70, 47.98, 47.88, 47.85, 41.46, 41.42, 41.38, 31.77, 30.01, 29.96, 29.92, 25.92, 22.78, 20.19, 20.12, 14.19, 13.86, 13.80, 13.76, 13.72, 13.66; ESIMS m/z 455 $[\text{M}+\text{H}^+]$.

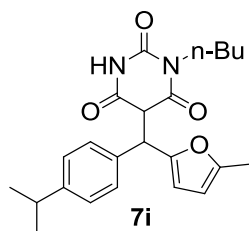


Yellow oil, analytical TLC (silica gel 60) (50% ethyl acetate in n-hexane) $R_f = 0.4$; 65% isolated yield; $^1\text{H NMR}$ (400 MHz, CDCl_3) δ 8.28-8.3 (br s, 1H), 6.60 (d, $J = 3.6$ Hz, 2H), 5.98-6.02 (m, 1H), 5.90-2.92 (m, 1H), 4.96 (d, $J = 6.8$ Hz, 1H), 4.19 (d, $J = 3.6$ Hz, 1H), 3.83 (s, 3H), 3.81 (s, 6H), 3.62-3.77 (m, 2H), 2.27 (s, 3H), 1.34-1.50 (m, 2H), 1.18-1.32 (m, 2H), 0.87-0.92 (m, 3H); $^{13}\text{C NMR}$ (100 MHz, CDCl_3) δ 167.77, 167.67, 167.11, 166.84, 153.38, 153.35, 151.98, 151.89, 150.69, 150.66, 148.98, 149.93, 138.15, 138.10, 132.41, 132.09, 109.83, 109.75, 106.79, 106.78, 106.73, 106.59, 106.51, 61.02, 56.37, 56.35, 53.52, 48.57, 48.27, 41.54, 41.44, 30.06, 20.16, 20.09, 13.84, 13.76, 13.70; ESIMS m/z 445 $[\text{M}+\text{H}^+]$.

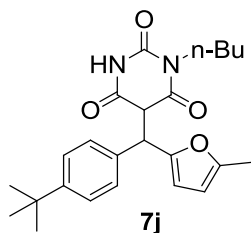


Yellow oil, analytical TLC (silica gel 60) (30% ethyl acetate in n-hexane) $R_f = 0.5$; 47% isolated yield; $^1\text{H NMR}$ (400 MHz, CDCl_3) δ 8.66-8.70 (br d, 1H), 6.81-6.91 (m,

1H), 6.57-6.62 (m, 1H), 6.04 (d, $J = 25.6$ Hz, 1H), 5.89 (br s, 1H), 5.29 (br s, 1H), 4.13-4.16 (m, 1H), 3.95 (s, 3H), 3.82-3.83 (m, 6H), 3.61-3.78 (m, 2H), 2.24 (s, 3H), 1.20-1.54 (m, 4H), 0.86-0.92 (m, 3H); ^{13}C NMR (100 MHz, CDCl_3) δ 168.21, 167.81, 167.65, 167.47, 153.51, 153.50, 152.00, 151.97, 151.43, 150.86, 150.73, 150.68, 150.63, 141.87, 124.52, 124.44, 123.92, 123.74, 109.74, 107.02, 106.95, 106.68, 106.64, 61.26, 61.18, 60.90, 56.05, 56.02, 52.70, 52.66, 41.85, 41.51, 41.44, 41.33, 30.08, 29.98, 20.21, 20.13, 13.89, 13.87, 13.75, 13.65; ESIMS m/z 445 $[\text{M}+\text{H}^+]$.



Yellow oil, analytical TLC (silica gel 60) (30% ethyl acetate in n-hexane) $R_f = 0.6$; 66% isolated yield; ^1H NMR (400 MHz, CDCl_3) δ 8.37 (br s, 1H), 7.15-7.26 (m, 4H), 5.98 (dd, $J = 2.8, 10.4$ Hz, 1H), 5.89-5.90 (m, 1H), 4.98 (br s, 1H), 4.17 (dd, $J = 3.6, 6.8$ Hz, 1H), 3.61-3.76 m, 2H), 2.83-2.93 (m, 1H), 2.26 (s, 3H), 1.30-1.46 (m, 2H), 1.15-1.23 (m, 8H), 0.86-0.92 (m, 3H); ^{13}C NMR (100 MHz, CDCl_3) δ 167.83, 167.65, 167.30, 166.94, 151.95, 151.90, 150.72, 150.67, 150.10, 149.08, 149.02, 133.94, 133.93, 133.82, 129.00, 128.97, 126.89, 126.84, 109.88, 109.82, 106.68, 106.65, 53.64, 53.61, 48.17, 41.46, 41.38, 33.92, 29.94, 24.11, 24.08, 24.03, 20.18, 20.11, 13.88, 13.78, 13.72; ESIMS m/z 397 $[\text{M}+\text{H}^+]$.



Brown oil, analytical TLC (silica gel 60) (25% ethyl acetate in n-hexane) $R_f = 0.5$;

73% isolated yield; $^1\text{H NMR}$ (400 MHz, CDCl_3) δ 8.47 (d, $J = 7.2$ Hz, 1H), 7.22-7.34

(m, 4H), 5.98 (dd, $J = 2.8, 12.8$ Hz, 1H), 5.88-5.90 (m, 1H), 4.98-5.00 (m, 1H), 4.16

(dd, $J = 3.6, 6.8$ Hz, 1H), 3.61-3.76 (m, 2H), 2.26 (s, 3H), 1.33-1.44 (m, 2H), 1.33 (s,

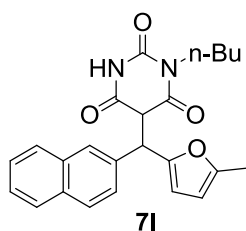
9H), 1.14-1.29 (m, 2H), 0.86-0.92 (m, 3H); $^{13}\text{C NMR}$ (100 MHz, CDCl_3) δ 167.85,

167.72, 167.49, 167.17, 151.94, 151.88, 151.33, 151.28, 150.73, 150.66, 150.23,

133.64, 133.53, 128.75, 128.72, 125.73, 125.69, 109.89, 109.83, 106.68, 106.65,

53.62, 53.59, 48.20, 48.03, 41.44, 41.36, 34.72, 31.48, 29.95, 20.18, 20.11, 13.91,

13.78, 13.72; ESIMS m/z 410 $[\text{M}+\text{H}^+]$.

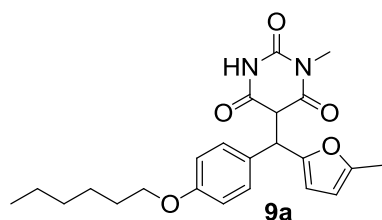


Yellow oil, analytical TLC (silica gel 60) (25% ethyl acetate in n-hexane) $R_f = 0.4$;

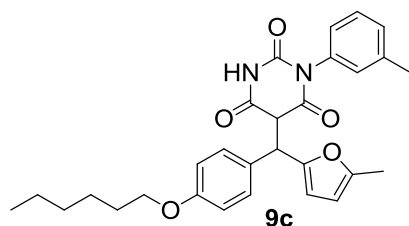
35% isolated yield; $^1\text{H NMR}$ (400 MHz, CDCl_3) δ 8.10-8.24 (m, 1H), 7.82-7.91 (m,

2H), 7.41-7.61 (m, 4H), 6.01 (dd, $J = 2.8, 10.8$ Hz, 1H), 5.92-5.94 (m, 2H), 4.17 (dd,

$J = 3.6, 14.8$ Hz, 1H), 3.72-3.87 (m, 1H), 3.66 (t, $J = 7.6$ Hz, 1H), 2.27 (s, 3H), 1.44-1.51 (m, 1H), 1.13-1.31 (m, 4H), 0.80-0.94 (m, 3H); ^{13}C NMR (100 MHz, CDCl_3) δ 168.76, 167.78, 167.22, 166.56, 152.23, 152.17, 150.27, 150.17, 150.13, 134.10, 133.69, 133.62, 130.92, 130.85, 129.62, 129.58, 128.89, 127.82, 127.68, 127.15, 127.12, 125.94, 125.92, 125.35, 122.31, 122.23, 110.24, 110.18, 106.96, 52.36, 52.33, 43.92, 43.24, 41.58, 41.43, 30.01, 29.85, 20.16, 20.10, 13.89, 13.83, 13.80, 13.67; ESIMS m/z 404 $[\text{M}+\text{H}^+]$.



Brown oil, analytical TLC (silica gel 60) (25% ethyl acetate in n-hexane) $R_f = 0.5$; 20% isolated yield; ^1H NMR (400 MHz, CDCl_3) δ 7.96 (br s, 1H), 7.17-7.22 (m, 2H), 6.81-6.84 (m, 2H), 5.97 (dd, $J = 2.8, 8.4$ Hz, 1H), 5.90 (br s, 1H), 4.91-4.93 (m, 1H), 4.19 (dd, $J = 3.6, 15.2$ Hz, 1H), 3.93 (t, $J = 6.4$ Hz, 2H), 3.13 (s, 3H), 2.26 (d, $J = 4.8$ Hz, 3H), 1.73-1.80 (m, 2H), 1.61 (br s, 2H), 1.45-1.47 (m, 2H), 1.33-1.35 (m, 4H), 0.89-0.92 (m, 3H); ^{13}C NMR (100 MHz, CDCl_3) δ 168.10, 167.62, 159.12, 159.01, 151.80, 150.64, 150.43, 150.12, 129.93, 129.83, 128.11, 127.62, 114.56, 109.62, 109.53, 106.46, 106.43, 68.02, 53.81, 53.64, 47.97, 47.92, 31.60, 29.23, 27.64, 27.56, 25.74, 22.61, 14.04, 13.06; ESIMS m/z 413 $[\text{M}+\text{H}^+]$.



Brown oil, analytical TLC (silica gel 60) (25% ethyl acetate in n-hexane) $R_f = 0.3$;

46% isolated yield; ^1H NMR (400 MHz, CDCl_3) δ 8.54 (d, $J = 9.6$ Hz, 1H), 7.20-7.34

(m, 3H), 6.66-6.89 (m, 4H), 5.99 (dd, $J = 2.8, 15.2$ Hz, 1H), 5.92 (dd, $J = 2.4, 8.8$ Hz,

1H), 5.01 (dd, $J = 3.6, 9.2$ Hz, 1H), 4.32 (t, $J = 3.2$ Hz, 1H), 3.93-3.97 (m, 2H), 2.35

(s, 3H), 2.27-2.31 (d, $J = 14$ Hz, 3H), 1.74-1.82 (m, 2H), 1.46 (m, 2H), 1.33-1.35 (m,

4H), 0.89-0.92 (m, 3H); ^{13}C NMR (100 MHz, CDCl_3) δ 168.08, 167.66, 167.43,

166.93, 159.46, 159.38, 152.12, 152.10, 149.97, 139.62, 133.44, 130.41, 130.41,

130.34, 129.35, 129.02, 128.21, 128.00, 125.38, 114.91, 114.86, 110.04, 106.77,

106.71, 68.28, 54.21, 54.07, 48.56, 48.30, 31.80, 29.45, 29.42, 25.95, 25.94, 22.80,

21.48, 14.23, 13.86, 13.76; ESIMS m/z 488 $[\text{M}+\text{H}^+]$.

3.5 Reference

- (1) For reviews of history of barbiturate: a) <http://science.kennesaw.edu/mhermes/phenol/pheno01.htm>. ChemCases.Com., sponsored by NSF, written by Prof. Sally Boudint. b) Goth, A. *Medical Pharmacology Principles and Concepts*; C. V. Mosby Co. St. Louis, MO. 1968. c) Windholtz, M. Editor, *The Merck Index*. 10th ed. Rahway; **1983**. d) DeRuiter, J. *Principles of Drug Action* 2. http://web6.duc.auburn.edu/~deruija/GABA_BarbAnalog2002.pdf. e) Gulliya, K. S. U. S. Patent 5,869,494; *Chem Abstr.* **1999**. f) Sakai, K.; Satoh, Y. International Patent WO9950252A3; *Chem Abstr.* **2000**.
- (2) Figueroa-Villar, J. D.; Rangel, C. E.; Dos Santos, L. N. *Synth. Commun.* **1992**, *22*, 1159.
- (3) Tanaka, K.; Cheng, X.; Yoneda, F. *Tetrahedron* **1988**, *44*, 3241.
- (4) Tanaka, K.; Cheng, X.; Kimura, T.; Yoneda, F. *Chem. Pharm. Bull.* **1986**, *34*, 3945.
- (5) Ikeda, A.; Kawabe, Y.; Sakai, T.; Kaeasaki, K. *Chem. Lett.* **1989**, 1803.
- (6) a) Villemin, D; Labiad, B. *Synth. Commun.* **1990**, 3333. b) Obrador, E.; Castro, M.; Tamariz, J.; Zepeda, G.; Miranda, R.; Delgado, F. *Synth. Commun.* **1998**, *28*,

4696. c) Alcerreca, G.; Sanabria, R.; Miranda, R.; Arroyo, G.; Tamariz, J.; Delgado, F. *Synth. Commun.* **2000**, *30*, 1295. d) Bigi, F.; Conforti, M. L., Maggi, R.; Piccinno, A.; Satori, G. *Green Chemistry*, **2000**, *2*, 101. e) Vvedenskii, V. D., *Khim. Geterotski. Soedin*, **1969**, *5*, 1092. f) Bandgar, B. P., Zirange, S. M., Wadgaonkar, P. P., *Synth. Commun.*, **1997**, *27*, 1153. g) Villemin, D. *Chem. Commun.* **1983**, 1092. h) Kim, S., Kwon, P., Kwon, T., *Synth. Commun.* **1997**, *27*, 533. i) Jourdain, F., Pommelet, J. C., *Synth. Commun.* **1997**, *27*, 483.
- (7) a) Figueroa-Villar, J. D.; Rangel, C. E.; Dos Santos, L. N. *Synth. Commun.* **1992**, *22*, 1159. b) Tanaka, K.; Cheng, X.; Yoneda, F. *Tetrahedron* **1988**, *44*, 3241. c) Tanaka, K.; Cheng, X.; Kimura, T; Yoneda, F. *Chem.Pharm. Bull.* **1986**, *34*, 3945. d) Ikeda, A.; Kawabe, Y.; Sakai, T.; Kaeasaki. K. *Chem.Lett.* **1989**, 1803.
- (8) a) Xu, Y.; Dolbier, W. R. *Tetrahedron* **1998**, *54*, 6319-6328. b) Figueroa-Villar, J. D.; Carneiro, C. L.; Cruz, E. R. *Heterocycles* **1992**, *34*, 891-894. c) Seeliger, F.; Berger, S. T. A.; Remennikov, G. Y.; Polborn, K.; Mayr, H, *J. Org. Chem.* **2007**, *72*, 9170-9180. d) Jursic, B. S.; Stevens, E. D. *Tetrahedron Lett.* **2003**, *44*, 2203-2210. e) Vieira, A. A.; Gomes, N. M.; Matheus, M. E.; Fernandes, P. D.; Figueroa-Villar, J. D. *J. Braz. Chem. Soc.* **2011**, *22*, 364-371. f) Shaabani, A.;

Teimouri, M. B.; Bijanzadehb, H. R.; *Tetrahedron Lett.* **2002**, *43*, 9151-9154. g)

Figuroa-Villar, J. D.; Oliveira, S. C. G.; *J. Braz. Chem. Soc.* **2011**, *20*,

2101-2107.

Chapter 4

Kinetic and Binding Studies of Amide-Based HB-DAD

Organocatalysis

4.1 Introduction

4.1.1 Kinetics Studies of Hydrogen Bonding Organocatalysts

Chemical kinetics is the study of reaction rate.^[1,2] One of the primary goals of chemical kinetics experiments is to determine the rate law for a chemical reaction.

Pseudo-first-order kinetics is one of the commonly used approaches.^[3]

The rate law is shown in equation 1. In pseudo-first-order method, the concentration of B (large excess) is regarded as a constant. In this regard, the actual rate constant (k) with the constant concentration of B ($[B]_o$) forming a new constant called k_{obs} and shown in equation 2.

$$r = k[A]^n[B]^m = (k[B]_o^m) [A]^n = k_{obs}[A]^n \quad \text{(Equation 1)}$$

$$k_{obs} = k[B]_o^m \quad \text{(Equation 2)}$$

Hydrogen bonding catalysts are able to accelerate organic transformations.^[4-6] In particular, hydrogen bonding donor-donor (bidentate) catalysts (such as thioureas), catalyze Diels-Alder reactions.^[7] Schreiner and coworkers reported that using ^1H NMR to investigate the relative rate constant (k_{rel}) of thioureas in catalyzing

Diels-Alder reaction of α,β -unsaturated carbonyl compounds with 10-fold excess of cyclopentadiene by pseudo-first-order method.

In this chapter, we use the reaction of benzylidene barbiturate **6a** with 2-methylfuran to determine the relative rate constants of a series of HB-DAD organocatalysts by ^1H NMR spectroscopy.

4.1.2 UV / Vis. Titration Binding Constant Study

One of the fundamental issues in supramolecular chemistry is the quantification of intermolecular interaction e.g. hydrogen bond.^[8] Optical spectroscopy is the widely applied experimental method^[9] for binding constant investigation of supramolecular complexes involving hydrogen bonding interaction.^[10]

In 2011, Spange and co-workers reported the benzylidene barbiturate chromophore for binding study of their HB-DAD structures.^[11] The UV / Vis. titration method has been applied for this binding study. The binding isotherms of HB-DAD structures and benzylidene barbiturate chromophores were constructed to determine binding constants of the corresponding hydrogen bond complexes.

In this regard, we employ the benzylidene barbiturate chromophore to study the binding constants of a series of our HB-DAD organocatalysts by UV / Vis. titration method.

4.1.3 The Objectives of This Chapter

We set out to investigate (1) the kinetics studies of conjugate additions of benzylidene barbiturate **6a** and 2-methylfuran with HB-DAD organocatalysts by ^1H NMR spectroscopy, (2) the binding studies of benzylidene barbiturate chromophore with HB-DAD organocatalysts by UV / Vis. titration method, and (3) the correlation of rate constants and binding constants.

4.2 Results and Discussion

4.2.1 Kinetics Study of Amide-Based HB-DAD Organocatalysts

Studies on the catalytic activities of 20 mol% of HB-DAD organocatalysts **1a**, **1b**, **1c**, **2a**, **2b**, and **3a** in conjugate additions of benzylidene barbiturate **6a** (0.025 mmol, 0.05 M) with 2-methylfuran (0.25 mmol, 0.5 M) to give adduct **7a** in CDCl₃ at 25 °C in 2 h were conducted. In the course of reaction, the ¹H NMR spectra were recorded every 5 minutes for a total of 120 minutes. With reference to the internal standard, the concentration and yield of adduct **7a** were determined (Figure 4.1 and Table 4.1).

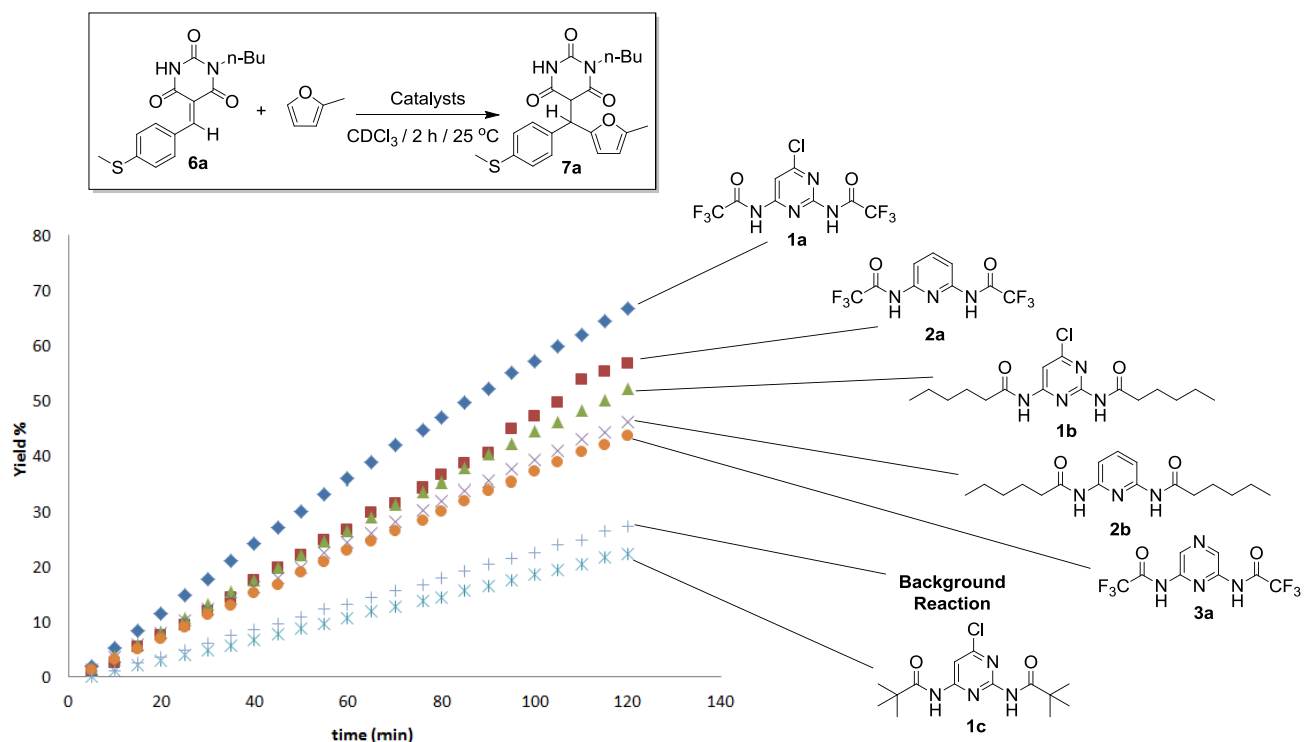
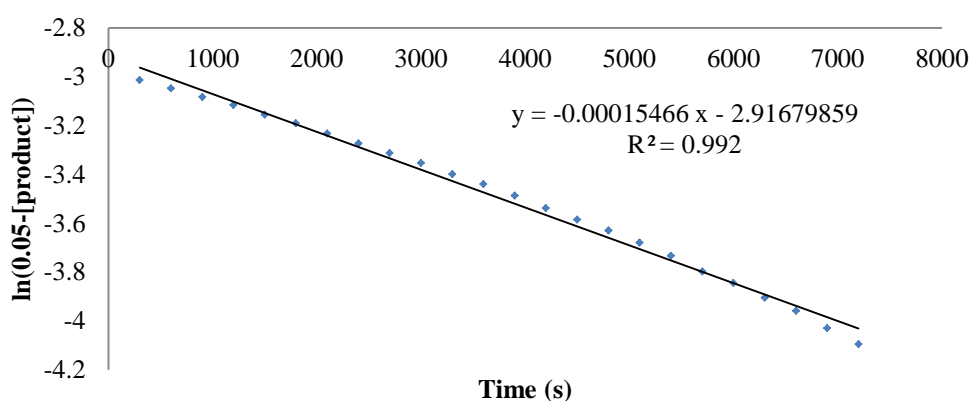


Figure 4.1 Kinetics data of conjugate addition of **6a** and 2-methylfuran catalyzed by HB-DAD organocatalysts

As depicted in Figure 4.1, the yields of adduct **7a** were recorded and plotted with reaction time. The reaction, using 20 mol% of **1a**, gave the highest yield of adduct **7a** (66%) while using **2a** gave adduct **7a** in 56% yield. Both **1b** and **2b** were found to be catalytically active, giving **7a** in 52% and 49% yields, respectively. In addition, the conjugate addition using **3a** could lead to adduct **7a** in 44% yield. However, **1c** was found to be inactive to catalyze conjugate addition of **6a** with 2-methylfuran (yield = 22%). The yield of adduct **7a** is lower than that of the reaction conducted without catalyst (yield = 28%).

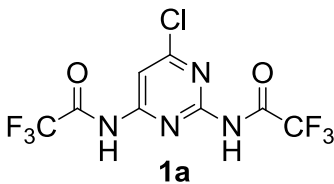
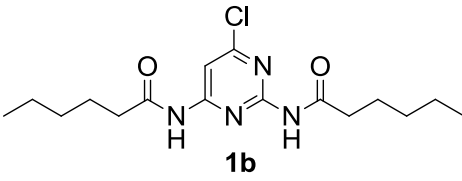
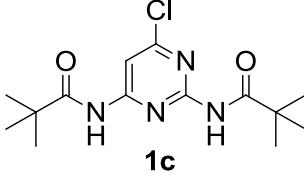
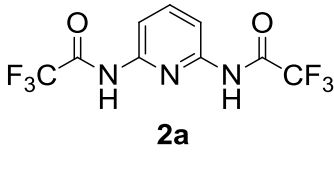
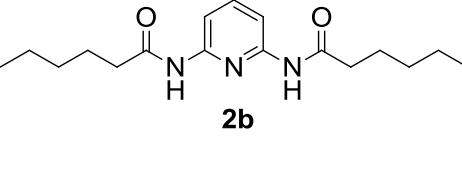
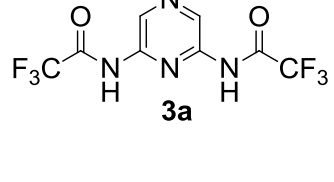
With a 10-fold excess of 2-methylfuran, all conjugate additions of **6a** were pseudo-first-order, and the corresponding rate constant k_{obs} were determined and depicted in Table 4.1. For the determination of k_{obs} , the kinetic data was plotted as $\ln[\text{concentration of benzylidene barbiturate } \mathbf{6a}]$ against time.^[7] The rate constant k_{obs} is determined by the negative slope of the plot.



In kinetics studies, the rate constant k_{obs} of **1a** (chloro-pyrimidine HBA and

trifluoroacetyl activator) was found to be $1.48 \times 10^{-4} \text{ s}^{-1}$ (entry 1) while **2a** (pyridine HBA and trifluoroacetyl activator) was $1.22 \times 10^{-4} \text{ s}^{-1}$ (entry 4). The rate constants (k_{obs}) were observed for **1b** (chloro-pyrimidine HBA and hexanoyl activator) and **2b** (pyridine HBA and hexanoyl activator) in $1.04 \times 10^{-4} \text{ s}^{-1}$ and $0.96 \times 10^{-4} \text{ s}^{-1}$, respectively (entries 2 and 5). In addition, the k_{obs} of **3a** (pyrazine HBA and trifluoroacetyl activator) and **1c** (chloro-pyrimidine HBA and *t*-butyl activator) were $0.82 \times 10^{-4} \text{ s}^{-1}$ and $0.37 \times 10^{-4} \text{ s}^{-1}$, respectively (entries 3 and 6). The rate constant of the reaction without catalyst was $0.39 \times 10^{-4} \text{ s}^{-1}$ (entry 7).

Table 4.1 Rate constant determinations by ^1H NMR studies

Entr y	HB-DAD Organocatalyst	$k_{obs} \times 10^{-4}$ (s^{-1}) ^[a]	$k_{cat} \times 10^{-4}$ (s^{-1}) ^[b]	k_{rel} ^[c]
1	 1a	1.484	1.091	2.78
2	 1b	1.043	0.650	1.68
3	 1c	0.366	-0.027	-0.068
4	 2a	1.221	0.828	2.11
5	 2b	0.960	0.567	1.45
6	 3a	0.818	0.425	1.08
7	-----	0.3928	$k_{uncata} = 0.3928$	-----

^[a] k_{obs} is obtained from kinetic result directly. ^[b] $k_{cata} = k_{obs} - k_{uncata}$. ^[c] $k_{rel} = k_{cata} / k_{uncata}$.

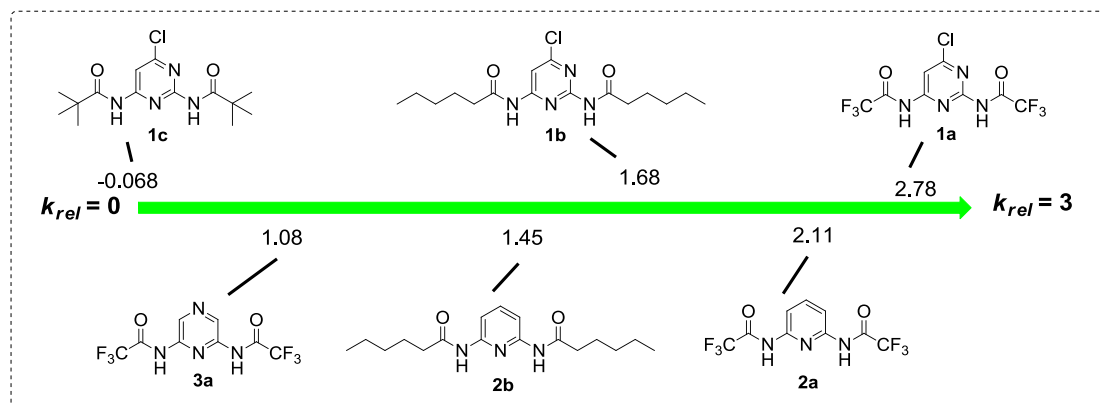
The calculation of k_{rel}	For instance, (Table 4.1, entry 1)
1a catalyzed reaction: $k_{obs} = 0.00014843 \text{ s}^{-1}$	
Uncatalyzed reaction: $k_{obs} = k_{uncata} = 0.00003928 \text{ s}^{-1}$	
$k_{cata} = k_{obs} - k_{uncata}$	
$= 0.00014843 - 0.00003928$	
$= 0.00010915 \text{ s}^{-1}$	
$k_{rel} = k_{cata} / k_{uncata}$	
$= 0.00010915 / 0.00003928$	
$= 2.78$ at 20 mol% of 1a	

Scheme 4.1 The calculation of the relative rate constant of HB-DAD organocatalyst

1a

From the kinetics constant (k_{obs}), the relative rates of HB-DAD organocatalysts were calculated (Scheme 4.1). The relative rate constant (k_{rel}) was 2.78 for **1a**-catalyzed conjugate addition of **6a** (Table 4.1; entry 1). It means that 20 mol% of amide-based HB-DAD organocatalyst **1a** increases the conjugate addition rate by a factor of ≈ 2 . The k_{rel} of **2a** was 2.11 (entry 4) while the k_{rel} of **3a** was obtained as 1.08 (entry 6). In addition, the k_{rel} of **1b** and **2b** were 1.68 and 1.45, respectively (entries 2 and 5). The k_{rel} of **1c** was -0.068 (entry 3), meaning that 20 mol% of **1c** gave no catalytic activity to conjugate addition of **6a** with 2-methylfuran. This result indicates that the more electron deficient activator (trifluoroacetyl group) afforded the higher catalytic activities than the hexanoyl group as the activator.

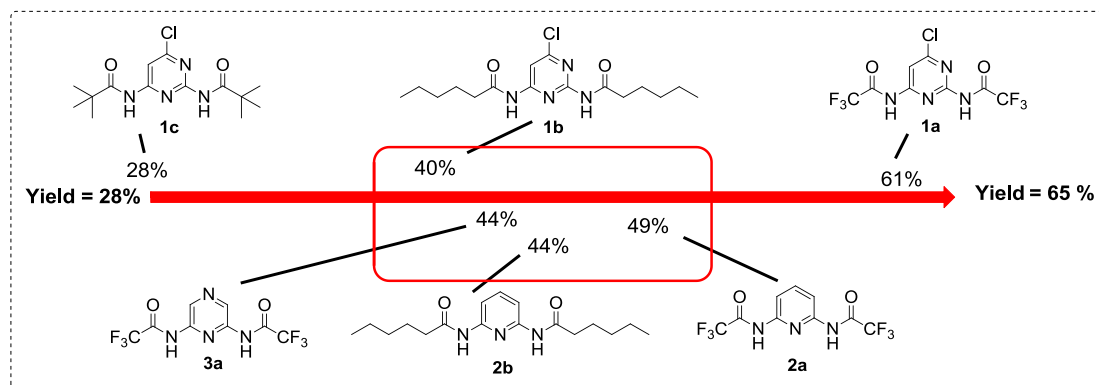
A gradually increasing trend in the relative rate constants of HB-DAD organocatalysts in catalyzing conjugate addition of **6a** is shown (Scheme 4.2). The corresponding relative rate increased from -0.068 to 2.78 because of the increase of electrophilicity of amide- based HB-DAD organocatalysts.



Scheme 4.2 The relative rate constants scale of HB-DAD organocatalysts in catalyzing conjugate addition of benzylidene barbiturate **6a**

As mentioned in chapter 2, HB-DAD organocatalysts **1a-1c**, **2a**, **2b** and **3a** in catalyzing conjugate addition of **6a** with 2-methylfuran gave adduct **7a** in 28-61% yields. Using these data from chapter 2, a scale of yield of adduct **7a** was constructed (Scheme 4.3). However, the correlation of product yield and electrophilicity of HB-DAD organocatalysts cannot be obtained as the **2b**- and **3a**-catalyzed conjugate addition of **6a** gave 44% yields. The results in Schemes 4.2, 4.3 indicates that determination of relative rate constants is a better method to understand catalytic activities of HB-DAD organocatalysts in conjugate addition of **6a** than product yield

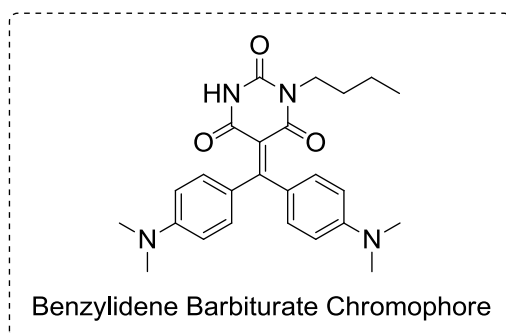
determination because subtle changes of catalytic activities of amide-based HB-DAD organocatalysts in relative rate constant studies could be observed.



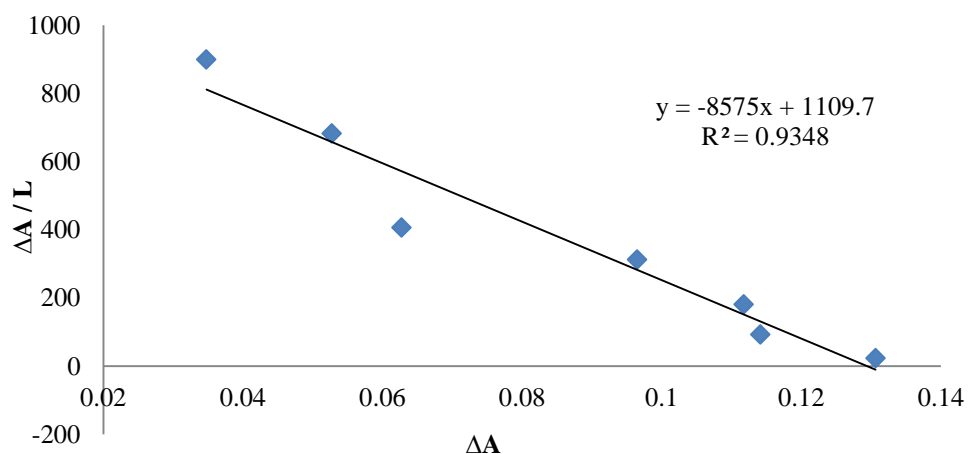
Scheme 4.3 The scale of yield of **7a** of HB-DAD organocatalysts in catalyzing conjugate addition of benzylidene barbiturate **6a**

4.2.2 Binding Study of Amide-Based HB-DAD Organocatalysts

Studies on the binding constants of HB-DAD organocatalysts (concentration of amide-based HB-DAD organocatalyst: $[R] = 4 \times 10^{-5} - 5.8 \times 10^{-3}$ M) **1a**, **1b**, **2a**, and **2c** with benzylidene barbiturate chromophore (concentration of benzylidene barbiturate chromophore: $[S] = 2 \times 10^{-5}$ M) were conducted with UV / Vis. spectroscopy by monitoring the change of absorbance (ΔA).



By plotting of ΔA at 525 nm of UV / Vis. spectra against the ratio of ($[R] / [S]$), binding isotherms could be obtained. The binding constants were obtained by nonlinear regression using equation 3. In addition, by plotting the ($\Delta A / [R]$) against ΔA at 525 nm of UV / Vis. spectra, the linearized Scatchard plot was drawn. The binding constant could be obtained from the negative slope of the linearized Scatchard plot (equation 4). The linearized Scatchard plot was used in determination of the binding constants of **1a**, **1b**, **2a**, and **2b**.



Linearized Scatchard plot of **1a**

$$\Delta A = \frac{\Delta \varepsilon \cdot K \cdot d \cdot [S] \cdot [R]}{1 + K \cdot [R]} \quad \text{(Equation 3)}$$

$$\frac{\Delta A}{d \cdot [R]} = - \frac{\Delta A \cdot K}{d} + K \cdot \Delta \varepsilon \cdot [S] \quad \text{(Equation 4)}$$

[S]: Concentration of benzylidene barbiturate chromophore

[R]: Concentration of amide-based HB-DAD organocatalysts

K: Binding Constant

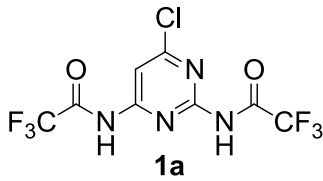
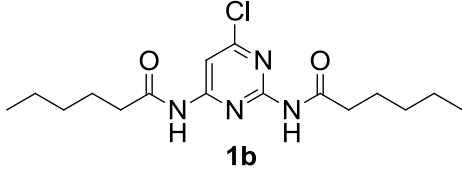
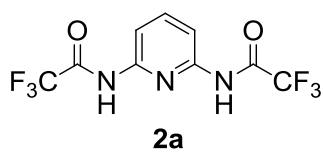
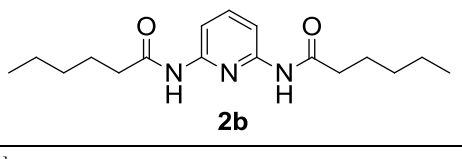
ΔA : Change of absorbance

$\Delta \varepsilon$: Molar absorptivity

d: Path length

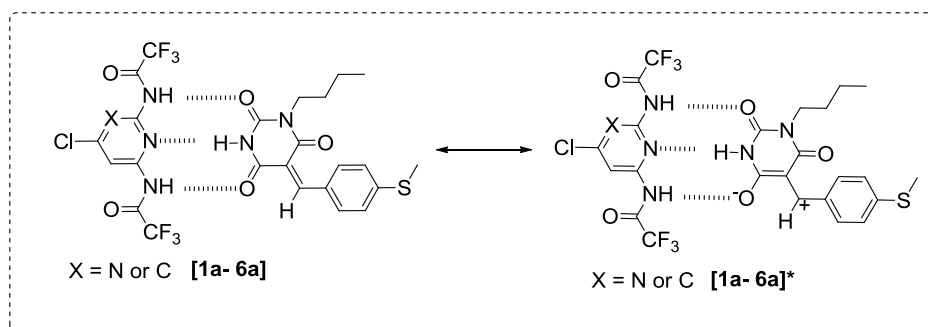
The highest binding constant for **1a** (chloro-pyrimidine HBA and trifluoroacetyl activator) ($K_A = 8936 (\pm 723) \text{ M}^{-1}$; Table 4.2, entry 1) was obtained. The binding constant $7747 (\pm 380) \text{ M}^{-1}$ of **2a** (pyridine HBA and trifluoroacetyl activator) was obtained (entry 3). The binding constants of **1b** (chloro-pyrimidine HBA and hexanoyl activator) and **2b** (pyridine HBA and hexanoyl activator) were $6447 (\pm 367) \text{ M}^{-1}$ and $4895 (\pm 1019) \text{ M}^{-1}$, respectively (entries 2 and 4). These results indicate that the electron withdrawing trifluoroacetyl activator led to a significant increase in binding strength. Notably, chloro-pyrimidine is a better HBA than pyridine in achieving high binding strength.

Table 4.2 Binding constants of HB-DAD organocatalysts^[a]

Entry	HB-DAD Organocatalyst	K_A (M^{-1})
1	 1a	8936 (\pm 723)
2	 1b	6447 (\pm 367)
3	 2a	7747 (\pm 380)
4	 2b	4895 (\pm 1019)

^[a] K_A is the binding constant obtained by linearized Scatchard plot.

In 2003, Rotello and co-workers reported the different energetic components of a hydrogen bond. The polarization term played a major role for changes of electronic structure of hydrogen bonded substrates.^[12] For the hydrogen bonded substrate benzylidene barbiturate **6a** (Scheme 4.4), a shift is induced if electron density towards the hydrogen bond acceptor group (carbonyl-group) enhances the polarization of the benzylidene barbiturate **6a** and further enhance the electron deficiency of C-C double bond as electrophilic center.^[11]



Scheme 4.4 The polarization of [1a-6a]

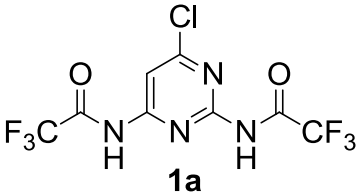
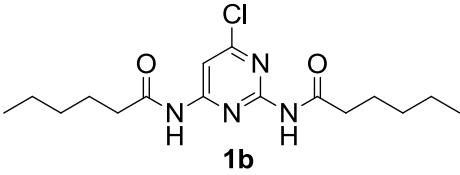
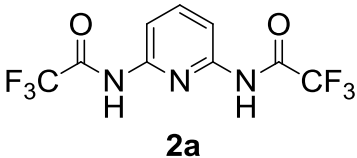
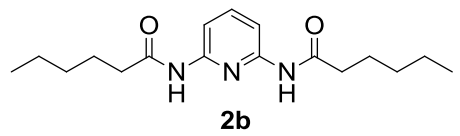
The polarization effect in benzylidene barbiturate **6a** became stronger by increasing the electron deficiency of HBD (N-H) of HB-DAD organocatalyst **1a**. As a result, in a higher binding energy of the hydrogen bonds of DAD-ADA binding mode is observed. Hence, both DAD-ADA hydrogen bond complex stability and electrophilicity of HB-DAD organocatalysts increased in the order **2b** < **1b** < **2a** < **1a**.

4.2.3 Correlation of Rate Constants and Binding Constants of Amide-Based HB-DAD

Organocatalysts

A gradually escalating trend of relative rate constants of conjugate addition of **6a** was obtained in kinetics studies while an increasing order of electrophilicity of HB-DAD organocatalysts **2b** < **1b** < **2a** < **1a** was determined in binding studies. Particularly, a correlation was observed between kinetics and binding studies (Table 4.3 and Figure 4.2).

Table 4.3 Treatment of relative rate and binding constants of HB-DAD organocatalysts

Entry	Catalysts	K_A (M^{-1})	$\ln K_A$	k_{rel}	$\ln k_{rel}$
1	 <p style="text-align: center;">1a</p>	8936	9.10	2.78	1.02
2	 <p style="text-align: center;">1b</p>	6447	8.96	1.68	0.52
3	 <p style="text-align: center;">2a</p>	7747	8.77	2.11	0.75
4	 <p style="text-align: center;">2b</p>	4895	8.50	1.45	0.37

The natural logarithm of binding constants and relative rate constants were obtained in Table 4.3.^[13] By plotting of $\ln K_A$ against $\ln k_{rel}$ of HB-DAD organocatalysts, a linear correlation was obtained ($R^2 = 0.92$). The results indicated that higher binding constant gave higher relative rate of the conjugate addition.

The stronger binding of amide-based HB-DAD organocatalysts and HB-ADA benzylidene barbiturate chromophore through DAD-ADA binding mode gave the higher relative rate constants of conjugate addition of benzylidene barbiturate **6a** with 2-methylfuran. Therefore, the higher electrophilicities of HB-DAD organocatalysts

are correlated with the relative rate constants.^[11,12]

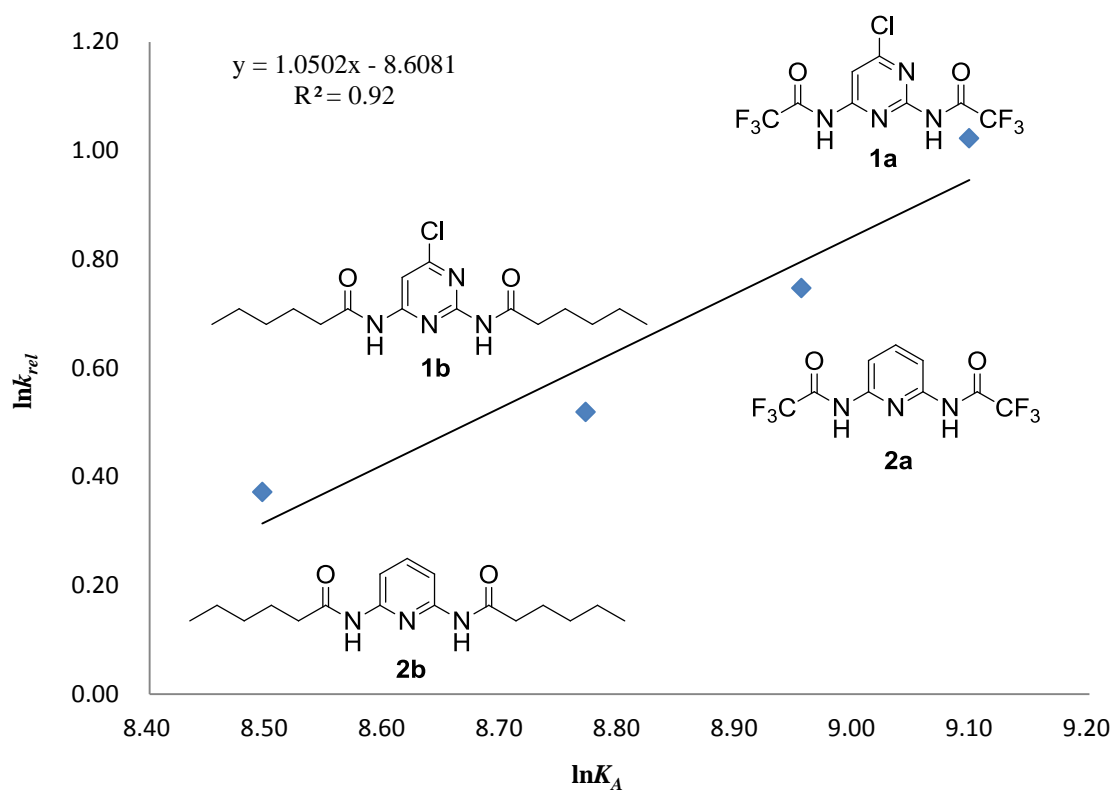


Figure 4.2 Correlation of natural logarithm relative rates and binding constants of HB-DAD organocatalysts

4.3 Conclusion

Kinetics and binding studies of conjugate addition of benzylidene barbiturates catalyzed by amide-based HB-DAD organocatalysts have been conducted. Particularly, **1a** was found to have the highest binding constant $K_A = 8936 (\pm 723) \text{ M}^{-1}$ and relative rate constant $k_{rel} = 2.78$.

Furthermore, the adjustable electrophilicity of conjugate addition of HB-ADA benzylidene barbiturates catalyzed by amide-based HB-DAD organocatalysts have been supported by linear correlation in $\ln K_A$ against $\ln k_{rel}$ ($R^2 = 0.92$).

4.4 Experimental Section

4.4.1 ¹H NMR Kinetics Study of Conjugate Addition of Benzylidene Barbiturate ^[7]

All reactions were conducted with 0.05 M of benzylidene barbiturate **6a**, 0.025 mmol of 2-methylfuran, 0.03 mmol of internal standard dichloromethane and 20 mol % HB-DAD organocatalysts. Stocks solutions of **6a** (0.083 M) and the HB-DAD organocatalysts (0.05 M) in deuterated CDCl₃ were prepared in 2 mL vials. An NMR tube was charged with 0.3 mL of **6a** stock solution followed by 0.1 mL of HB-DAD organocatalysts stock solution, 1.98 μL of dichloromethane and made up to 0.5 mL with CDCl₃. After adding 22.3 μL of 2-methylfuran, the solutions were mixed thoroughly. The first NMR spectrum was taken after 5 min after the addition of 2-methylfuran and additional ¹H NMR spectra were recorded every 5 min for 120 min.

The methylene peak of dichloromethane (DCM) (5.3, singlet, 2H) was monitored with the ratio of product signal (4.91, multiplet, 1H) that was calibrated as 1. The number of mole of product was calculated based on the known number of mole of internal standard (DCM) in the reaction using:

No. of mmol of product = [mmol of DCM x 2 / Ratio of DCM signal]

[Concentration of product] = No. of mmol of product/ 0.5mL

The k_{obs} of each reactions was determine using the slope of the plot of the ln (0.05 –

[Concentration of product]) vs time.

4.4.2 Results in ¹H NMR Kinetic Study of Conjugate Addition of Benzylidene

Barbiturates^[7]

Table 4.4 Rate constants determinations with ¹H NMR studies

Catalysts	$k_{obs} \times 10^{-4} \text{ (s}^{-1}\text{)}$	$k_{cat} \times 10^{-4} \text{ (s}^{-1}\text{)}$	k_{rel}
-----	0.4612	$k_{uncata} = 0.4612$	1.0
-----	0.3244	$k_{uncata} = 0.3244$	1.0
1a	1.5466	1.1538	2.94
1a	1.4221	1.0293	2.62
1b	1.0437	0.6509	1.66
1b	1.0548	0.6620	1.69
1c	0.3662	-0.0266	-0.0677
2a	1.2174	0.8246	2.10
2a	1.2239	0.8311	2.12
2b	0.8725	0.4797	1.22
2b	1.0475	0.6547	1.67
3a	0.8178	0.4250	1.08

The calculation of relative rate

1a catalyzed reaction: $k_{obs} = 0.00015466 \text{ s}^{-1}$

Uncatalyzed reaction: $k_{obs} = k_{uncata} = 0.00004612 \text{ s}^{-1}$

$$\begin{aligned}k_{cat} &= k_{obs} - k_{uncata} \\ &= 0.00015466 - 0.00004612 \\ &= 0.00010854 \text{ s}^{-1}\end{aligned}$$

$$\begin{aligned}k_{rel} &= k_{cat} / k_{uncata} \\ &= 0.00010854 / 0.00004612 \\ &= 2.35 \text{ at } 20\text{mol \% of } \mathbf{1a}\end{aligned}$$

4.4.3 UV / Vis. Titration Binding Study of Benzylidene Barbiturate Chromophore with Amide-Based HB-DAD Organocatalysts ^[11]

Ten graduated flasks (5 mL) were treated with 0.5 mL of stock solution of benzylidene barbiturate chromophore (final concentration: $2 \times 10^{-5} \text{ molL}^{-1}$) and 20-3000 μL (corresponding to a 2-290 folds excess) of a stock solution of amide-based HB-DAD organocatalyst, and filled up to 5 mL. The change in absorbance was monitored and evaluated by linearized Scatchard plot (S1). The given values of K were the average of two runs.

$$\frac{\Delta A}{d \cdot [R]} = - \frac{\Delta A \cdot K}{d} + K \cdot \Delta \varepsilon \cdot [S] \quad (\text{S1})$$

[S]: Concentration of benzylidene barbiturate chromophore

[R]: Concentration of amide-based HB-DAD organocatalysts

K: Binding Constant

ΔA : Change of absorbance

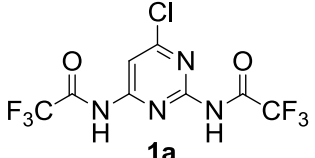
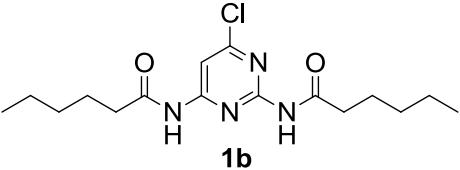
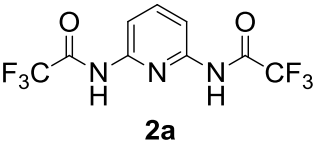
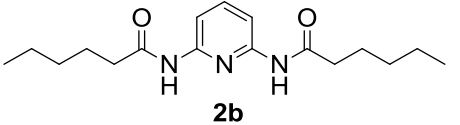
$\Delta \varepsilon$: Molar absorptivity

In Scatchard Plot

$K = - (\text{slope})$

$\Delta \varepsilon = (\text{x-intercept}) / [S]$

Table 4.5 Binding constant determinations with UV / Vis. titration method

Entr y	HB-DAD Organocatalysts	1 st Trial K_A (M^{-1})	2 nd Trial K_A (M^{-1})	Averaged K_A (M^{-1})
1	 1a	8575	9298	8936 (±723)
2	 1b	6264	6631	6447 (±367)
3	 2a	7557	7937	7747 (±380)
4	 2b	5404	4385	4895 (±1019)

4.5 References

- (1) Denisov, E. T.; Sarkisov, O. M.; Likhtenshtein, G. I. *Chemical Kinetics Fundamentals and New Developments*, Elsevier, 2003. b) Logan, S. R. *Fundamentals of Chemical Kinetics*, Longman, 1996. c) Masel, R. I. *Chemical Kinetics and Catalysis*, Wiley-VCH, Weinheim, 2001. d) Logan, S. R. *Introductory Reaction Kinetics – an unacknowledged difficulty. Education in Chemistry*, **1984**, *21*, 20-22.
- (2) a) Logan, S. R. *J. Chem. Educ.* **1982**, *59*, 279-281. b) Viossat, V.; Ben-Aim, R. I. *J. Chem. Educ.* **1993**, *70*, 732-738. c) McCracken, D. R.; Buxton, G. V. *Nature* **1982**, *292*, 439-441. d) Tardy, D. C.; Cater, E. D. *J. Chem. Educ.* **1983**, *60*, 109-111. e) Brosseau, V. A.; Basila, J. R.; Smalley, J. F.; Strong, R. L. *J. Am. Chem. Soc.* **1972**, *94*, 716-719. f) Edwards, J. O.; Greene, E. F.; Ross, J. *J. Chem. Educ.* **1968**, *45*, 381-385.
- (3) a) Espenson, J. H. *Chemical Kinetics and Reaction Mechanisms*. New York: McGraw-Hill, 1995. b) MacAlduff, E. J. *J. Chem. Educ.* **1980**, *57*, 627-628. c) Nordman, C. E.; Blinder, S. M. *J. Chem. Educ.* **1975**, *51*, 790-791. d) Moss, S. J.; Coady, C. J. *J. Chem. Educ.* **1983**, *60*, 455-461.
- (4) a) Schreiner, P. R.; Wittkopp, A. *Org. Lett.* **2002**, *4*, 217-220. b) Kelly, T. R.; Meghani, P.; Ekkundi, V. S. *Tetrahedron Lett.* **1990**, *31*, 3381-3384.

- (5) Curran, D. P.; Kuo, L. H. *Tetrahedron Lett.* **1995**, *36*, 6647-6650.
- (6) a) Curran, D. P.; Kuo, L. H. *J. Org. Chem.* **1994**, *59*, 3259-3261. b) Schuster, T.; Kurtz, M.; Göbel, M. W. *J. Org. Chem.* **2000**, *65*, 1697-1701.
- (7) Wittkopp, A.; Schreiner, P. R. *Chem. Eur. J.* **2003**, *9*, 407-414.
- (8) a) Thordarson, P. *Chem. Soc. Rev.* **2011**, *40*, 1305-1323. b) Connors, K. A. *Comprehensive Supramolecular Chemistry* ed. Atwood, J. L.; Davies, J. E. D.; McNicol, D. D.; Vogtle, F., Pergamon, Oxford, 1996, vol. 3, ch. 6, pp. 205-241. c) Tskube, H.; Furuta, H.; Odani, A.; Takeda, Y.; Kudo, Y.; Inoue, Y.; Liu, Y.; Sakamoto, H.; Kimura, K. *Comprehensive Supramolecular Chemistry* ed. Atwood, J. L.; Davies, J. E. D.; McNicol, D. D.; Vogtle, F., Pergamon, Oxford, 1996, vol. 8, ch. 10, pp. 425-482. d) Goodrich, J. A.; Kugel, J. F. *Binding and Kinetics for Molecular Biologists*, Cold Spring Harbour Laboratory Press, New York, 2007.
- (9) a) Connors, K. A. *Binding Constants: The Measurement of Molecular Complex Stability*, Wiley-VCH, Weinheim, 1987. b) Davies, C. W. *Ion Association*, Butterworths, Washington, 1962, ch. 4. c) Andrews, L. J.; Keefer, R. M. *Molecular Complexes in Organic Chemistry*, Holden-Day, San Francisco, 1964, Ch.4. d) Nancollas, G. H. *Interactions in Electrolyte Solutions*, Elsevier,

Amsterdam, 1966, ch. 2. e) Ross, J. *Molecular Complexes*, Pergamon, Oxford, 1967, ch. 3. f) Ramette, R. W. *J. Chem. Educ.* **1967**, *44*, 647-649. g) Mulliken, R. S.; Person, W. B. *Molecular Complexes*, Wiley-Interscience, New York, 1969, ch. 7. h) Gur'yanova, E. N.; Gol'dshtein, I. P.; Romm, I. P. *Donor-Acceptor Bond*, Halsted, Wiley, New York, 1975, ch. 2.

(10) a) Schalley C. A. *Analytical Methods in Supramolecular Chemistry* Wiley-VCH, Weinheim, Germany, 2007. b) Schneider, H. J.; Juneva, R. K.; Simova, S.; *Chem. Ber.* **1989**, *122*, 1211. c) Beijer, F. H.; Sijbesma, R. P.; Kooijman, H.; Spek, A. L.; Meijer, E. W. *J. Am. Chem. Soc.* **1998**, *120*, 6761-6769. d) Beijer, F. H.; Kooijman, H.; Spek, A. L.; Sijbesma, R. P.; Meijer, E. W. *Angew. Chem. Int. Ed.* **1998**, *37*, 75-78. e) Corbin, P. S.; Zimmerman, S. C. *J. Am. Chem. Soc.* **1998**, *120*, 9710-9711. f) Wang, X. Z.; Li, X. Q.; Shao, X. B.; Zhao, X.; Deng, P.; Jiang, X. K.; Li, Z. T.; Chen, Y. Q. *Chem. Eur. J.* **2003**, *9*, 2904-2913. g) Chang, S. K.; Hamilton, A. D. *J. Am. Chem. Soc.* **1988**, *110*, 1318-1319. h) Park, T.; Todd, E. M.; Nakashima, S.; Zimmerman, S. C. *J. Am. Chem. Soc.* **2005**, *127*, 18133-18142. i) Ligthart, G. B. W. L.; Phkawa, H.; Sijbesma, R. P.; Meijer, E. W. *J. Org. Chem.* **2006**, *71*, 375-378.

- (11) Bauer, M.; Spange, S. *Angew. Chem. Int. Ed.* **2011**, *50*, 9727-9730.
- (12) a) Gray, M; Guello, A. O.; Cooke, G.; Rotello, V. M. *J. Am. Chem. Soc.* **2003**, *125*, 7882-7888. b) Deans, R.; Cuello, A. O.; Galow, T. H.; Ober, M.; Rotello, V. *M. J. Chem. Soc. Perkin Trans.2* **2000**, 1309-1313.
- (13) Huynh, P. N. H.; Walvoord, R. R.; Kozlowski, M. C. *J. Am. Chem. Soc.* **2003**, *134*, 15621-15623.

Chapter 5

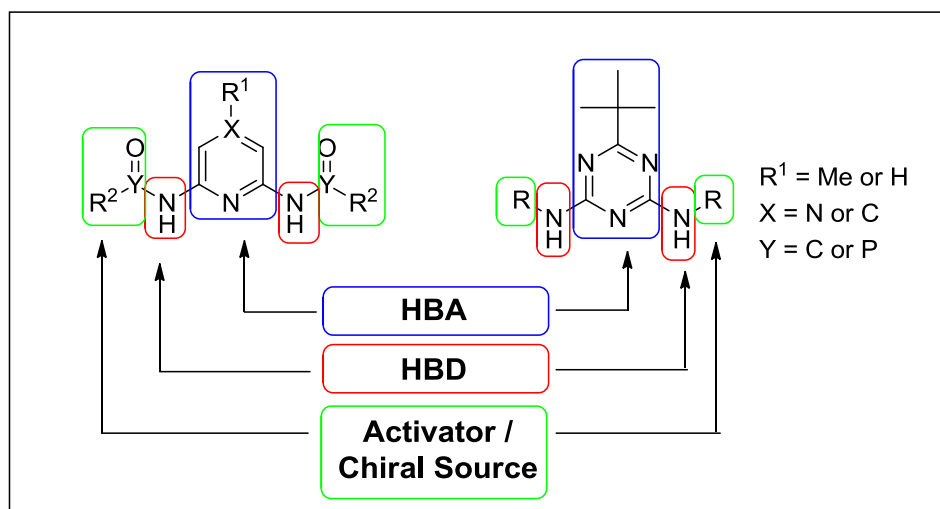
Studies on Asymmetric Conjugate Addition by C_2 -Symmetric Chiral Hydrogen Bond Donor-Acceptor-Donor Organocatalysts

5.1 Introduction

Chemical synthesis has been making a significant contribution to the modernization of our society through providing a wide diversity of commodity ranging from plastics, agrochemicals to pharmaceuticals. Traditionally, transition metal catalysis is the mainstay technology used in those chemical processes.^[1,2] However, to enable the future development of our world in a sustainable manner, stringent constraints owing to the limited supply, high market price, and toxicity of these precious metals need to be addressed. Thus, a formidable challenge of chemical synthesis in this century is to develop efficient synthetic technologies on the basis of robust, abundant, inexpensive, and environmentally friendly catalysts.

For decades, two major classes of asymmetric catalysis have been developed: enzymes and transition metal complexes^[3]. Since 2000, organocatalysts have emerged as a new class of powerful chiral catalysts^[4].

5.1.1 Design of C_2 -Symmetric Chiral HB-DAD Organocatalysts



Scheme 5.1 Design of C_2 -Symmetric chiral HB-DAD organocatalysts

The design of C_2 -Symmetric chiral HB-DAD organocatalysts consists of three moieties (1) Hydrogen bond acceptor (HBA), (2) Hydrogen bond donor (HBD), and (3) Chiral element (Figure 5.1).

HBA is N-heterocyclic aromatic ring. Pyridine, triazine, pyrazine and N-methyl-pyrazine were selected to be the HBA. Nitrogen-hydrogen (N-H) bond was chosen as HBD in our design.

Chiral acyl groups and alkyl groups were selected for the synthesis of C_2 -Symmetric chiral HB-DAD organocatalysts.

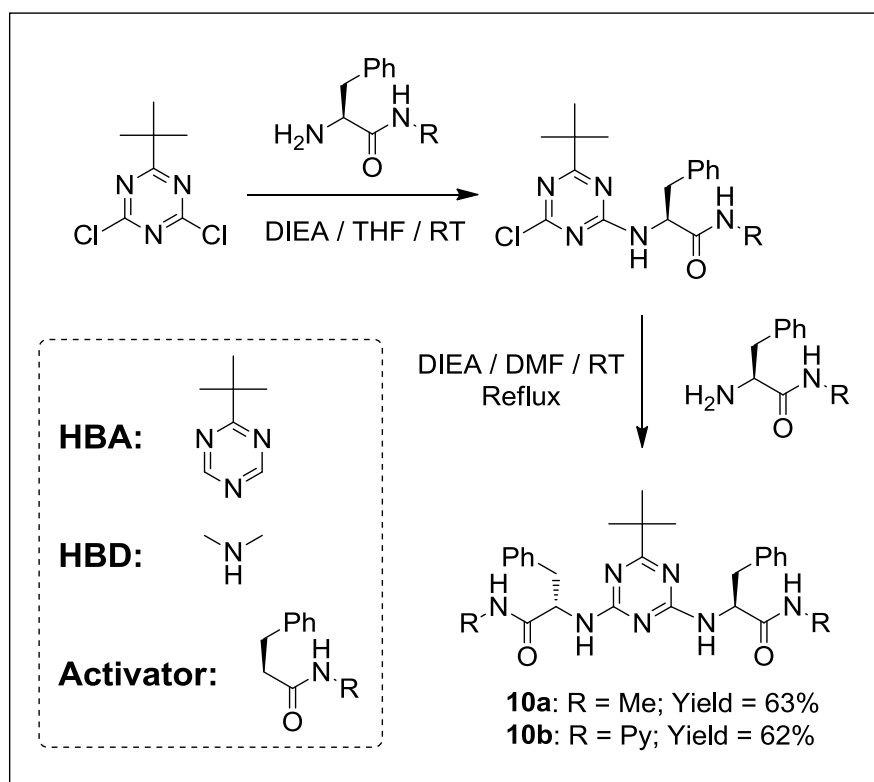
5.1.2 The Objective of This Chapter

We set out to incorporate chiral elements to the C_2 -Symmetric HB-DAD organocatalysts and to study their activities in catalytic asymmetric conjugate addition.

5.2 Results and Discussion

5.2.1 Synthesis of C_2 -Symmetric Chiral HB-DAD Organocatalysts

Chiral amine-based HB-DAD organocatalysts **10a** and **10b** were prepared in good isolated yield (63% and 62%) by a two-step synthesis (Scheme 5.1).^[5] In brief, C_2 -Symmetric chiral HB-DAD organocatalysts **10a** and **10b** consisted of (1) *t*-butyl-triazine as HBA, (2) N-H as HBD, and (3) phenylalanine derivatives as the activator and chiral element. The molecular structure of C_2 -Symmetric chiral HB-DAD organocatalyst **10a** was revealed by X-ray crystallography (Figure 5.1).



Scheme 5.1 Synthetic route of **10a** and **10b**

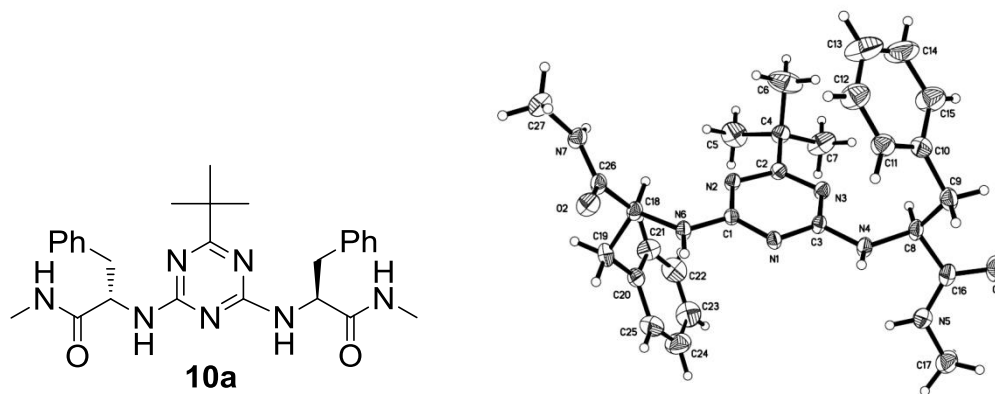


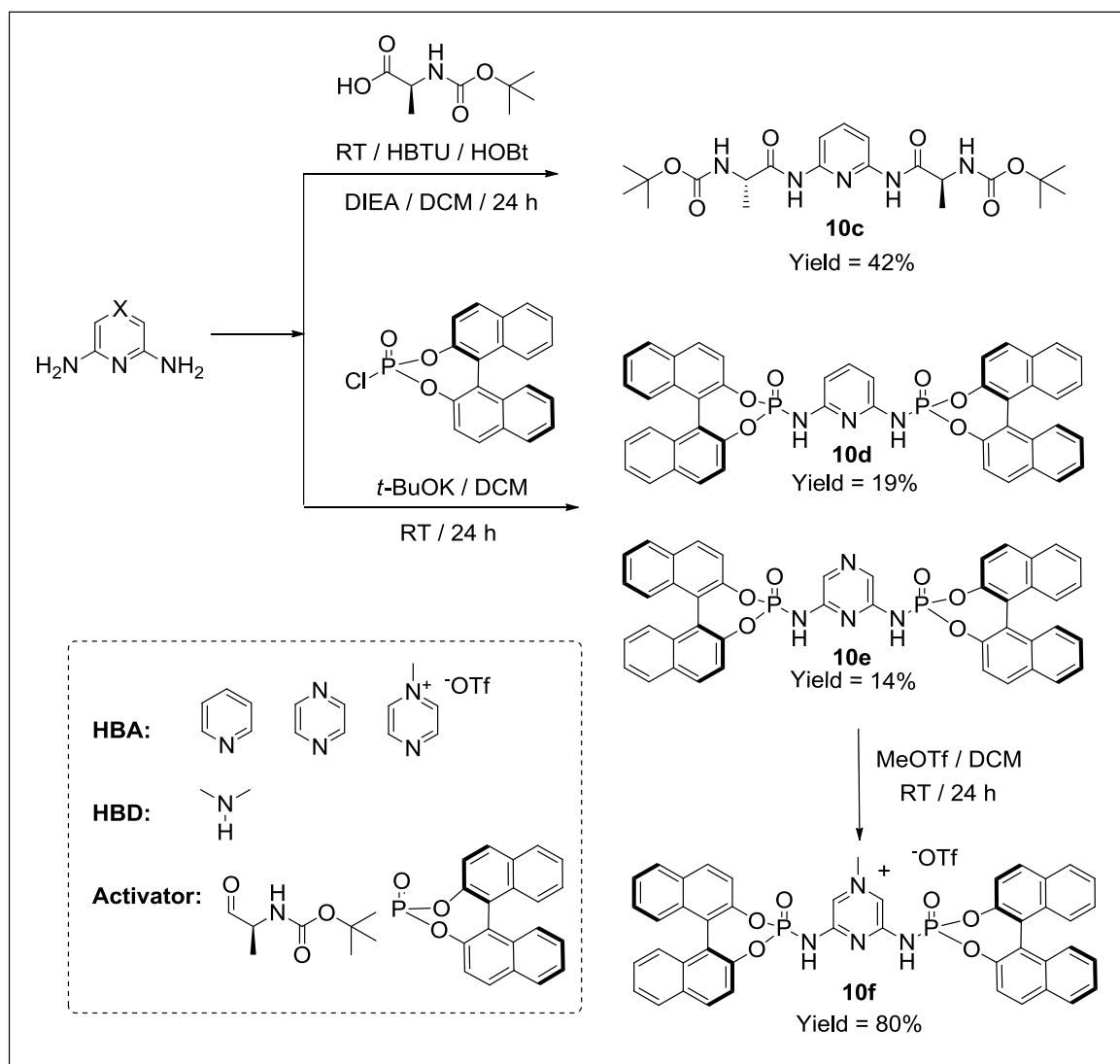
Figure 5.1 X-ray crystallography structure of **10a**

A series of C_2 -Symmetric chiral amide-based HB-DAD organocatalysts have also been synthesized (Scheme 5.2). **10c** was synthesized in 42% yield from amide coupling of 2,6-diaminopyridine (1 mmol) and *N*-[(1,1-dimethylethoxy)carbonyl] L-alanine (2 mmol).^[6] C_2 -Symmetric chiral HB-DAD organocatalysts **10d** and **10e** were prepared from amide coupling of 2,6-diaminopyridine (1 mmol) / 2,6-diaminopyrazine (1 mmol) and (+)-1,1'-binaphthyl-2,2'-diyl-phosphorochloridate (2 mmol) (isolated yield = 19% and 14%, respectively).^[7] Furthermore, **10e** was converted to **10f** in excellent isolated yield (80%) by methylation with methyl trifluoromethanesulfonate under nitrogen atmosphere.

The C_2 -Symmetric chiral amide-based HB-DAD organocatalysts **10c-10f** were constructed with (1) pyridine, pyrazine and methylated-pyrazine as HBA, (2) N-H as HBD, and (3) alanine derivative and BINOL phosphinic group as activator and chiral elements.

In this regard, these C_2 -Symmetric chiral HB-DAD organocatalysts were used

for investigation of asymmetric conjugate additions of maleimide with dibenzoylmethane.



Scheme 5.2 Synthetic route of C_2 -Symmetric chiral HB-DAD organocatalysts **10c**,

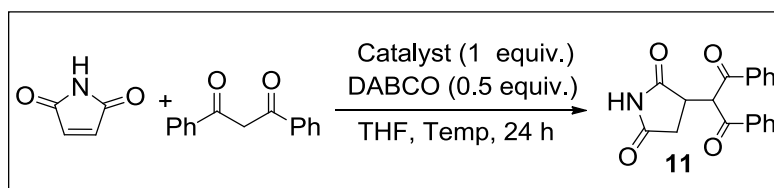
10d, **10e** and **10f**

5.2.2 Catalytic Activity Studies - C_2 -Symmetric Chiral HB-DAD Organocatalysts in

Conjugate Additions of Maleimide with Dibenzoylmethane

Studies on catalytic activities of C_2 -Symmetric chiral HB-DAD organocatalysts **10a** and **10b** (0.1 mmol) in conjugate addition of maleimide (0.1 mmol), dibenzoylmethane (0.1 mmol) and DABCO (0.05 mmol) to give adduct **11** is depicted in Table 5.1. No adduct **11** was observed in the absence of DABCO (entry 1).

The reaction (carried out with DABCO only) gave adduct **11** in 54% isolated yield at 20 °C in THF in 24 h (entry 2). Using C_2 -Symmetric chiral HB-DAD organocatalyst **10a** with DABCO, adduct **11** in 60% isolated yield and enantioselectivity of 9 %*ee* (entry 3) was obtained.

Table 5.1 **10a** and **10b** in catalyzing conjugate addition of maleimide^[a]

Entry ^[a]	Catalysts	Temperature (°C)	Isolated Yield (%)	<i>ee</i> (%) ^[d]
1 ^[b,c]	-----	25	0	-----
2 ^[b]	-----	25	54	-----
3	10a	25	60	9
4	10a	-15	<5	5
5	10a	-78	<5	15
6	10b	-78	<5	9

^[a] Unless noted otherwise, reaction were performed with maleimide (0.1 mmol), dibenzoylmethane (0.1 mmol), **10a** and **10b** (0.1 mmol) and DABCO (0.05 mmol) in THF (1 mL), 24 h. ^[b] Without addition of catalyst. ^[c] Without addition of DABCO. ^[d] Enantiomeric excesses determined by HPLC analysis using Chiralpak AD-H column.

The temperature of **10a**-catalyzed conjugate addition of maleimide was lowered in $-15\text{ }^{\circ}\text{C}$ to give adduct **11** with 9 %*ee* (Table 5.1; entry 4) while that of 15 %*ee* was obtained in $-78\text{ }^{\circ}\text{C}$ (entry 5). In addition, using **10b**, gave adduct **11** was obtained in 9 %*ee* (entry 6).

The catalytic activity studies of **10c**, **10d**, **10e**, and **10f** (0.01 mmol) in the conjugate addition of maleimide (0.05 mmol), dibenzoylmethane (0.05 mmol) and DABCO (0.025 mmol) giving adduct **11** are delineated in Table 5.2. Using of **10c**,

adduct **11** was obtained in 67% isolated yield at 20 °C in dichloromethane (8 %*ee*; entry 1) while the reaction conducted without catalyst gave 46% isolated yield (entry 5). The reaction using **10d** and **10e** led to adduct **11** in 46% and 33% isolated yields with 0 %*ee* and 8 %*ee*, respectively (entries 2 and 3). A poor isolated yield (13%) was obtained using **10f** (0 %*ee*; entry 4).

Table 5.2 **10c**, **10d**, **10e** and **10f** in catalyzing conjugate addition of maleimide^[a]

Entry ^[a]	Catalysts	Isolated Yield (%)	ee (%) ^[b]
1	10c	67	8
2	10d	46	0
3	10e	33	8
4	10f	13	0
5 ^[c]	-----	46	-----

^[a] Unless noted otherwise, reaction were performed with maleimide (0.05 mmol), dibenzoylmethane (0.05 mmol), **10c-f** (0.01 mmol) and DABCO (0.025 mmol) in DCM (1 mL), 25 °C, 24 h. ^[b] Enantiomeric excesses determined by HPLC analysis using Chiralpak AD-H column. ^[c] Without addition of catalyst

Future work will be directed towards focus on the design and synthesis of C₂-Symmetric chiral sulfonamide-based HB-DAD organocatalysts and the study of their activities in catalytic asymmetric conjugate additions.

5.3 Conclusion

Six C_2 -Symmetric chiral HB-DAD organocatalysts were synthesized and characterized. The reaction adduct **11** were obtained in good yield (up to 67%) with enantioselectivities of 8-15 %*ee* suggesting the feasibility of catalyst-to-product chirality transfer.

5.4 Experimental Section

5.4.1 Experimental Procedures

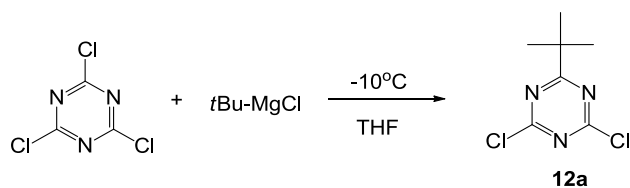
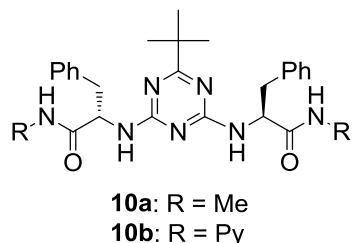
Procedure for Conjugate Additions of Maleimide and Dibenzoylmethane in THF

A mixture of melaimide (0.1 mmol), dibenzoylmethane (0.1 mmol), DABCO (0.5 mmol) and HB-DAD organocatalysts (0.1 mmol) in THF (1 mL) was stirred at -78 °C to 25 °C for 24 h. The reaction mixture was concentrated. The residue was purified by flash column chromatography on silica gel using ethyl acetate-hexane as eluent.

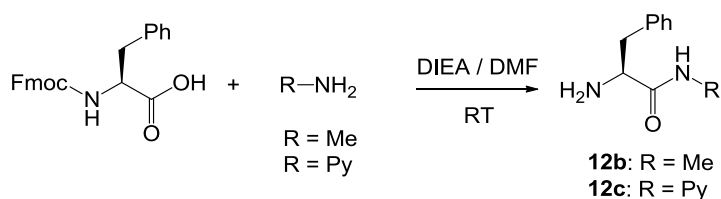
Procedure for Conjugate Additions of Maleimide and Dibenzoylmethane in DCM

A mixture of melaimide (0.05 mmol), dibenzoylmethane (0.05 mmol), DABCO (0.025 mmol) and HB-DAD organocatalysts (0.01 mmol), in DCM (1 mL) was stirred at 25 °C for 24 h. The reaction mixture was concentrated. The residue was purified by flash column chromatography on silica gel using ethyl acetate-hexane as eluent.

Synthetic Procedure of **10a** and **10b**

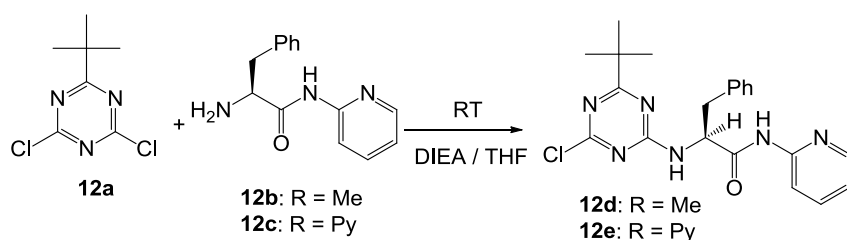


In a dried round-bottom Schlenk flask under nitrogen, anhydrous THF (1 mL) is added to the cyanuric chloride (1.0 mmol) and CuI (5 mol%). The mixture was cooled to $-10\text{ }^{\circ}\text{C}$ with stirring. A solution of the Grignard reagent (1.0–2.5 mmol) in THF was added slowly, and the reaction mixture stirred from $0\text{ }^{\circ}\text{C}$ to $25\text{ }^{\circ}\text{C}$, until reaction completion indicated by TLC. The reaction mixture was treated with water (5 mL), and extracted with ethyl acetate ($3 \times 10\text{ mL}$). The combined organic layers were dried over anhydrous Na_2SO_4 , filtered, and concentrated. The residue was purified by flash column chromatography on silica gel using ethyl acetate-hexane as eluent.

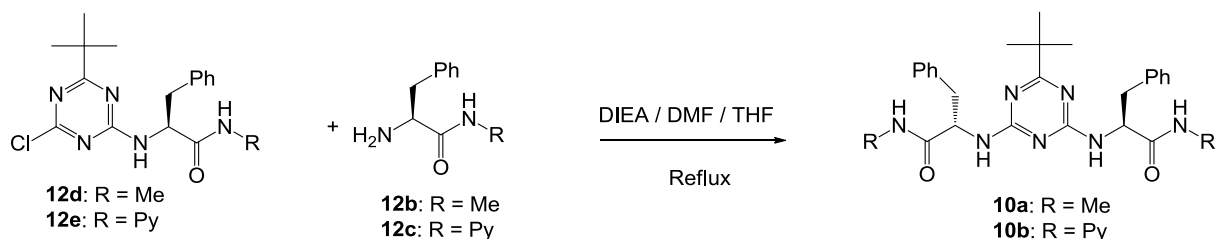


To a mixture of Fmoc-Phe-OH (2 mmol), 2-aminopyridine or methylamine (5 mmol),

HBTU (2 mmol) and HOBT (2mmol) in DMF (10ml) was added diisopropylamine (5 mmol) at room temperature under nitrogen atmosphere for 24 h. The methanol and DCM added as solvent with the piperidine (5 mmol) stirred at room temperature for another 24 h. The reaction mixture was treated with water (5 mL), and extracted with ethyl acetate (3 × 10 mL). The combined organic layers were dried over anhydrous Na₂SO₄, filtered, and concentrated. The residue was purified by flash column chromatography on silica gel using ethyl acetate-hexane as eluent.

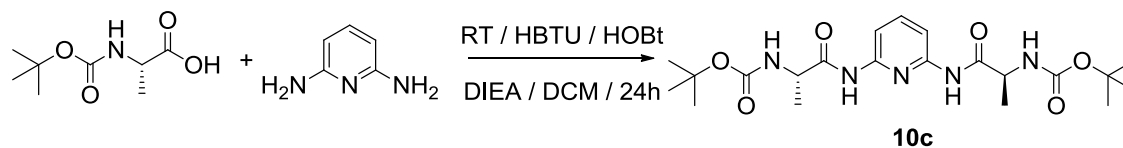


To a mixture of **12a** (1 mmol), **12b** or **12c** (1.05 mmol) and diisopropylamine (5 mmol) in DCM (10 mL) is stirred at room temperature under nitrogen atmosphere for 24 h. The reaction mixture was treated with water (5 mL), and extracted with ethyl acetate (3 × 10 mL). The combined organic layers were dried over anhydrous Na₂SO₄, filtered, and concentrated. The residue was purified by flash column chromatography on silica gel using ethyl acetate-hexane as eluent.

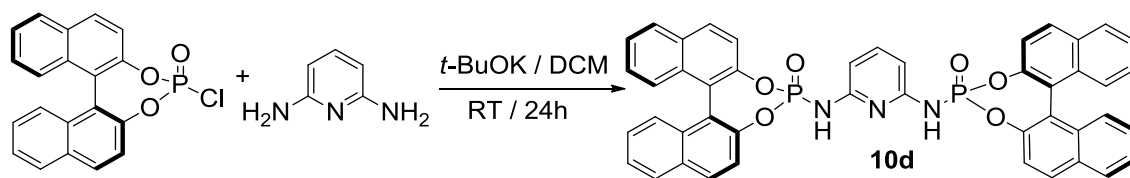


To a mixture of **12d** or **12e** (0.5 mmol), **12b** or **12c** (1.05 mmol) and diisopropylamine (5 mmol) in THF (10 mL) and DMF (2 mL) is refluxed under nitrogen atmosphere for 24 h. The reaction mixture was treated with water (5 mL), and extracted with ethyl acetate (3 × 10 mL). The combined organic layers were dried over anhydrous Na₂SO₄, filtered, and concentrated. The residue was purified by flash column chromatography on silica gel using ethyl acetate-hexane as eluent.

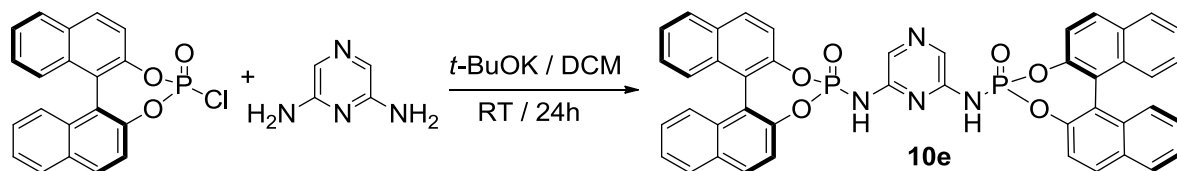
Synthetic Procedure of 10c -10f



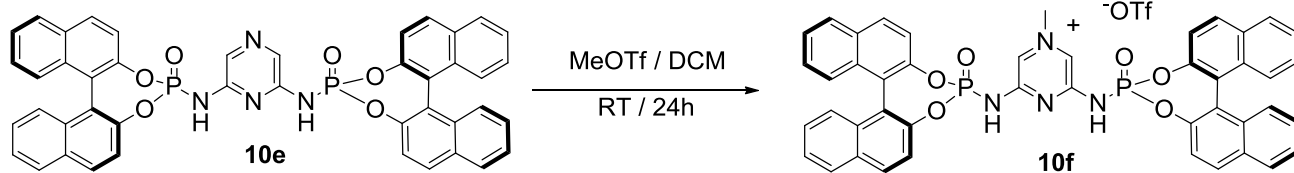
To a mixture of Boc-Ala-OH (2 mmol), 2,6-diaminopyridine (1 mmol), HBTU (2.5 mmol) and HOBT (2.5 mmol) in DCM (10ml) was added diisopropylamine (5 mmol) at room temperature under nitrogen atmosphere for 24 h. The reaction mixture was treated with water (5 mL), and extracted with ethyl acetate (3 × 10 mL). The combined organic layers were dried over anhydrous Na₂SO₄, filtered, and concentrated. The residue was purified by flash column chromatography on silica gel using ethyl acetate-hexane as eluent.



To a mixture of (+)-1,1'-binaphthyl-2,2'-diyl-phosphorochloridate (1 mmol), 2,6-diaminopyridine (2 mmol) and *t*-BuOK (2.5 mmol) in DCM (10ml) was stirred at room temperature under nitrogen atmosphere for 24 h. The reaction mixture was treated with water (5 mL), and extracted with ethyl acetate (3 × 10 mL). The combined organic layers were dried over anhydrous Na₂SO₄, filtered, and concentrated. The residue was purified by flash column chromatography on silica gel using ethyl acetate-hexane as eluent.



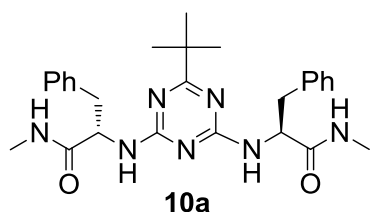
To a mixture of (+)-1,1'-binaphthyl-2,2'-diyl-phosphorochloridate (1 mmol), 2,6-diaminopyrazine (2 mmol) and *t*-BuOK (2.5 mmol) in DCM (10ml) was stirred at room temperature under nitrogen atmosphere for 24 h. The reaction mixture was treated with water (5 mL), and extracted with ethyl acetate (3 × 10 mL). The combined organic layers were dried over anhydrous Na₂SO₄, filtered, and concentrated. The residue was purified by flash column chromatography on silica gel using ethyl acetate-hexane as eluent.



To a mixture of **10e** (0.2 mmol) and methyl trifluoromethanesulfonate (1.2 mmol) in DCM (5 ml) was stirred at room temperature under nitrogen atmosphere for 24 h. The reaction mixture was treated with water (5 mL), and extracted with ethyl acetate (3 × 10 mL). The combined organic layers were dried over anhydrous Na₂SO₄, filtered, and concentrated. The residue was purified by flash column chromatography on silica gel using methanol-ethyl acetate as eluent.

5.4.2 Characterizations

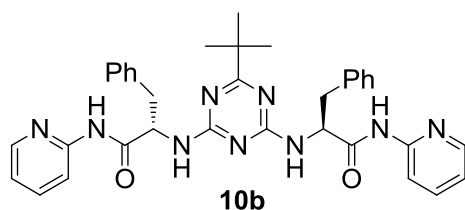
Characterization of **10a-10f** and **11**



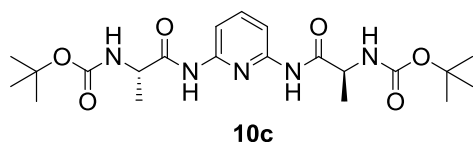
Transparent crystal, analytical TLC (silica gel 60) (10 % MeOH in dichloromethane)

R_f = 0.6; 63% isolated yield; ¹H NMR (500 MHz, CDCl₃) δ 7.19-7.30 (m, 10H), 6.54 (br s, 1H), 5.53 (br s, 1H), 4.76 (br s, 1H), 4.29 (br s, 1H), 3.12 (br s, 4H), 2.7 (br s, 6H), 2.04 (s, 1H), 1.16-1.26 (m, 10H); ¹H NMR (500 MHz, CD₃OD) δ 7.23 (br s,

10H), 3.31 (m, 3H), 3.11 (m, 2H), 2.97 (m, 2H), 2.67-2.69 (br s, 6H), 1.19 (br s, 9H);
 ^{13}C NMR (100 MHz, CDCl_3) δ 171.33, 165.73, 129.41, 128.89, 128.69, 60.58, 56.44,
38.39, 38.03, 28.01, 28.28, 21.21, 14.39, 0.19; ESIMS m/z 491 $[\text{M}+\text{H}^+]$; X-ray
crystallography obtained.

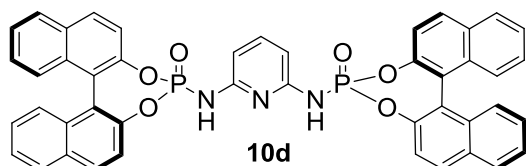


Yellow solid, analytical TLC (silica gel 60) (25% ethyl acetate in n-hexane) $R_f = 0.6$;
62% isolated yield; ^1H NMR (400 MHz, CDCl_3) δ 9.94 (br s, 1H), 9.53-9.70 (b, 1H),
8.20-8.36 (m, 4H), 7.72-7.83 (m, 2H), 6.72-7.33 (m, 11H), 6.70 (s, 1H), 5.13 (br s,
1H), 4.93 (br s, 1H), 3.14-3.31 (m, 4H), 1.10-1.29 (m, 9H); ^{13}C NMR (100 MHz,
 CDCl_3) δ 171.83, 166.00, 152.21, 152.20, 148.36, 138.08, 129.52, 129.40, 128.46,
126.69, 119.93, 119.64, 114.44, 113.75, 57.60, 56.95, 37.47, 28.36; ESIMS m/z 616
 $[\text{M}+\text{H}^+]$.

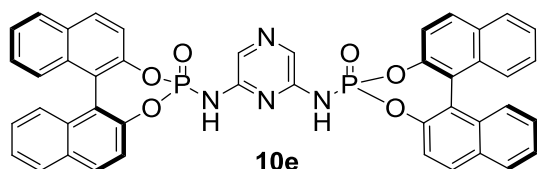


Yellow solid, analytical TLC (silica gel 60) (25% ethyl acetate in n-hexane) $R_f = 0.6$;
42% isolated yield; ^1H NMR (400 MHz, CDCl_3) δ 9.17 (br s, 1H), 7.90 (d, $J = 8.0$ Hz,

2H), 7.76 (t, $J = 8.4$ Hz, 1H), 6.41 (br s, 1H), 4.35 (br s, 2H), 2.83 (br s, 2H), 1.42 (br d, 24H); ^{13}C NMR (100 MHz, CDCl_3) δ 172.03, 155.87, 150.50, 140.42, 108.98, 79.07, 79.04, 51.12, 27.89, 17.29, 17.27; ESIMS m/z 452 $[\text{M}+\text{H}^+]$.

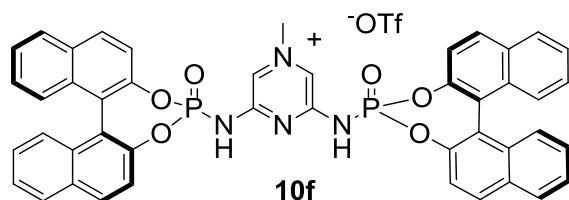


White solid, analytical TLC (silica gel 60) (75% ethyl acetate in n-hexane) $R_f = 0.6$; 19% isolated yield; ^1H NMR (400 MHz, CDCl_3) δ 8.09 (d, $J = 7.6$ Hz, 1H), 7.99 (s, 1H), 7.96 (d, $J = 8.4$ Hz, 1H), 7.88 (d, $J = 9.2$ Hz, 1H), 7.55 (d, $J = 4.0$ Hz, 1H), 7.36 (d, $J = 4.2$ Hz, 1H), 7.38 (t, $J = 7.6$ Hz, 1H), 7.29 (t, $J = 7.2$ Hz, 1H), 7.17 (t, $J = 7.6$ Hz, 1H), 7.05-7.12 (m, 2H), 6.97 (d, $J = 8.4$ Hz, 1H); ^{13}C NMR (100 MHz, D-Acetone) δ 148.03, 147.98, 147.87, 146.15, 146.07, 132.38, 132.23, 132.11, 131.97, 131.57, 128.86, 128.80, 127.65, 127.09, 126.93, 126.76, 126.62, 126.09, 125.86, 121.61, 121.35, 121.29, 121.26, 121.11; ESIMS m/z 770 $[\text{M}+\text{H}^+]$.

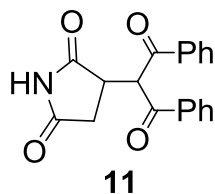


White solid, analytical TLC (silica gel 60) (75% ethyl acetate in n-hexane) $R_f = 0.4$; 14% isolated yield; ^1H NMR (400 MHz, CDCl_3) δ 8.25 (d, $J = 8.8$ Hz, 1H), 8.10-8.14

(m, 2H), 8.03 (d, $J = 8.8$ Hz, 1H), 7.97 (d, $J = 8.0$ Hz, 1H), 7.68-7.72 (m, 2H), 7.54 (t, $J = 7.6$ Hz, 1H), 7.45 (t, $J = 7.6$ Hz, 1H), 7.33 (t, $J = 8.8$ Hz, 1H), 7.21-7.27 (m, 2H), 7.13 (d, $J = 8.8$ Hz, 1H); ^{13}C NMR (100 MHz, CDCl_3) δ 148.03, 147.98, 147.87, 146.15, 146.07, 132.38, 132.23, 132.11, 131.97, 131.57, 128.86, 128.80, 127.65, 127.09, 126.93, 126.76, 126.62, 126.09, 125.86, 121.61, 121.35, 121.29, 121.26, 121.11; ESIMS m/z 771 $[\text{M}+\text{H}^+]$.



Yellow solid, analytical TLC (silica gel 60) (25% methanol in ethyl acetate) $R_f = 0.6$; 80% isolated yield; ^1H NMR (500 MHz, D-Acetone) δ 9.76 (br s, 1H), 8.22-8.23 (br d, 2H), 8.10-8.15 (m, 4H), 8.06 (d, $J = 8.5$ Hz, 2H), 7.72 (t, $J = 10.5$ Hz, 4H), 7.52-7.59 (m, 4H), 7.25-7.38 (m, 8H), 4.51 (s, 3H); ^{13}C NMR (100 MHz, D-Acetone) δ 153.40, 153.34, 147.36, 147.25, 145.70, 145.62, 132.28, 132.20, 131.95, 129.00, 127.41, 127.29, 126.80, 126.46, 126.30, 121.52, 121.22, 121.20, 120.79, 120.77, 49.72; ESIMS m/z 785 $[\text{M}^+]$.

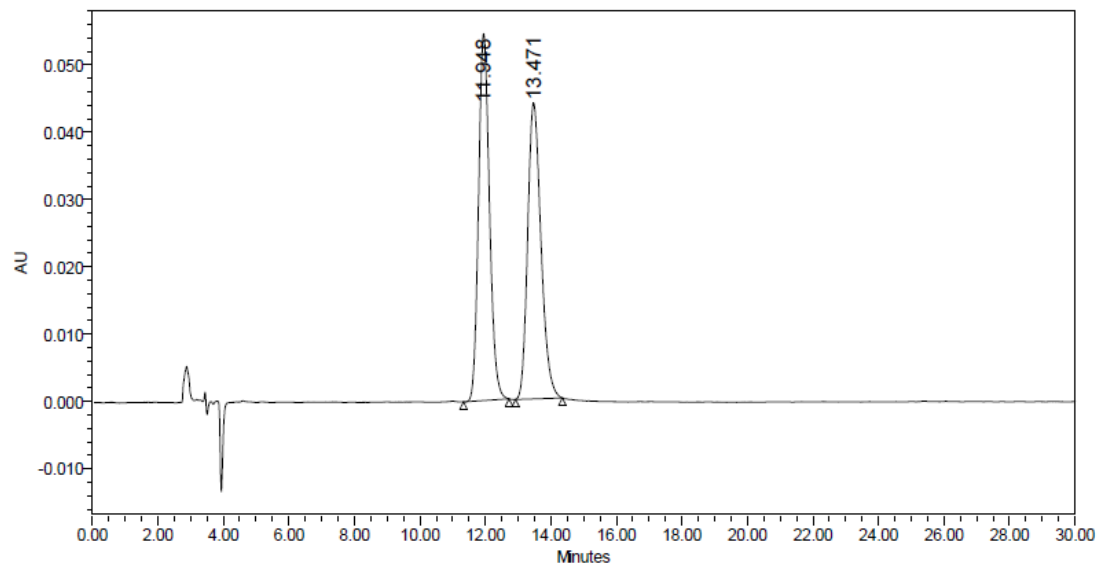


White solid, analytical TLC (silica gel 60) (50% methanol in ethyl acetate) $R_f = 0.4$;
67% isolated yield; $^1\text{H NMR}$ (400 MHz, CDCl_3) δ 8.85 (br s, 1H), 8.08 (d, $J = 7.6$ Hz
2H), 7.81 (d, $J = 7.6$ Hz, 2H), 7.69 (t, $J = 7.2$ Hz, 2H), 7.50-7.58 (m, 3H), 7.38 (t, $J =$
8.0 Hz, 2H), 6.01 (d, $J = 4.4$ Hz, 1H), 3.42-3.47 (m, 1H), 3.07 (dd, $J = 5.6, 18$ Hz, 1H),
2.60 (dd, $J = 9.6, 18$ Hz, 1H); $^{13}\text{C NMR}$ (100 MHz, CDCl_3) δ 195.28, 194.99, 178.38,
176.45, 135.51, 134.82, 134.71, 134.10, 129.67, 129.08, 128.93, 128.66, 54.38, 41.47,
32.90; ESIMS m/z 322 $[\text{M}+\text{H}^+]$; HPLC analysis: Chiralpak ADH (Hex / IPA = 7:3,
1.0 mL / min, 20 °C) 11.7 (major), 13.2 min. 0-15 % *ee*.

5.4.3 HPLC Spectra of **11**

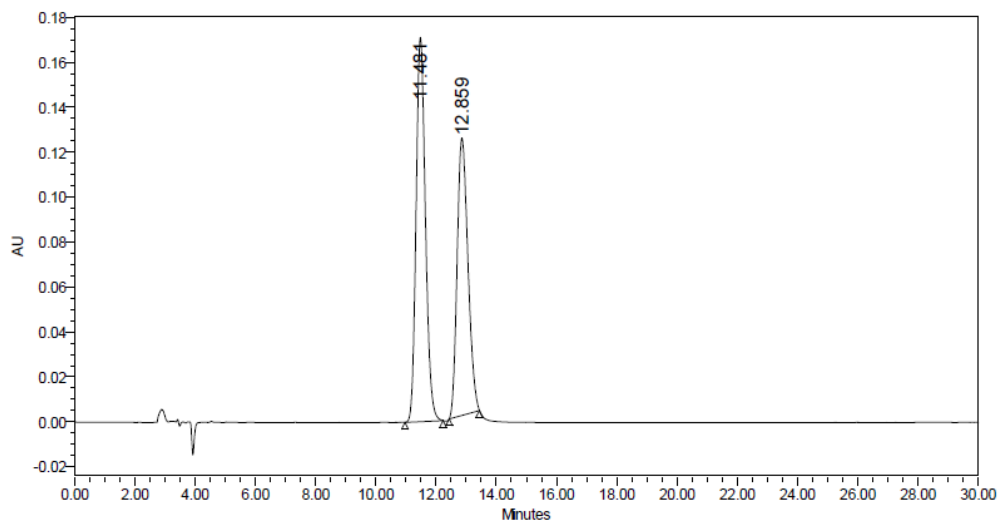
11 (Chiralcel ADH column 0.46 cm x 25 cm, 30 % IPA in hexane, 1.0 mL / min)

Racemic



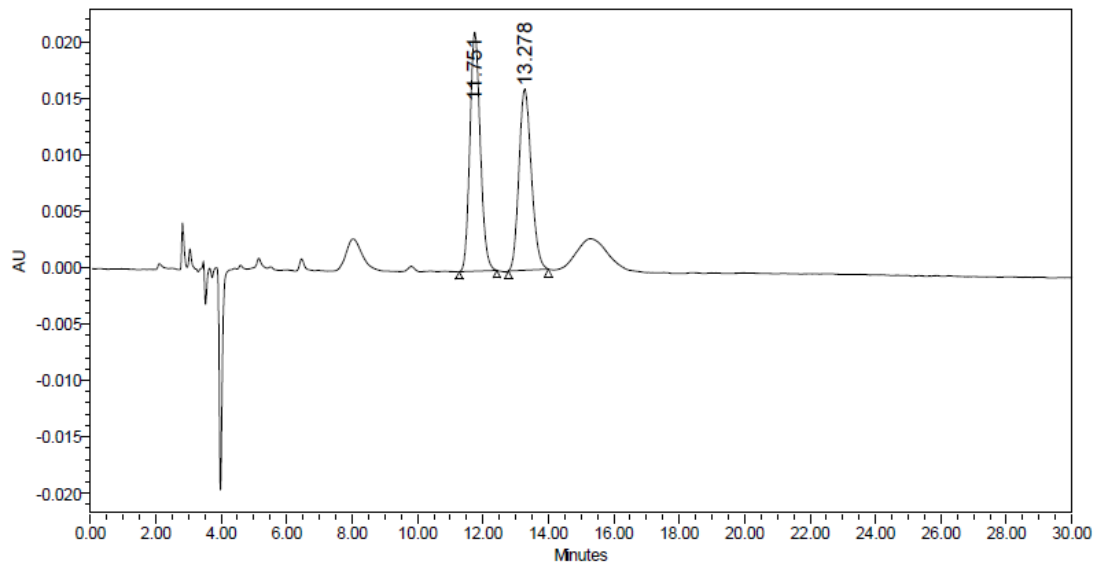
	RT	Area	% Area	Height
1	11.948	1259499	50.35	54490
2	13.471	1241812	49.65	43981

11, for Table 5.1, entry 3



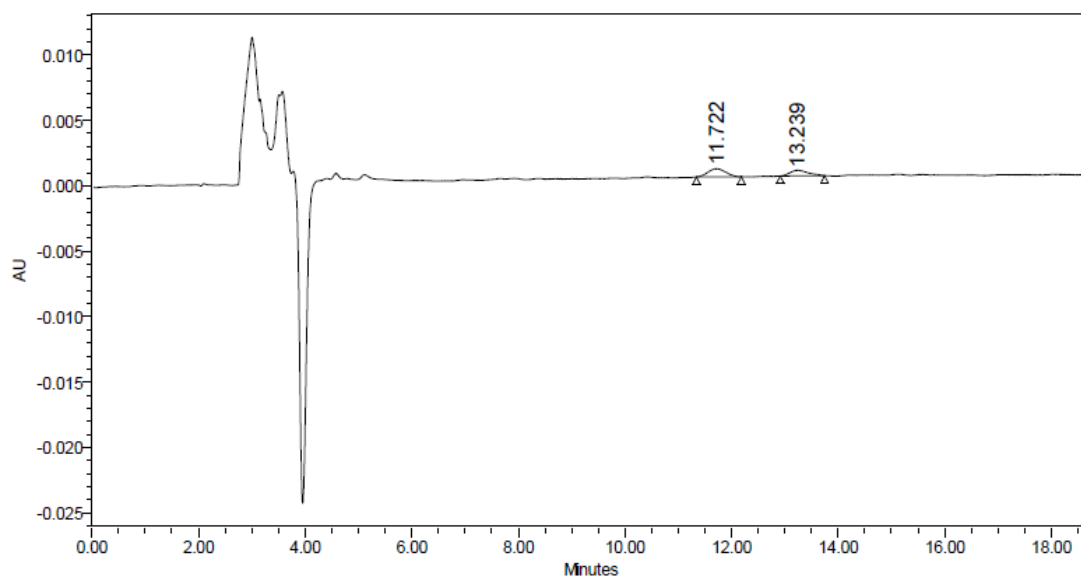
	RT	Area	% Area	Height
1	11.481	3681503	54.54	171019
2	12.859	3068597	45.46	123425

11, for Table 5.1, entry 4



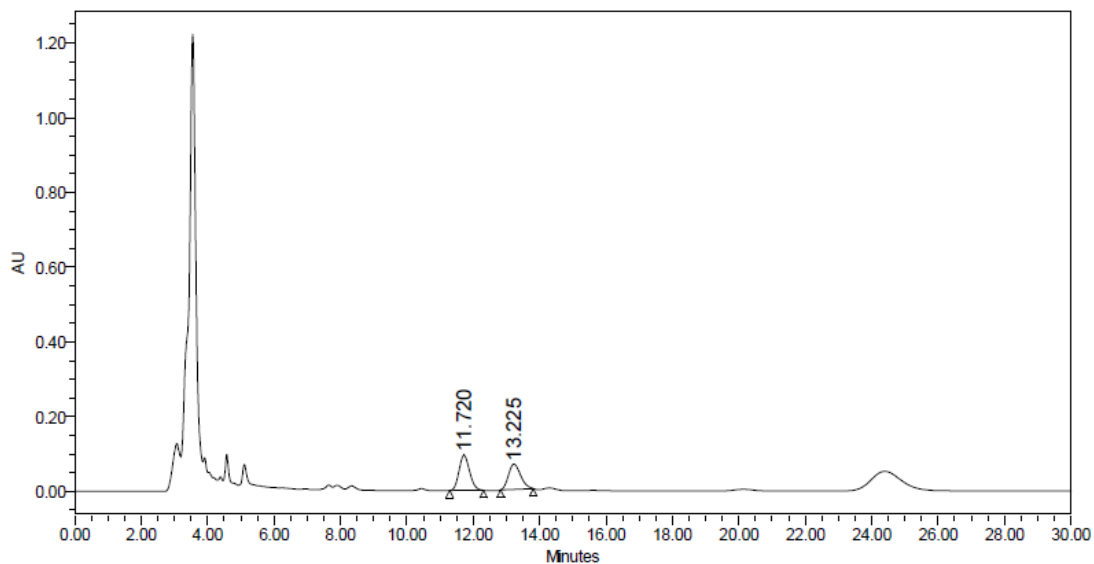
	RT	Area	% Area	Height
1	11.751	467377	52.51	21145
2	13.278	422654	47.49	16039

11, for Table 5.1, entry 5



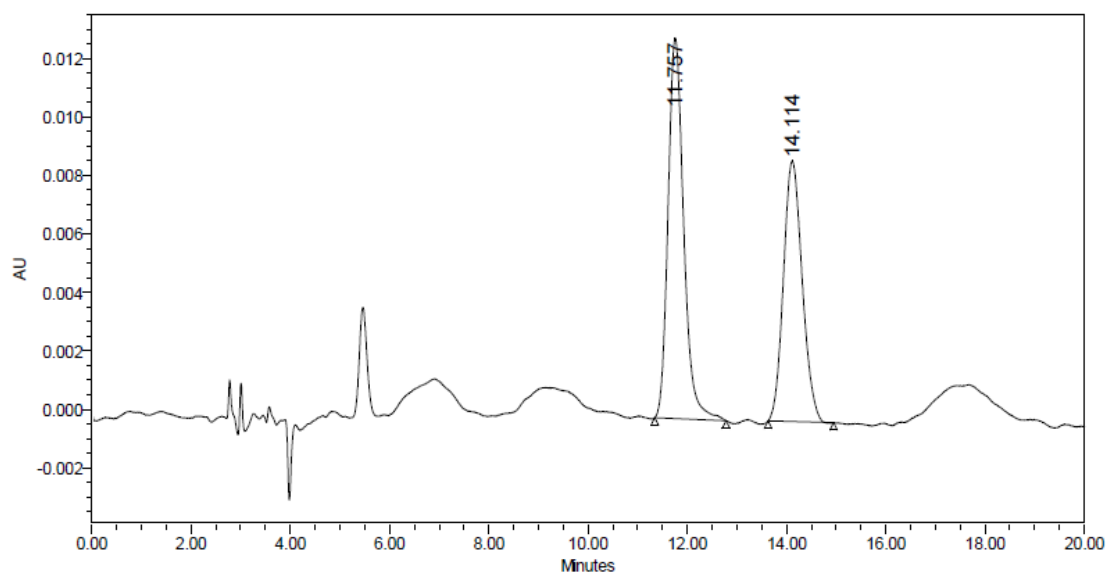
	RT	Area	% Area	Height
1	11.722	14430	58.98	630
2	13.239	10036	41.02	429

11, for Table 5.1, entry 6



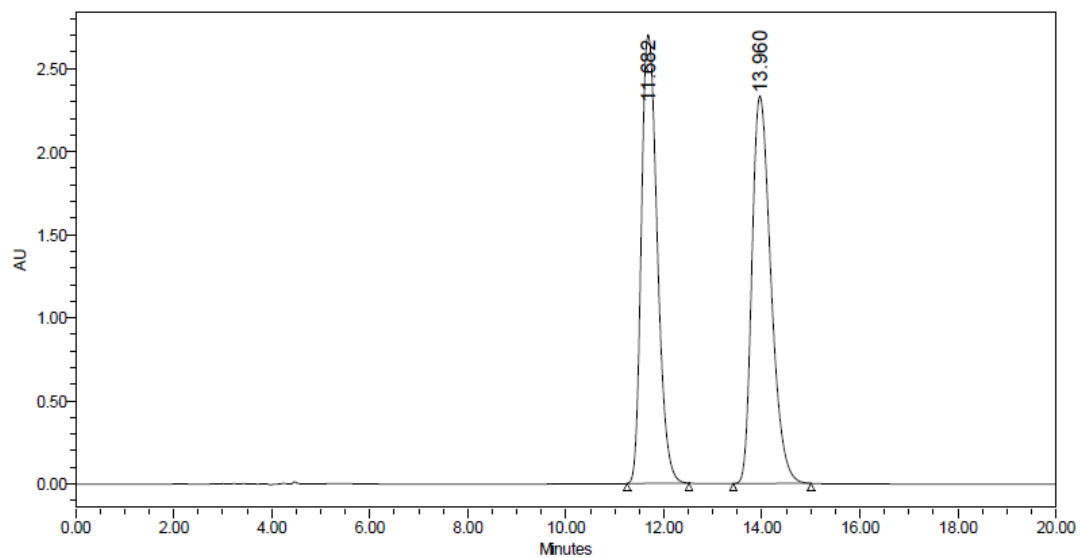
	RT	Area	% Area	Height
1	11.720	2082158	54.76	94150
2	13.225	1720186	45.24	67727

11, for Table 5.2, entry 1



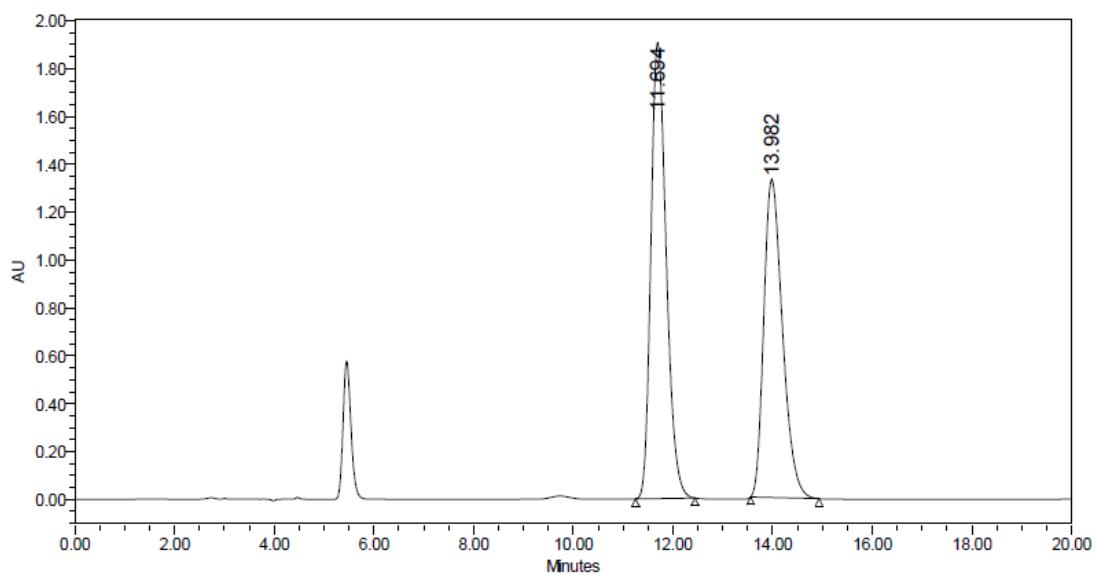
	RT	Area	% Area	Height
1	11.757	285017	54.89	13028
2	14.114	234261	45.11	8922

11, for Table 5.2, entry 2



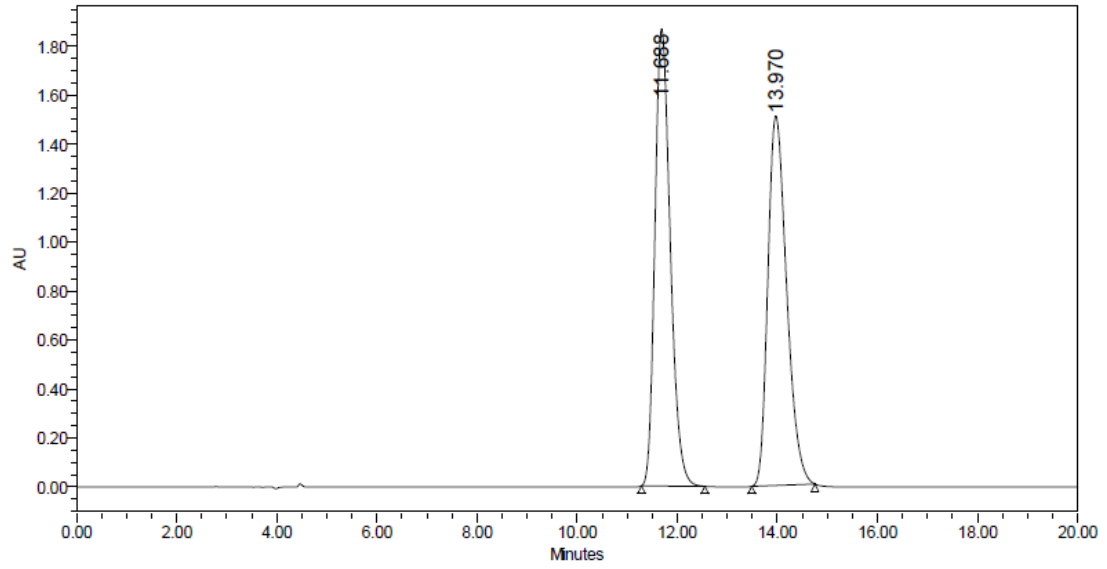
	RT	Area	% Area	Height
1	11.682	60880261	49.28	2698886
2	13.960	62659111	50.72	2330727

11, for Table 5.2, entry 3



	RT	Area	% Area	Height
1	11.694	40655693	54.02	1905866
2	13.982	34600330	45.98	1328639

11, for Table 5.2, entry 4



	RT	Area	% Area	Height
1	11.688	39815480	50.31	1866625
2	13.970	39320528	49.69	1509410

5.5 References

- (1) a) Nicolaou, K. C.; Sorensen, E. J. *Classics in Total Synthesis*, Wiley-VCH, Weinheim, 1996, p. 344. b) Corbet, J. P.; Mignani, G. *Chem. Rev.* **2006**, *106*, 2651-2710. c) Roglans, A.; Pla-Quintana, A.; Moreno-Manas, M. *Chem. Rev.* **2006**, *106*, 4622-4643. d) Yin, L. X.; Liebscher, J. *Chem. Rev.* **2007**, *107*, 133-173. e) Agharahimi, M. R.; LeBel, N. A. *J. Org. Chem.* **1995**, *60*, 1856-1863. f) Forsyth, C. J.; Clardy, J. *J. Am. Chem. Soc.* **1990**, *112*, 3497-3505. g) Neogi, P.; Doundoulakis, T.; Yazbak, A.; Sinha, S. C.; Sinha, S. C.; Keinan, E., *J. Am. Chem. Soc.* **1998**, *120*, 11279-11284. h) James, C. A.; Snieckus, V. *Tetrahedron Lett.* **1997**, *38*, 8149-8152. i) Jung, M. E.; Jung, Y. H., *Tetrahedron Lett.* **1988**, *29*, 2517-2520. j) Larsen, R. D.; King, A. O.; Chen, C. Y.; Corley, E. G.; Foster, B. S.; Roberts, F. E.; Yang, C. H.; Lieberman, D. R.; Reamer, R. A.; Tschaen, D. M.; Verhoeven, T. R.; Reider, P. J., *J. Org. Chem.* **1994**, *59*, 6391-6394.
- (2) a) Hapern, J.; Trost, B. M. *Proc. Natl. Acad. Sci. U.S.A.* **2004**, *101*, 5347. b) Walsh, P. J.; Kozlowski, M. C. *Fundamental of Asymmetric Catalysis*; University Science Books: Mill Valley, CA, 2009. c) Lough, W. J.; Wainer, I. W. *Chirality in Nature and Applied Science*. CRC press / Blackwall Pub., **2002**. d) Noyori, R. Ed. *Asymmetric Catalysis in Organic Synthesis*; Wiley: New York, **1994**. e)

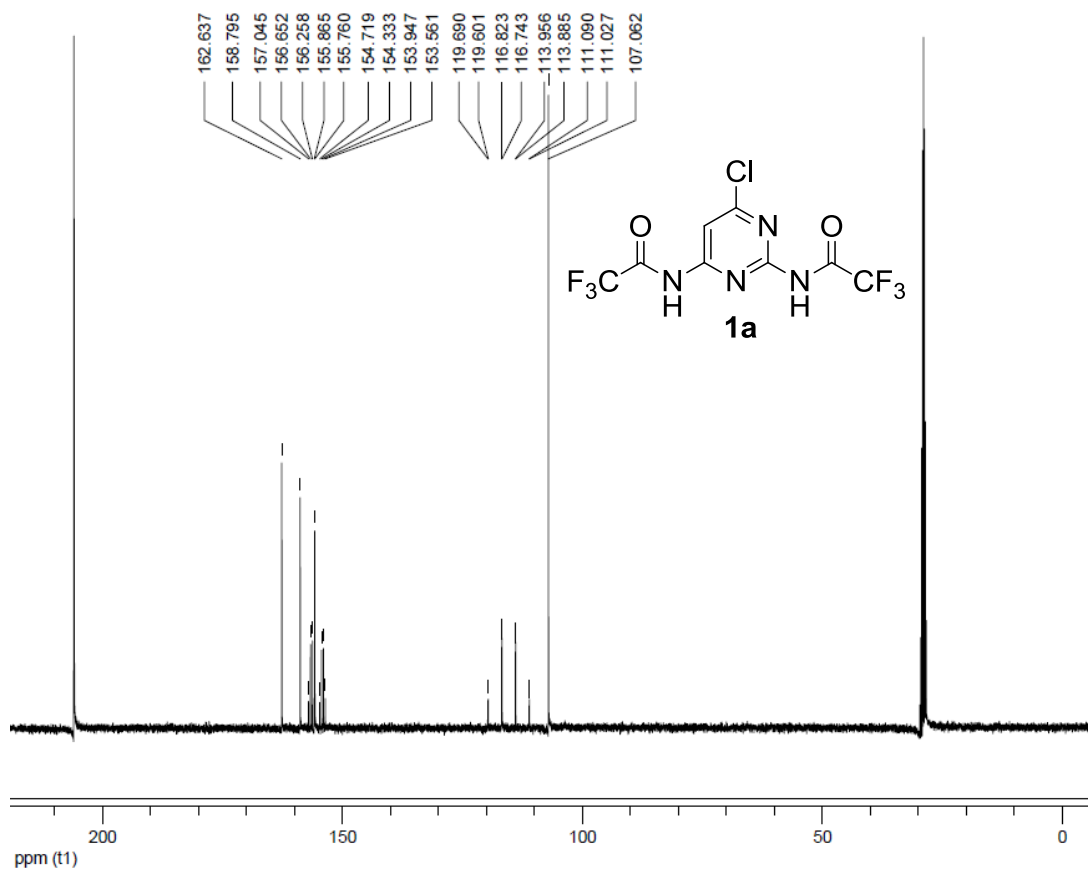
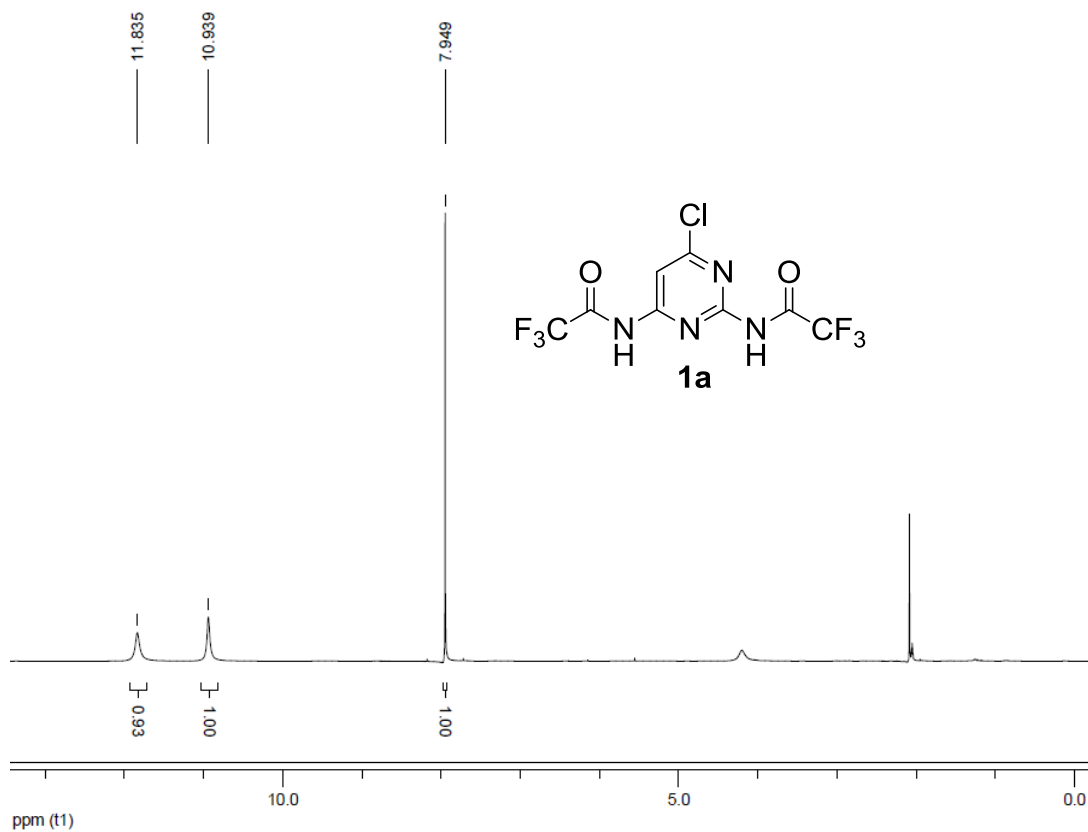
Jacobsen, E. N., Pfaltz, A. Yamamoto, H. Eds. *Comprehensive Asymmetric Catalysis*; Springer: Berlin, **1999**, Vol. 1. f) Ojima, I. Ed. *Catalytic Asymmetric Synthesis*; Wiley-VCH: New York, **2000**. g) Lin, G. Q., Li, Y. M., Chan, A. S. C. Eds. *Principles and Applications of Asymmetric Synthesis*; Wiley: New York, **2001**. h) Knowles, W. S. *Angew. Chem. Int. Ed.* **2002**, *41*, 1998. i) Sharpless, K. B. *Angew. Chem. Int. Ed.* **2002**, *41*, 2024.

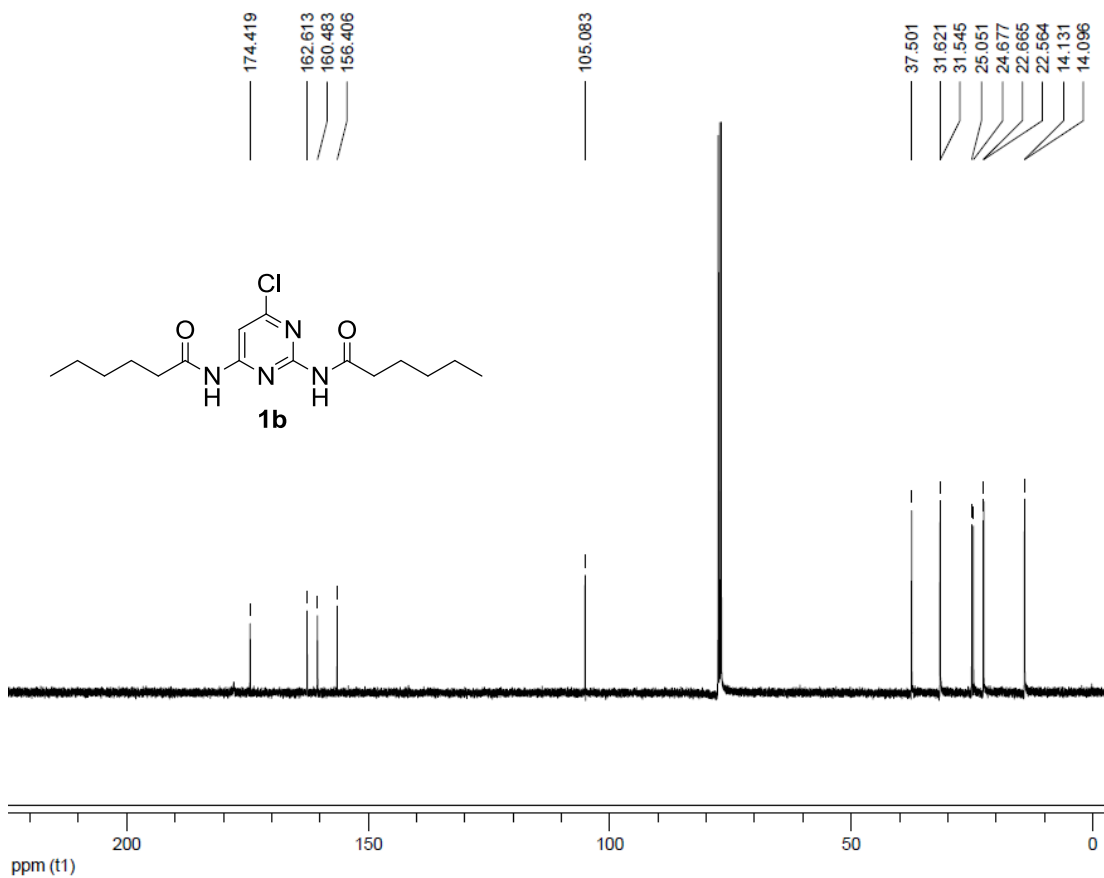
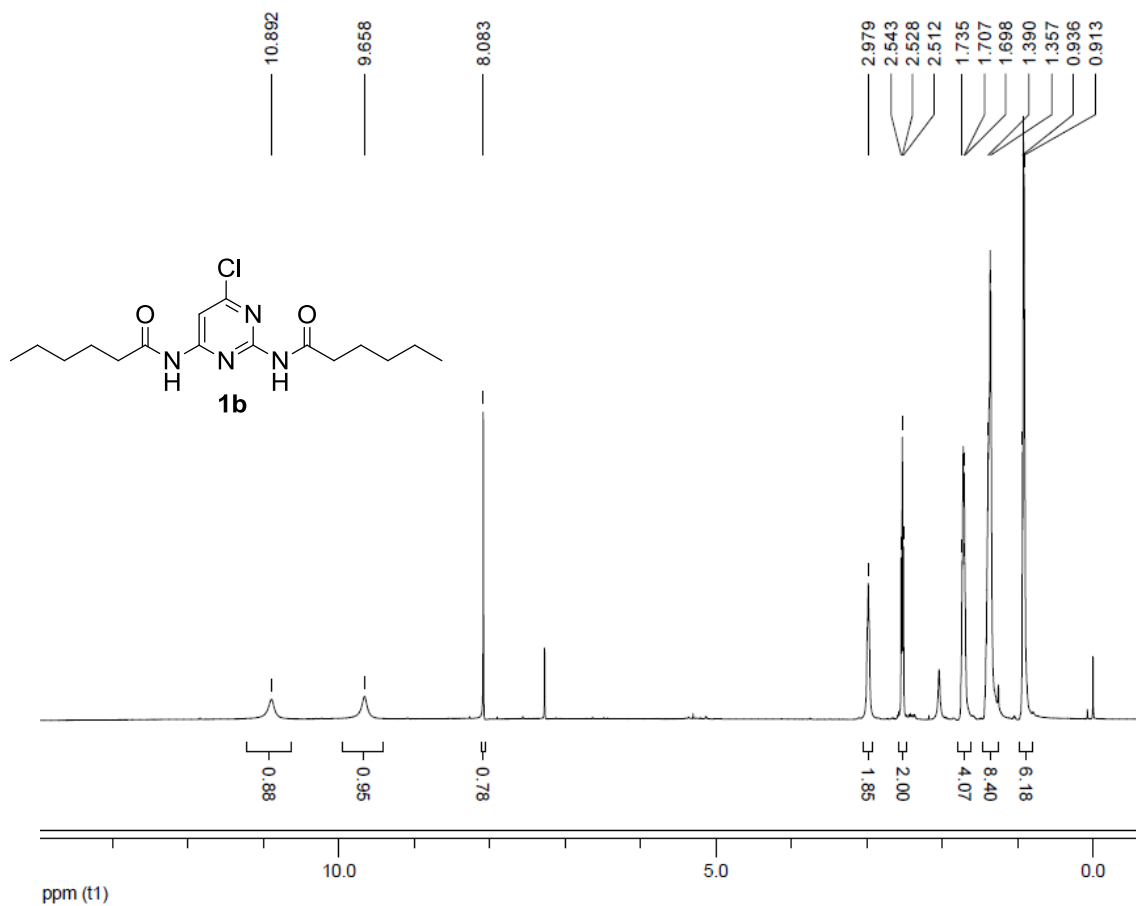
(3) a) List B.; Yang, J. W. *Science* **2006**, *313*, 1584-1586. b) Berkessel, A.; Groeger, H. *Asymmetric Organocatalysis: from Biomimetic Concepts to Applications in Asymmetric Synthesis*; University Science Books: Mill Valley, CA, 2005. c) MacMillan, D. W. C. *Nature* **2008**, *455*, 304-308. b) Hegedus, L.S. *J. Am. Chem. Soc.* **2009**, *131*, 177995-17997. d) List, B. *Chem. Rev.* **2007**, *107*, 5413-5415. e) Jacobsen, E. N.; MacMillan, D. W. C. *Proc. Natl. Acad. Sci. USA* **2010**, *107*, 20618-20619.

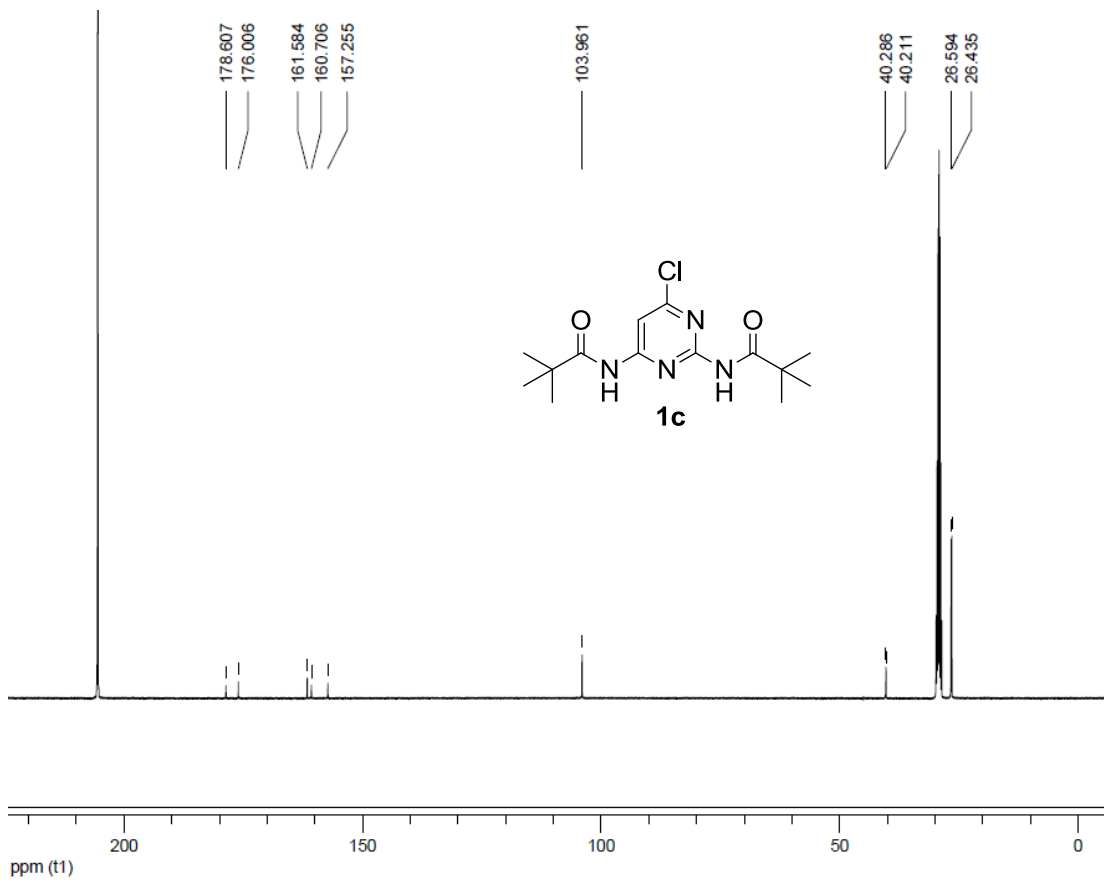
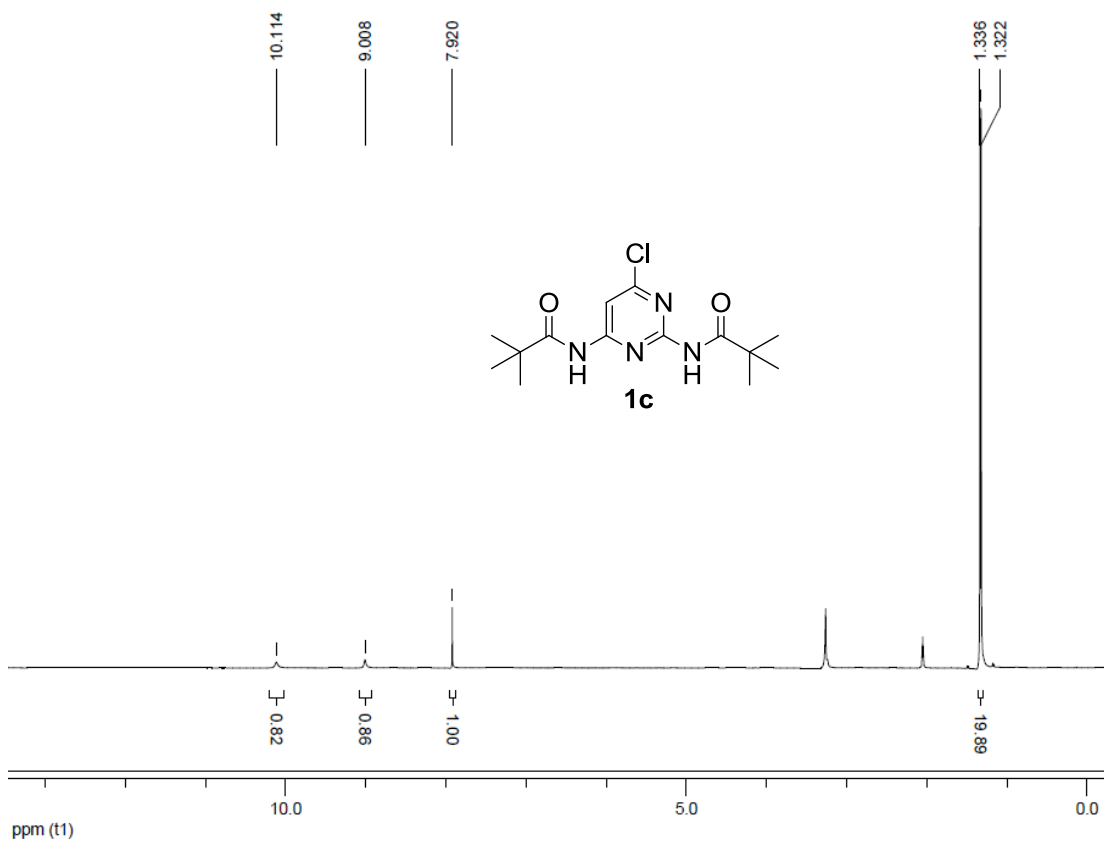
(4) a) Ahrendt, K. A.; Borths, C. J.; MacMillan, D. W. C. *J. Am. Chem. Soc.* **2000**, *122*, 4243-4244. b) Jen, W. S.; Wiener, J. J. M.; MacMillan, D. W. C. *J. Am. Chem. Soc.* **2000**, *122*, 9874-9875. c) Paras, N. A.; MacMillan, D. W. C. *J. Am. Chem. Soc.* **2001**, *123*, 4370-4371. d) Fu, X.; Tan, C. H. *Chem. Commun.* **2011**, *47*, 8210-8222. b) Leow, D.; Tan, C. H. *Synlett* **2010**, *11*, 1589-1605. e) Leow, D.;

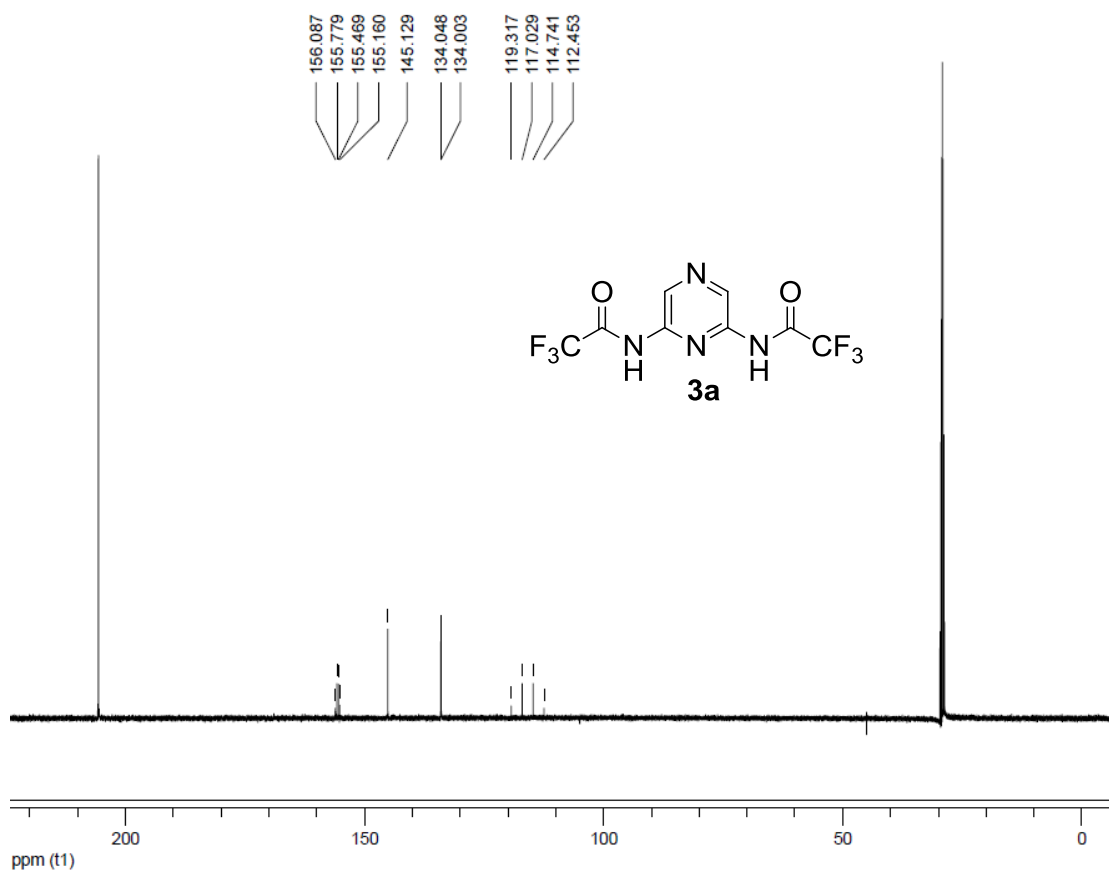
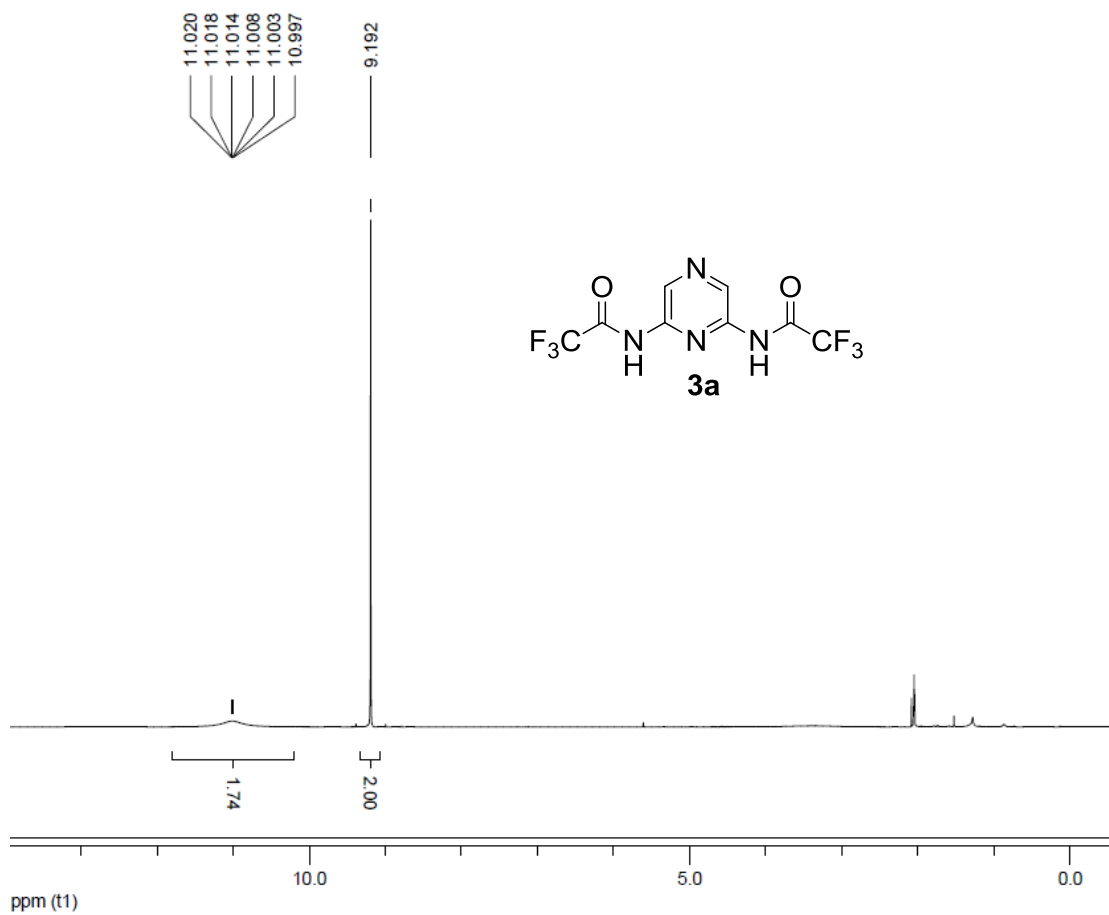
- Tan, C. H. *Chem. Asian. J.* **2009**, *4*, 488-507. f) Shen, J.; Tan, C. H. *Org. Biomol. Chem.* **2007**, *6*, 3229-3236. g) Ender, D.; niemeier, O.; Henseler, A. *Chem. Rev.* **2007**, *107*, 5606-5655. h) Grossmann, A.; Ender, D. *Angew. Chem. Int. Ed.* **2012**, *51*, 314-325. i) Biju, A. T.; Kuhl, N.; Glorius, F. *Acc. Chem. Res.* **2011**, *44*, 1182-1195. j) Zhang, Z.; Schreiner, P. R. *Chem. Soc. Rev.* **2009**, *38*, 1187-1198. k) Yu, X.; Wang, W. *Chem.-Asian J.* **2008**, *3*, 516-532. l) Doyle, A. G.; Jacobsen, E. N. *Chem. Rev.* **2007**, *107*, 5713-5743. m) Connon, S. J. *Chem.-Eur. J.* **2006**, *12*, 5418-5427. n) Taylor, M. S.; Jacobsen, E. N. *Angew. Chem. Int. Ed.* **2006**, *45*, 1520-1543. o) Takemoto, Y. *Org. Biomol. Chem.* **2005**, *3*, 4299-4306. p) Schreiner, P. R. *Chem. Soc. Rev.* **2003**, *32*, 289-296. q) Brak, K.; Jacobsen, E. N. *Angew. Chem. Int. Ed.* **2013**, *52*, 534-561. r) Mahlau, M.; List, B. *Angew. Chem. Int. Ed.* **2013**, *52*, 518-533.
- (5) Hintermann, L.; Xiao, L.; Labonne, A. *Angew. Chem. Int. Ed.* **2008**, *47*, 8246-8250.
- (6) Xu, Z.; Liu, L.; Wheeler, K.; Wang, H. *Angew. Chem. Int. Ed.* **2011**, *50*, 3484-3488.
- (7) Kim, S. H.; Jung, D. Y.; Chang, S. J. *Org. Chem.* **2007**, *72*, 9769-9771.

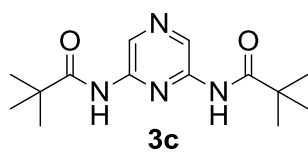
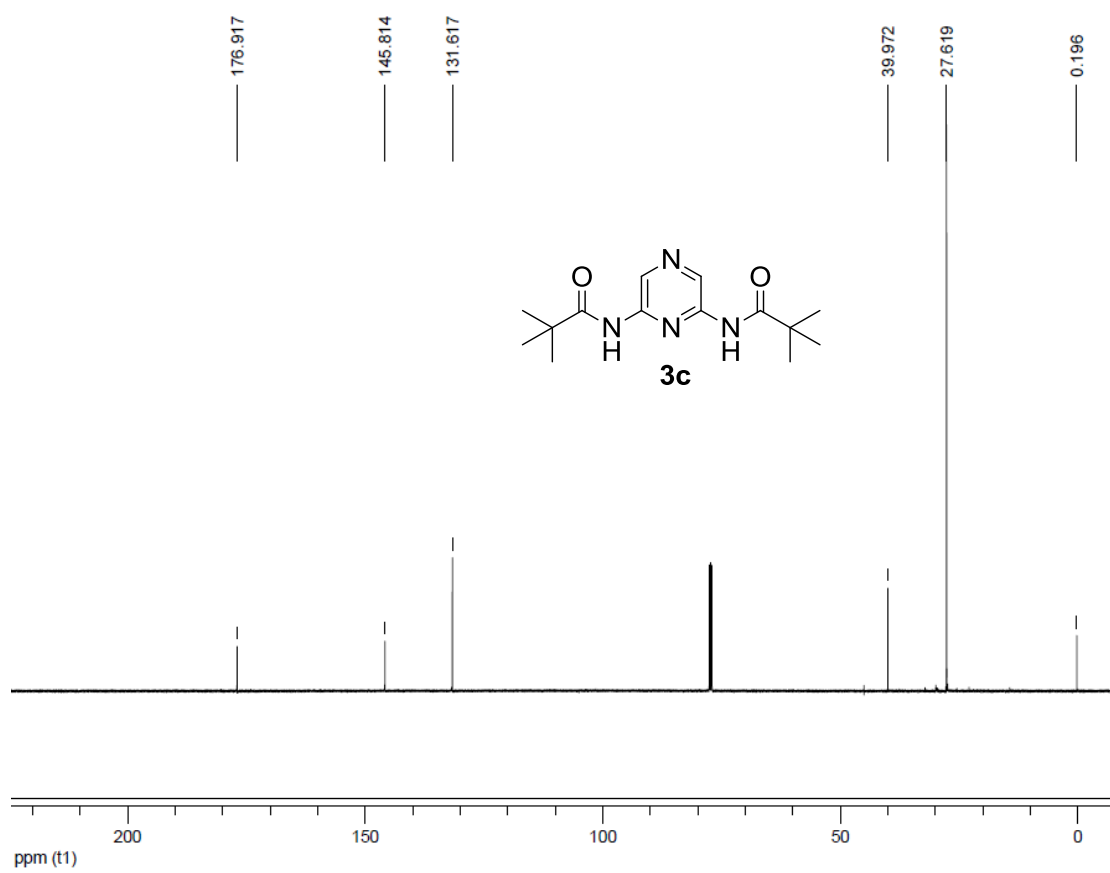
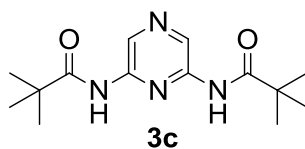
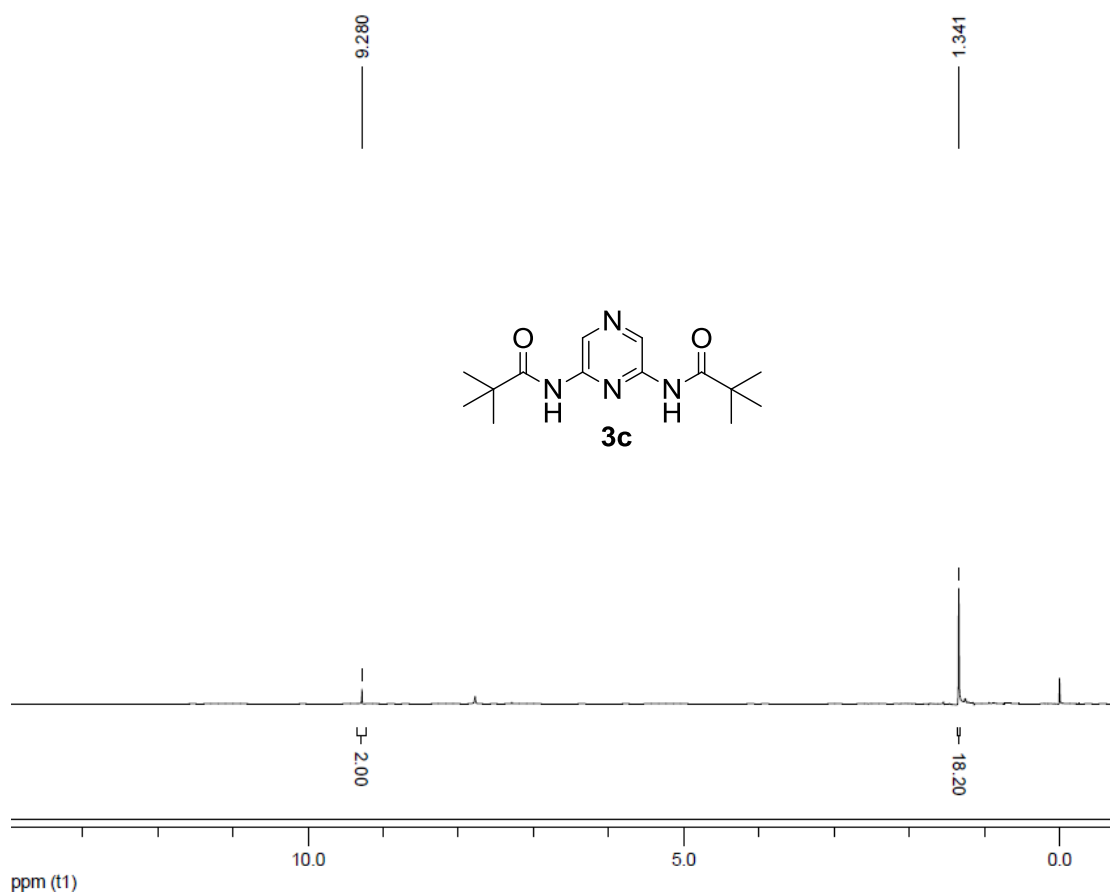
Appendices

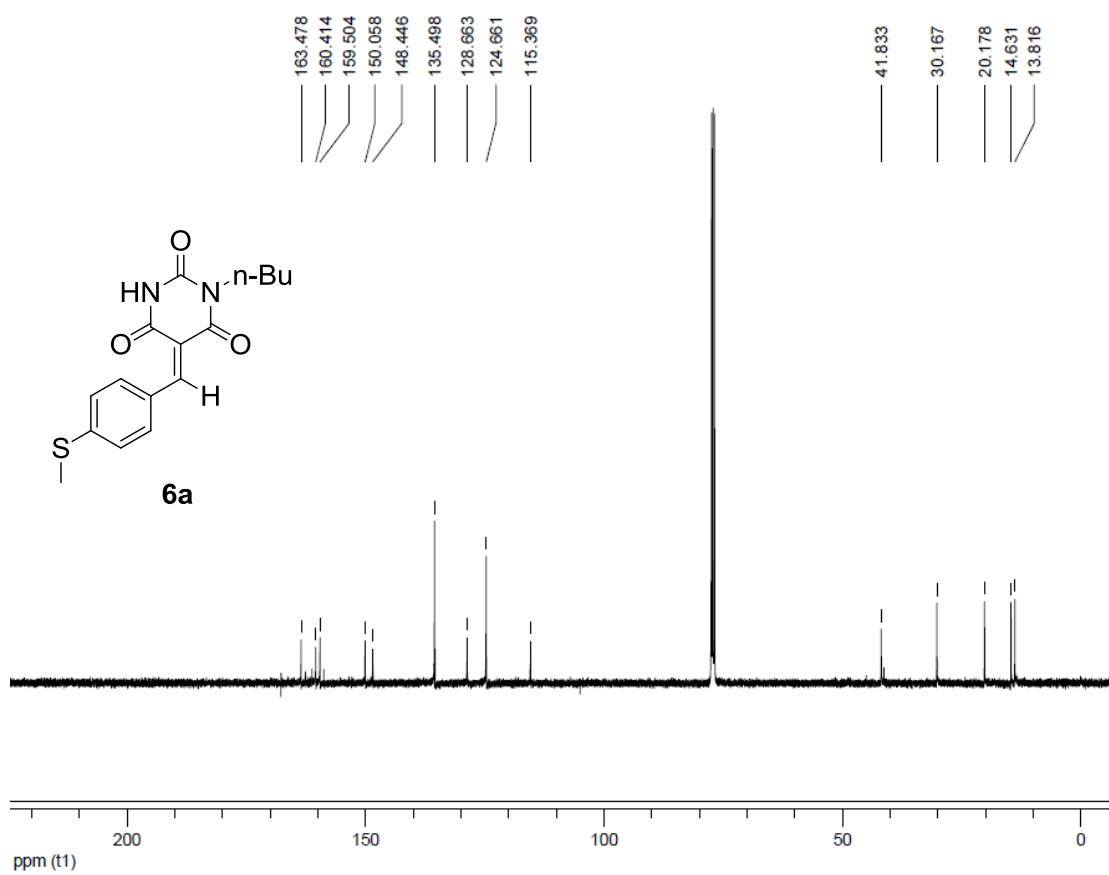
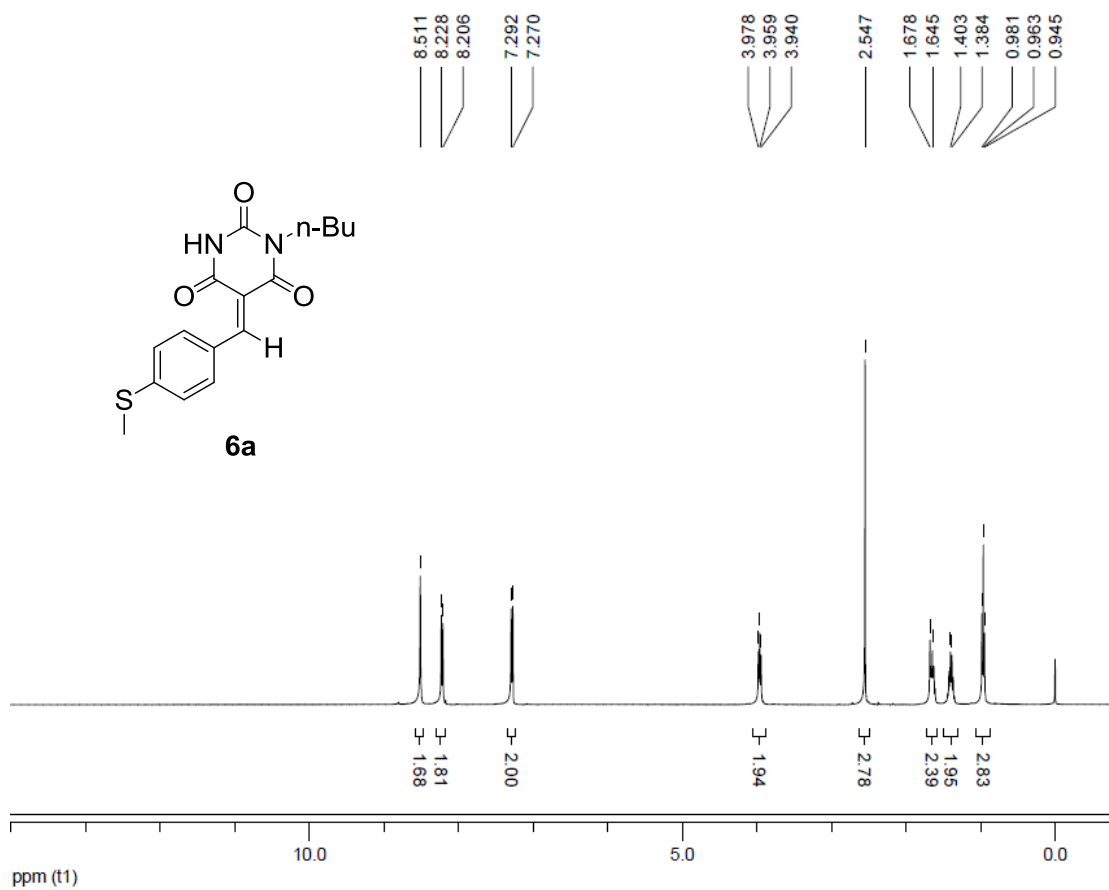


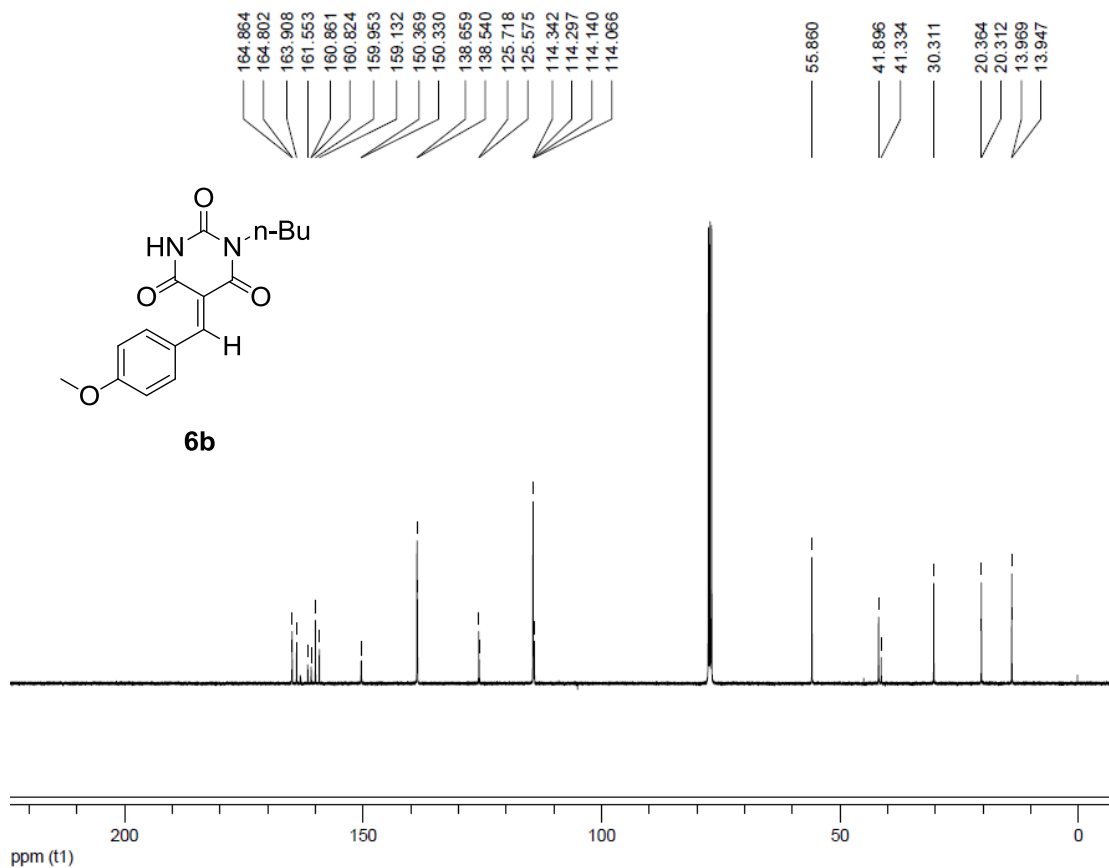
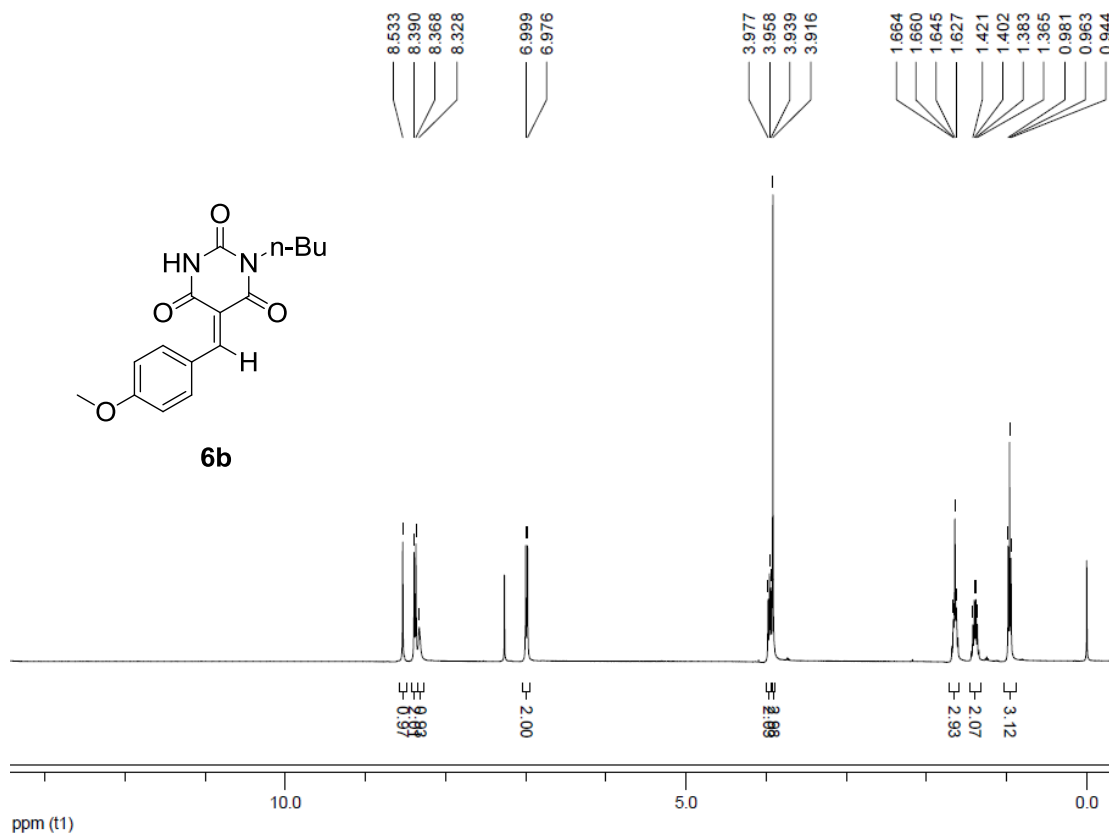


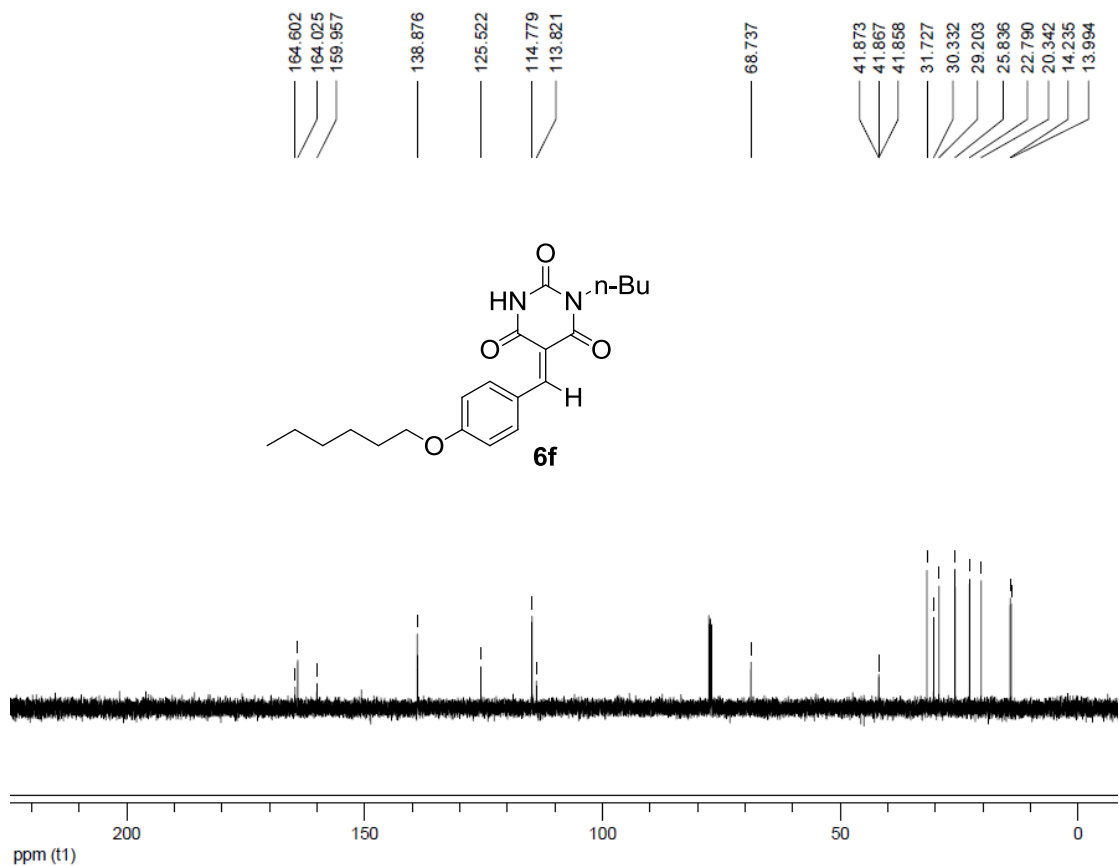
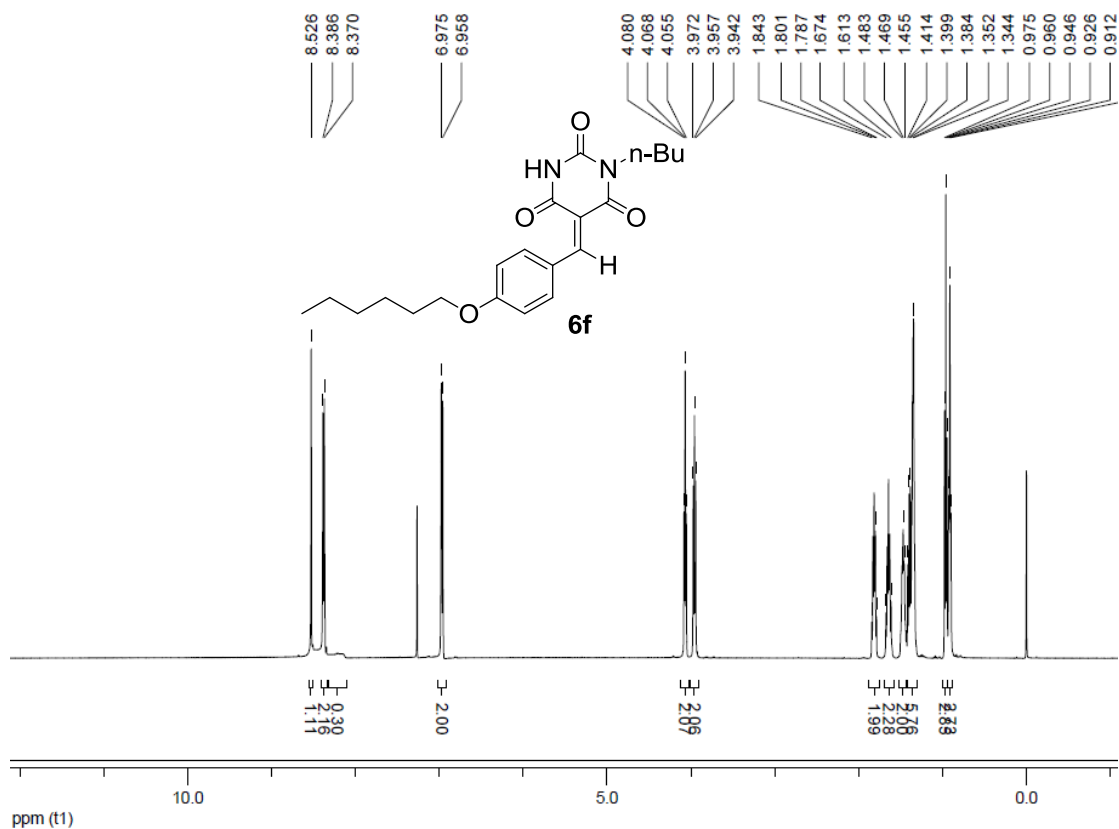


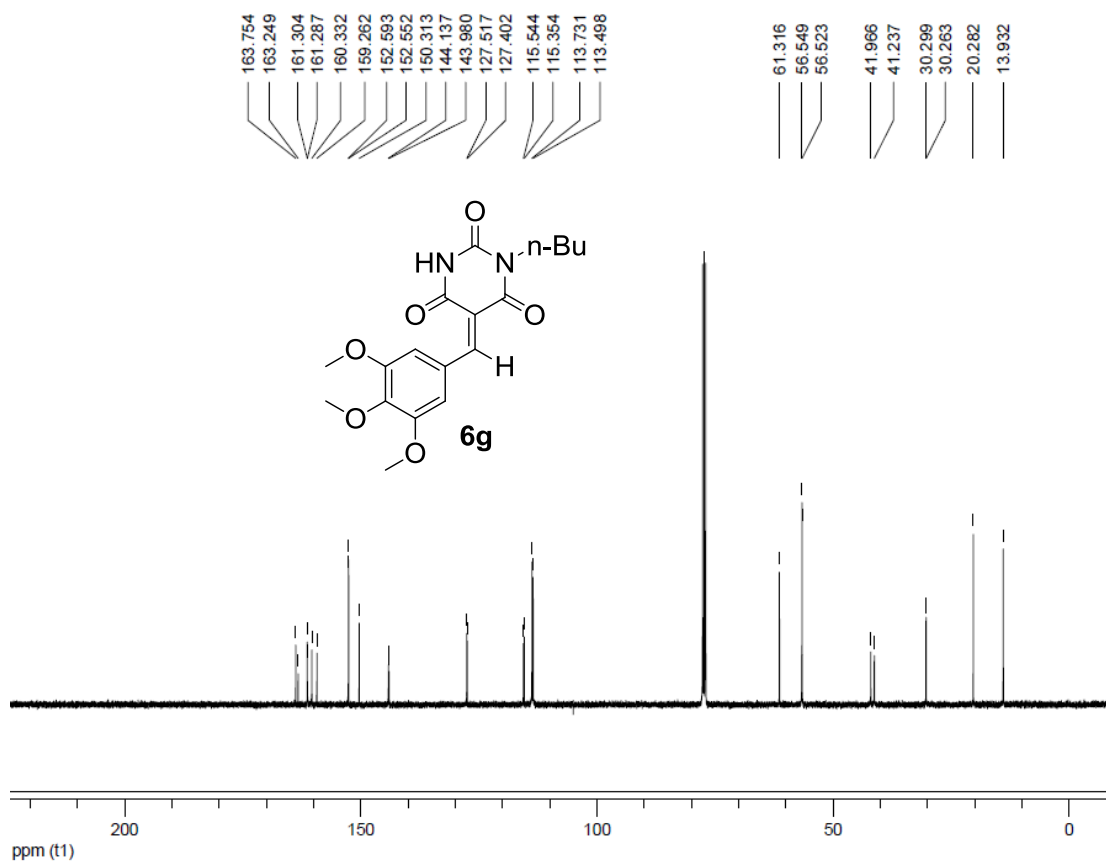
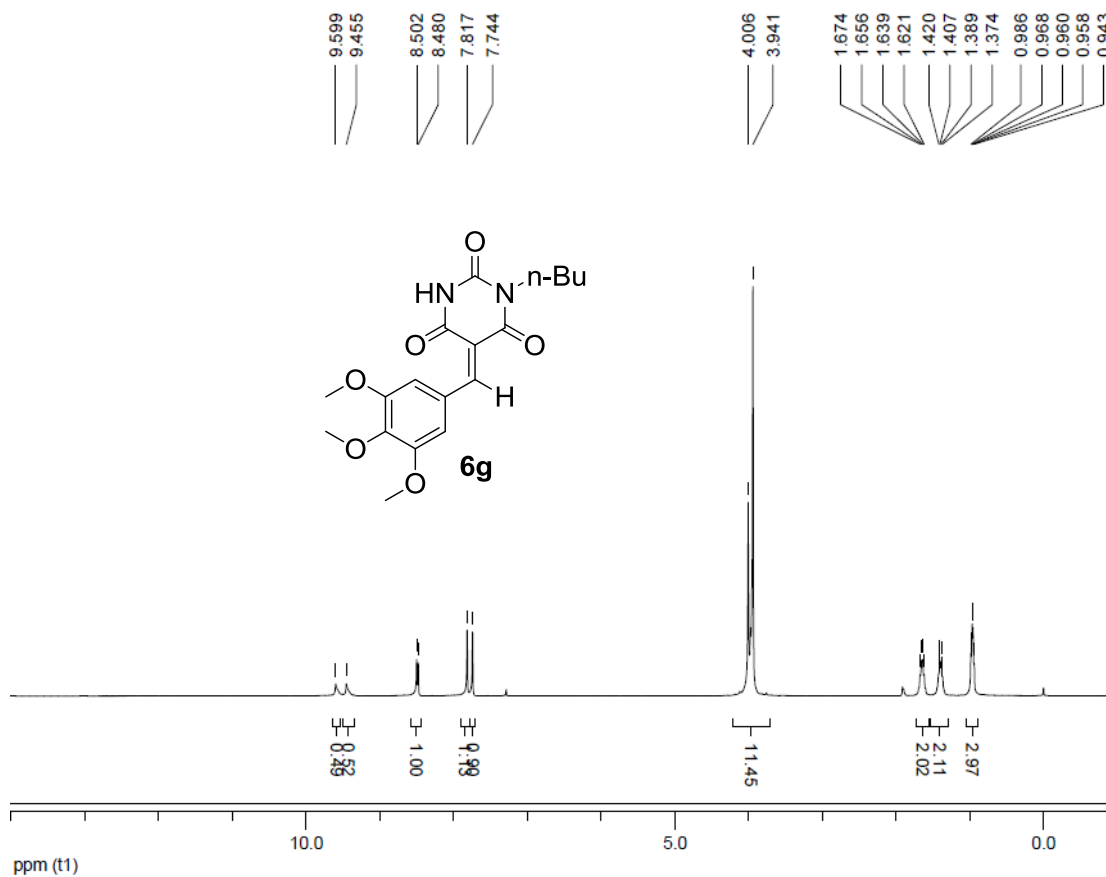


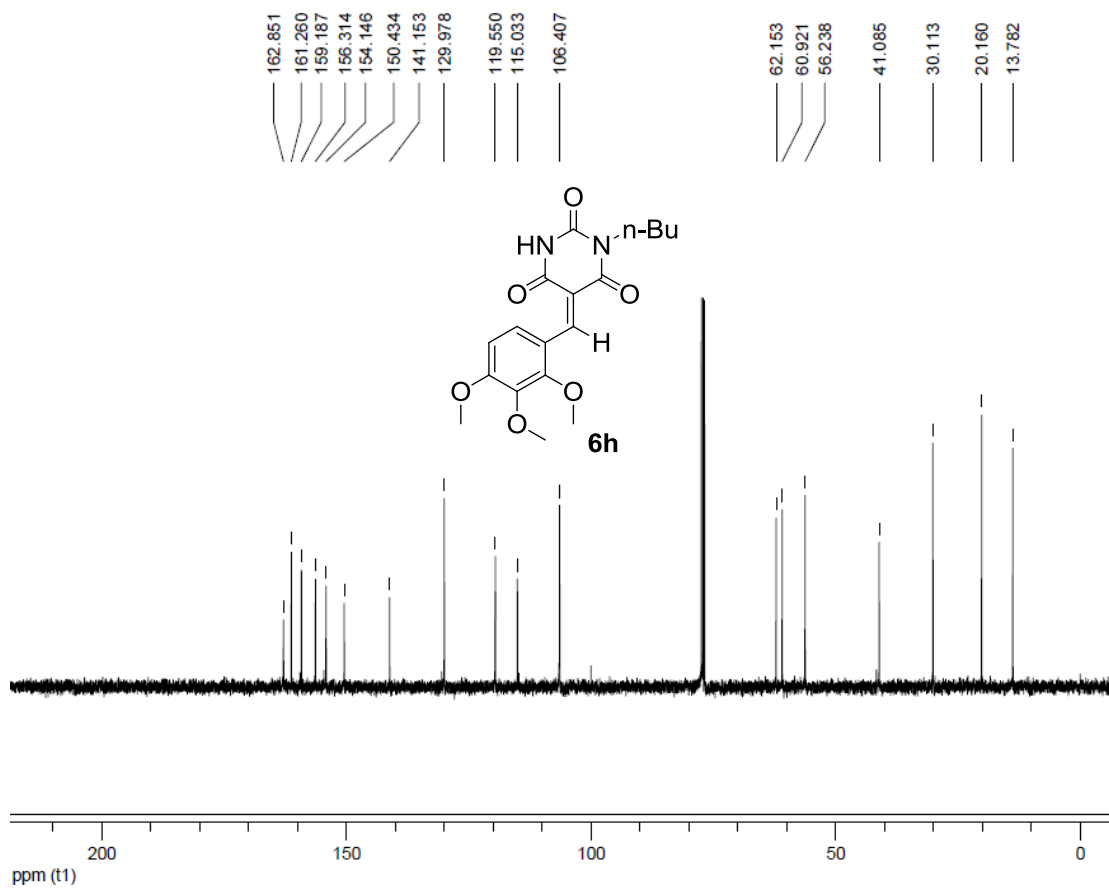
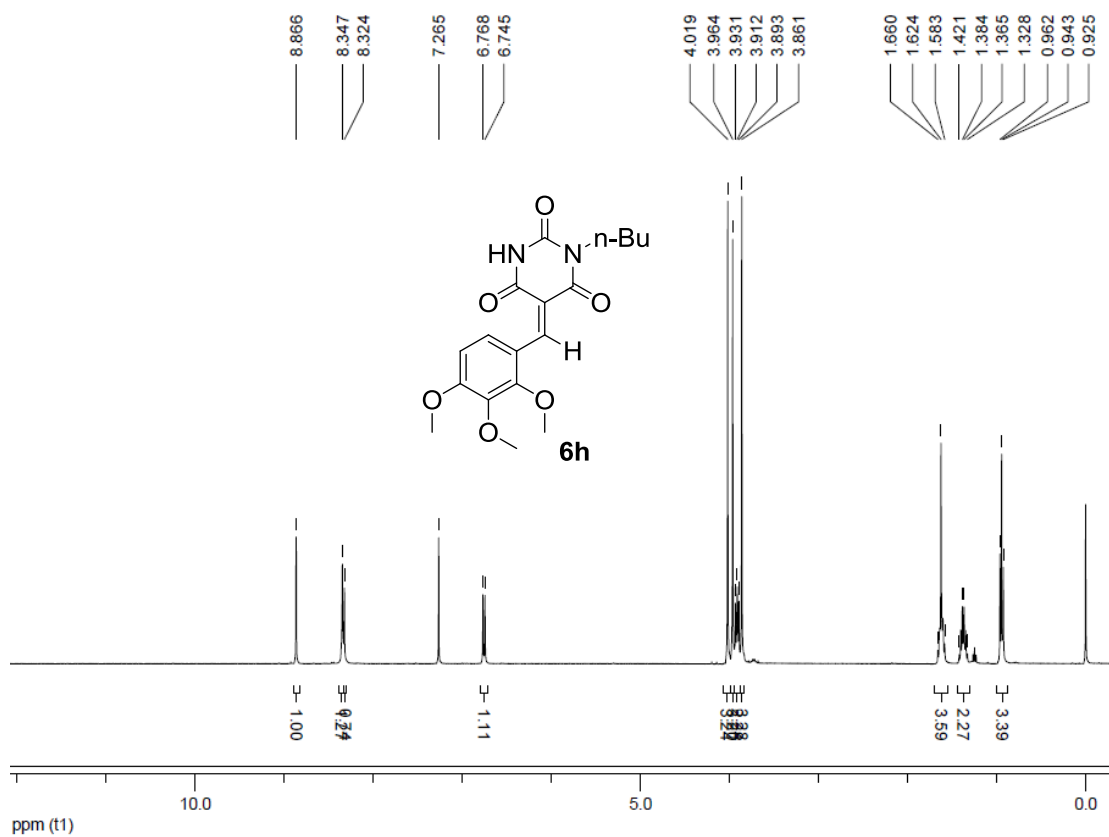


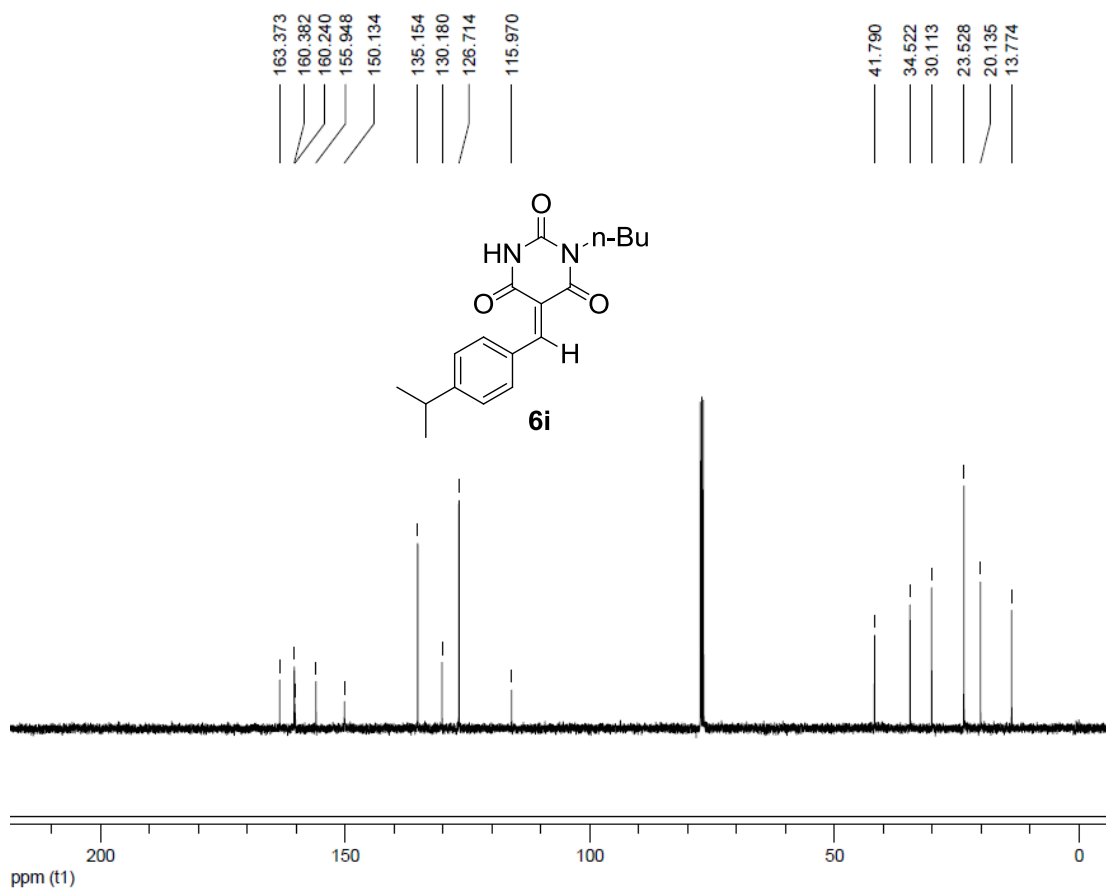
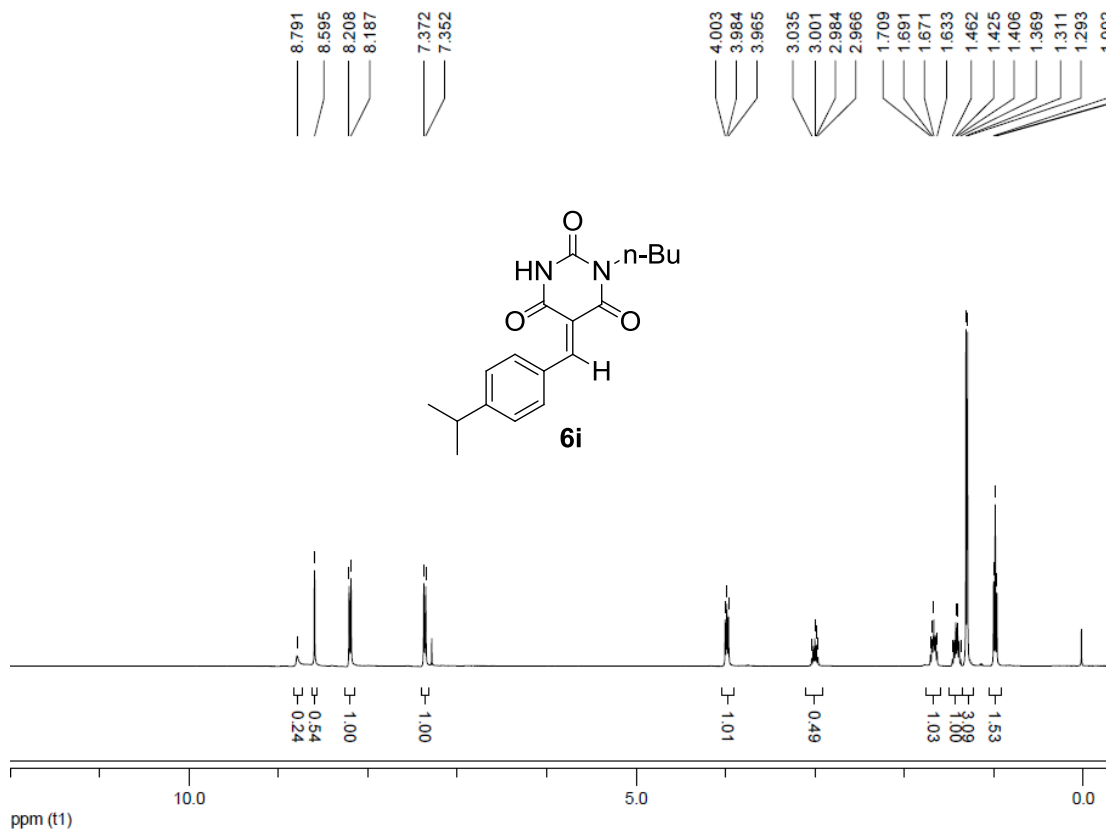


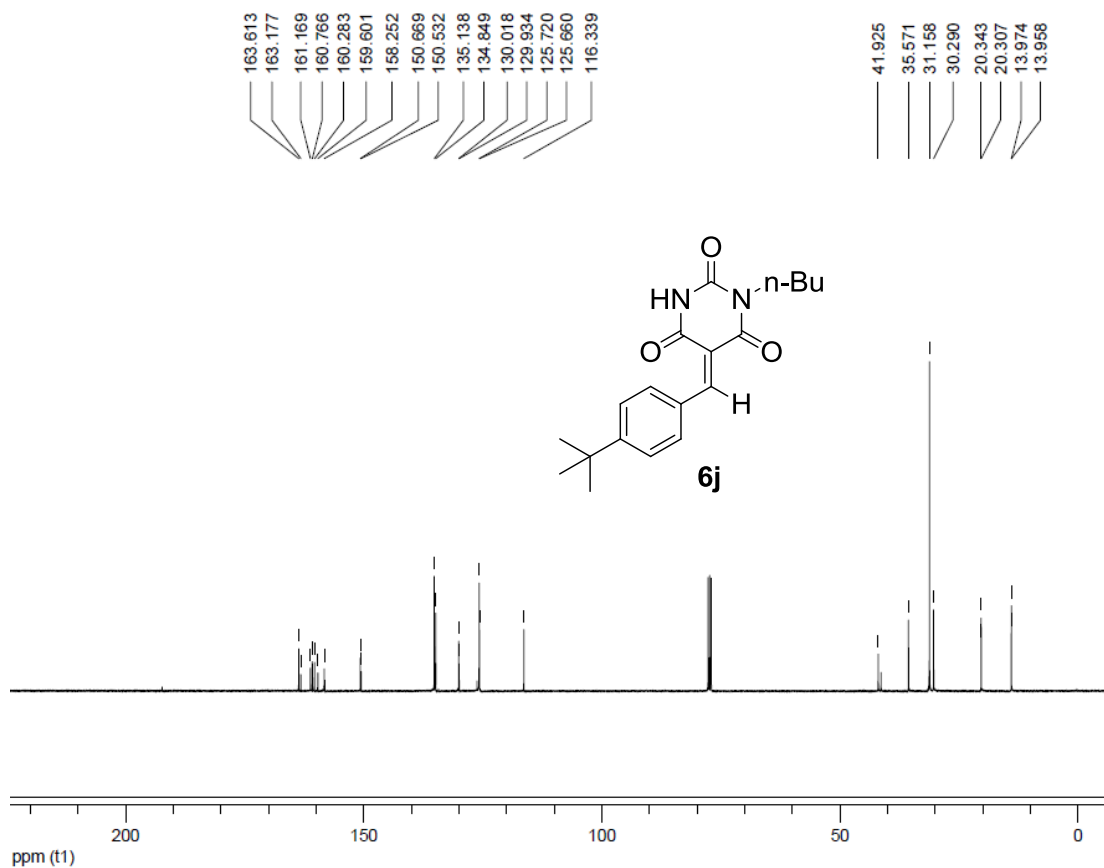
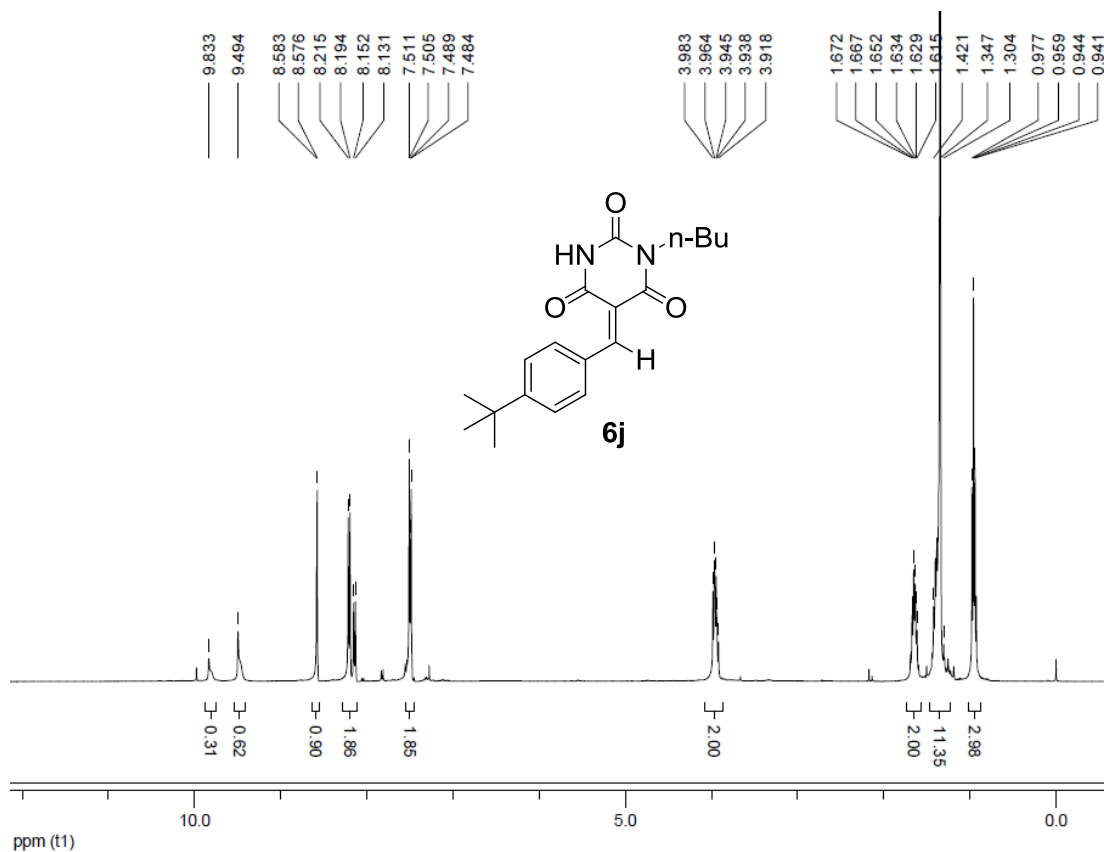


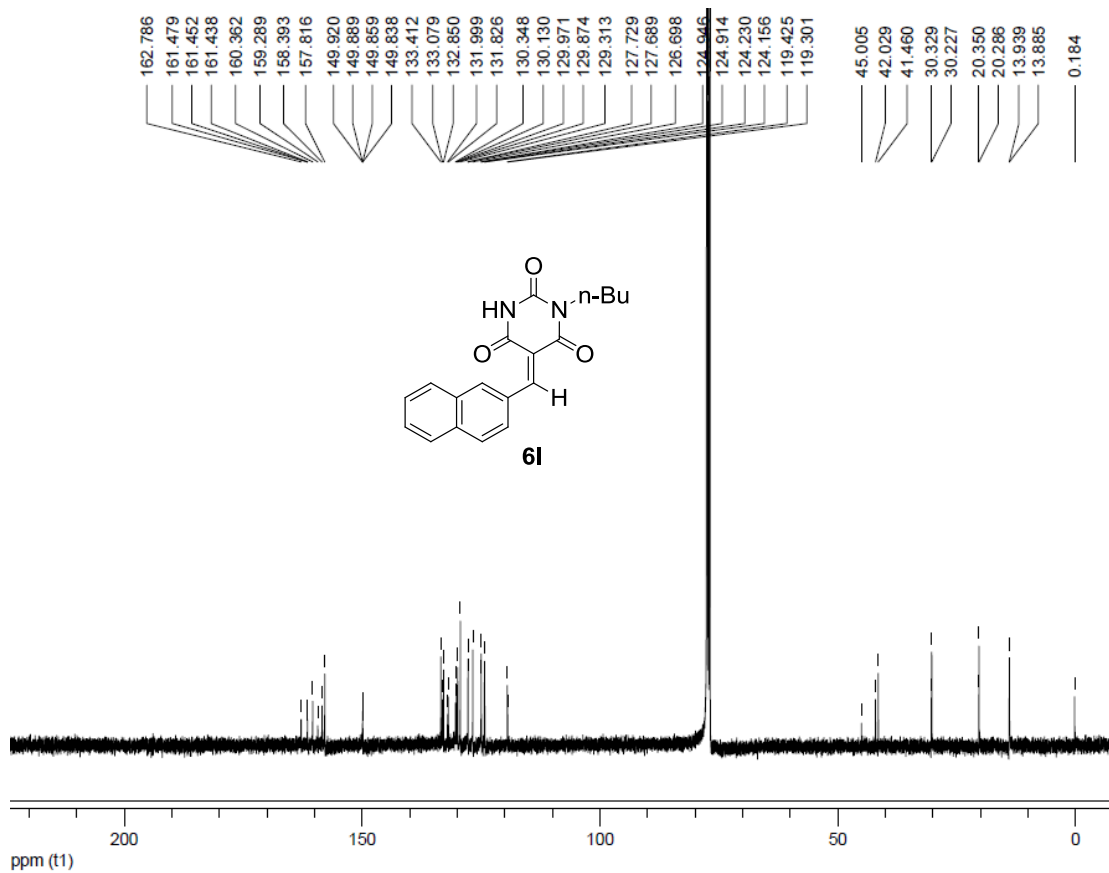
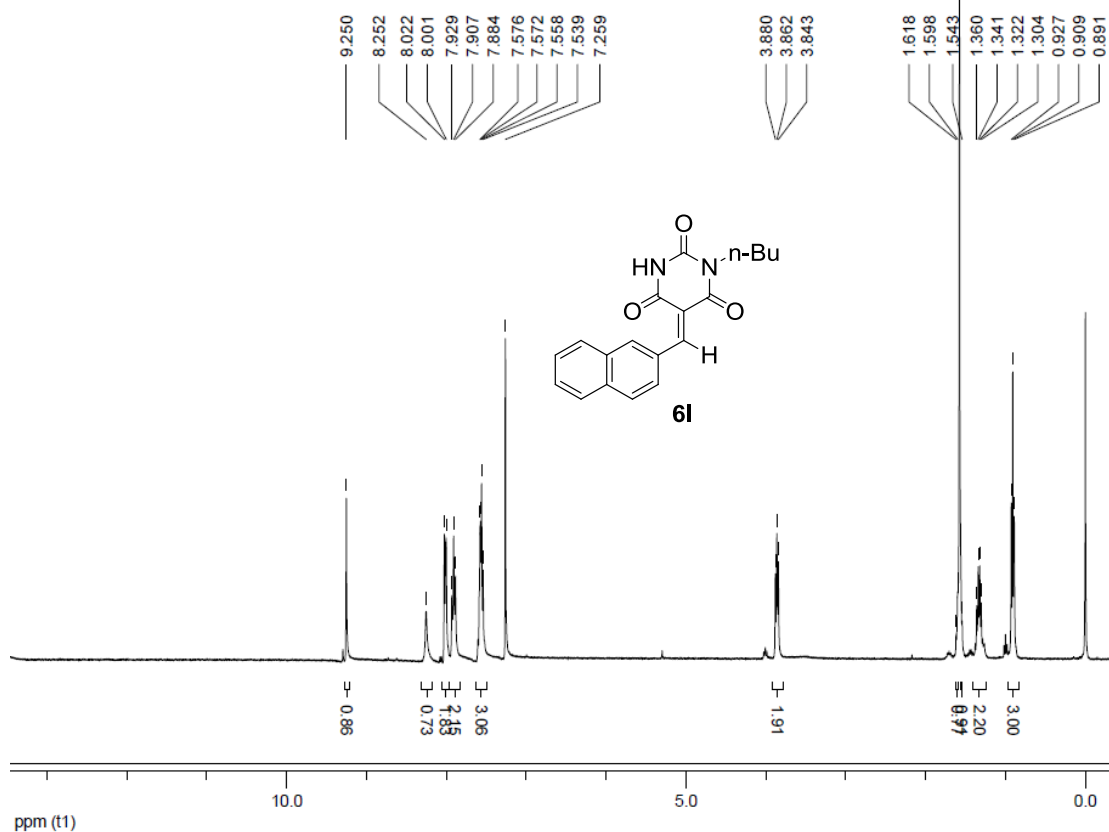


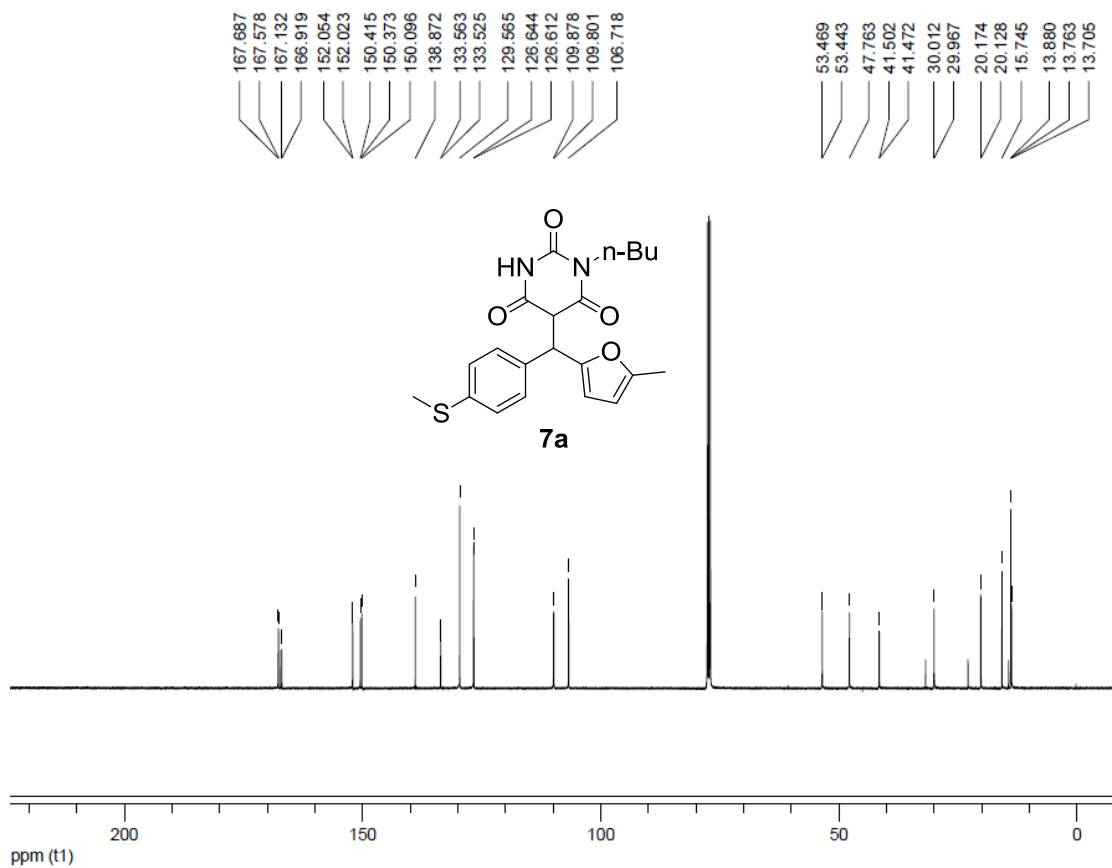
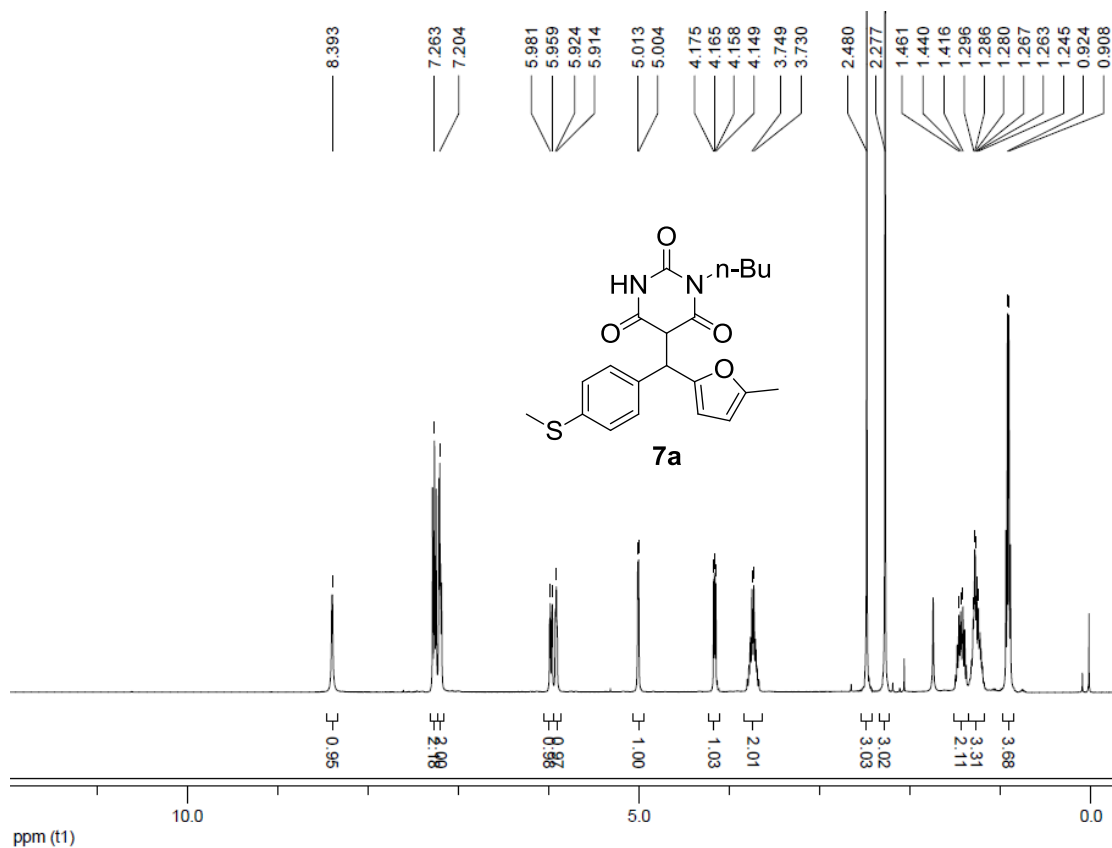


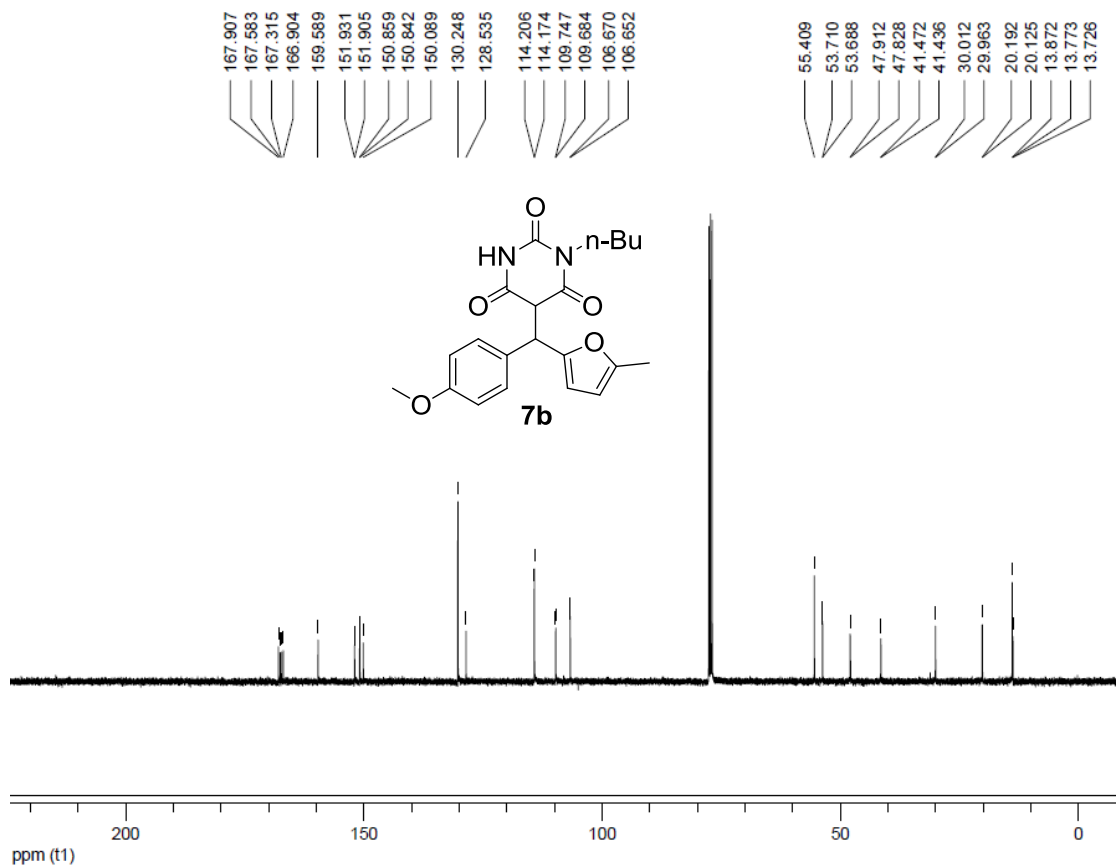
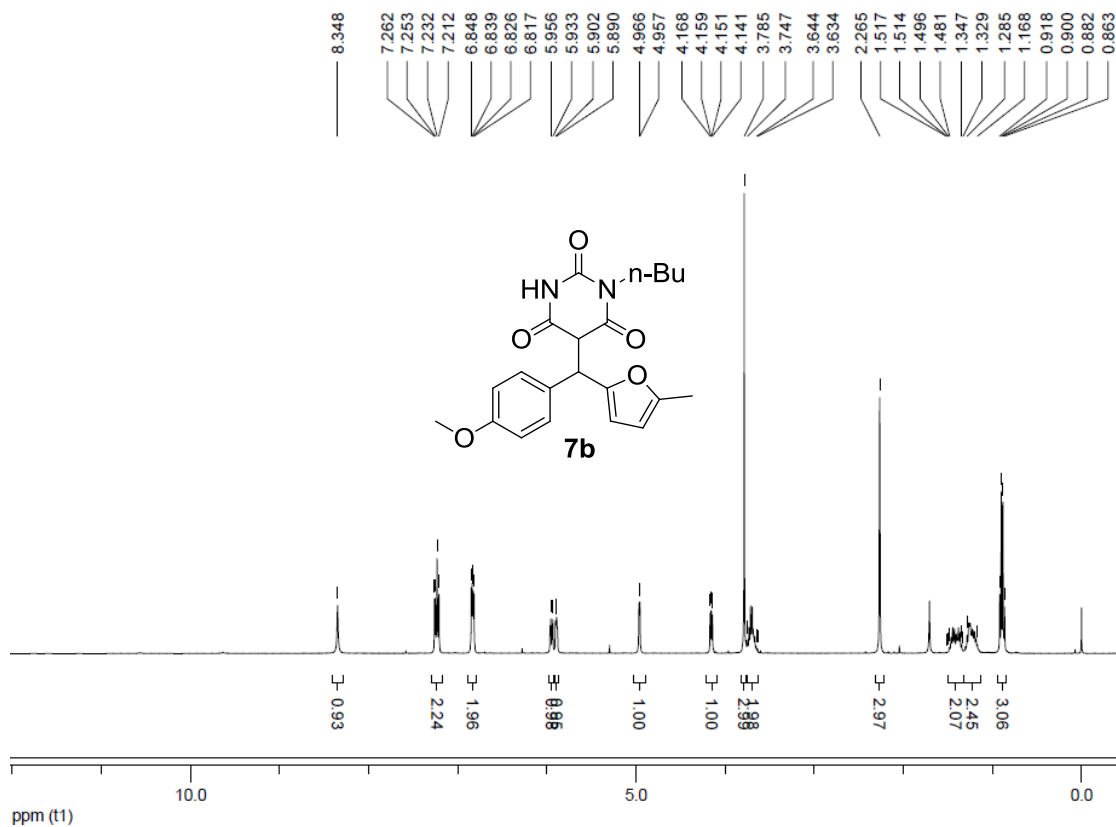


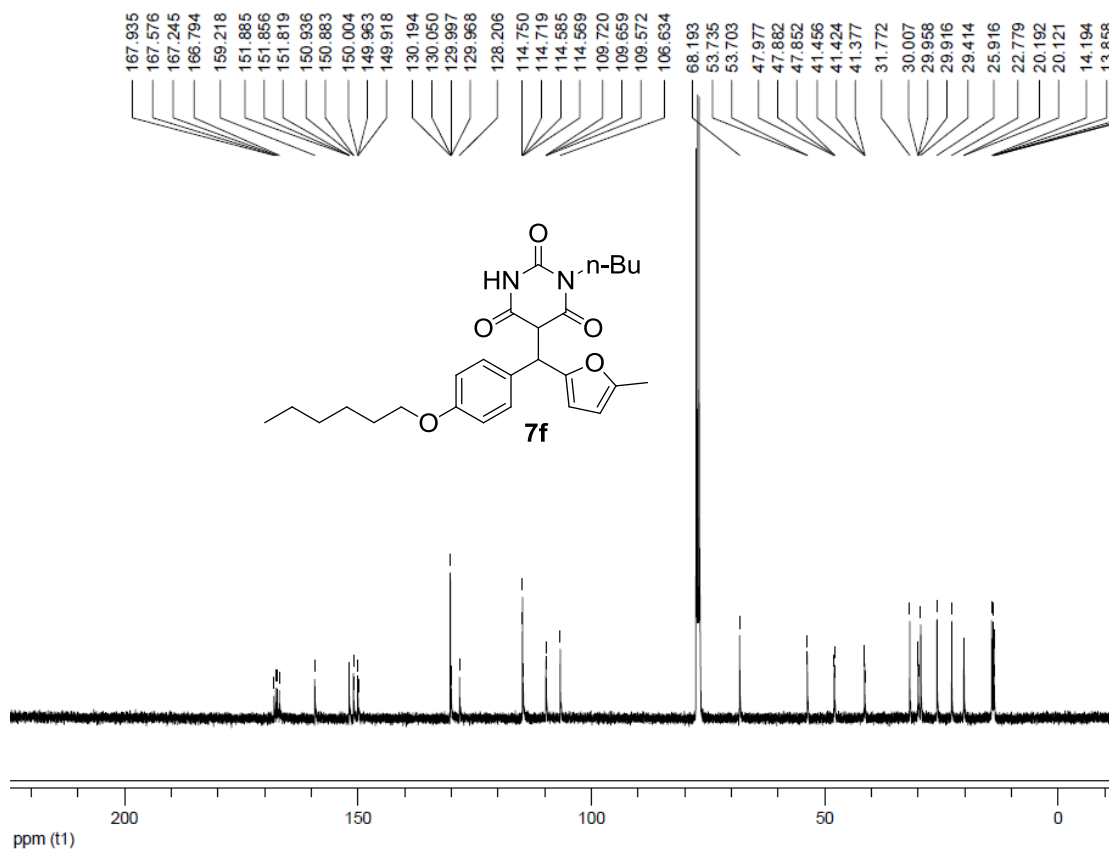
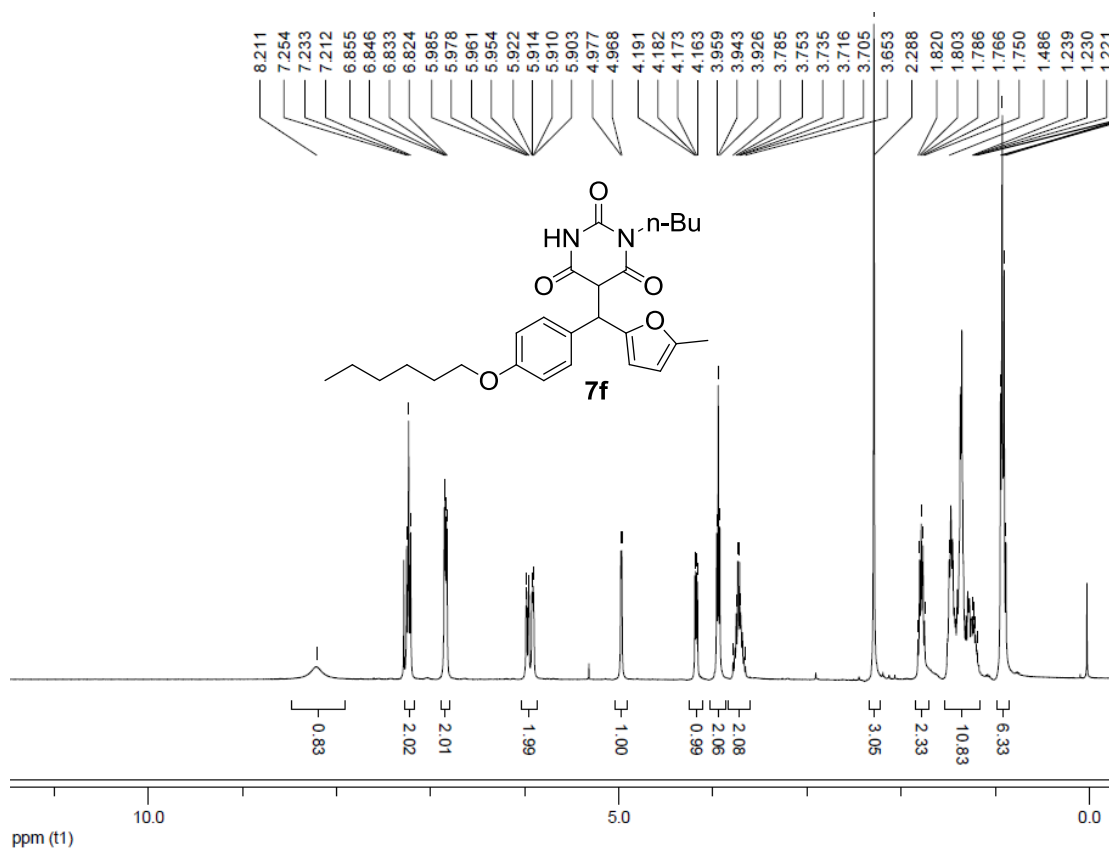


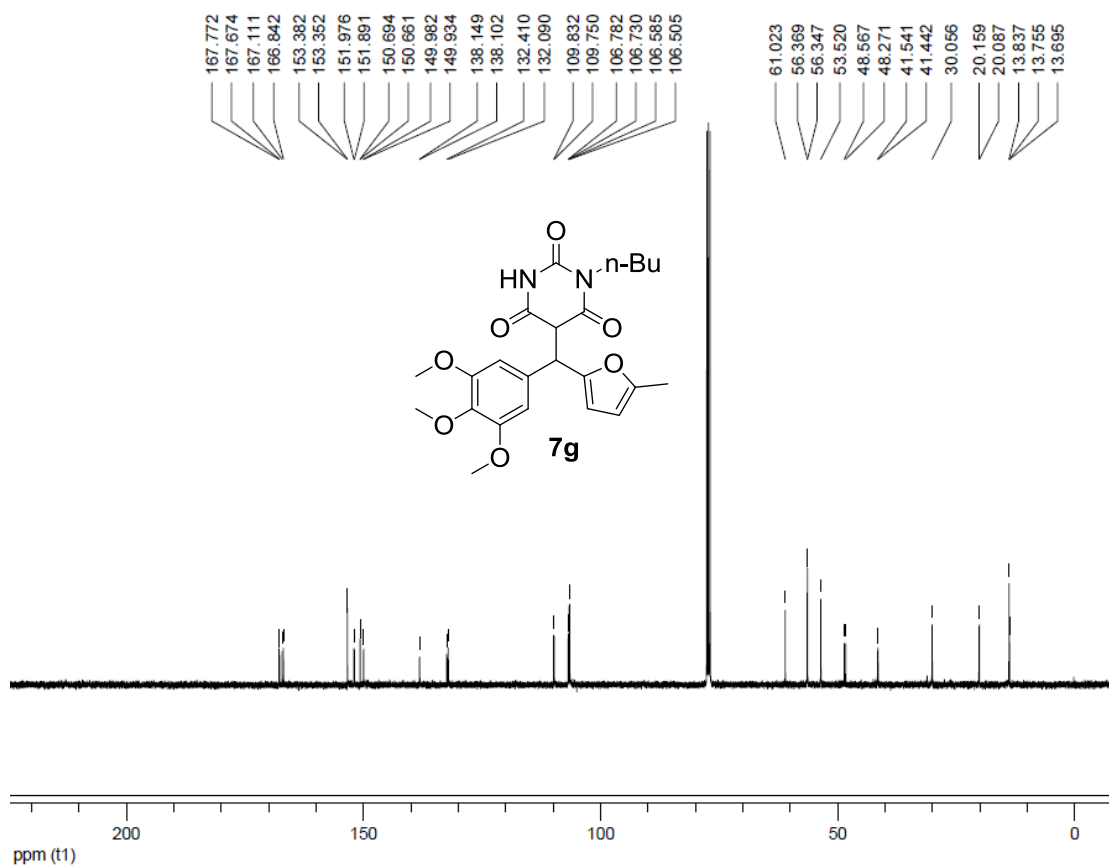
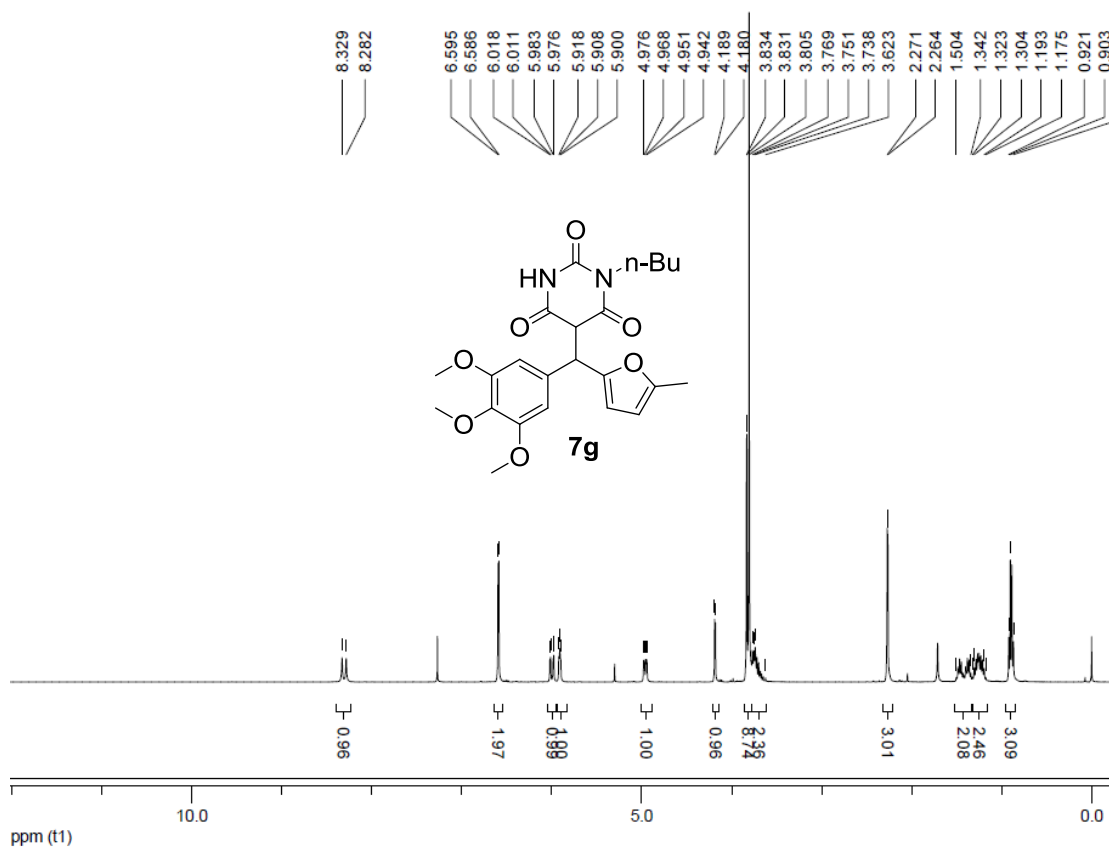


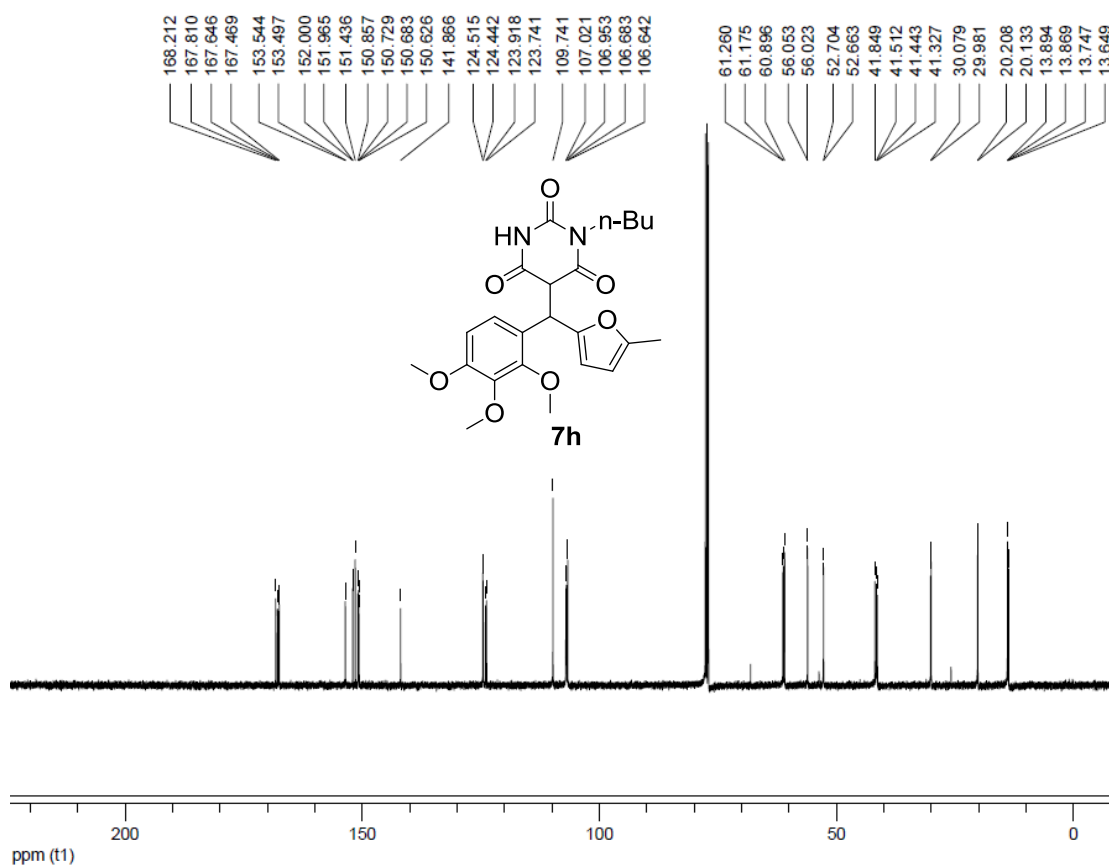
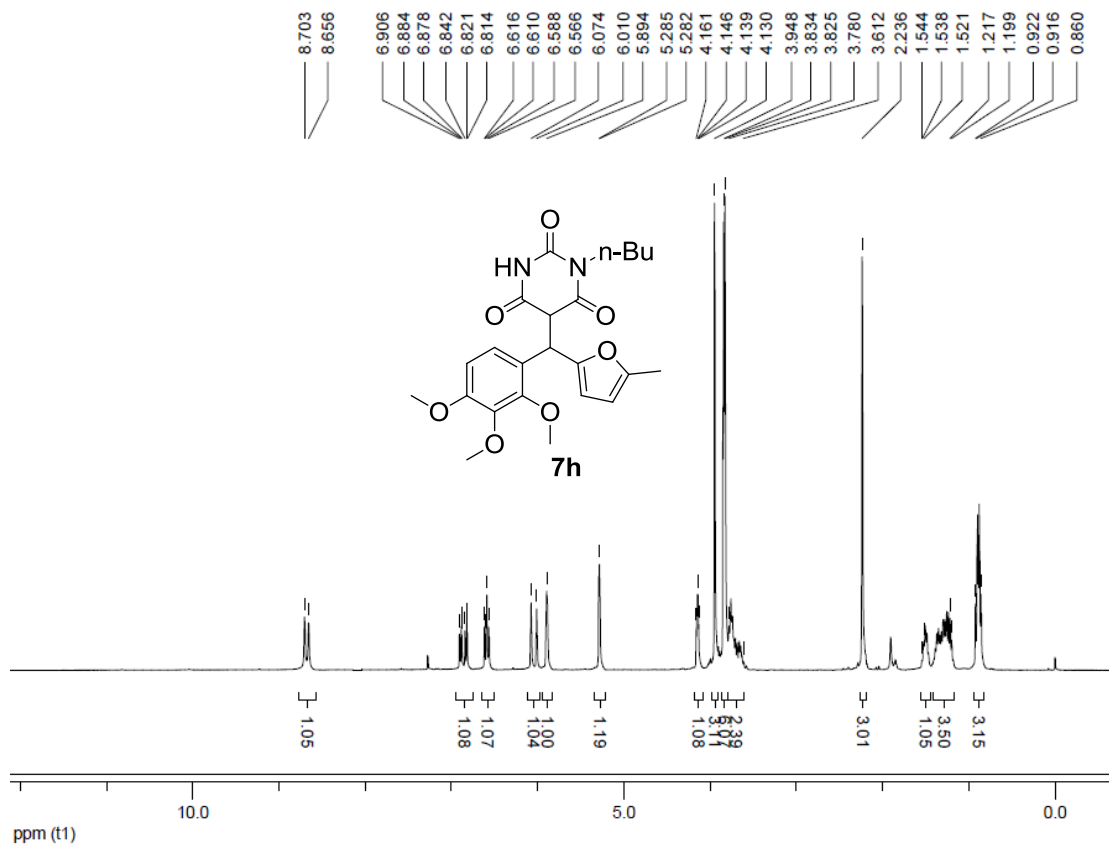


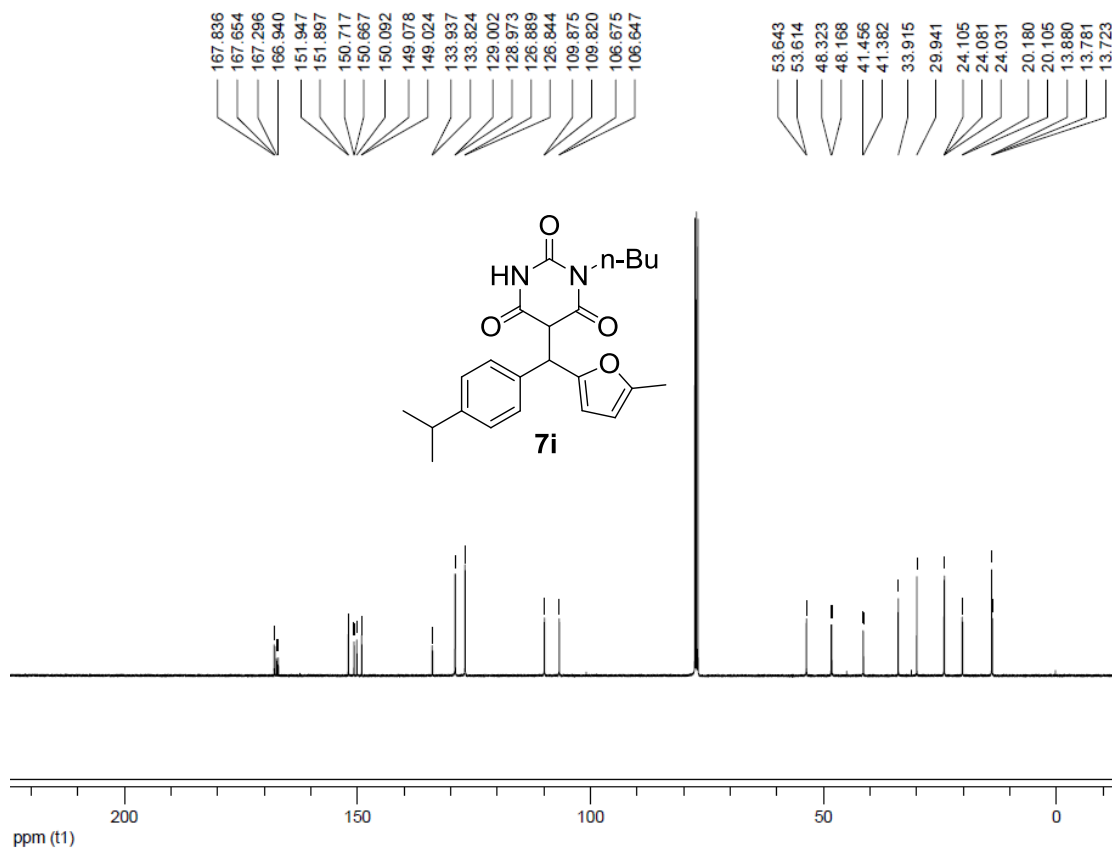
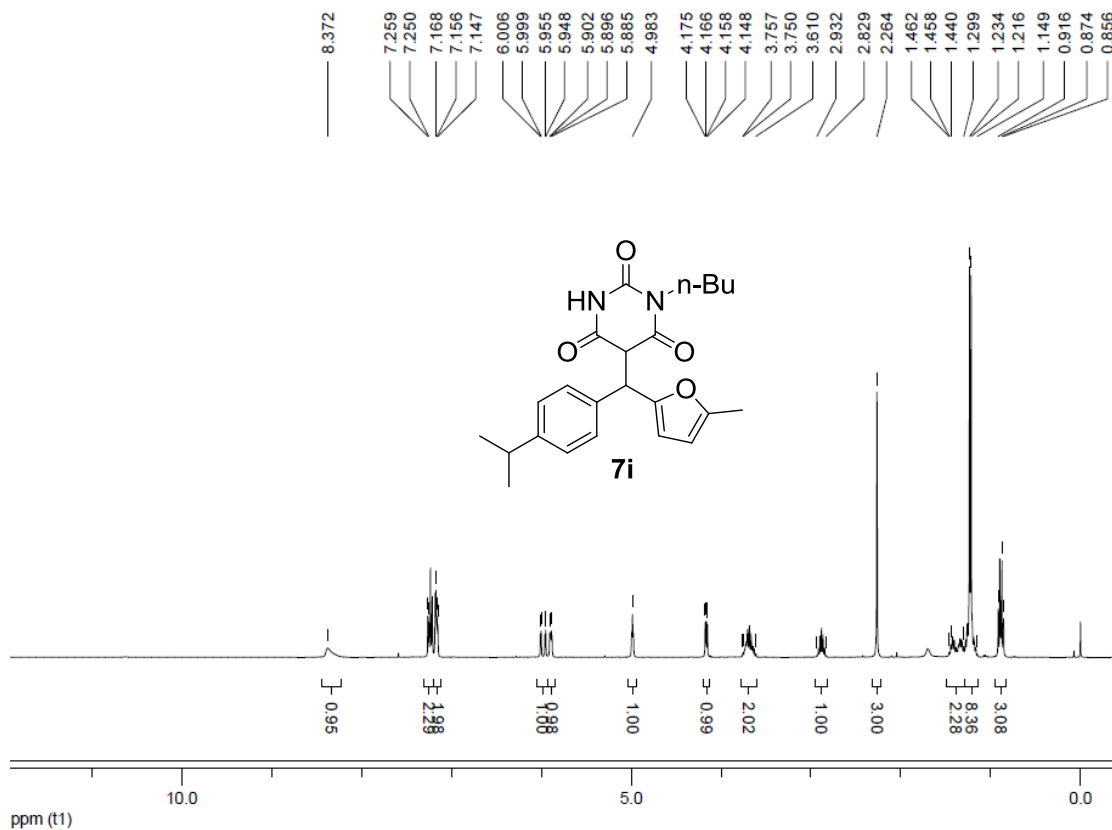


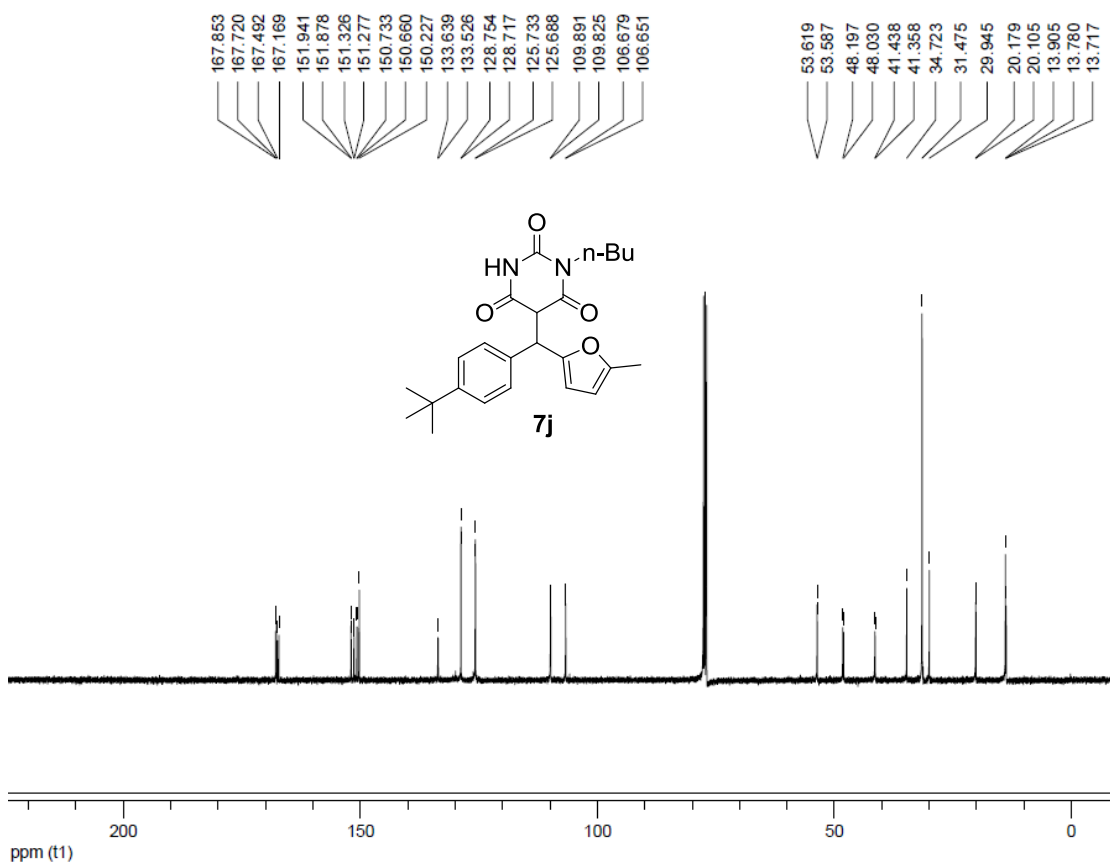
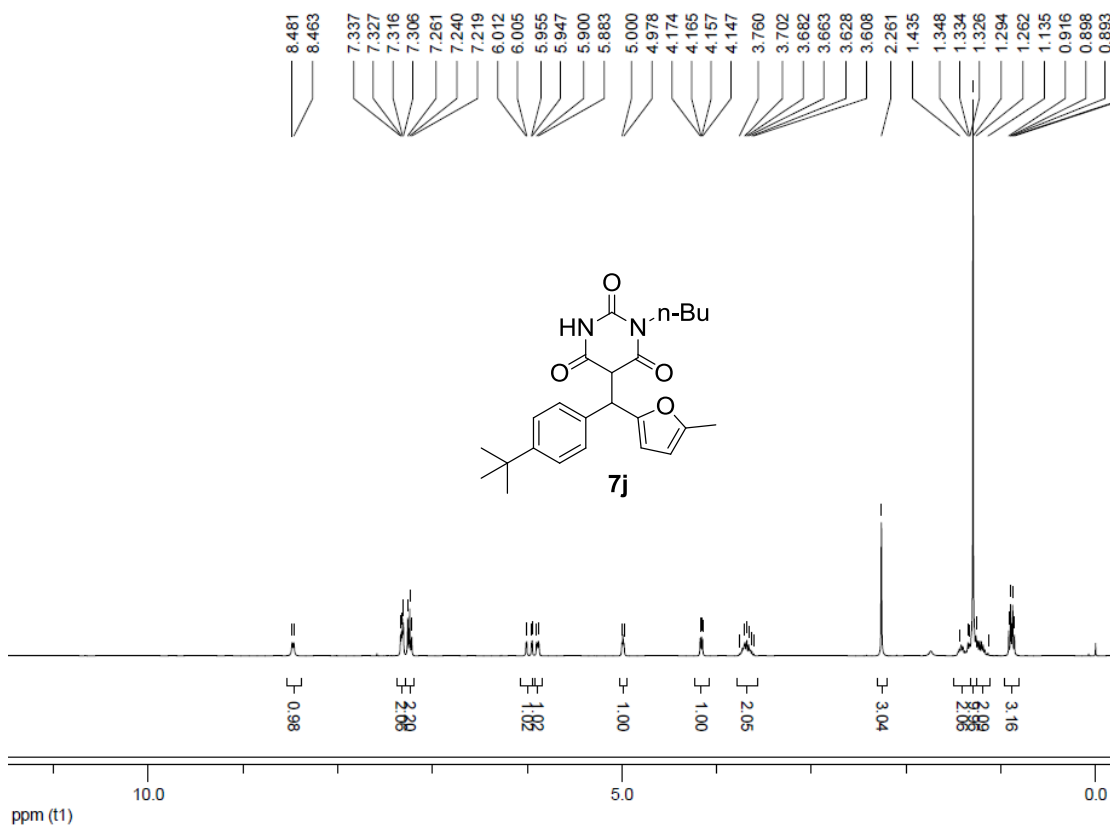


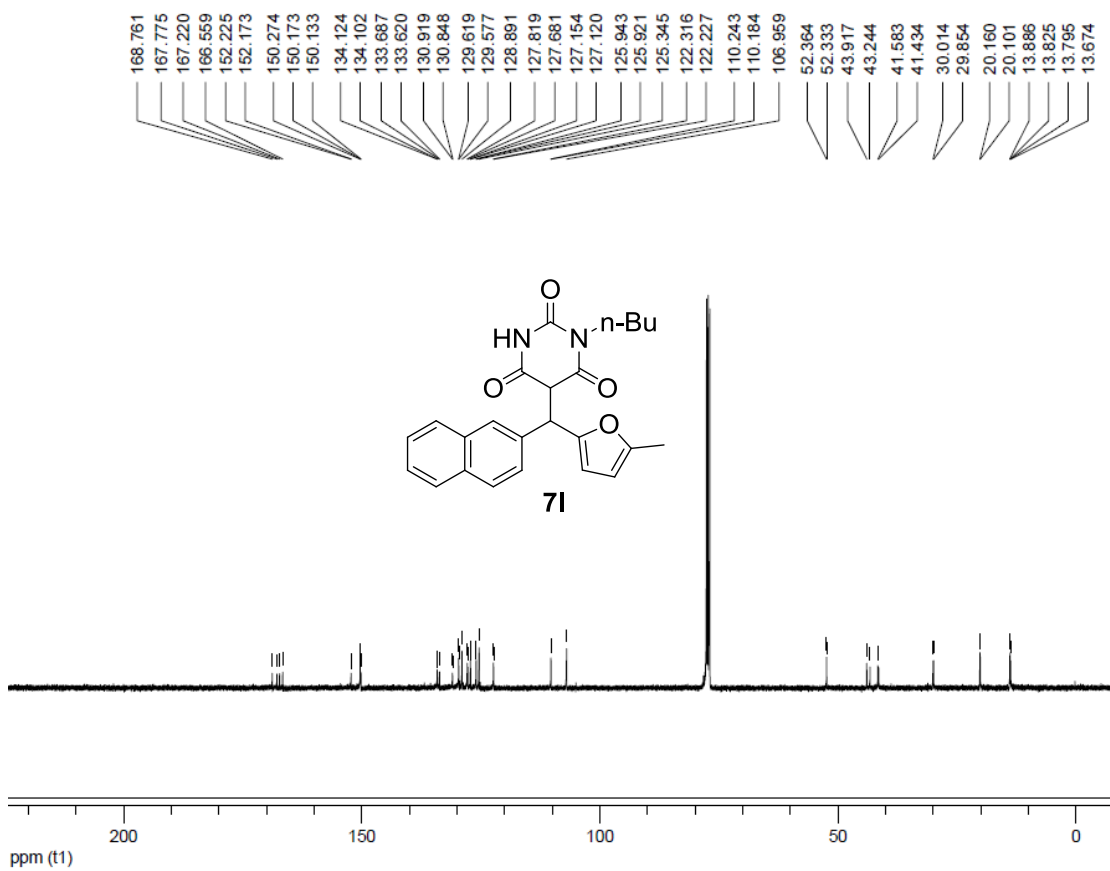
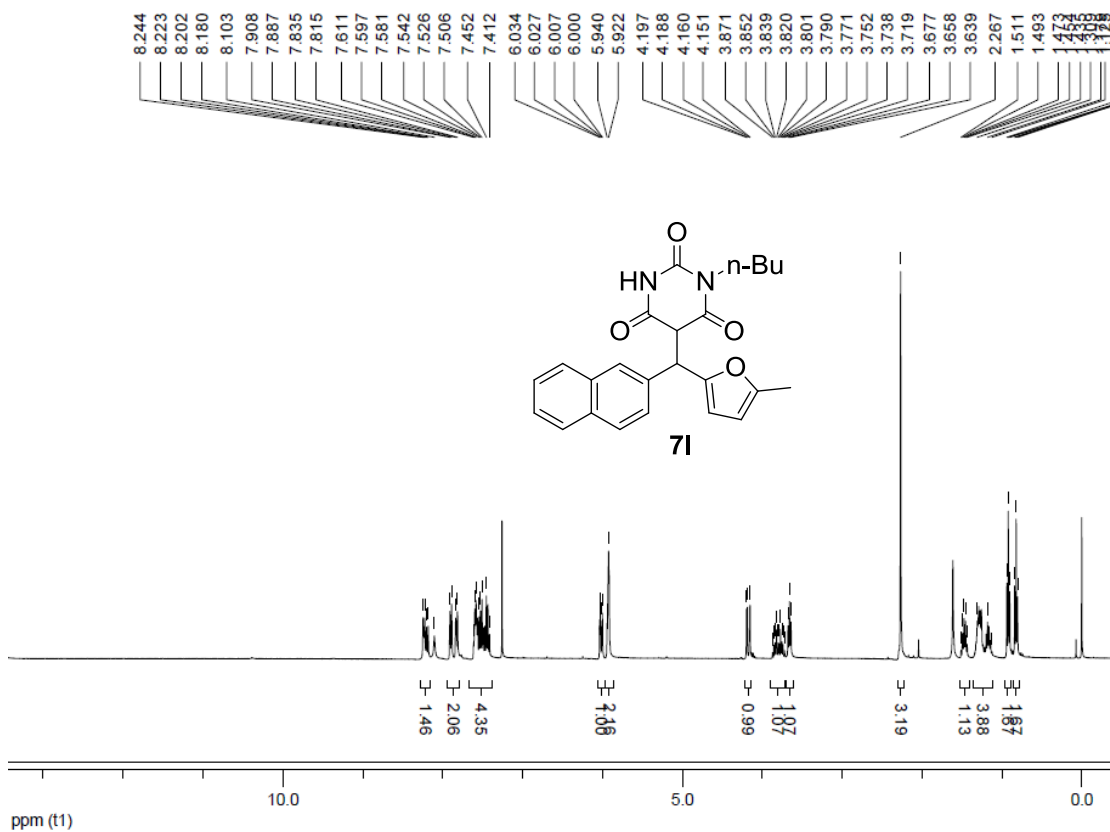


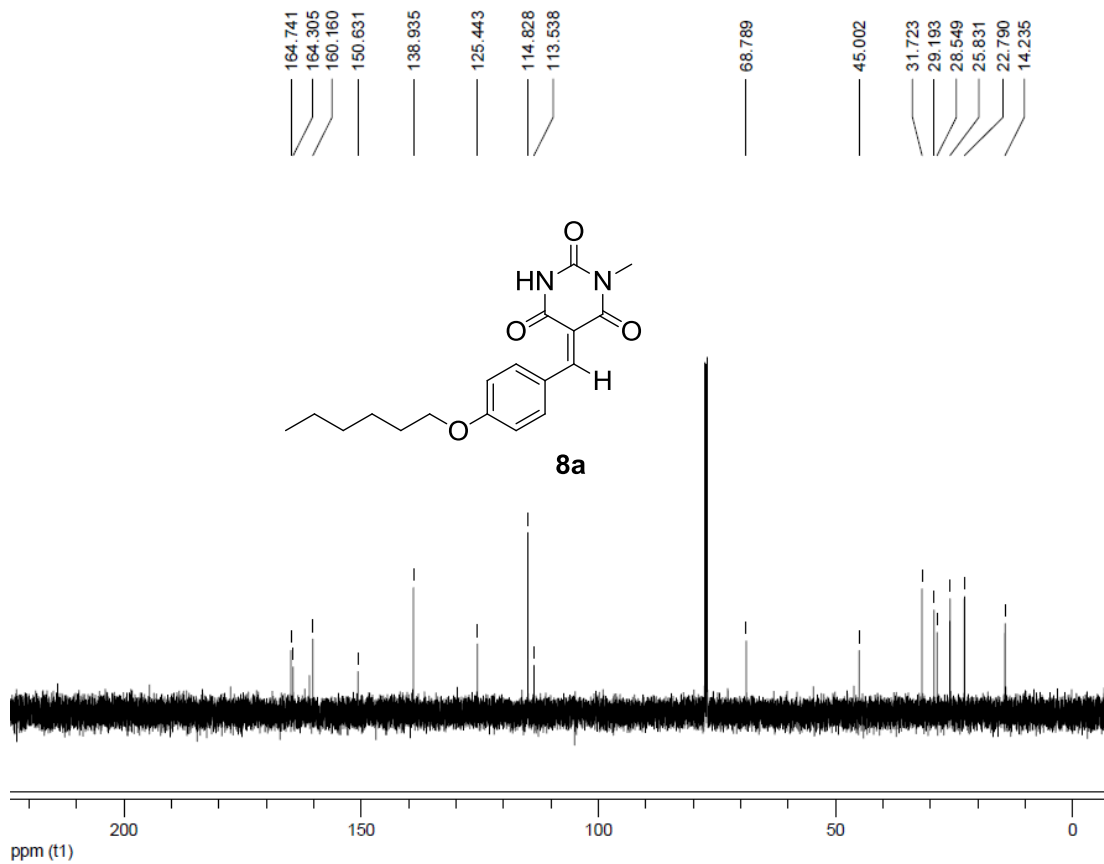
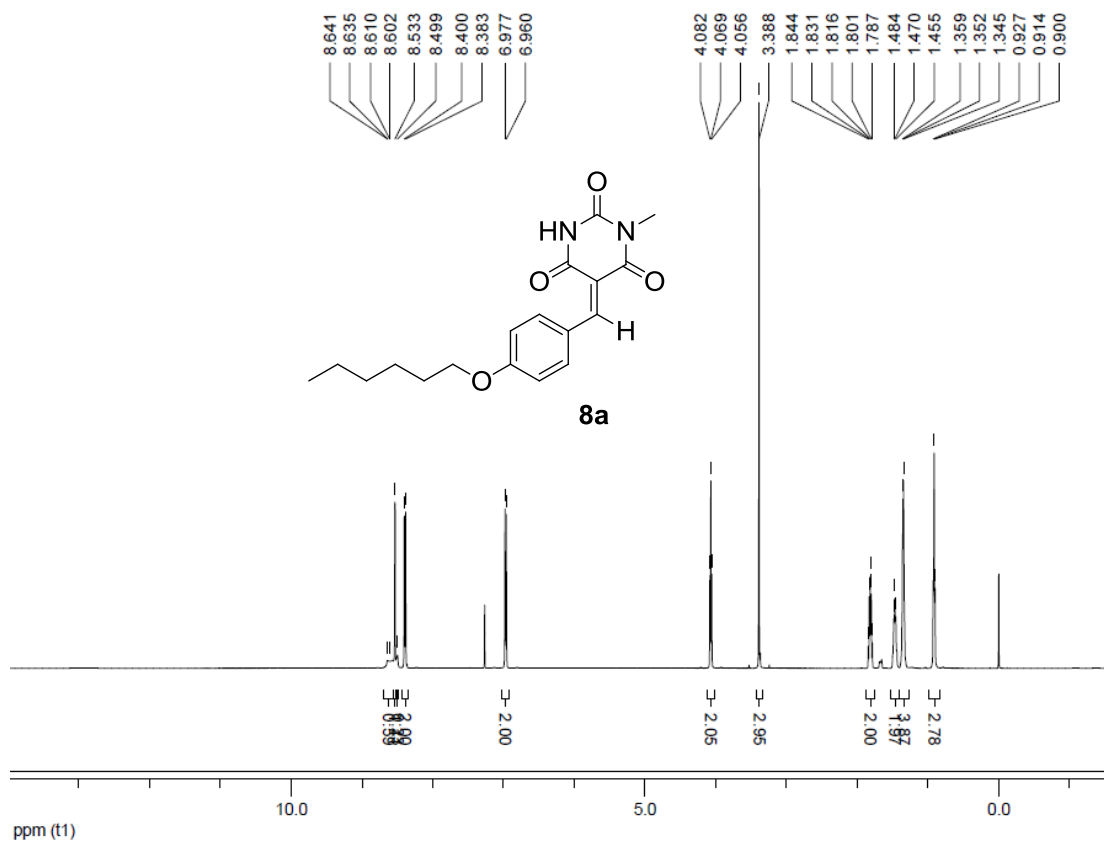


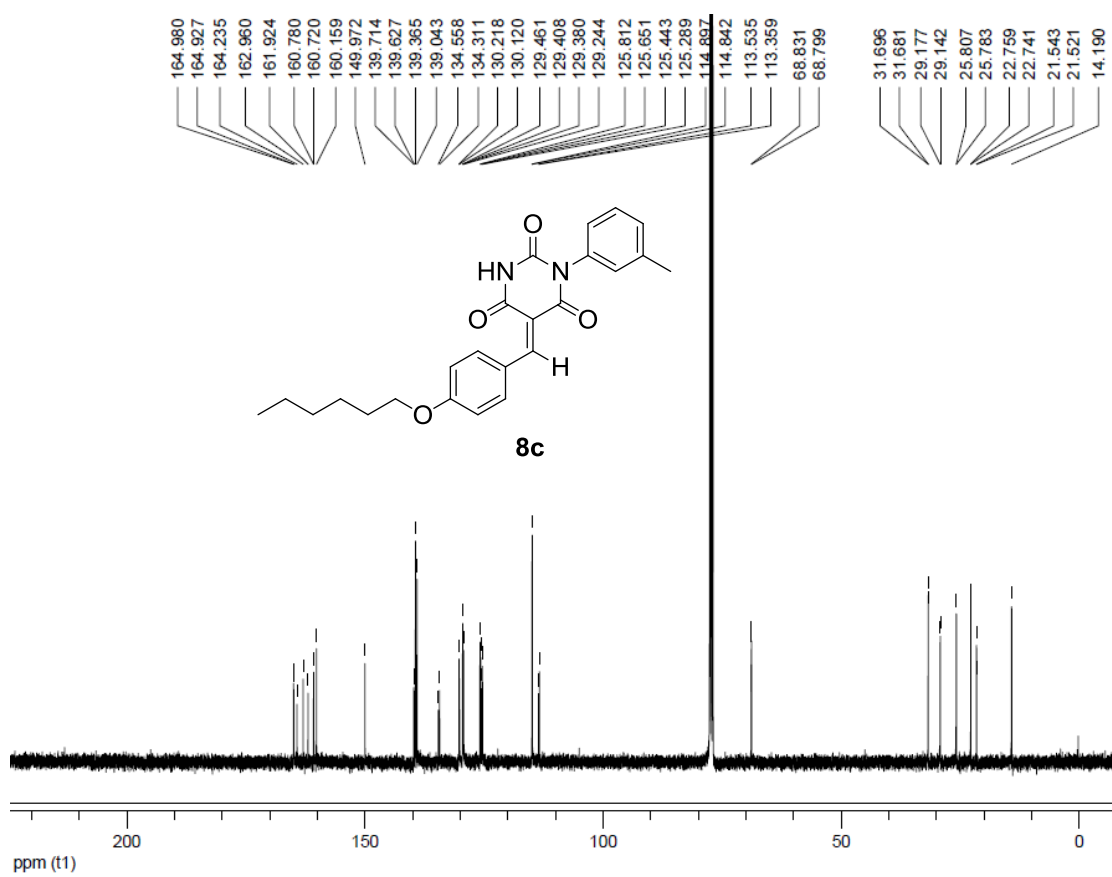
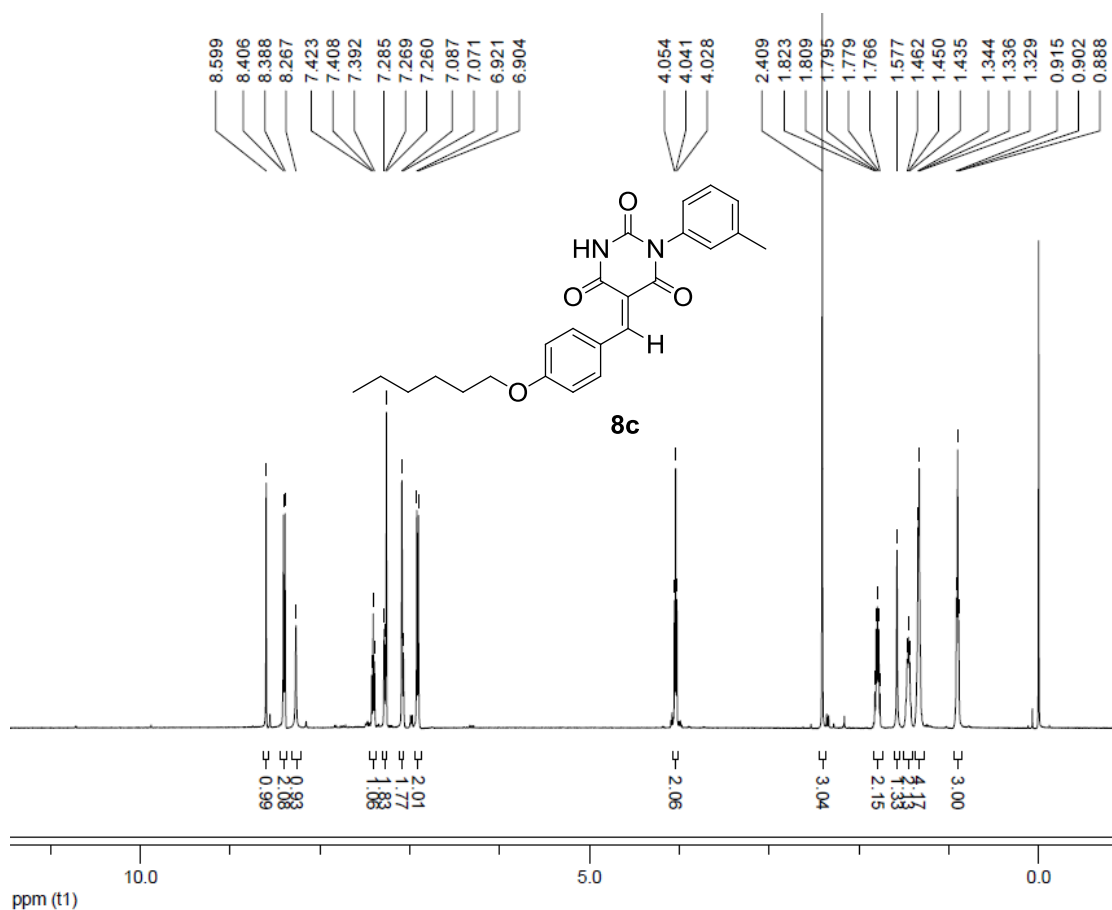


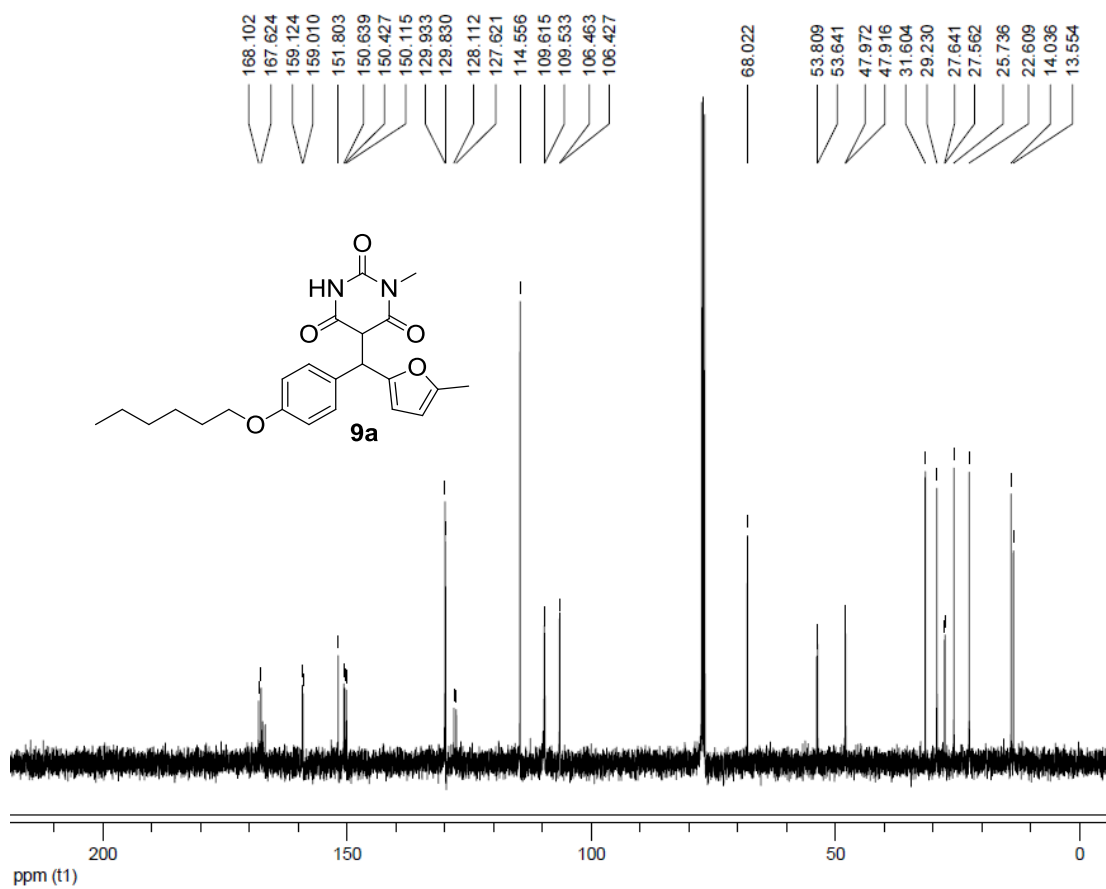
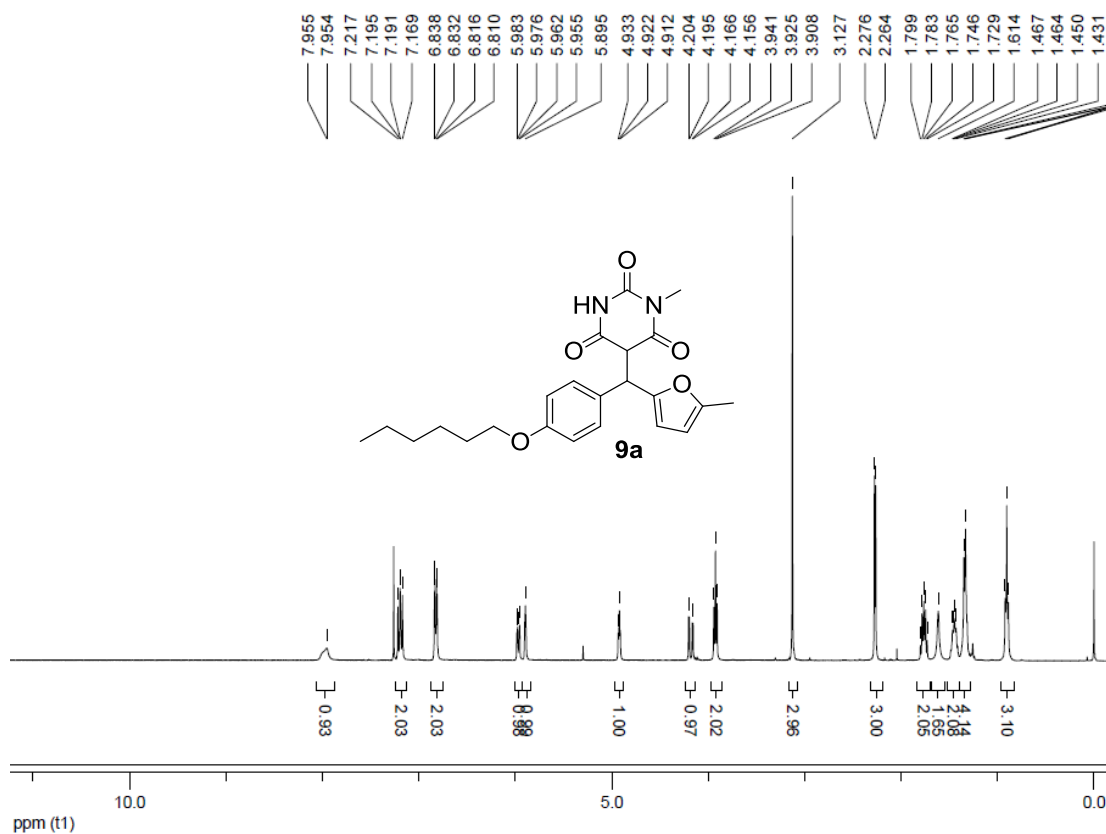


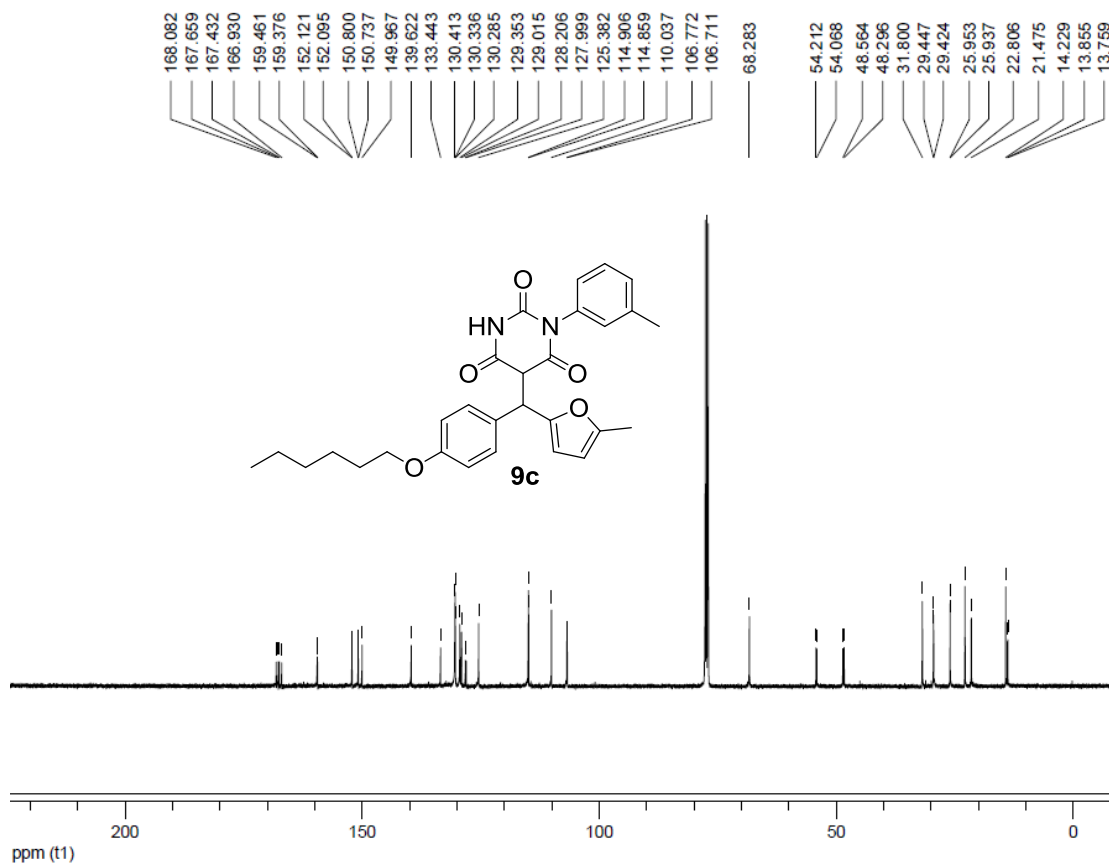
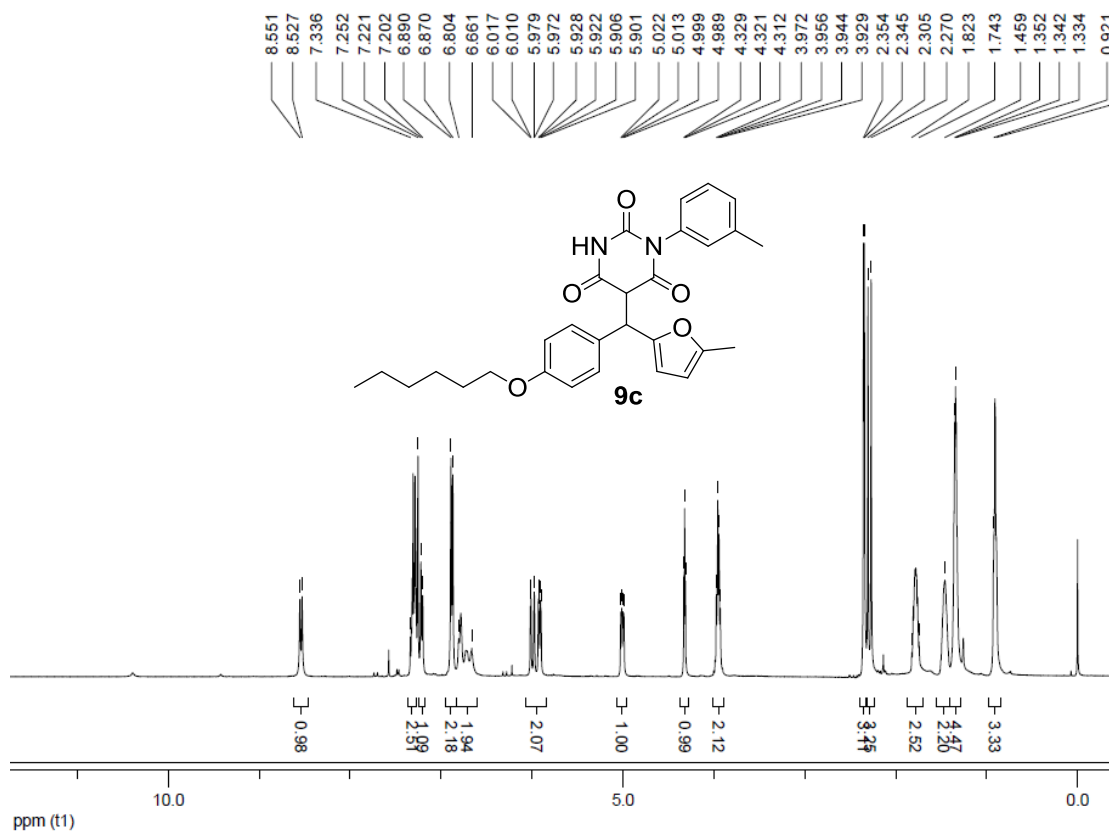


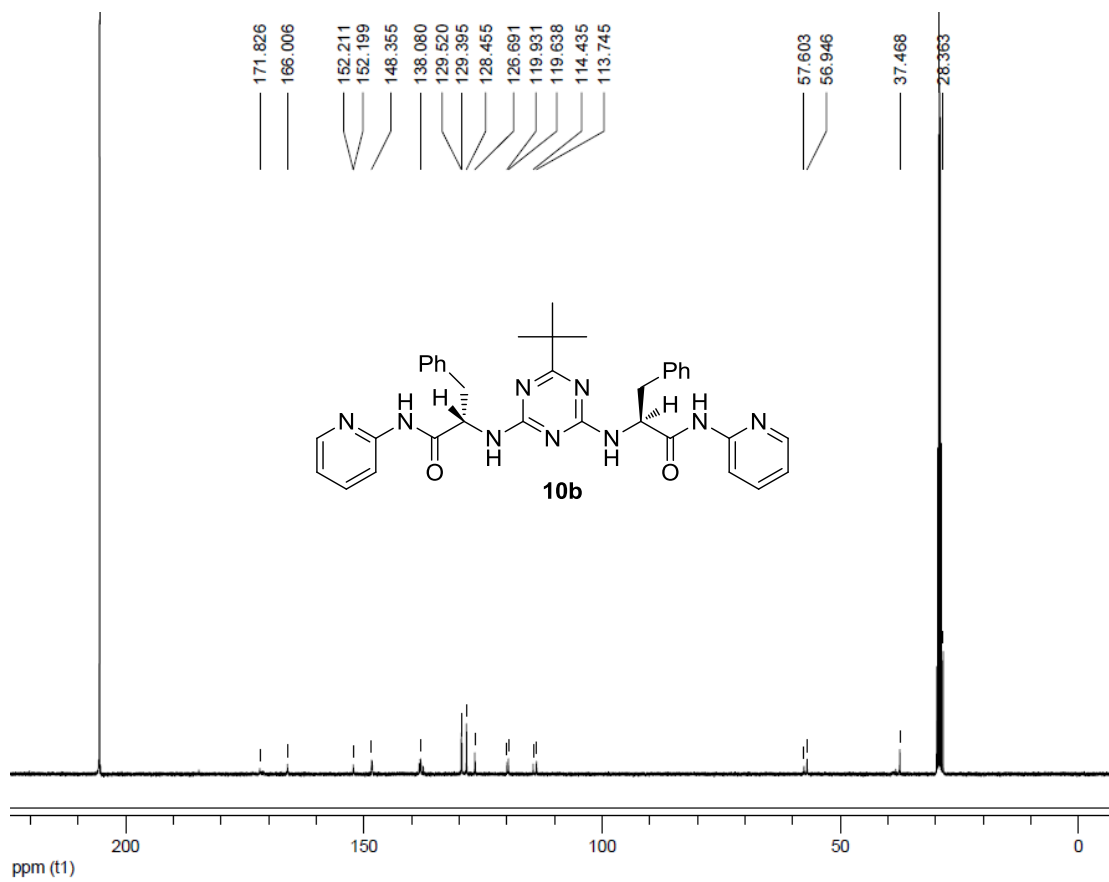
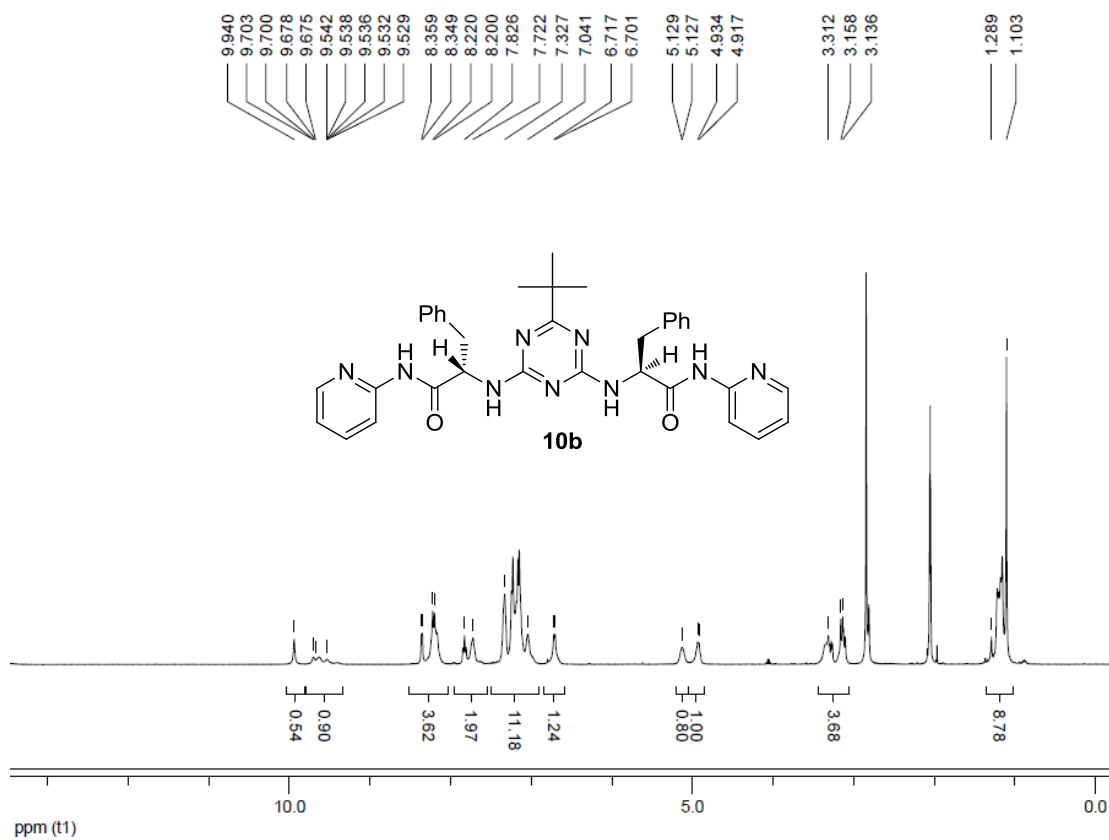


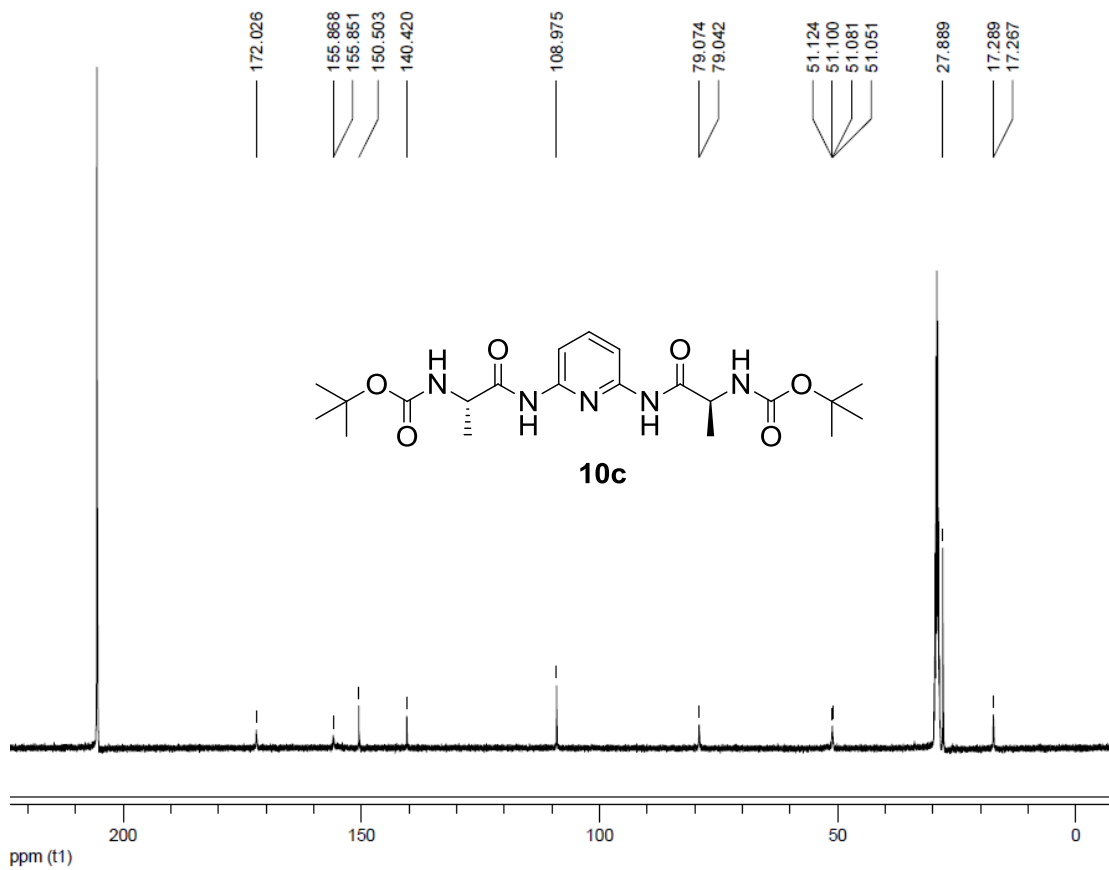


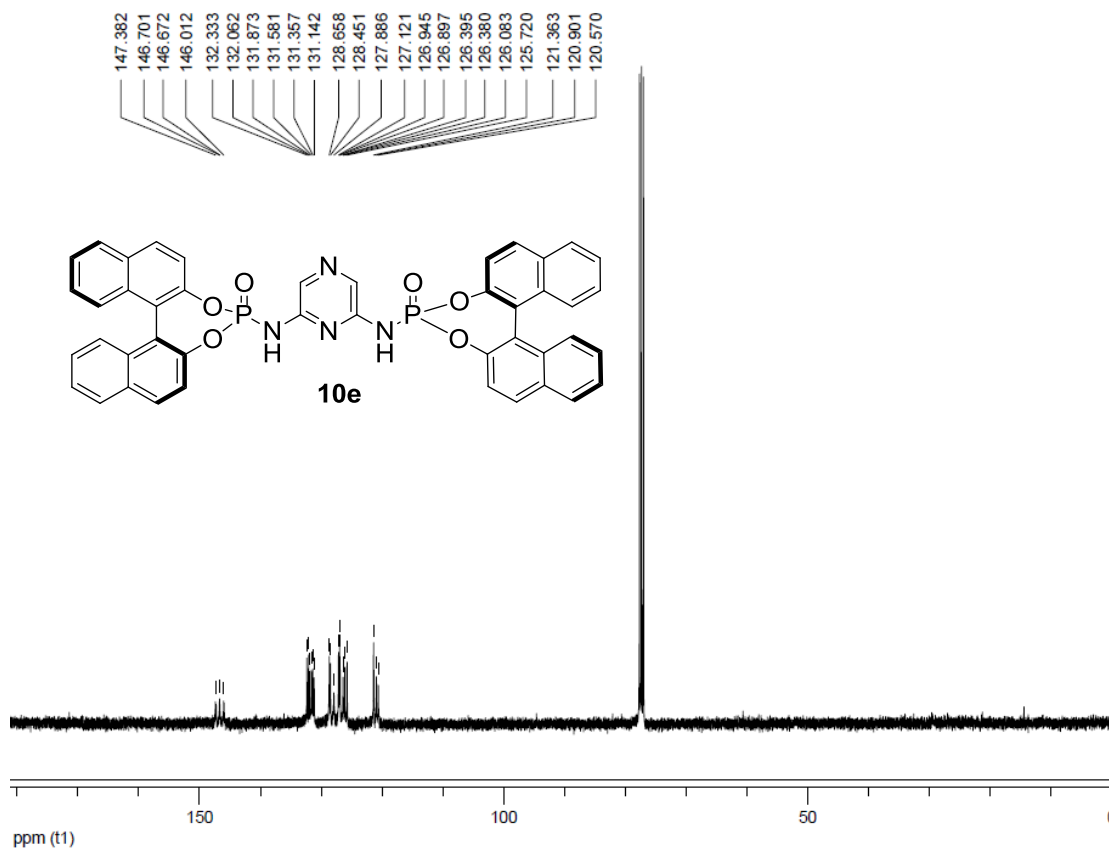
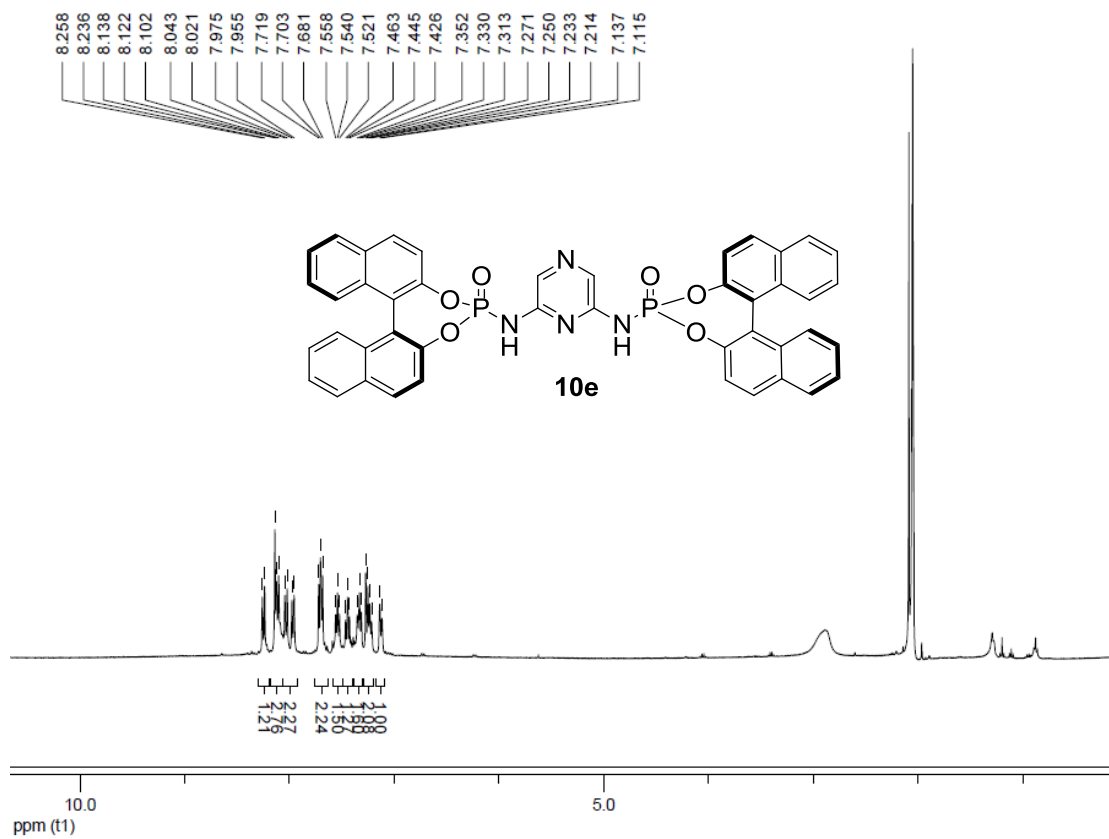


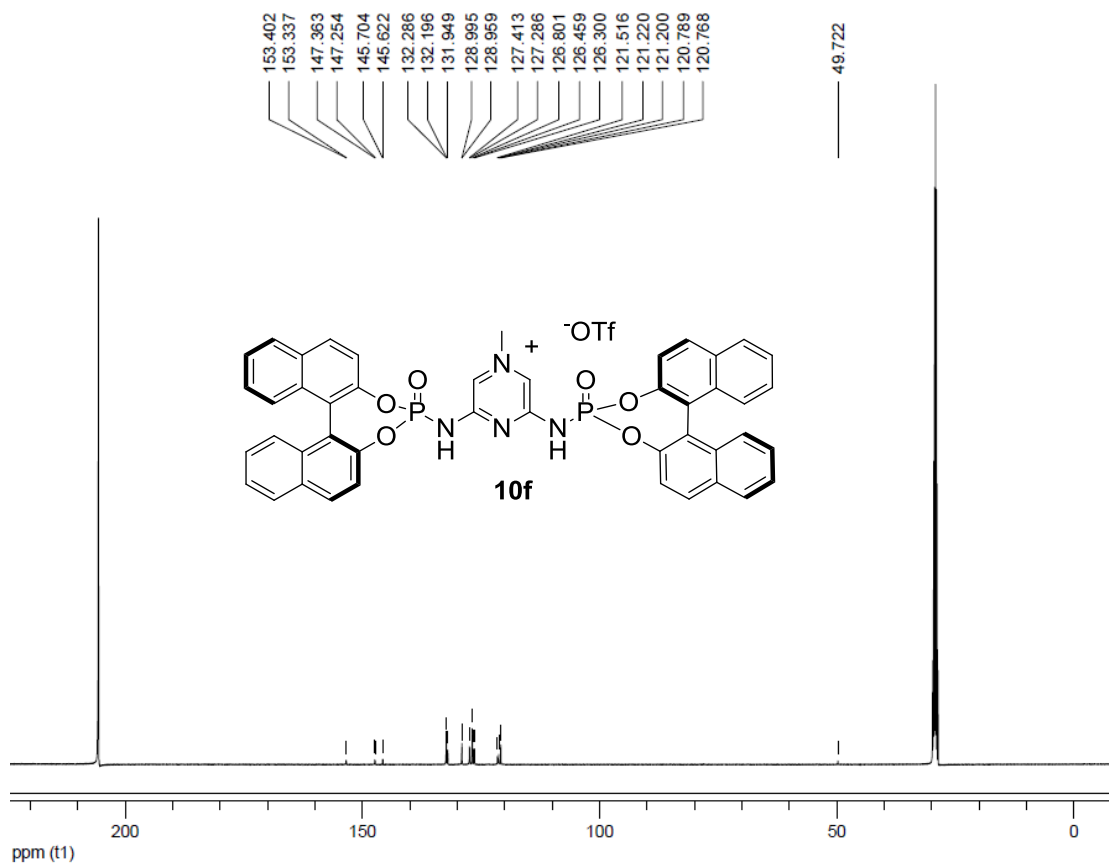
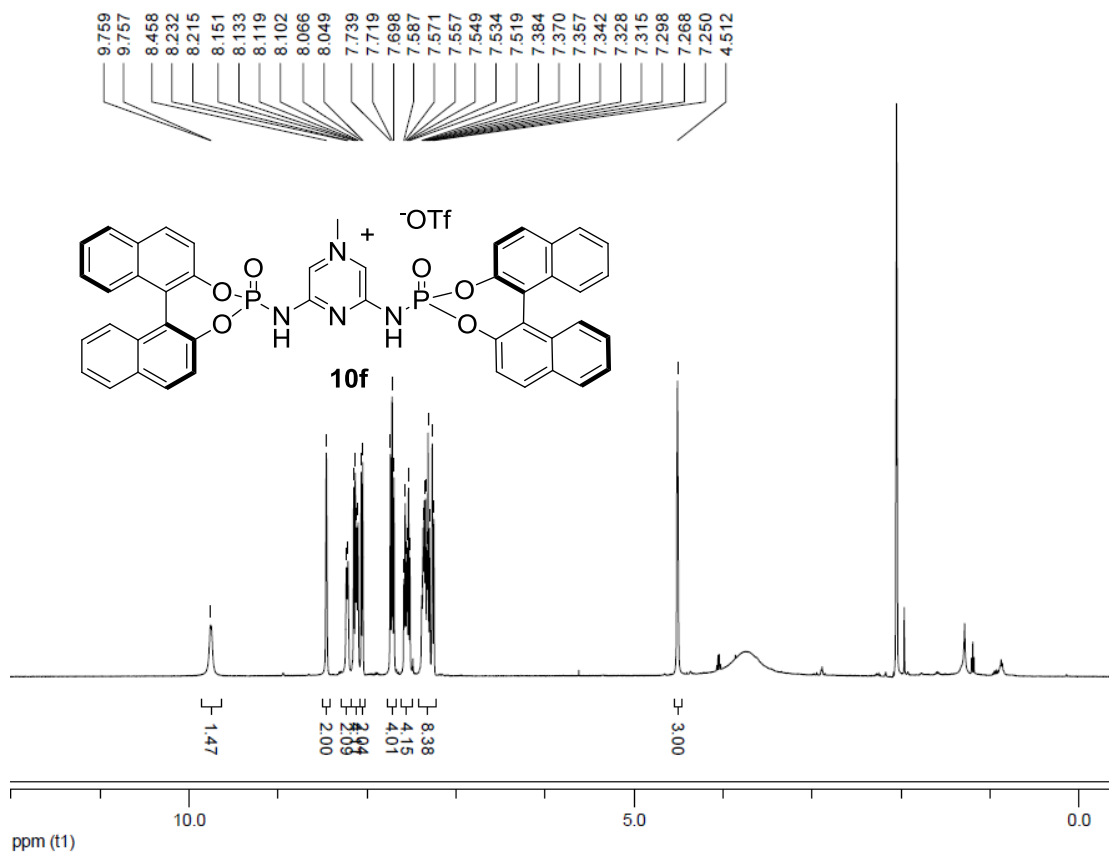


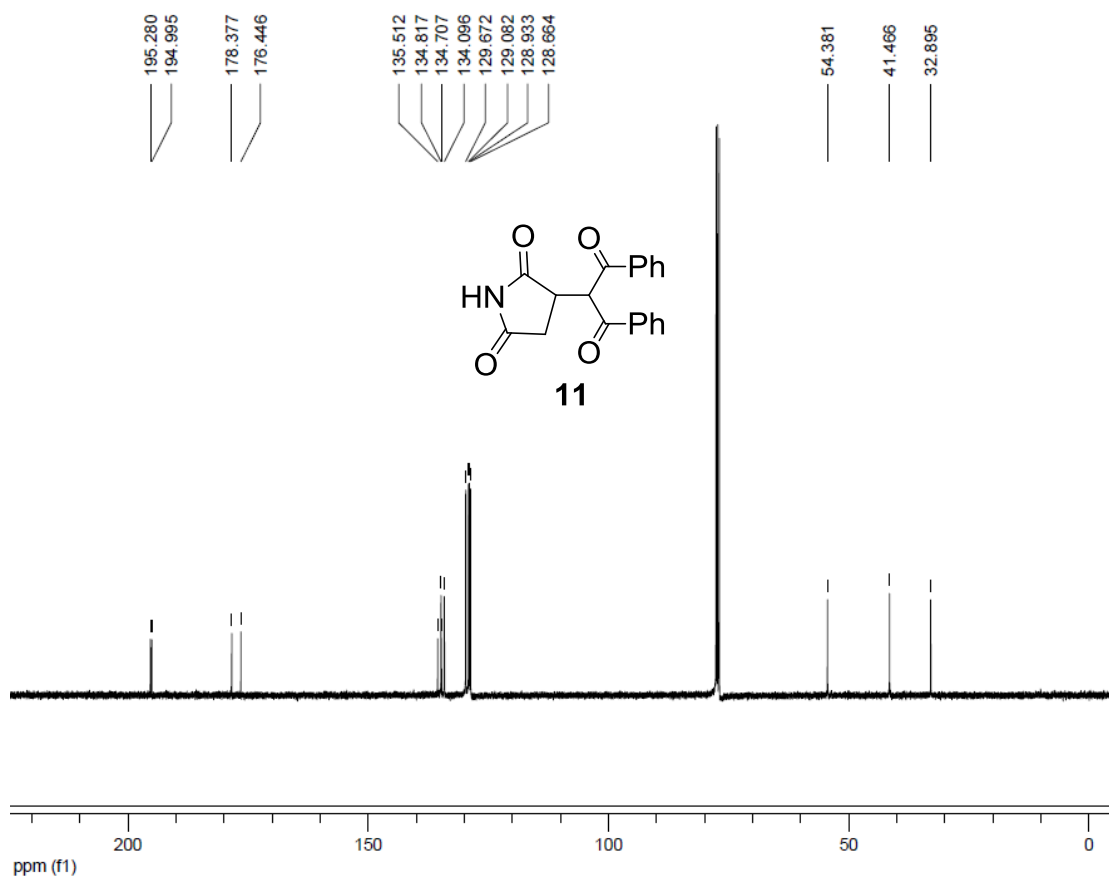
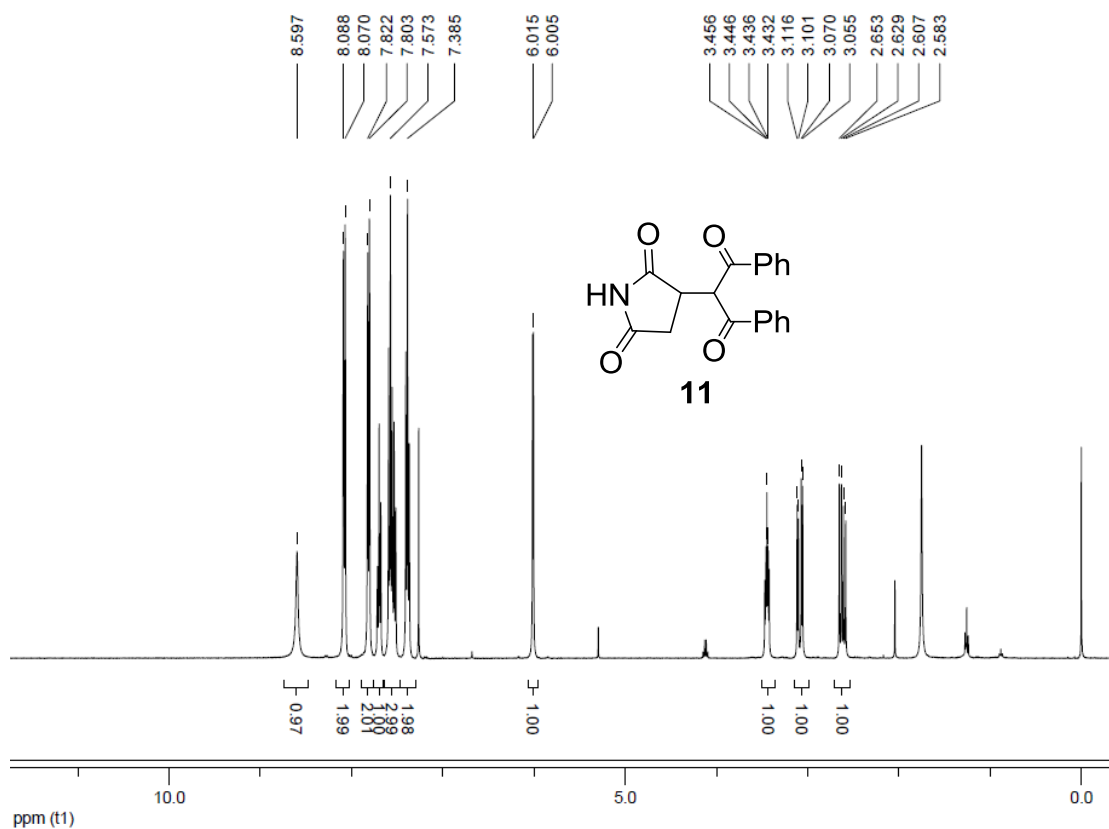


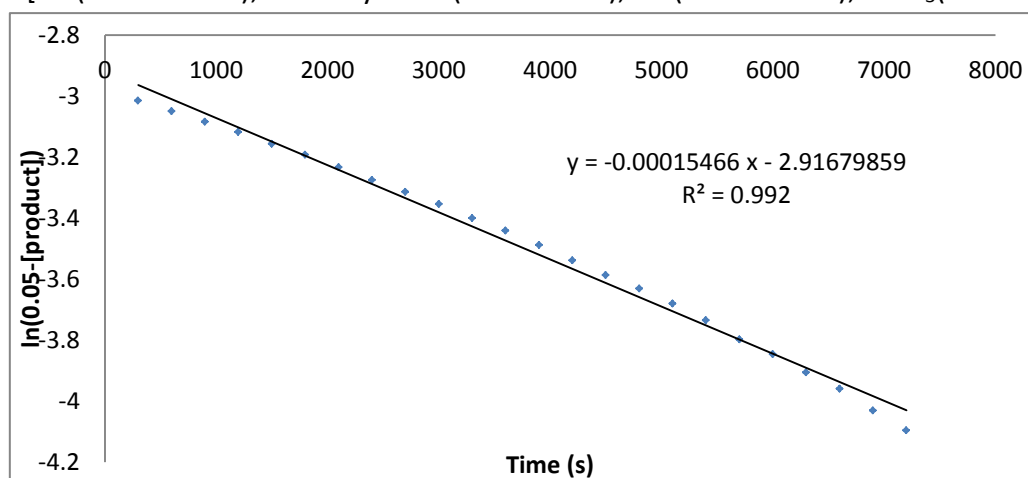






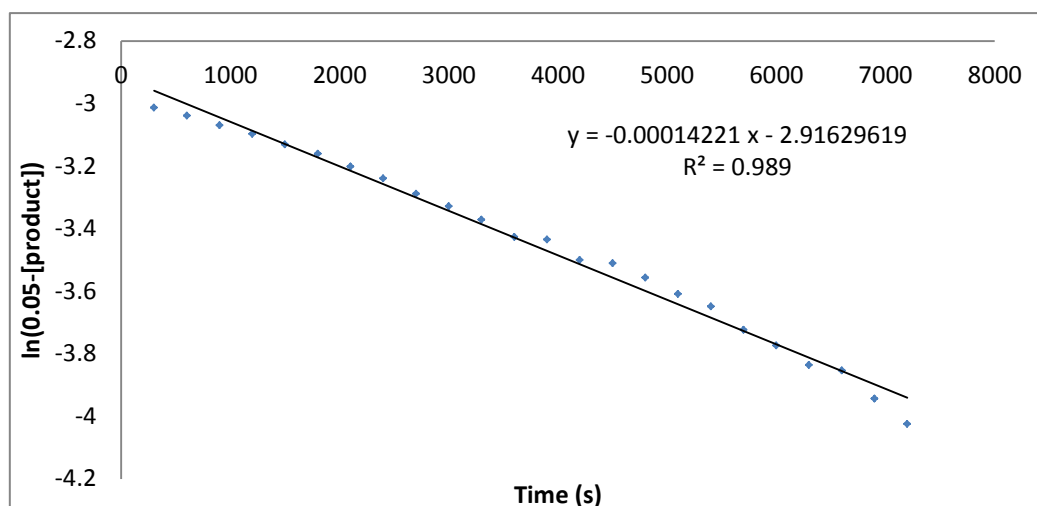




*¹H NMR Kinetics Study of Conjugate Addition of Benzylidene Barbiturate*First Trial – [6a (0.025 mmol); 2-methylfuran(0.25 mmol); 1a (0.005 mmol); CDCl₃(0.5 mL)]

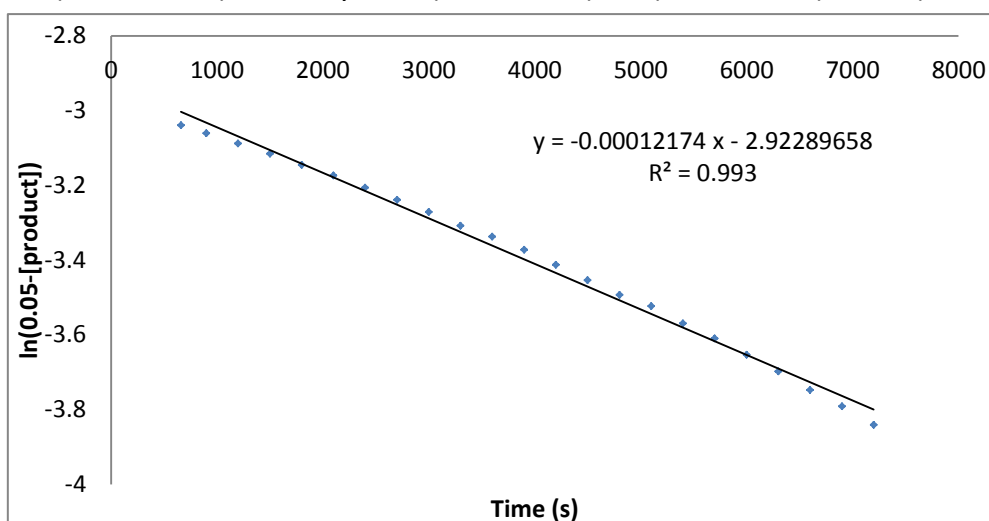
Time (min)	Time (s)	Integration	mmol	NMR Yield (%)	[product]	0.05-[product]	ln(0.05-[product])
5	300	137.608	0.00044	1.7	0.0009	0.0491	-3.013
10	600	56.381	0.00106	4.3	0.0021	0.0479	-3.039
15	900	33.776	0.00178	7.1	0.0036	0.0464	-3.069
20	1200	20.943	0.00286	11.5	0.0057	0.0443	-3.117
25	1500	16.149	0.00372	14.9	0.0074	0.0426	-3.157
30	1800	13.483	0.00445	17.8	0.0089	0.0411	-3.192
35	2100	11.359	0.00528	21.1	0.0106	0.0394	-3.233
40	2400	9.863	0.00608	24.3	0.0122	0.0378	-3.275
45	2700	8.819	0.00680	27.2	0.0136	0.0364	-3.313
50	3000	7.976	0.00752	30.1	0.0150	0.0350	-3.354
55	3300	7.220	0.00831	33.2	0.0166	0.0334	-3.400
60	3600	6.684	0.00898	35.9	0.0180	0.0320	-3.441
65	3900	6.173	0.00972	38.9	0.0194	0.0306	-3.488
70	4200	5.729	0.01047	41.9	0.0209	0.0291	-3.539
75	4500	5.381	0.01115	44.6	0.0223	0.0277	-3.586
80	4800	5.108	0.01175	47.0	0.0235	0.0265	-3.630
85	5100	4.842	0.01239	49.6	0.0248	0.0252	-3.680
90	5400	4.596	0.01306	52.2	0.0261	0.0239	-3.734
95	5700	4.351	0.01379	55.2	0.0276	0.0224	-3.798
100	6000	4.192	0.01431	57.3	0.0286	0.0214	-3.846
105	6300	4.016	0.01494	59.8	0.0299	0.0201	-3.906
110	6600	3.880	0.01546	61.9	0.0309	0.0191	-3.959
115	6900	3.723	0.01611	64.5	0.0322	0.0178	-4.030
120	7200	3.598	0.01668	66.7	0.0334	0.0166	-4.096

Second Trial – [6a (0.025 mmol); 2-methylfuran(0.25 mmol); 1a (0.005 mmol); CDCl₃(0.5 mL)]



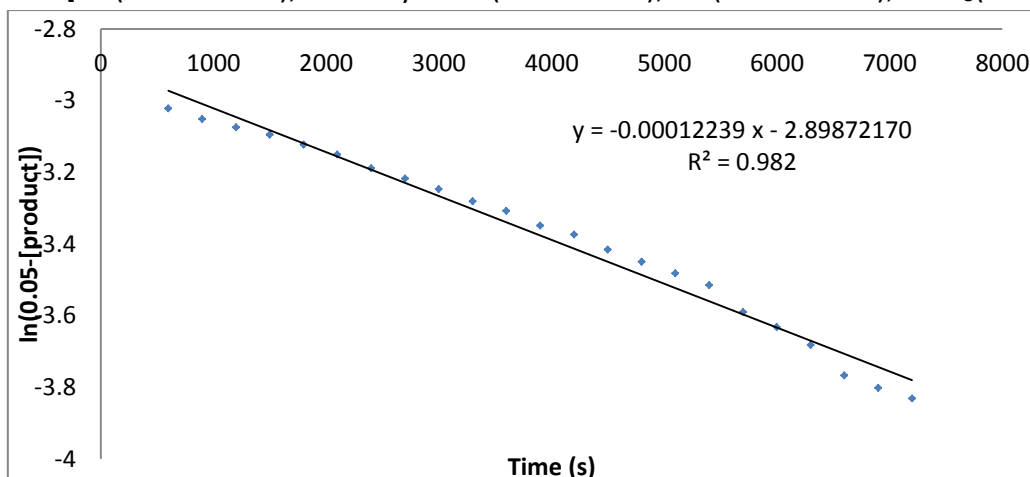
Time (min)	Time (s)	Integration	mmol	NMR Yield (%)	[product]	0.05-[product]	ln(0.05-[product])
5	300	137.608	0.00044	1.7	0.0009	0.0491	-3.013
10	600	56.381	0.00106	4.3	0.0021	0.0479	-3.039
15	900	33.776	0.00178	7.1	0.0036	0.0464	-3.069
20	1200	24.711	0.00243	9.7	0.0049	0.0451	-3.098
25	1500	18.949	0.00317	12.7	0.0063	0.0437	-3.131
30	1800	15.761	0.00381	15.2	0.0076	0.0424	-3.161
35	2100	12.889	0.00466	18.6	0.0093	0.0407	-3.202
40	2400	11.096	0.00541	21.6	0.0108	0.0392	-3.239
45	2700	9.441	0.00636	25.4	0.0127	0.0373	-3.289
50	3000	8.466	0.00709	28.3	0.0142	0.0358	-3.329
55	3300	7.653	0.00784	31.4	0.0157	0.0343	-3.372
60	3600	6.856	0.00875	35.0	0.0175	0.0325	-3.427
65	3900	6.750	0.00889	35.6	0.0178	0.0322	-3.435
70	4200	6.056	0.00991	39.6	0.0198	0.0302	-3.500
75	4500	5.958	0.01007	40.3	0.0201	0.0299	-3.511
80	4800	5.587	0.01074	43.0	0.0215	0.0285	-3.557
85	5100	5.235	0.01146	45.8	0.0229	0.0271	-3.609
90	5400	5.002	0.01200	48.0	0.0240	0.0260	-3.649
95	5700	4.641	0.01293	51.7	0.0259	0.0241	-3.724
100	6000	4.436	0.01352	54.1	0.0270	0.0230	-3.774
105	6300	4.222	0.01421	56.8	0.0284	0.0216	-3.836
110	6600	4.165	0.01441	57.6	0.0288	0.0212	-3.854
115	6900	3.919	0.01531	61.2	0.0306	0.0194	-3.944
120	7200	3.734	0.01607	64.3	0.0321	0.0179	-4.025

First Trial – [6a (0.025 mmol); 2-methylfuran(0.25 mmol); 2a (0.005 mmol); CDCl₃(0.5 mL)]



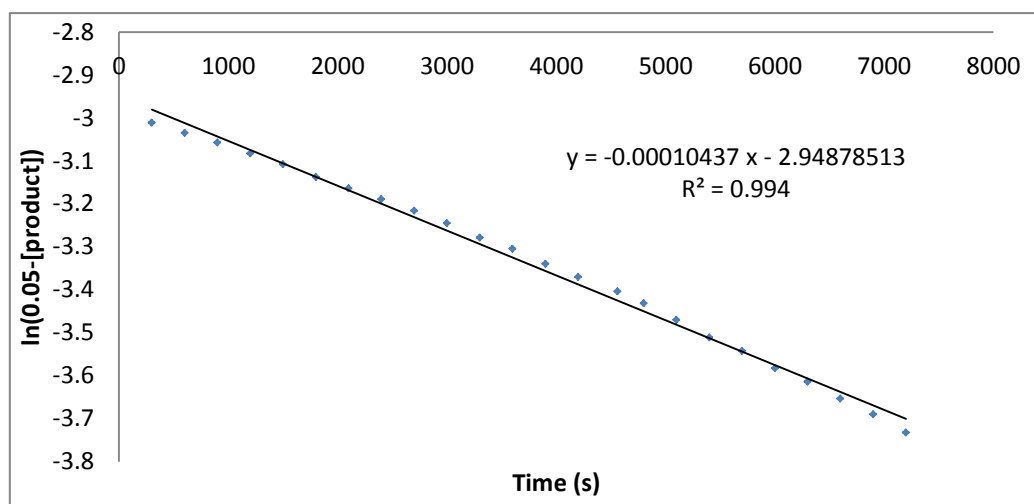
Time (min)	Time (s)	Integration	mmol	NMR Yield (%)	[product]	0.05-[product]	ln(0.05-[product])
11	660	55.682	0.00108	4.3	0.0022	0.0478	-3.040
15	900	37.982	0.00158	6.3	0.0032	0.0468	-3.061
20	1200	27.212	0.00220	8.8	0.0044	0.0456	-3.088
25	1500	21.283	0.00282	11.3	0.0056	0.0444	-3.115
30	1800	17.254	0.00348	13.9	0.0070	0.0430	-3.146
35	2100	14.687	0.00409	16.3	0.0082	0.0418	-3.174
40	2400	12.634	0.00475	19.0	0.0095	0.0405	-3.206
45	2700	11.124	0.00539	21.6	0.0108	0.0392	-3.239
50	3000	9.957	0.00603	24.1	0.0121	0.0379	-3.272
55	3300	8.942	0.00671	26.8	0.0134	0.0366	-3.308
60	3600	8.285	0.00724	29.0	0.0145	0.0355	-3.338
65	3900	7.642	0.00785	31.4	0.0157	0.0343	-3.373
70	4200	7.038	0.00852	34.1	0.0170	0.0330	-3.413
75	4500	6.532	0.00919	36.7	0.0184	0.0316	-3.454
80	4800	6.122	0.00980	39.2	0.0196	0.0304	-3.493
85	5100	5.853	0.01025	41.0	0.0205	0.0295	-3.523
90	5400	5.494	0.01092	43.7	0.0218	0.0282	-3.570
95	5700	5.228	0.01148	45.9	0.0230	0.0270	-3.610
100	6000	4.982	0.01204	48.2	0.0241	0.0259	-3.653
105	6300	4.756	0.01262	50.5	0.0252	0.0248	-3.698
110	6600	4.540	0.01322	52.9	0.0264	0.0236	-3.748
115	6900	4.374	0.01372	54.9	0.0274	0.0226	-3.791
120	7200	4.207	0.01426	57.1	0.0285	0.0215	-3.841

Second Trial – [6a (0.025 mmol); 2-methylfuran(0.25 mmol); 2a (0.005 mmol); CDCl₃(0.5 mL)]



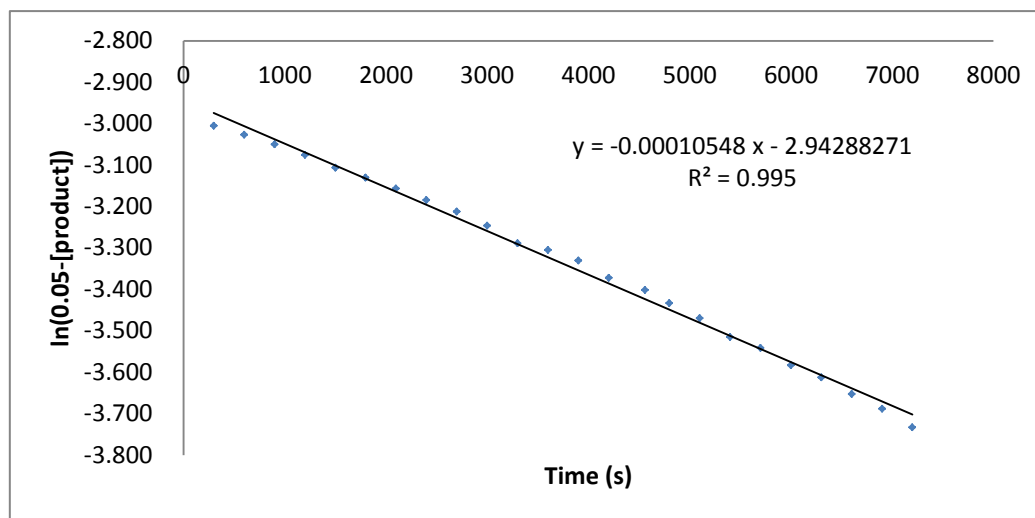
Time (min)	Time (s)	Integration	mmol	NMR Yield (%)	[product]	0.05-[product]	ln(0.05-[product])
5	300	242.841	0.00025	1.0	0.0005	0.0495	-3.006
10	600	92.072	0.00065	2.6	0.0013	0.0487	-3.022
15	900	44.052	0.00136	5.4	0.0027	0.0473	-3.052
20	1200	31.731	0.00189	7.6	0.0038	0.0462	-3.074
25	1500	25.261	0.00238	9.5	0.0048	0.0452	-3.096
30	1800	20.107	0.00298	11.9	0.0060	0.0440	-3.123
35	2100	16.723	0.00359	14.4	0.0072	0.0428	-3.151
40	2400	13.651	0.00440	17.6	0.0088	0.0412	-3.189
45	2700	12.061	0.00497	19.9	0.0099	0.0401	-3.218
50	3000	10.807	0.00555	22.2	0.0111	0.0389	-3.247
55	3300	9.668	0.00621	24.8	0.0124	0.0376	-3.281
60	3600	8.956	0.00670	26.8	0.0134	0.0366	-3.308
65	3900	8.065	0.00744	29.8	0.0149	0.0351	-3.349
70	4200	7.628	0.00787	31.5	0.0157	0.0343	-3.374
75	4500	7.001	0.00857	34.3	0.0171	0.0329	-3.416
80	4800	6.576	0.00912	36.5	0.0182	0.0318	-3.450
85	5100	6.231	0.00963	38.5	0.0193	0.0307	-3.482
90	5400	5.922	0.01013	40.5	0.0203	0.0297	-3.515
95	5700	5.353	0.01121	44.8	0.0224	0.0276	-3.591
100	6000	5.100	0.01176	47.1	0.0235	0.0265	-3.632
105	6300	4.834	0.01241	49.7	0.0248	0.0252	-3.682
110	6600	4.466	0.01343	53.7	0.0269	0.0231	-3.767
115	6900	4.338	0.01383	55.3	0.0277	0.0223	-3.802
120	7200	4.237	0.01416	56.6	0.0283	0.0217	-3.832

First Trial – [6a (0.025 mmol); 2-methylfuran(0.25 mmol); 1b (0.005 mmol); CDCl₃(0.5 mL)]



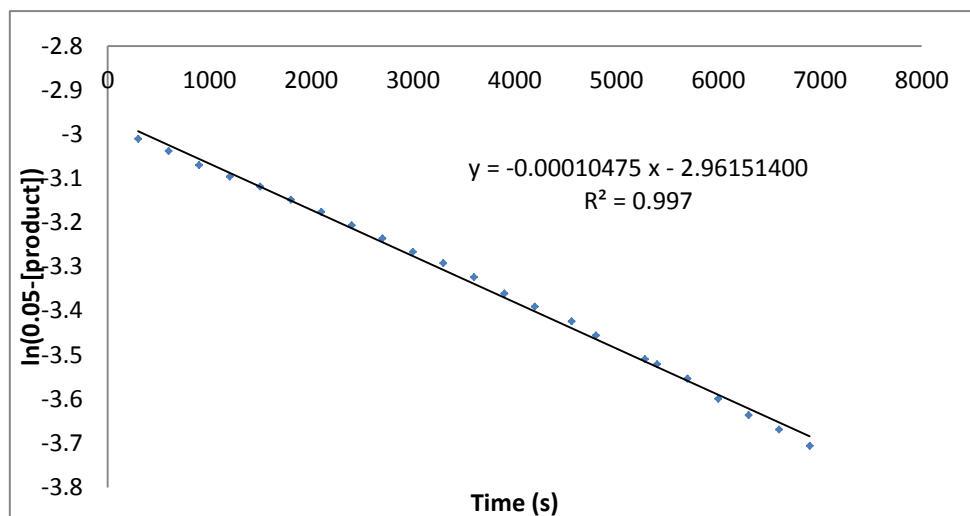
Time (min)	Time (s)	Integration	mmol	NMR Yield (%)	[product]	0.05-[product]	ln(0.05-[product])
5	300	154.393	0.00039	1.6	0.0008	0.0492	-3.011
10	600	62.603	0.00096	3.8	0.0019	0.0481	-3.035
15	900	40.411	0.00148	5.9	0.0030	0.0470	-3.057
20	1200	28.940	0.00207	8.3	0.0041	0.0459	-3.082
25	1500	22.553	0.00266	10.6	0.0053	0.0447	-3.108
30	1800	18.152	0.00331	13.2	0.0066	0.0434	-3.138
35	2100	15.512	0.00387	15.5	0.0077	0.0423	-3.164
40	2400	13.650	0.00440	17.6	0.0088	0.0412	-3.189
45	2700	12.135	0.00494	19.8	0.0099	0.0401	-3.216
50	3000	10.870	0.00552	22.1	0.0110	0.0390	-3.245
55	3300	9.741	0.00616	24.6	0.0123	0.0377	-3.279
60	3600	9.035	0.00664	26.6	0.0133	0.0367	-3.304
65	3900	8.247	0.00728	29.1	0.0146	0.0354	-3.340
70	4200	7.678	0.00781	31.3	0.0156	0.0344	-3.371
76	4560	7.161	0.00838	33.5	0.0168	0.0332	-3.404
80	4800	6.798	0.00883	35.3	0.0177	0.0323	-3.431
85	5100	6.352	0.00945	37.8	0.0189	0.0311	-3.470
90	5400	5.961	0.01006	40.3	0.0201	0.0299	-3.511
95	5700	5.698	0.01053	42.1	0.0211	0.0289	-3.543
100	6000	5.405	0.01110	44.4	0.0222	0.0278	-3.583
105	6300	5.204	0.01153	46.1	0.0231	0.0269	-3.614
110	6600	4.980	0.01205	48.2	0.0241	0.0259	-3.653
115	6900	4.795	0.01251	50.1	0.0250	0.0250	-3.690
120	7200	4.604	0.01303	52.1	0.0261	0.0239	-3.732

Second Trial – [6a (0.025 mmol); 2-methylfuran(0.25 mmol); 1b (0.005 mmol); CDCl₃(0.5 mL)]



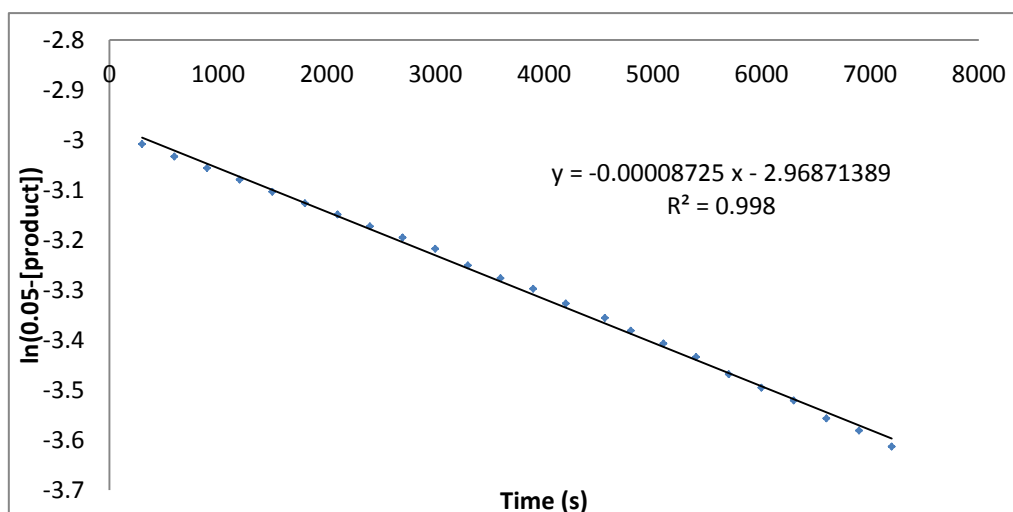
Time(min)	Time(s)	Integration	mmol	NMR Yield (%)	[product]	0.05-[product]	ln(0.05-[product])
5	300	241.987	0.00025	1.0	0.0005	0.0495	-3.006
10	600	77.849	0.00077	3.1	0.0015	0.0485	-3.027
15	900	45.425	0.00132	5.3	0.0026	0.0474	-3.050
20	1200	31.206	0.00192	7.7	0.0038	0.0462	-3.076
25	1500	22.889	0.00262	10.5	0.0052	0.0448	-3.107
30	1800	18.958	0.00316	12.7	0.0063	0.0437	-3.131
35	2100	16.114	0.00372	14.9	0.0074	0.0426	-3.157
40	2400	13.918	0.00431	17.2	0.0086	0.0414	-3.185
45	2700	12.299	0.00488	19.5	0.0098	0.0402	-3.213
50	3000	10.812	0.00555	22.2	0.0111	0.0389	-3.247
55	3300	9.446	0.00635	25.4	0.0127	0.0373	-3.289
60	3600	9.011	0.00666	26.6	0.0133	0.0367	-3.305
65	3900	8.436	0.00711	28.4	0.0142	0.0358	-3.330
70	4200	7.646	0.00785	31.4	0.0157	0.0343	-3.372
76	4560	7.190	0.00835	33.4	0.0167	0.0333	-3.402
80	4800	6.772	0.00886	35.4	0.0177	0.0323	-3.433
85	5100	6.357	0.00944	37.8	0.0189	0.0311	-3.470
90	5400	5.923	0.01013	40.5	0.0203	0.0297	-3.515
95	5700	5.704	0.01052	42.1	0.0210	0.0290	-3.542
100	6000	5.399	0.01111	44.5	0.0222	0.0278	-3.584
105	6300	5.211	0.01151	46.1	0.0230	0.0270	-3.613
110	6600	4.982	0.01204	48.2	0.0241	0.0259	-3.653
115	6900	4.801	0.01250	50.0	0.0250	0.0250	-3.689
120	7200	4.598	0.01305	52.2	0.0261	0.0239	-3.734

First Trial – [6a (0.025 mmol); 2-methylfuran(0.25 mmol); 2b (0.005 mmol); CDCl₃(0.5 mL)]



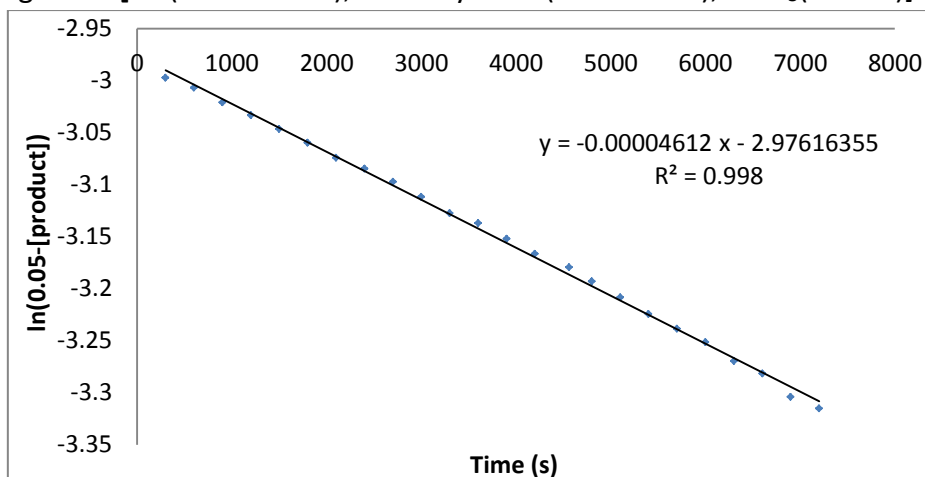
Time (min)	Time (s)	Integration	mmol	NMR Yield (%)	[product]	0.05-[product]	ln(0.05-[product])
5	300	160.730	0.00037	1.5	0.0007	0.0493	-3.011
10	600	57.705	0.00104	4.2	0.0021	0.0479	-3.038
15	900	33.389	0.00180	7.2	0.0036	0.0464	-3.070
20	1200	25.176	0.00238	9.5	0.0048	0.0452	-3.096
25	1500	20.691	0.00290	11.6	0.0058	0.0442	-3.119
30	1800	16.938	0.00354	14.2	0.0071	0.0429	-3.149
35	2100	14.570	0.00412	16.5	0.0082	0.0418	-3.176
40	2400	12.629	0.00475	19.0	0.0095	0.0405	-3.206
45	2700	11.222	0.00535	21.4	0.0107	0.0393	-3.236
50	3000	10.115	0.00593	23.7	0.0119	0.0381	-3.267
55	3300	9.361	0.00641	25.6	0.0128	0.0372	-3.292
60	3600	8.572	0.00700	28.0	0.0140	0.0360	-3.324
65	3900	7.845	0.00765	30.6	0.0153	0.0347	-3.361
70	4200	7.350	0.00816	32.7	0.0163	0.0337	-3.391
76	4560	6.888	0.00871	34.8	0.0174	0.0326	-3.424
80	4800	6.502	0.00923	36.9	0.0185	0.0315	-3.456
88	5280	5.973	0.01005	40.2	0.0201	0.0299	-3.510
90	5400	5.873	0.01022	40.9	0.0204	0.0296	-3.521
95	5700	5.612	0.01069	42.8	0.0214	0.0286	-3.554
100	6000	5.296	0.01133	45.3	0.0227	0.0273	-3.599
105	6300	5.070	0.01183	47.3	0.0237	0.0263	-3.637
110	6600	4.896	0.01225	49.0	0.0245	0.0255	-3.669
115	6900	4.717	0.01272	50.9	0.0254	0.0246	-3.707
120	7200	4.516	0.01329	53.1	0.0266	0.0234	-3.754

Second Trial – [6a (0.025 mmol); 2-methylfuran(0.25 mmol); 2b (0.005 mmol); CDCl₃(0.5 mL)]

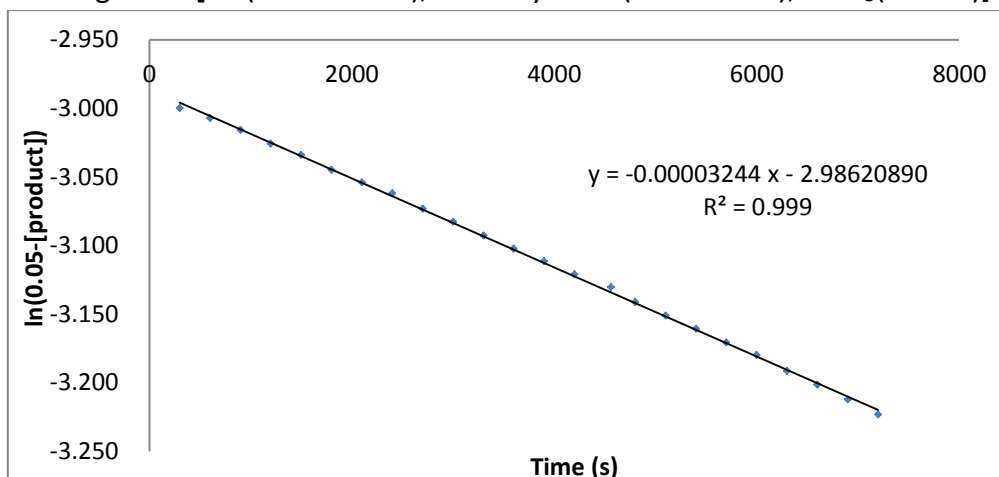


Time (min)	Time (s)	Integration mmol	NMR Yield (%)	[product]	0.05-[product]	ln(0.05-[product])	
5	300	194.663	0.00031	1.2	0.0006	0.0494	-3.008
10	600	65.329	0.00092	3.7	0.0018	0.0482	-3.033
15	900	40.720	0.00147	5.9	0.0029	0.0471	-3.056
20	1200	30.016	0.00200	8.0	0.0040	0.0460	-3.079
25	1500	23.477	0.00256	10.2	0.0051	0.0449	-3.104
30	1800	19.556	0.00307	12.3	0.0061	0.0439	-3.127
35	2100	16.861	0.00356	14.2	0.0071	0.0429	-3.149
40	2400	14.775	0.00406	16.2	0.0081	0.0419	-3.173
45	2700	13.278	0.00452	18.1	0.0090	0.0410	-3.195
50	3000	12.074	0.00497	19.9	0.0099	0.0401	-3.217
55	3300	10.657	0.00563	22.5	0.0113	0.0387	-3.251
60	3600	9.813	0.00611	24.5	0.0122	0.0378	-3.276
65	3900	9.213	0.00651	26.0	0.0130	0.0370	-3.298
70	4200	8.508	0.00705	28.2	0.0141	0.0359	-3.327
76	4560	7.943	0.00755	30.2	0.0151	0.0349	-3.356
80	4800	7.498	0.00800	32.0	0.0160	0.0340	-3.382
85	5100	7.114	0.00843	33.7	0.0169	0.0331	-3.407
90	5400	6.766	0.00887	35.5	0.0177	0.0323	-3.434
95	5700	6.375	0.00941	37.7	0.0188	0.0312	-3.468
100	6000	6.104	0.00983	39.3	0.0197	0.0303	-3.495
105	6300	5.877	0.01021	40.8	0.0204	0.0296	-3.521
110	6600	5.589	0.01073	42.9	0.0215	0.0285	-3.557
115	6900	5.416	0.01108	44.3	0.0222	0.0278	-3.581
120	7200	5.210	0.01152	46.1	0.0230	0.0270	-3.613

First Trial–Background [6a (0.025 mmol); 2-methylfuran(0.25 mmol); CDCl₃(0.5 mL)]

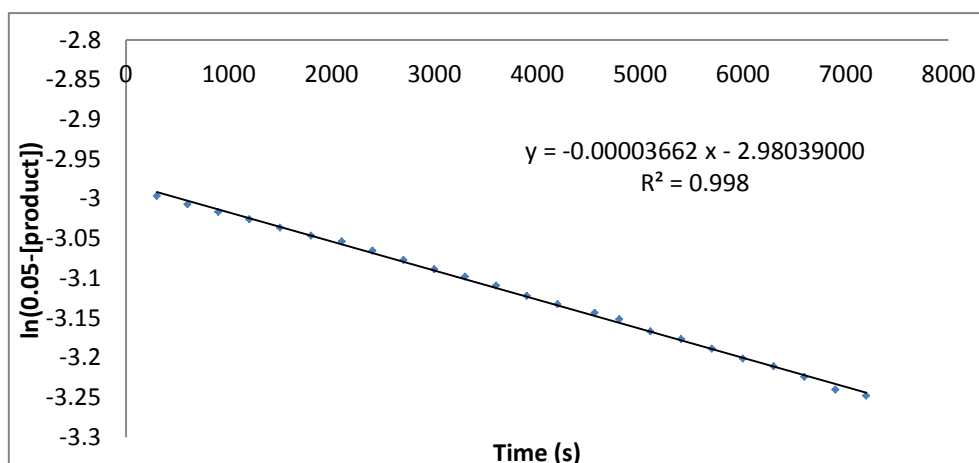


Time (min)	Time (s)	Integration	mmol	NMR Yield (%)	[product]	0.05-[product]	$\ln(0.05-[product])$
5	300	1566.141	0.00004	0.2	0.0001	0.0499	-2.997
10	600	215.476	0.00028	1.1	0.0006	0.0494	-3.007
15	900	96.880	0.00062	2.5	0.0012	0.0488	-3.021
20	1200	65.055	0.00092	3.7	0.0018	0.0482	-3.033
25	1500	48.592	0.00123	4.9	0.0025	0.0475	-3.046
30	1800	38.785	0.00155	6.2	0.0031	0.0469	-3.060
35	2100	31.809	0.00189	7.5	0.0038	0.0462	-3.074
40	2400	28.188	0.00213	8.5	0.0043	0.0457	-3.085
45	2700	24.886	0.00241	9.6	0.0048	0.0452	-3.097
50	3000	21.936	0.00274	10.9	0.0055	0.0445	-3.112
55	3300	19.449	0.00308	12.3	0.0062	0.0438	-3.127
60	3600	18.204	0.00330	13.2	0.0066	0.0434	-3.137
65	3900	16.578	0.00362	14.5	0.0072	0.0428	-3.152
70	4200	15.287	0.00392	15.7	0.0078	0.0422	-3.167
76	4560	14.294	0.00420	16.8	0.0084	0.0416	-3.180
80	4800	13.403	0.00448	17.9	0.0090	0.0410	-3.193
85	5100	12.536	0.00479	19.1	0.0096	0.0404	-3.208
90	5400	11.740	0.00511	20.4	0.0102	0.0398	-3.224
95	5700	11.128	0.00539	21.6	0.0108	0.0392	-3.239
100	6000	10.632	0.00564	22.6	0.0113	0.0387	-3.252
105	6300	10.018	0.00599	24.0	0.0120	0.0380	-3.270
110	6600	9.653	0.00622	24.9	0.0124	0.0376	-3.282
115	6900	9.043	0.00664	26.5	0.0133	0.0367	-3.304
120	7200	8.779	0.00683	27.3	0.0137	0.0363	-3.315

Second Trial–Background [6a (0.025 mmol); 2-methylfuran(0.25 mmol); CDCl₃(0.5 mL)]

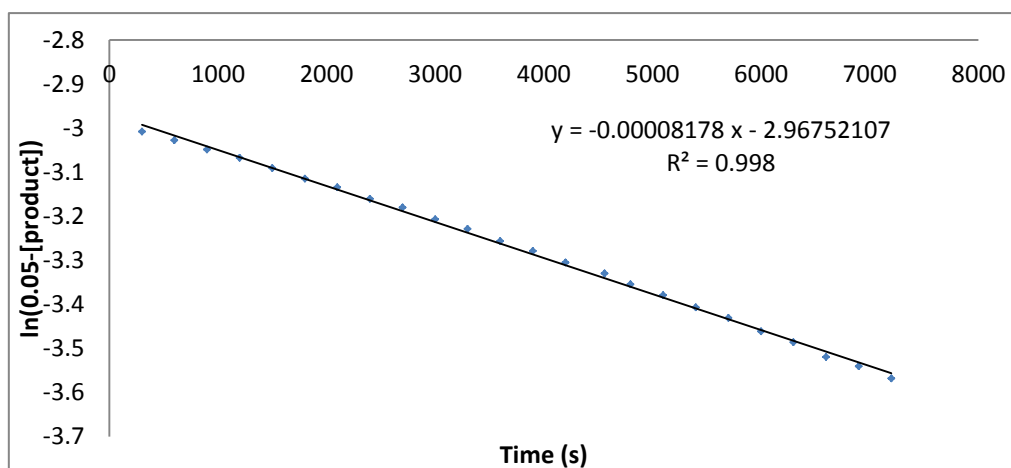
Time (min)	Time (s)	Integration	mmol	NMR Yield (%)	[product]	0.05-[product]	ln(0.05-[product])
5	300	575.814	0.00010	0.4	0.0002	0.0498	-3.000
10	600	210.331	0.00029	1.1	0.0006	0.0494	-3.007
15	900	120.639	0.00050	2.0	0.0010	0.0490	-3.016
20	1200	81.136	0.00074	3.0	0.0015	0.0485	-3.026
25	1500	63.773	0.00094	3.8	0.0019	0.0481	-3.034
30	1800	49.850	0.00120	4.8	0.0024	0.0476	-3.045
35	2100	42.290	0.00142	5.7	0.0028	0.0472	-3.054
40	2400	37.384	0.00160	6.4	0.0032	0.0468	-3.062
45	2700	32.203	0.00186	7.5	0.0037	0.0463	-3.073
50	3000	28.821	0.00208	8.3	0.0042	0.0458	-3.083
55	3300	25.938	0.00231	9.3	0.0046	0.0454	-3.093
60	3600	23.709	0.00253	10.1	0.0051	0.0449	-3.102
65	3900	21.975	0.00273	10.9	0.0055	0.0445	-3.111
70	4200	20.373	0.00295	11.8	0.0059	0.0441	-3.121
76	4560	19.067	0.00315	12.6	0.0063	0.0437	-3.130
80	4800	17.712	0.00339	13.6	0.0068	0.0432	-3.141
85	5100	16.676	0.00360	14.4	0.0072	0.0428	-3.151
90	5400	15.773	0.00380	15.2	0.0076	0.0424	-3.161
95	5700	14.941	0.00402	16.1	0.0080	0.0420	-3.171
100	6000	14.278	0.00420	16.8	0.0084	0.0416	-3.180
105	6300	13.494	0.00445	17.8	0.0089	0.0411	-3.192
110	6600	12.907	0.00465	18.6	0.0093	0.0407	-3.201
115	6900	12.324	0.00487	19.5	0.0097	0.0403	-3.212
120	7200	11.792	0.00509	20.4	0.0102	0.0398	-3.223

First Trial –[**6a** (0.025 mmol); 2-methylfuran(0.25 mmol); **1c** (0.005 mmol); CDCl_3 (0.5 mL)]



Time (min)	Time (s)	Integration	mmol	NMR Yield (%)	[product]	0.05-[product]	$\ln(0.05-[product])$
5	300	2814.067	0.00002	0.1	0.0000	0.0500	-2.997
10	600	218.620	0.00027	1.1	0.0005	0.0495	-3.007
15	900	116.964	0.00051	2.1	0.0010	0.0490	-3.016
20	1200	80.702	0.00074	3.0	0.0015	0.0485	-3.026
25	1500	60.503	0.00099	4.0	0.0020	0.0480	-3.036
30	1800	48.430	0.00124	5.0	0.0025	0.0475	-3.047
35	2100	42.585	0.00141	5.6	0.0028	0.0472	-3.054
40	2400	35.740	0.00168	6.7	0.0034	0.0466	-3.065
45	2700	30.681	0.00196	7.8	0.0039	0.0461	-3.077
50	3000	27.006	0.00222	8.9	0.0044	0.0456	-3.089
55	3300	24.711	0.00243	9.7	0.0049	0.0451	-3.098
60	3600	22.356	0.00268	10.7	0.0054	0.0446	-3.109
65	3900	20.226	0.00297	11.9	0.0059	0.0441	-3.122
70	4200	18.771	0.00320	12.8	0.0064	0.0436	-3.133
76	4560	17.451	0.00344	13.8	0.0069	0.0431	-3.144
80	4800	16.638	0.00361	14.4	0.0072	0.0428	-3.152
85	5100	15.251	0.00393	15.7	0.0079	0.0421	-3.167
90	5400	14.492	0.00414	16.6	0.0083	0.0417	-3.177
95	5700	13.674	0.00439	17.6	0.0088	0.0412	-3.189
100	6000	12.918	0.00464	18.6	0.0093	0.0407	-3.201
105	6300	12.403	0.00484	19.4	0.0097	0.0403	-3.211
110	6600	11.748	0.00511	20.4	0.0102	0.0398	-3.224
115	6900	11.057	0.00543	21.7	0.0109	0.0391	-3.240
120	7200	10.769	0.00557	22.3	0.0111	0.0389	-3.248

First Trial –[**6a** (0.025 mmol); 2-methylfuran(0.25 mmol); **3a** (0.005 mmol); CDCl_3 (0.5 mL)]



Time (min)	Time (s)	Integration	mmol	NMR Yield (%)	[product]	0.05-[product]	ln(0.05-[product])
5	300	194.764	0.00031	1.2	0.0006	0.0494	-3.008
10	600	76.885	0.00078	3.1	0.0016	0.0484	-3.027
15	900	46.615	0.00129	5.1	0.0026	0.0474	-3.049
20	1200	34.786	0.00172	6.9	0.0034	0.0466	-3.067
25	1500	26.536	0.00226	9.0	0.0045	0.0455	-3.091
30	1800	21.372	0.00281	11.2	0.0056	0.0444	-3.115
35	2100	18.515	0.00324	13.0	0.0065	0.0435	-3.135
40	2400	15.788	0.00380	15.2	0.0076	0.0424	-3.161
45	2700	14.266	0.00421	16.8	0.0084	0.0416	-3.180
50	3000	12.618	0.00475	19.0	0.0095	0.0405	-3.207
55	3300	11.541	0.00520	20.8	0.0104	0.0396	-3.229
60	3600	10.459	0.00574	22.9	0.0115	0.0385	-3.256
65	3900	9.732	0.00617	24.7	0.0123	0.0377	-3.279
70	4200	9.013	0.00666	26.6	0.0133	0.0367	-3.305
76	4560	8.457	0.00709	28.4	0.0142	0.0358	-3.330
80	4800	7.964	0.00753	30.1	0.0151	0.0349	-3.354
85	5100	7.536	0.00796	31.8	0.0159	0.0341	-3.379
90	5400	7.118	0.00843	33.7	0.0169	0.0331	-3.407
95	5700	6.799	0.00882	35.3	0.0176	0.0324	-3.431
100	6000	6.446	0.00931	37.2	0.0186	0.0314	-3.461
105	6300	6.194	0.00969	38.7	0.0194	0.0306	-3.486
110	6600	5.885	0.01020	40.8	0.0204	0.0296	-3.520
115	6900	5.714	0.01050	42.0	0.0210	0.0290	-3.541
120	7200	5.505	0.01090	43.6	0.0218	0.0282	-3.568

UV / Vis. Titration Binding Study of Benzylidene Barbiturate Chromophore with Amide-Based HB-DAD Organocatalysts

Ten graduated flasks (5 mL) were treated with 0.5 mL of stock solution of benzylidene barbiturate chromophore (final concentration: $2 \times 10^{-5} \text{ molL}^{-1}$) and 20-3000 μL (corresponding to a 2-290 folds excess) of a stock solution of amide-based HB-DAD organocatalyst, and filled up to 5 mL. The change in absorbance was monitored and evaluated by linearized Scatchard plot (S1). The given values of K were the average of two runs.

$$\frac{\Delta A}{d \cdot [R]} = - \frac{\Delta A \cdot K}{d} + K \cdot \Delta \varepsilon \cdot [S] \quad (\text{S1})$$

[S]: Concentration of benzylidene barbiturate chromophore

[R]: Concentration of amide-based HB-DAD organocatalysts

K: Binding Constant

ΔA : Change of absorbance

$\Delta \varepsilon$: Molar absorptivity

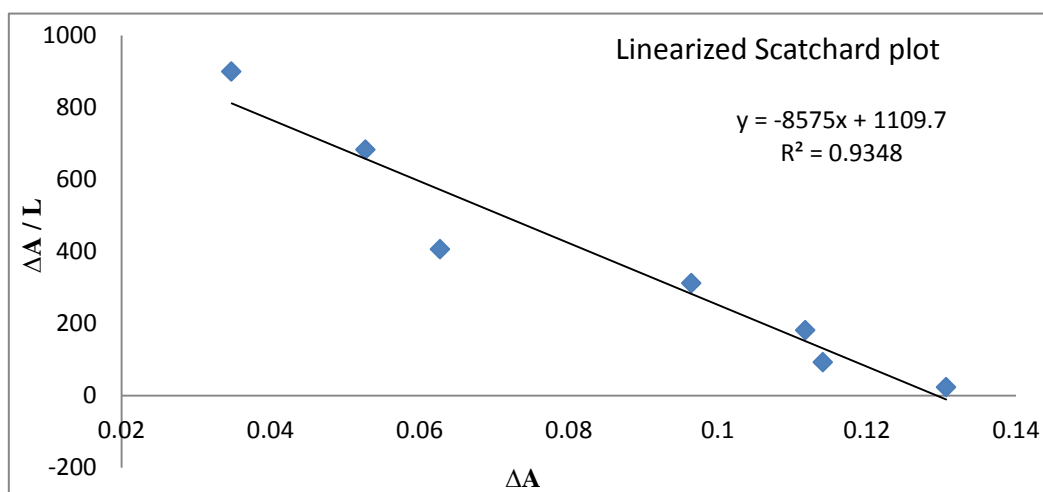
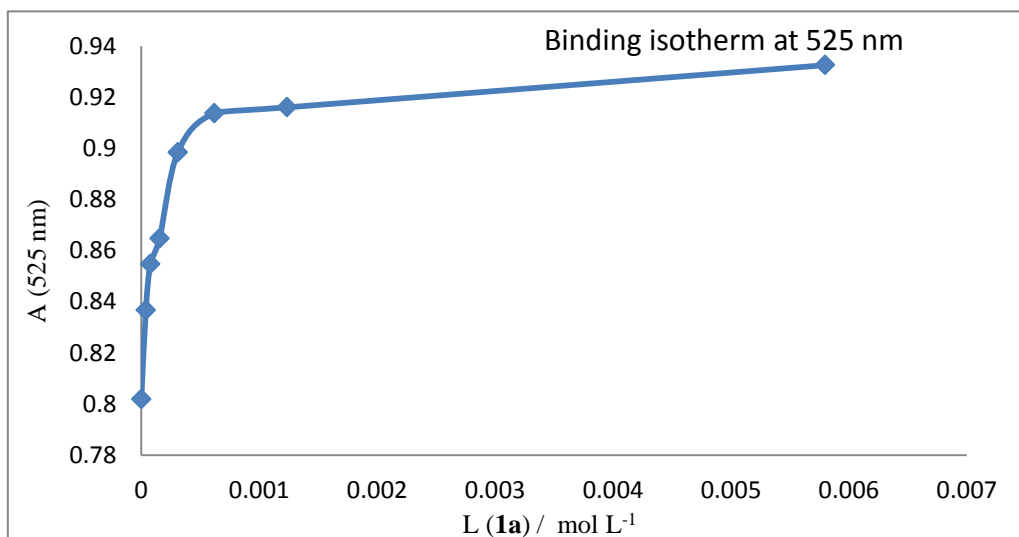
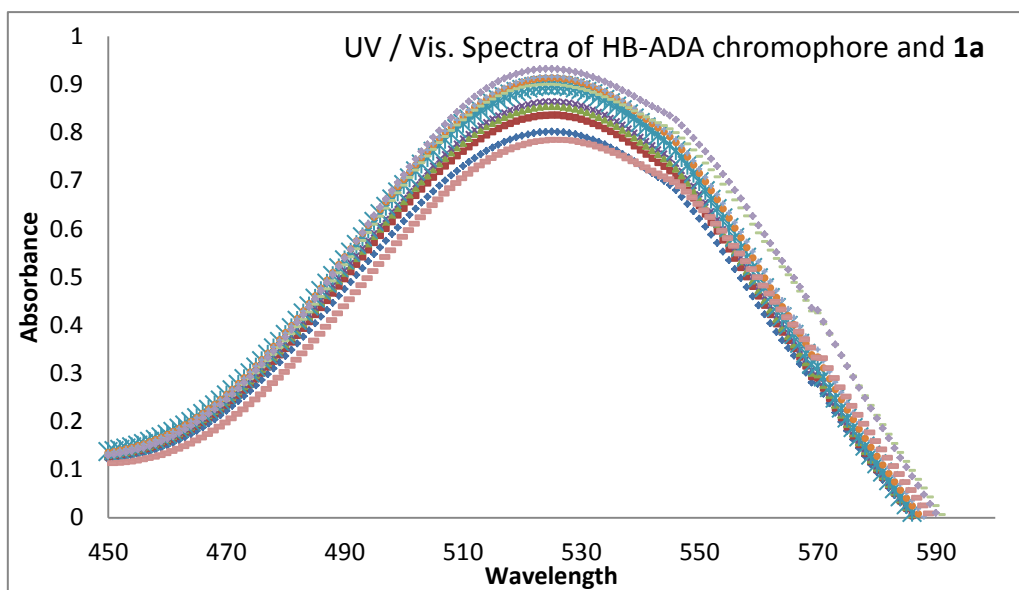
In Scatchard Plot

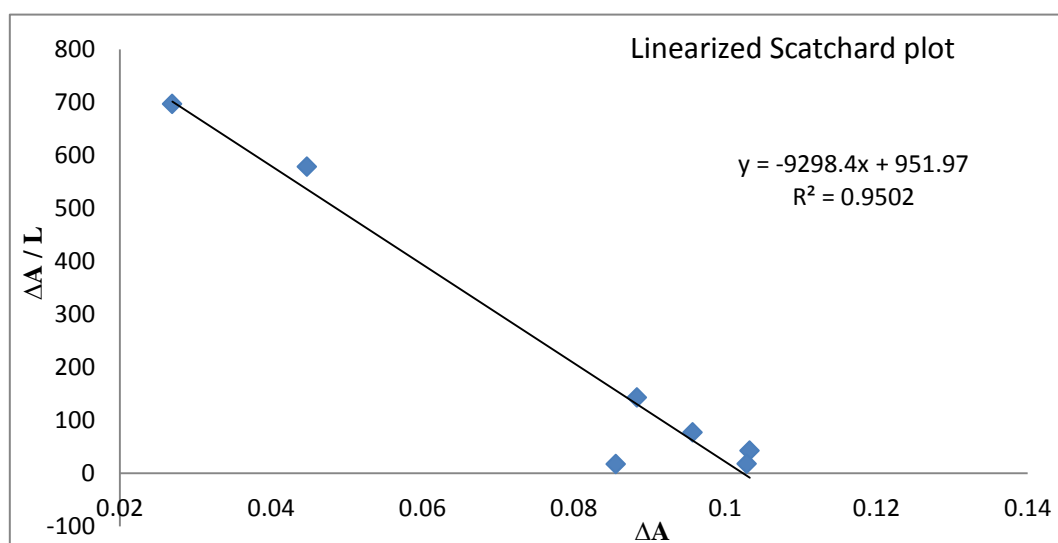
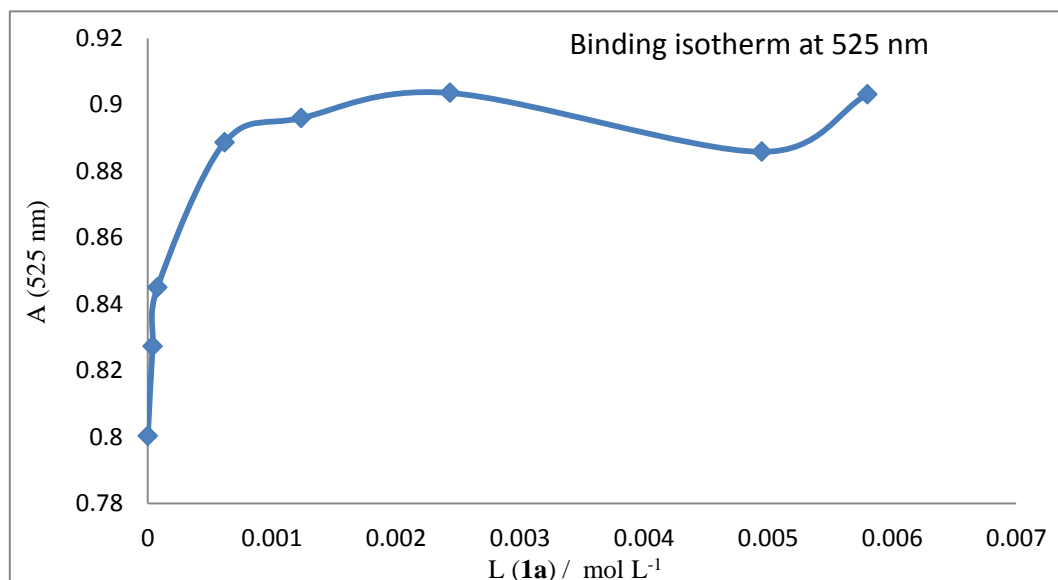
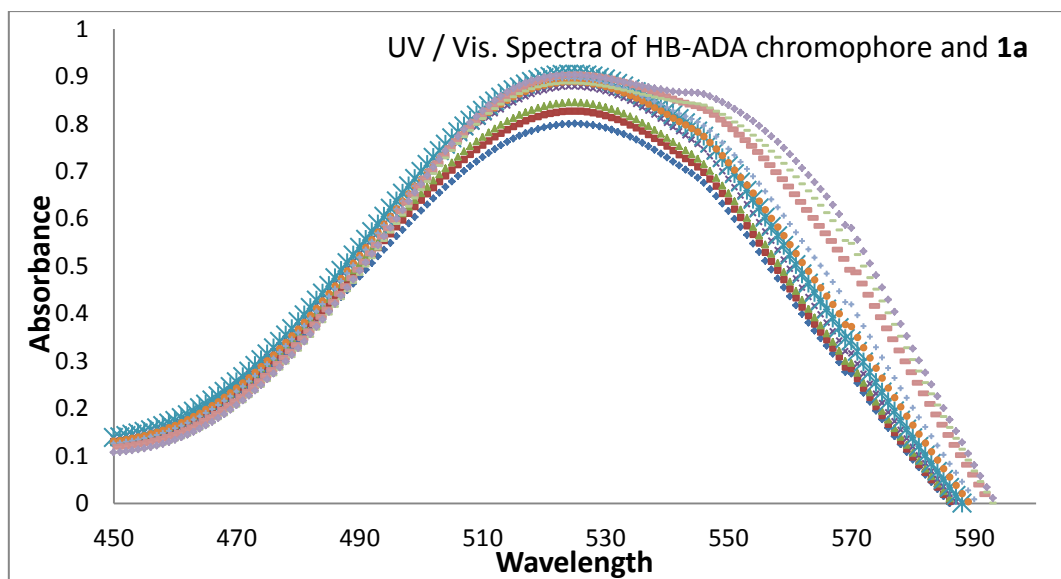
$K = - (\text{slope})$

$\Delta \varepsilon = (\text{x-intercept}) / [S]$

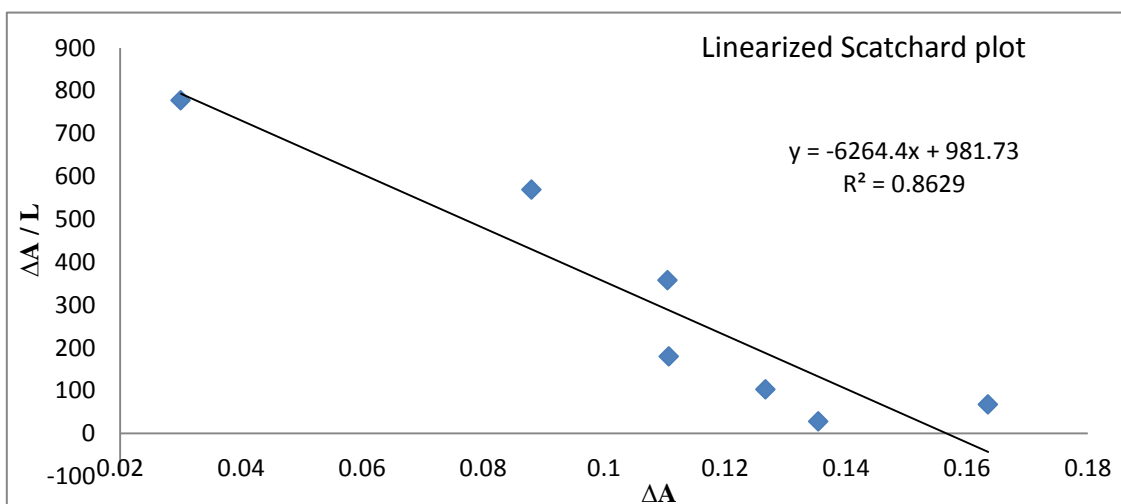
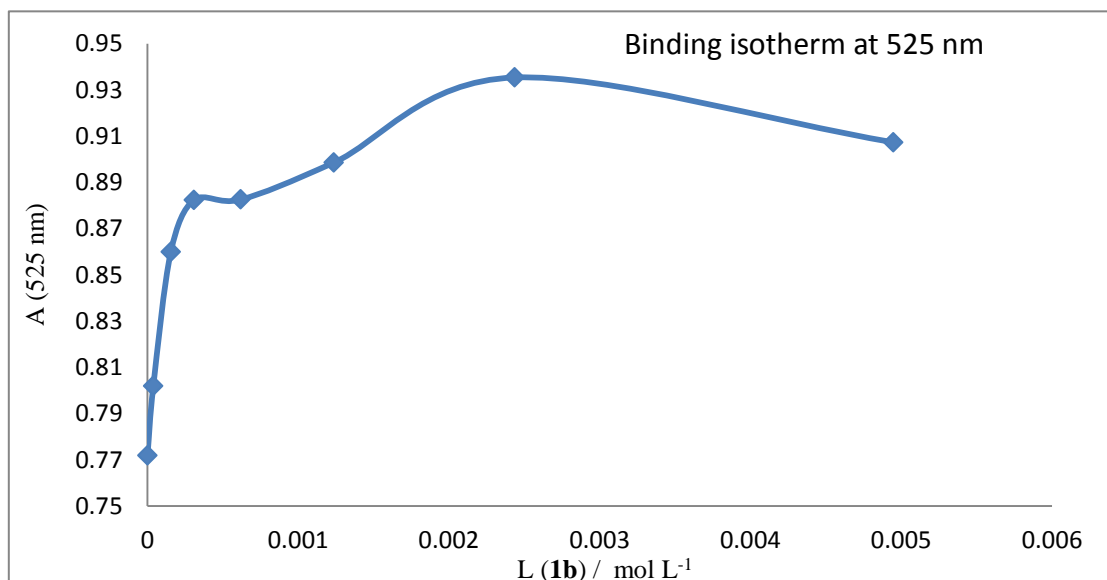
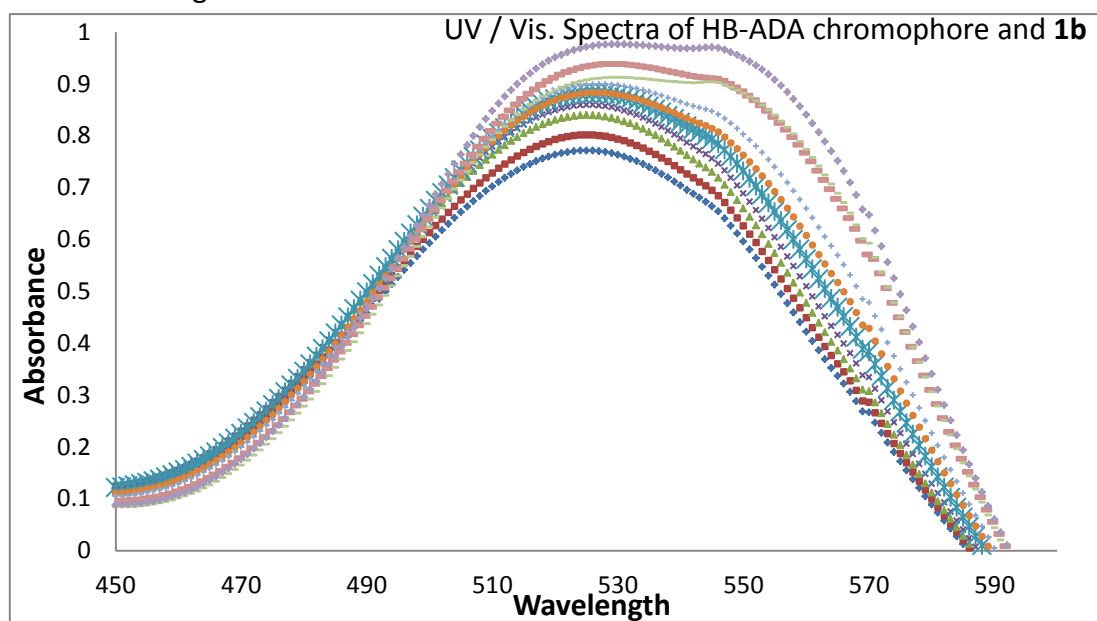
In UV / Vis. spectroscopy binding constant studies, the absorbance UV / Vis. spectra were recorded from 450 nm to 600nm and shown in UV / Vis. spectra. The absorbances at 525 nm were recorded in Binding isotherm to confirm binding stoichiometry. Furthermore, the change of absorbance was recorded according to linearized Scatchard equation to give linearized Scatchard plot.

First Trial of **1a** Binding Constant

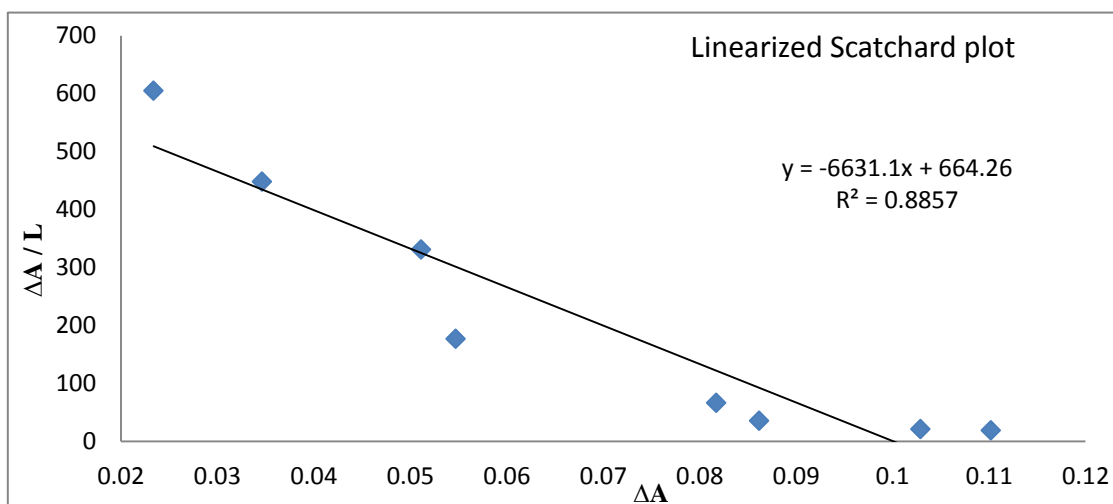
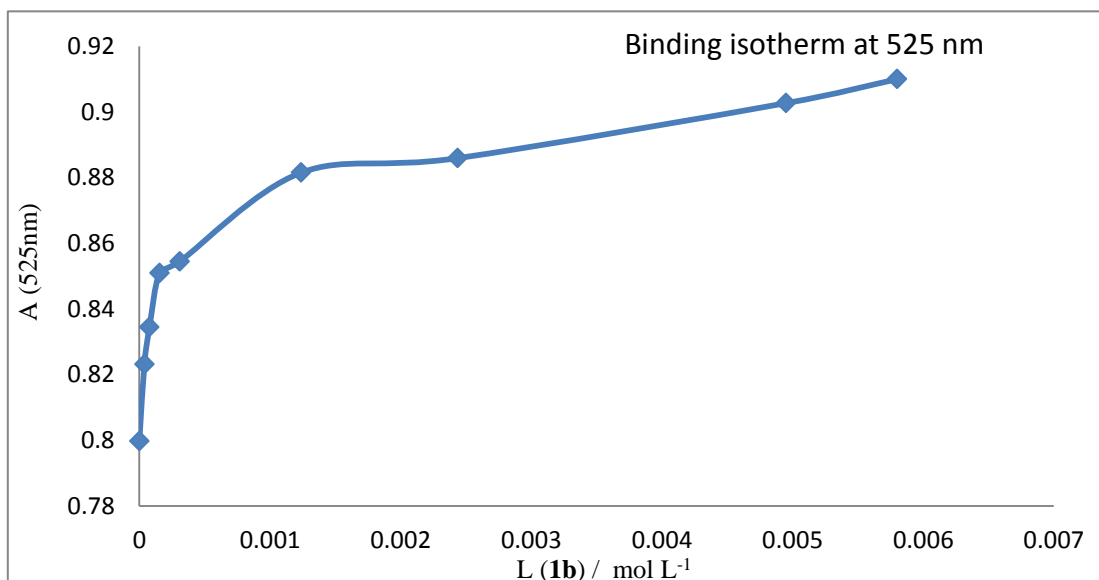
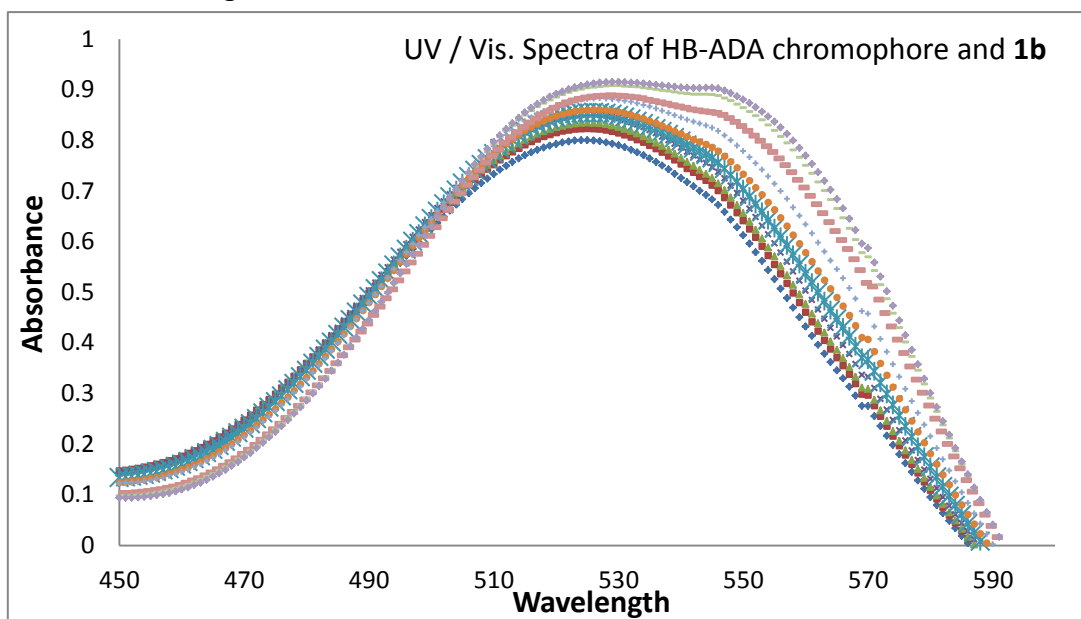


Second Trial of **1a** Binding Constant

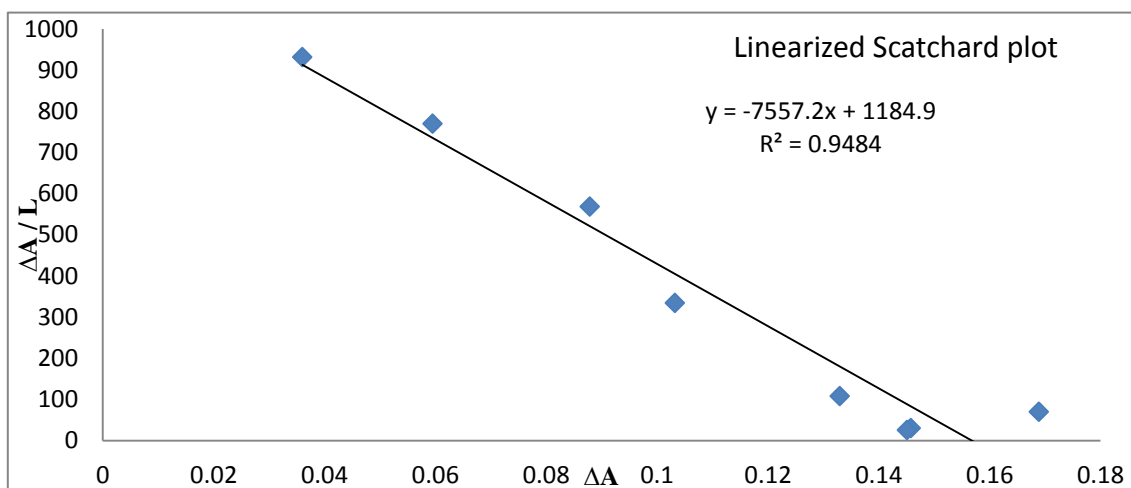
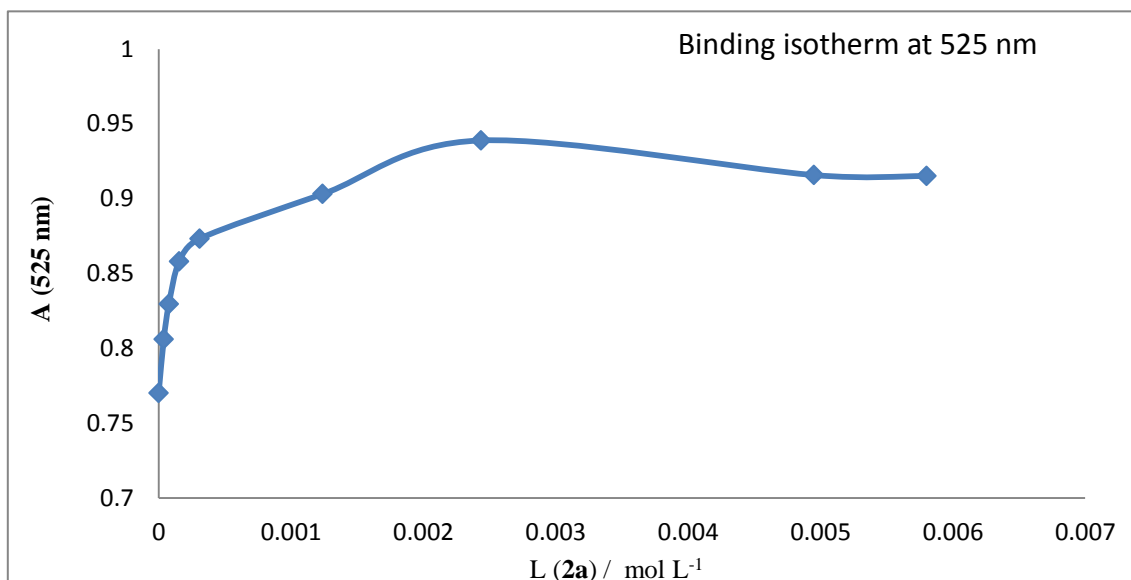
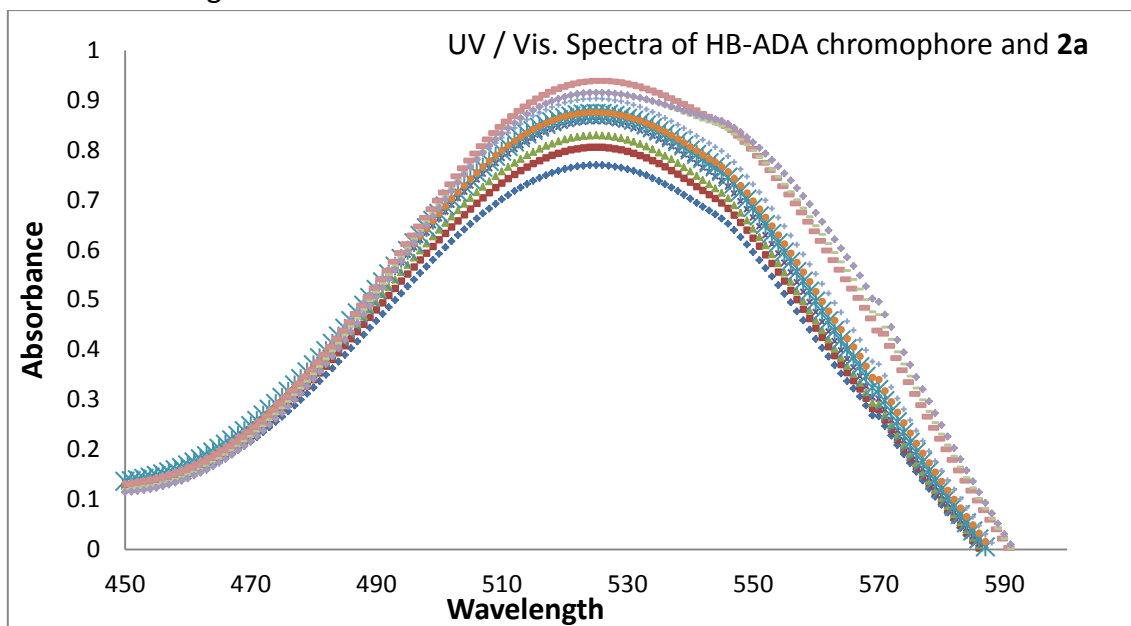
First Trial of **1b** Binding Constant



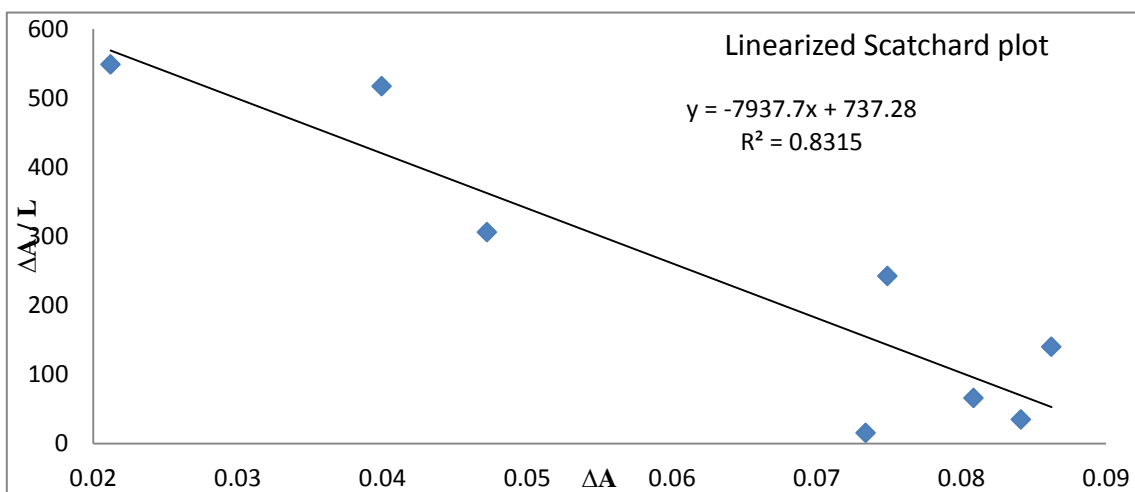
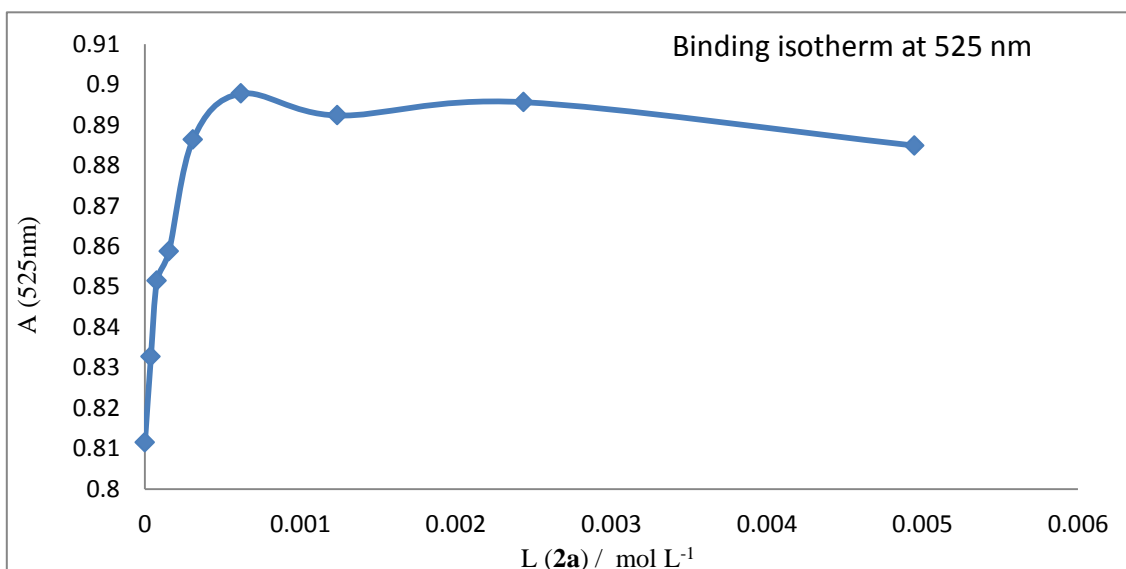
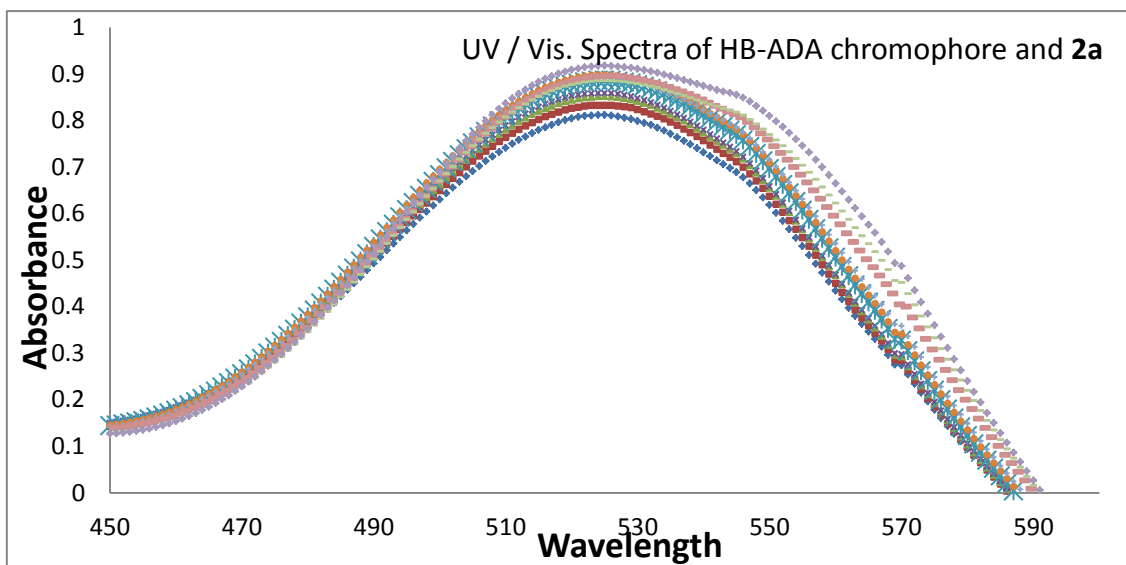
Second Trial of **1b** Binding Constant



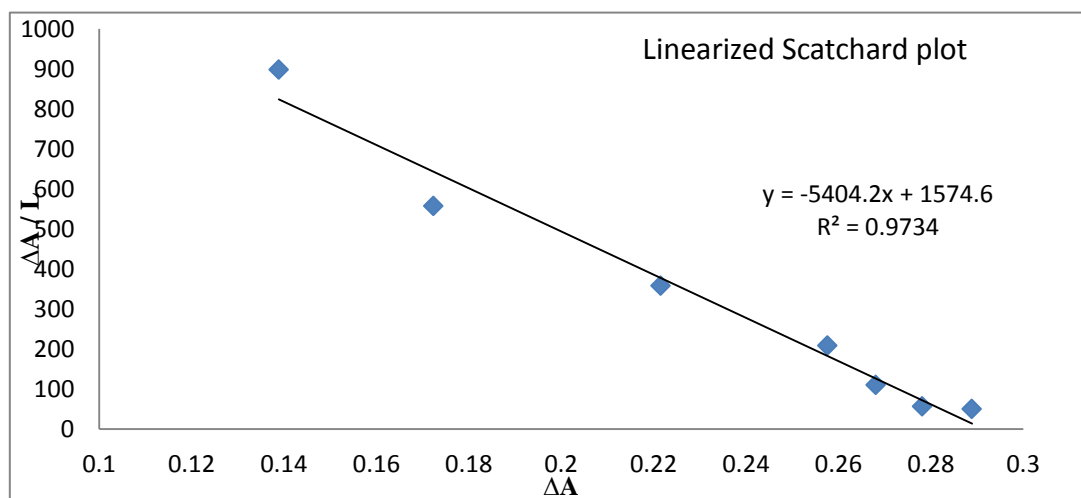
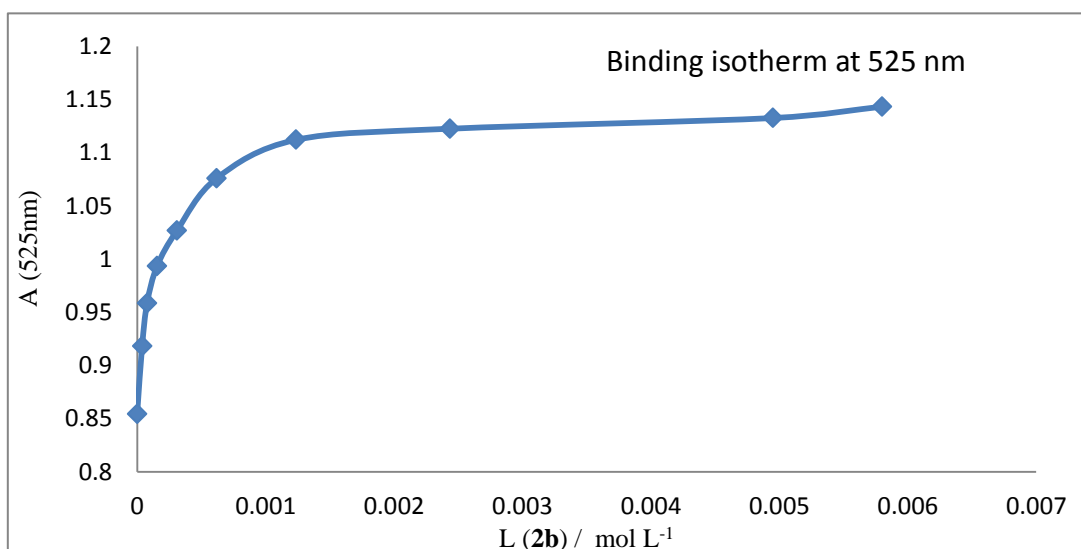
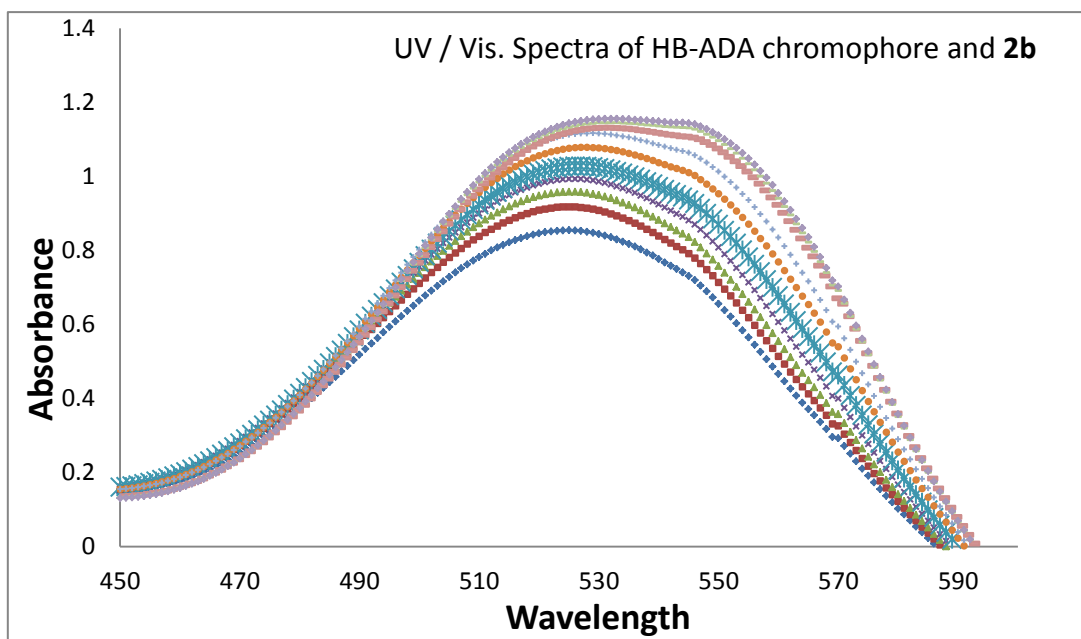
First Trial of **2a** Binding Constant



Second Trial of **2a** Binding Constant



First Trial of **2b** Binding Constant



Second Trial of **2b** Binding Constant

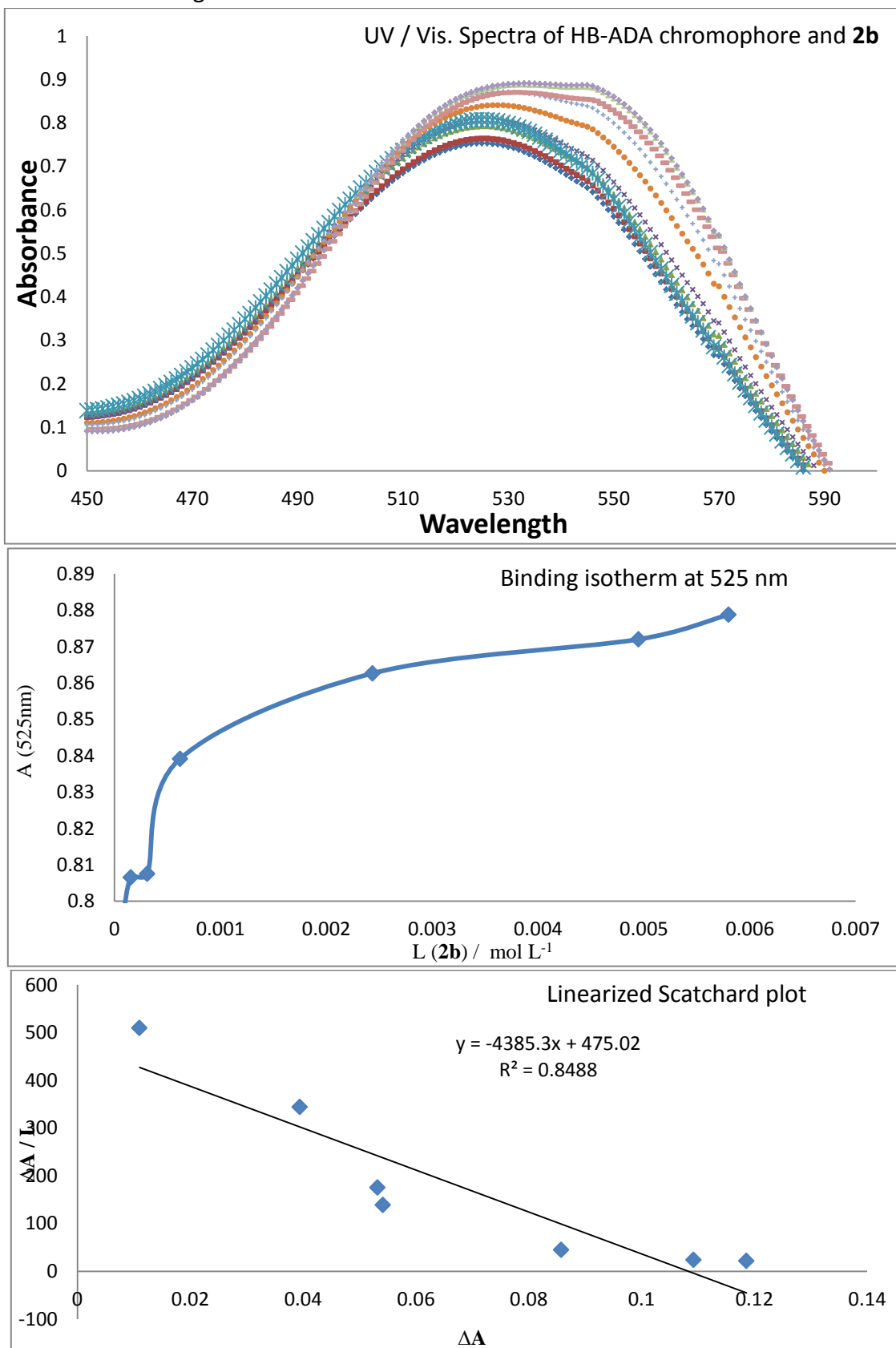


Table 1. Crystal data and structure refinement for BCLKC1 (22 Mar 2011).

Identification code	lkc1	
Empirical formula	C ₂₇ H ₃₅ N ₇ O ₂	
Formula weight	489.62	
Temperature	296(2) K	
Wavelength	0.71073 Å	
Crystal system	Orthorhombic	
Space group	P2(1)2(1)2	
Unit cell dimensions	a = 15.2409(6) Å	α = 90°.
	b = 21.6925(8) Å	β = 90°.
	c = 8.3346(3) Å	γ = 90°.
Volume	2755.53(18) Å ³	
Z	4	
Density (calculated)	1.180 Mg/m ³	
Absorption coefficient	0.078 mm ⁻¹	
F(000)	1048	
Crystal size	0.46 x 0.40 x 0.40 mm ³	
Theta range for data collection	1.63 to 27.38°.	
Index ranges	-19 ≤ h ≤ 17, -28 ≤ k ≤ 28, -10 ≤ l ≤ 10	
Reflections collected	26375	
Independent reflections	6209 [R(int) = 0.0693]	
Completeness to theta = 27.38°	100.0 %	
Absorption correction	Semi-empirical from equivalents	
Max. and min. transmission	0.745 and 0.667	
Refinement method	Full-matrix least-squares on F ²	
Data / restraints / parameters	6209 / 4 / 346	
Goodness-of-fit on F ²	1.002	
Final R indices [I > 2σ(I)]	R1 = 0.0651, wR2 = 0.1708	
R indices (all data)	R1 = 0.1392, wR2 = 0.2176	
Absolute structure parameter	0(2)	
Extinction coefficient	0.0031(7)	
Largest diff. peak and hole	0.375 and -0.275 e.Å ⁻³	

Table 2. Atomic coordinates ($\times 10^4$) and equivalent isotropic displacement parameters ($\text{\AA}^2 \times 10^3$) for lkc1. $U(\text{eq})$ is defined as one third of the trace of the orthogonalized U^{ij} tensor.

	x	y	z	U(eq)
O(1)	1241(1)	-2019(1)	5237(2)	80(1)
O(2)	5879(1)	1527(1)	2803(2)	66(1)
N(1)	3698(1)	25(1)	4423(2)	41(1)
N(2)	3030(1)	1021(1)	4516(2)	44(1)
N(3)	2138(1)	132(1)	4467(2)	46(1)
N(4)	2809(1)	-825(1)	4375(2)	49(1)
N(5)	2349(1)	-1621(1)	6693(2)	67(1)
N(6)	4534(1)	904(1)	4501(2)	45(1)
N(7)	4940(1)	2323(1)	2605(2)	57(1)
C(1)	3730(1)	642(1)	4481(2)	38(1)
C(2)	2255(1)	736(1)	4496(2)	44(1)
C(3)	2878(1)	-201(1)	4415(2)	41(1)
C(4)	1441(1)	1142(1)	4483(3)	60(1)
C(5)	1627(2)	1761(1)	5278(5)	104(1)
C(6)	1238(2)	1277(2)	2719(4)	130(1)
C(7)	684(2)	837(1)	5271(5)	107(1)
C(8)	1980(1)	-1142(1)	4143(3)	53(1)
C(9)	1910(1)	-1423(1)	2454(3)	63(1)
C(10)	1940(2)	-949(1)	1141(3)	65(1)
C(11)	2720(2)	-752(1)	490(3)	70(1)
C(12)	2758(2)	-313(1)	-672(4)	93(1)
C(13)	2044(2)	-37(2)	-1247(4)	125(1)
C(14)	1267(2)	-222(2)	-655(5)	135(1)
C(15)	1192(2)	-684(1)	523(4)	105(1)
C(16)	1831(1)	-1631(1)	5423(3)	57(1)
C(17)	2279(2)	-2052(1)	8000(3)	85(1)
C(18)	4673(1)	1569(1)	4658(3)	47(1)
C(19)	5124(1)	1719(1)	6255(3)	64(1)
C(20)	4603(1)	1536(1)	7673(3)	58(1)
C(21)	3803(2)	1819(1)	7991(3)	78(1)
C(22)	3315(2)	1648(1)	9320(4)	96(1)
C(23)	3594(2)	1206(2)	10304(4)	103(1)
C(24)	4368(2)	926(1)	10033(4)	105(1)

C(25)	4870(2)	1086(1)	8719(3)	86(1)
C(26)	5214(1)	1805(1)	3266(3)	50(1)
C(27)	5385(2)	2600(1)	1251(3)	78(1)

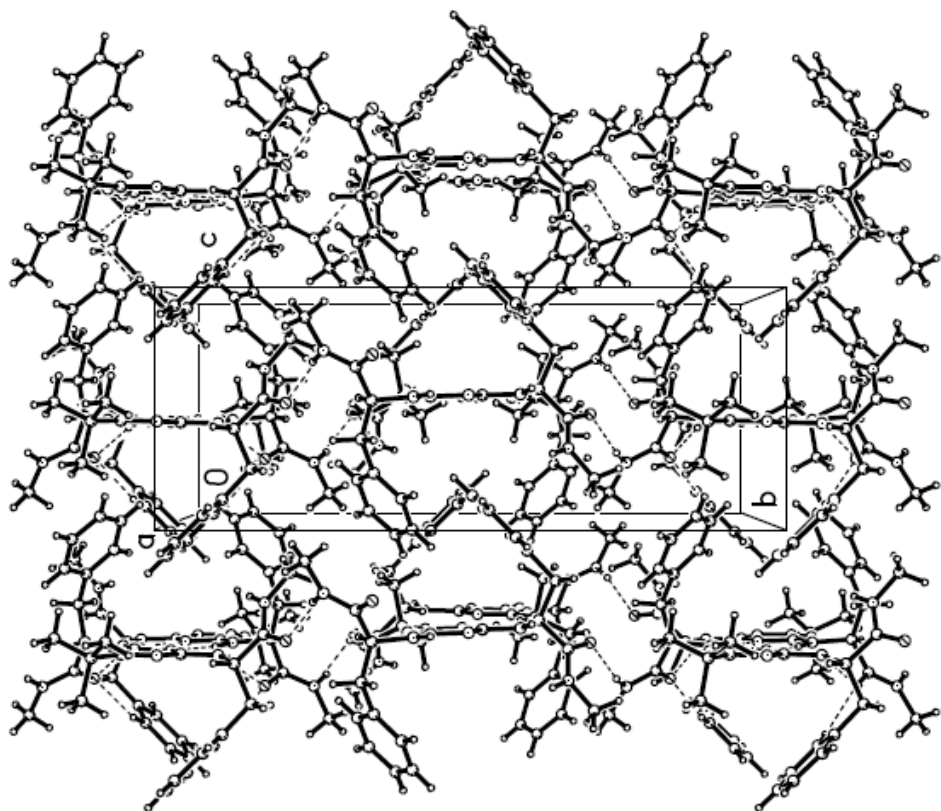
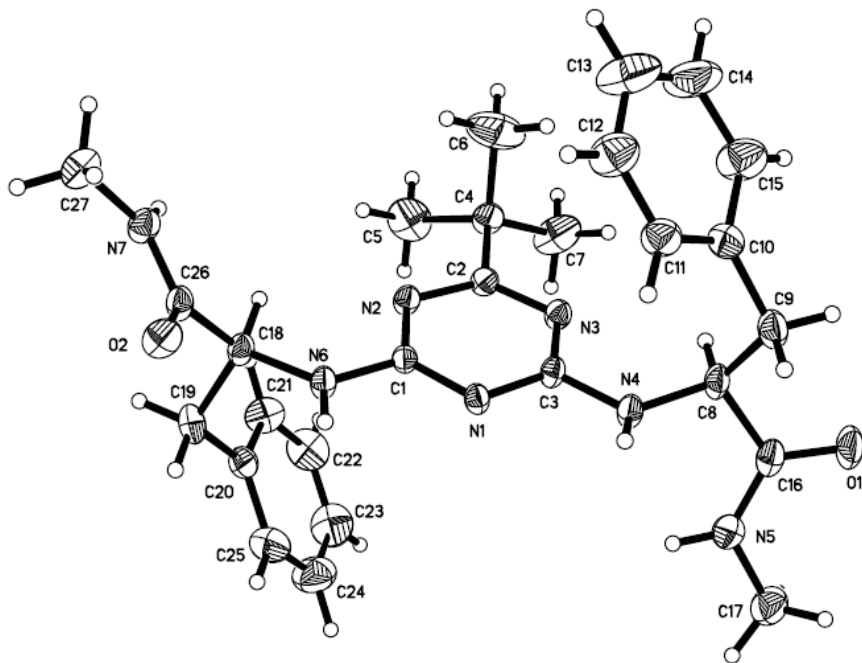


Table 1. Crystal data and structure refinement for BCLKC35 (13 Mar 2013).

Identification code	lkc35	
Empirical formula	(C ₈ H ₃ Cl F ₆ N ₄ O ₃)·H ₂ O	
Formula weight	354.61	
Temperature	296(2) K	
Wavelength	0.71073 Å	
Crystal system	Monoclinic	
Space group	P2(1)/n	
Unit cell dimensions	a = 5.0503(2) Å	α = 90°.
	b = 18.9742(7) Å	β = 97.537(2)°.
	c = 13.6338(5) Å	γ = 90°.
Volume	1295.18(8) Å ³	
Z	4	
Density (calculated)	1.819 Mg/m ³	
Absorption coefficient	0.389 mm ⁻¹	
F(000)	704	
Crystal size	0.60 x 0.40 x 0.30 mm ³	
Theta range for data collection	1.85 to 29.27°.	
Index ranges	-6<=h<=6, -25<=k<=25, -18<=l<=18	
Reflections collected	23780	
Independent reflections	3410 [R(int) = 0.0440]	
Completeness to theta = 29.27°	97.0 %	
Absorption correction	Semi-empirical from equivalents	
Max. and min. transmission	0.7456 and 0.5904	
Refinement method	Full-matrix least-squares on F ²	
Data / restraints / parameters	3410 / 0 / 220	
Goodness-of-fit on F ²	1.000	
Final R indices [I>2σ(I)]	R1 = 0.0844, wR2 = 0.2172	
R indices (all data)	R1 = 0.1113, wR2 = 0.2413	
Extinction coefficient	0.016(2)	
Largest diff. peak and hole	0.797 and -0.558 e.Å ⁻³	

Table 2. Atomic coordinates ($\times 10^4$) and equivalent isotropic displacement parameters ($\text{\AA}^2 \times 10^3$) for lkc35. $U(\text{eq})$ is defined as one third of the trace of the orthogonalized U^{ij} tensor.

	x	y	z	U(eq)
Cl(1)	5384(2)	692(1)	7024(1)	71(1)
O(1W)	-502(4)	2536(1)	7099(1)	56(1)
O(1)	69(5)	2846(1)	3379(2)	64(1)
O(2)	9961(5)	475(1)	3911(2)	66(1)
N(1)	3860(4)	1927(1)	4266(2)	45(1)
N(2)	3011(5)	1665(1)	5914(2)	45(1)
N(3)	749(4)	2560(1)	5032(2)	46(1)
N(4)	6850(5)	1331(1)	3481(2)	48(1)
C(1)	2635(5)	2018(1)	5055(2)	42(1)
C(2)	4830(5)	1159(1)	5945(2)	44(1)
C(3)	6257(5)	993(1)	5179(2)	45(1)
C(4)	5667(5)	1402(1)	4340(2)	42(1)
C(5)	-277(5)	2933(1)	4224(2)	46(1)
C(6)	-2026(7)	3557(2)	4466(2)	58(1)
C(7)	8784(5)	868(2)	3322(2)	48(1)
C(8)	9428(6)	877(2)	2245(2)	54(1)
F(1)	-3935(5)	3679(1)	3735(2)	88(1)
F(2)	-614(6)	4130(1)	4595(2)	109(1)
F(3)	-3169(5)	3446(1)	5266(2)	110(1)
F(4)	8798(6)	1474(2)	1792(2)	138(1)
F(5)	8169(8)	405(2)	1738(2)	173(1)
F(6)	11930(5)	799(2)	2210(2)	109(1)

